CLEAN WATER WATER POLLUTION CONTROL RESEARCH SERIES ● 16130 DJH 01/71

A PREDICTIVE MODEL FOR THERMAL STRATIFICATION AND WATER QUALITY IN RESERVOIRS

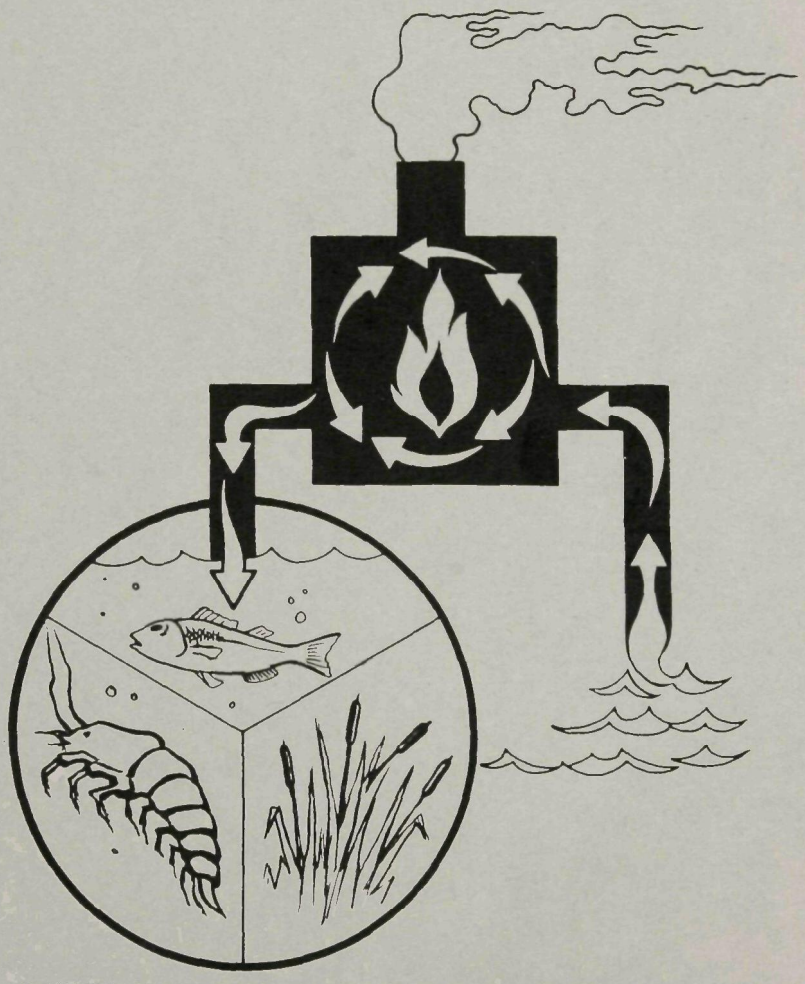

ENVIRONMENTAL PROTECTION AGENCY ● WATER QUALITY OFFICE

WATER POLLUTION CONTROL RESEARCH SERIES

The Water Pollution Control Research Series describes the results and progress in the control and abatement of pollution of our Nation's waters. They provide a central source of information on the research, development, and demonstration activities of the Water Quality Office, Environmental Protection Agency, through inhouse research and grants and contracts with Federal, State, and local agencies, research institutions, and industrial organizations.

Inquiries pertaining to the Water Pollution Control Research Reports should be directed to the Head, Project Reports System, Office of Research and Development, Water Quality Office, Environmental Protection Agency, Washington, D.C. 20242.

A PREDICTIVE MODEL FOR THERMAL STRATIFICATION AND WATER QUALITY IN RESERVOIRS

by

Mark Markofsky

and

Donald R. F. Harleman

RALPH M. PARSONS LABORATORY

FOR WATER RESOURCES AND HYDRODYNAMICS

Department of Civil Engineering

Massachusetts Institute of Technology

Cambridge, Massachusetts 02139

for the

WATER QUALITY OFFICE

ENVIRONMENTAL PROTECTION AGENCY

Research Grant No. 16130 DJH

January, 1971

EPA Review Notice

This report has been reviewed by the Water Quality Office, EPA, and approved for publication. Approval does not signify that the contents necessarily reflect the views and policies of the Environmental Protection Agency, nor does mention of trade names or commercial products constitute endorsement or recommendation for use.

FOREWARD

This is the third report issued in conjunction with a continuing research program on thermal stratification and water quality in lakes and reservoirs. The previous reports are as follows:

1. Dake, J.M.K. and D.R.F. Harleman, "An Analytical and Experimental Investigation of Thermal Stratification in Lakes and Ponds", M.I.T. Hydrodynamics Laboratory Technical Report No. 99, September 1966. (Portions of this report have also been published by the same authors under the title: "Thermal Stratification in Lakes: Analytical and Laboratory Studies", Water Resources Research, Vol. 5, No. 2, April 1969, pp. 484-495.)

2. Huber, W.C. and D.R.F. Harleman, "Laboratory and Analytical Studies of the Thermal Stratification of Reservoirs", M.I.T. Hydrodynamics Laboratory Technical Report No. 112, October 1968.

ABSTRACT

Previous research on thermal stratification in reservoirs has provided analytical methods for predicting the thermal structure and internal flow field of a reservoir characterized by horizontal isotherms. A one-dimensional analytical thermal stratification prediction method developed by Huber and Harleman is reviewed and modififed to include the time required for the inflowing water to reach the dam face.

Various "dispersion" approaches to water quality prediction, which depend on empirically determined dispersion coefficients, are reviewed. Application of these methods to water quality prediction in a stratified reservoir is discarded because of their inability to account for the transient nature of the internal flow pattern generated by changing meteorological and hydrological conditions.

A one-dimensional water quality mathematical model is developed which incorporates the internal flow pattern predicted for a stratified reservoir from the temperature model of Huber and Harleman. The water quality parameters of rivers and streams entering the reservoir are assumed to be known. After initial mixing, the entering water seeks its own density level within the horizontal stratification field of the reservoir. The outflow of water through the reservoir outlet is assumed to come from a withdrawal layer whose vertical thickness is a function of the time-dependent vertical temperature-density gradient. The water quality model is designed to predict the concentration of particular water quality parameters in the outflow water as a function of time. In the case of non-conservative pollutants, the model incorporates generation and/or decay rates for the substance under consideration.

The mathematical model is tested by comparisons with measurements of outlet concentrations resulting from pulse injections of a conservative tracer into a laboratory reservoir with time varying inflows, outflows and insolation. Good agreement is obtained between measured and predicted concentration values. Pulse injection tests of a conservative tracer in Fontana Reservoir are simulated by means of the mathematical model in order to illustrate the flowthrough time characteristics of a stratified reservoir. Field data for comparison with the theory is not available.

The application of the mathematical model to a field case of practical interest is demonstrated by solving the coupled set of water quality equations for B.O.D. and D.O. predictions in Fontana Reservoir. Field measurements of D.O. both within the reservoir and at the outlet of Fontana are available for the year 1966; however, measurements of incoming B.O.D. and of the long-term B.O.D decay rate were not made.

Direct comparisons of the water quality model predictions with the field measurements of dissolved oxygen are limited by the lack of input data. A sensitivity analysis to various assumptions on the input data is made in order to illustrate the mechanics of the water quality prediction model. It is concluded that the model is capable of predicting the effect of reservoir impoundments on water quality.

This report was submitted in fulfillment of Research Grant No. 16130 DJH between the Water Quality Office, Environmental Protection Agency and the Massachusetts Institute of Technology.

Key Words: reservoir water quality; thermal stratification in reservoirs; biochemical oxygen demand in reservoirs, dissolved oxygen in reservoirs.

ACKNOWLEDGEMENT

This investigation was supported by the Water Quality Office, Environmental Protection Agency, under Research Grant No. 16130 DJH as part of a research program entitled "Thermal Stratification and Reservoir Water Quality". The project officer was Mr. Frank Rainwater, Chief, National Thermal Pollution Research Program, FWQA Pacific Northwest Water Laboratory at Corvallis, Oregon. The cooperation of Mr. Rainwater and of Mr. Bruce A. Tichenor is gratefully acknowledged.

The authors wish to express their appreciation to Mr. Rex A. Elder, Chief of the Engineering Laboratory Branch of the T.V.A. Division of Water Control Planning and to Dr. W. O. Wunderlich of the same organization for their cooperation and assistance in supplying the field data for Fontana Reservoir.

Mr. Patrick Ryan, Research Assistant in the Water Resources and Hydrodynamics Laboratory, made substantial contributions in both the analytical and experimental phases of the research program. Appreciation is also extended to Messrs. Edward McCaffrey and Roy Milley for assistance in the instrumentation and construction of experimental equipment.

The research program was administered at M.I.T. under DSR 71381 and 72325. Numerical computations were done at the M.I.T. Information Processing Service Center. Our thanks to Miss Kathleen Emperor who typed most of the report and to Mrs. Barbara Yasney for assistance with the drafting.

The material contained in this report was submitted by Mr. Markofsky in partial fulfillment of the requirements for the degree of Doctor of Philosophy at M.I.T.

TABLE OF CONTENTS

CHAPTER 1. INTRODUCTION

1.1 Introduction

The construction of an impoundment on a river usually leads to substantial changes in water quality within the reservoir and in the river downstream of the reservoir. These changes reflect modifications of the physical, chemical, and biological regimes which are associated with the increase in depth,surface area and the reduction of velocity. The thermal structure of the reservoir and the temperature of the outlet water are important as primary water quality factors. In addition, the changing thermal structure has a dominant effect on the detention time which is related to the internal flow characteristics within the reservoir.

Thermal stratification occurs in practically all reservoir impoundments. In shallow "run of the river" reservoirs the isotherms tend to be tilted in the downstream direction and the stratification is relatively weak. In deep reservoirs, having a storage volume which is large compared to the annual through-flow, the isotherms are horizontal during most of the year and strong stratification may develop during certain seasons. This investigation is concerned mainly with the latter type of reservoir in which temperature and water quality parameters are functions of depth and time.

The thermal stratification process is governed by a heat balance involving solar radiation, surface losses by evaporation and conduction, and convective transfer of inflows and outflows. As a result of research in the past few years, the stratification process is now understood to the extent that reasonable predictions of the

internal temperature distributions and outflow temperature can be made for the purpose of planning new facilities or the operation of existing reservoirs. The thermal stratification, through the density variation, has a predominant influence on the flow pattern and circulation within a reservoir. Vertical motions are inhibited in density-stratified reservoirs and outflows tend to be drawn from a layer of restricted depth near the outlet. The flow pattern may involve numerous counterflowing currents. This complicated internal current structure is important in the convective and dispersive processes for any substance introduced into the reservoir.

Many water quality factors other than temperature are important in a reservoir. The majority of these are affected by the distribution, dilution, and detention time in the reservoir. An understanding of the internal flow structure of a stratified reservoir is a prerequisite to rational concentration predictions of various water quality parameters. The traditional methods of analysis, in which the concentration is assumed to depend on only the longitudinal coordinate, is inappropriate in a stratified reservoir because the localized horizontal currents may restrict the particular water quality parameter to a certain level within the reservoir for a long period of time.

The dissolved oxygen structure of a reservoir will be a primary consideration in water quality because the ecological balance in a reservoir is very sensitive to dissolved oxygen levels. The oxygen balance in a reservoir is dependent on numerous physical and

biological factors which include convective transport by internal currents, atmospheric reaeration at the surface, photosynthetic oxygen sources associated with plant life, oxygen demands of river inflows, bottom deposits, respiration and decomposition of aquatic organisms. Thermally stratified reservoirs exhibit oxygen stratification with an oxygen rich surface layer which is mixed by winds and convection currents. The lower layers of a reservoir are often deficient in oxygen because the oxygen demand of internal organic material exceeds the oxygen transfer from the surface layer. In addition, the biological and mass transfer processes are sensitive to temperature and thus the oxygen balance will depend on the thermal structure of the reservoir. In view of the oxygen stratification in reservoirs, the classical Streeter-Phelps analysis for streams, which assumes vertically mixed conditions, is not applicable in stratified reservoirs. The oxygen balance should include the vertical variation of dissolved oxygen as influenced by internal currents and the vertical distribution of oxygen sources and sinks.

In the following chapters a mathematical model for predicting the thermal stratification phenomena in a horizontally stratified reservoir is presented. The temperature model is based on modifications to the work of Huber and Harleman (18) in an earlier phase of the M.I.T. reservoir research program. The primary objective of the present investigation is the development of a water quality mathematical model which is coupled with the thermal stratification prediction model. The water quality model is initially verified by comparing the results with measurements made under controlled laboratory condi-

tions. A series of tests were made on the prediction of the transient reservoir outlet concentrations which resulted from pulse injections of a conservative tracer into a laboratory reservoir. Predictions are also given for a simulated pulse injection of a conservative tracer into Fontana Reservoir in the TVA system. In this context the concept of detention time in a stratified reservoir is discussed. Dissolved oxygen predictions are also presented for Fontana Reservoir and compared with available field data.

CHAPTER 2. INTRODUCTION AND BASIC CONCEPTS - THE TEMPERATURE MODEL

2.1 Introduction and Basic Concepts

The problem of predicting the temporal variation of the concentration of a particular water quality parameter in the outlet and at all points within a stratified reservoir is very difficult because of the complicated flow patterns which are generated. Additional complications arise if one considers a parameter such as dissolved oxygen (DO) which experiences a time dependent decay due to biological oxygen demand (BOD) and chemical oxygen demand (COD).

Previous work on the concentration distribution of a conservative tracer (48) and DO (54) in a stratified reservoir has attempted to circumvent the internal flow problem. (These papers will be discussed in detail in Sections 2.3.3.3 and 3.2 respectively.)

As a stream enters the main body of a thermally stratified reservoir there is a certain amount of mixing and entrainment which takes place. If the stream temperature differs from that of the reservoir water with which it is mixing, the effective inflow rate and temperature will depend on the amount of entrainment which takes place at the entrance. This "mixed" incoming water will then seek its own density level within the reservoir. If this water is warmer than the surface water it will enter and flow along the reservoir surface. If it is colder than any of the water within the reservoir, it will flow along the bottom until it reaches the deepest portion of the reservoir. If the incoming water is at some intermediate temperature, it will flow along the bottom until it reaches an elevation corresponding to its own density level, at which point it will begin to move horizontally.

As the vertical density gradient due to temperature at the outlet increases, the vertical zone of withdrawal, δ, from the reservoir decreases. This gives rise to a complicated series of flows and counterflows within the reservoir.

These phenomena are illustrated in Figure 2.1.

There are many time dependent factors which are involved in altering the thermal structure of a reservoir. Besides the changing temperature of the inflowing water, there are surface and internal heat sources due to incoming solar radiation. Evaporative cooling, back radiation and possible losses through the reservoir perimeter are also important contributors to the transient thermal structure. In addition, the operation of the reservoir discharge will control the amount of heat advected from the reservoir. Due to the changing temperature field, any pollutant or water quality parameter contained in the inflowing water will enter the reservoir at different elevations throughout the year, depending on the temperature of the inflowing water, and the thermal structure of the reservoir at that time.

The water which enters the reservoir in the spring and early summer is usually warmer than the water within the lake; it tends to enter at the surface and remain in the reservoir for a long period of time. The water entering in the late summer and fall is usually colder than the reservoir surface water, consequently, it enters at some intermediate depth. This colder water may find its way to the reservoir outlet much earlier than the warmer water which entered before it. This fact is important because the majority of the water quality parameters are affected by the length of time which the water spends in the reservoir.

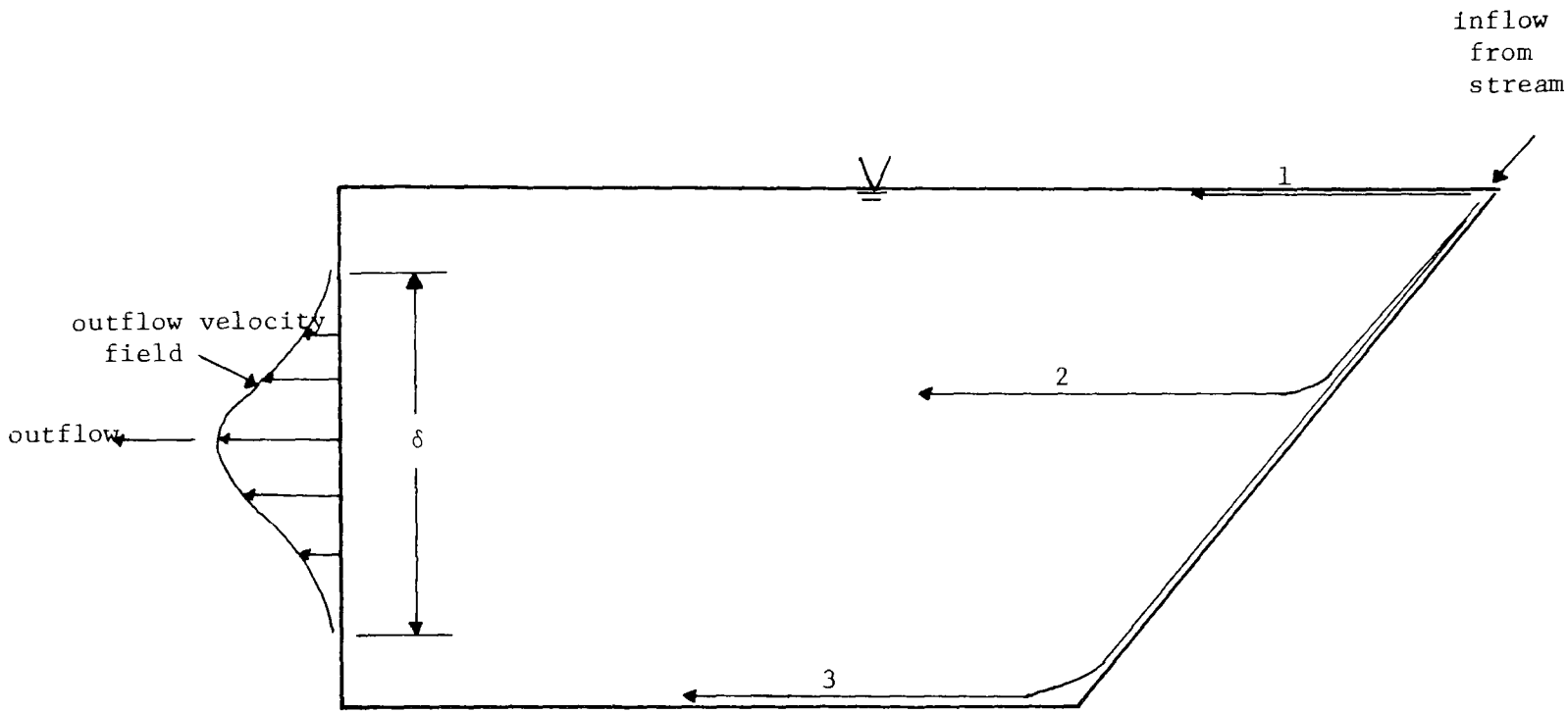

1 Warm Water Inflow

2 Intermediate Inflow

3 Cold Water Inflow

FIGURE 2.1 THE CHANGING INFLOW LEVEL AND WITHDRAWAL DISTRIBUTION IN A STRATIFIED RESERVOIR

The main objective of this investigation is to develop a method of predicting the temporal variation of the concentration distribution of a particular pollutant or water quality parameter in a stratified reservoir. In order to do this, a mechanism for evaluating the reservoir entrance mixing, the internal flow field and dispersion characteristics must be developed. It should be clear from the previous discussion that these phenomena are related to the changing temperature structure within the reservoir. Therefore, before concentration predictions can be made, a method of predicting the temperature field as a function of time is needed. A major contribution has been made by Huber and Harleman (18) who have developed a one-dimensional model for predicting the transient temperature and internal flow field in a deep reservoir having horizontal isotherms.

This investigation is also limited to deep reservoirs with horizontal isotherms. By means of this assumption the mass transport phenomena can also be treated in a one-dimensional approach similar to that taken by Huber and Harleman in treating the thermal prediction problem. In addition, the temperature and mass transport equations are coupled in that the same velocity field used in the temperature model can be used in the concentration prediction model.

The temperature model was verified by Huber and Harleman using both laboratory and field data. The mass transport model developed here is verified in the laboratory by means of a pulse injection of a conservative tracer into a laboratory reservoir. This type of experiment was run to further check the assumptions made in the temperature model

and to fully develop the method of analyzing this type of experiment because it is a potentially valuable field technique. The mathematical model is also applied to DO and BOD prediction in Fontana Reservoir in the TVA system.

In the following section the exact equations governing the prediction of the temporal and spatial distribution of conservative and non-conservative substances in a stratified reservoir are presented. The approximations and assumptions necessary to solve these equations follows. Since the prediction of the temperature field will be shown to be most crucial, the model of Huber and Harleman, along with certain modifications, will be discussed in detail in this chapter. In Chapter 3, the water quality prediction model will be developed. This is applied to laboratory tests in Chapter 4 and field data in Chapter 5.

2.2 The Exact Equations Governing Pollutant Concentration Predictions in a Stratified Reservoir

In order to solve for the concentration of a particular pollutant in a stratified reservoir one must have knowledge of the flow field, density distribution and conservation of mass for all substances under consideration. Mathematically, this involves the simultaneous solution of the equation of motion:

$$\rho\left[\frac{\partial \bar{u}_i}{\partial t} + \bar{u}_j \frac{\partial \bar{u}_i}{\partial x_j}\right] = -\rho g_i - \frac{\partial \bar{p}}{\partial x_i} + \mu \frac{\partial^2 \bar{u}_i}{\partial x_j^2} - \rho\left[\frac{\partial}{\partial x_j} \overline{(u_i' u_j')}\right] \quad (2\text{-}1)$$

continuity:

$$\frac{\partial \rho}{\partial t} + \rho \frac{\partial \bar{u}_j}{\partial x_j} + \bar{u}_j \frac{\partial \rho}{\partial x_j} = 0 \quad (2\text{-}2)$$

The conservation of heat equation:

$$\frac{\partial \bar{T}}{\partial t} + \bar{u}_j \frac{\partial \bar{T}}{\partial x_j} = D_T \frac{\partial^2 T}{\partial x_j^2} - \frac{\partial}{\partial x_j} (\overline{u_j' T'}) + \frac{\text{sources}_T}{\rho c_p} - \frac{\text{sinks}_T}{\rho c_p} \quad (2\text{-}3)$$

the equation of state:

$$\rho = \rho(T, \text{ dissolved substances}) \quad (2\text{-}4)$$

and conservation of mass:

$$\frac{\partial \bar{c}}{\partial t} + \bar{u}_j \frac{\partial \bar{c}}{\partial x_j} = D_M \frac{\partial^2 \bar{c}}{\partial x_j^2} - \frac{\partial}{\partial x_j} (\overline{u_j' c'}) + \frac{\text{sources}_m}{\rho} - \frac{\text{sinks}_m}{\rho} \quad (2\text{-}5)$$

for each pollutant under investigation where

$\bar{u}_i = \bar{u}_i (x,y,z,t)$ = velocity in the i^{th} direction ($i = 1,2,3$) at time t.

$\bar{u}_j = \bar{u}_j (x,y,z,t)$ = velocity in the j^{th} direction ($j = 1,2,3$) at time t.

$\bar{p} = \bar{p} (x,y,z,t)$ = pressure field at time t.

$\rho = \rho(x,y,z,t)$ = the density field at time t.

g = acceleration of gravity.

u_i', $u_j' = u_i' (x,y,z,t)$, $u_j' (x,y,z,t)$ = turbulent velocity fluctuation in the i and j direction.

$\bar{T} = \bar{T} (x,y,z,t)$ = temperature field at time t.

$T' = T' (x,y,z,t)$ = turbulent temperature fluctuation at time t.

$\mu = \mu(\bar{T})$ = dynamic viscosity.

D_T = molecular diffusivity of heat.

c_p = specific heat of water.

$sources_T$ = sources of heat per unit volume per unit time.

$sinks_T$ = sinks of heat per unit volume per unit time.

$\bar{c} = \bar{c}(x,y,z,t)$ = concentration field of a particular pollutant of time t.

$c' = c'(x,y,z,t)$ = turbulent concentration fluctuation.

D_M = molecular diffusivity of mass.

$source_m$ = source of mass per unit volume per unit time.

$sink_m$ = sink of mass per unit volume per unit time.

The last term in the equations of motion and the terms involving the cross products $u_j'T'$ and $u_j'c'$ in Equations 2.3 and 2.5 should be included only if the flow is turbulent. As Koh (23) has demonstrated, the amount of work, W, required to vertically transport a particle of fluid of volume, V, from depth y_o to y_1, (Figure 2.2) in a stably stratified fluid (i.e. $\frac{\partial \rho}{\partial y} \leq 0$) is given by

$$W = V \int_{y_o}^{y_1} [\rho(y_o) - \rho(y)]\, g\, dy \qquad (2\text{-}6)$$

Since this work is always positive whether $y_o > y_1$, $y_o < y_1$, any vertical motion requires an addition of energy, no matter how slowly the motion is carried out. Thus, the existence of a vertical density stratification tends to inhibit vertical motion. The ability of a density stratification to inhibit turbulence in the vertical direction will depend on the magnitude of $\frac{\partial \rho}{\partial y}$. This is usually expressed in the form of

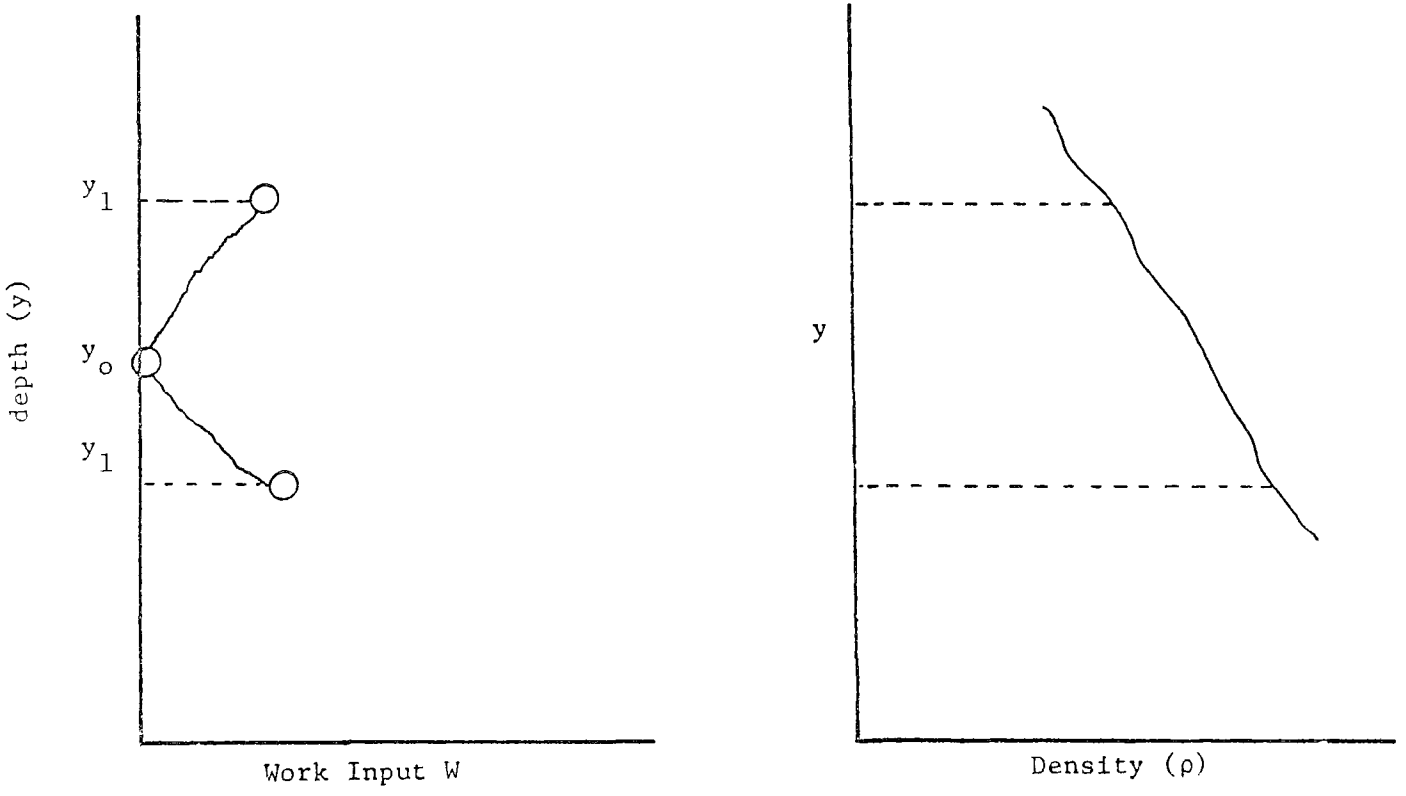

FIGURE 2.2 WORK INPUT TO DISPLACE A PARTICLE OF FLUID IN A STABLY STRATIFIED FLUID

a Richardson number.

The question of turbulent vs. laminar flow in a stratified reservoir is most crucial since this will dictate whether the turbulent fluctuation terms in Equations 2-1, 2-3 and 2-5, which considerably complicate the problem, should be considered. A basic premise of this investigation is that the existence of horizontal isotherms in a reservoir suppresses vertical motion to the extent that turbulent transport of momentum, heat or mass can be neglected. The only exceptions will be in the case of entrance mixing and that of a surface layer instability caused by evaporative cooling which results in an unstable density gradient. As will be shown in Sections 2.4.3 and 2.4.5 these two exceptions can be handled quite satisfactorily without specifying the exact form of the turbulence generated in each case. The ultimate verification of this assumption will be the ability or inability of a theory neglecting turbulence to match observed values.

Orlob and Selna (36), in developing a thermal prediction model for stratified reservoirs, employ a dispersion coefficient which is the order of 10^4 times the molecular value. This would, at first impression, tend to indicate a high degree of turbulence and invalidate the assumption just discussed. However, as is shown in Section 2.3.3.3 an apparent turbulent dispersion term may not indicate turbulence but rather the inability of certain assumptions in a mathematical model to account for a very complex pheonomena.

Orlob (54) and Huber and Harleman (18) have presented criteria (Table 2.1) for determining when reservoirs will tend to stratify hori-

zontally, vertically or in some intermediate stage. Huber and Harleman's criterion is based on the ratio, r_H, of the yearly volume of inflow, $\forall_Q$, to the reservoir volume, $\forall_r$. Orlob uses this criterion, replacing $\forall_Q$ by Q, the average discharge in m^3/sec through the reservoir multiplied by the ratio of the average reservoir depth, d, in meters to length in meters to define a reservoir Froude number, $\mathbb{F}_r$:

$$r_H = \frac{\forall_Q}{\forall_r} \tag{2-7}$$

$$\mathbb{F}_r = \frac{Q}{\forall_r} \frac{L}{d} \sqrt{\frac{\rho_o}{g\beta_o}} \tag{2-8}$$

where ρ_o = reference density

β_o = average vertical density gradient in the reservoir

Orlob suggests the use of 10^{-3} Kg m^{-4} and 10^3 Kg m^{-3} for β_o and ρ_o respectively, reducing Equation 2-8 to:

$$\mathbb{F}_r = 320 \frac{L}{d} \frac{Q}{\forall_r} \tag{2-9}$$

These criteria are combined and typical values presented in Table 2.1.

Orlob's modification, which introduces L/d into the reservoir criterion, is an indirect way of including the pheonomena of wind induced mixing and evaporative cooling. As L/d increases, the reservoir will be more susceptible to mixing due to either a large surface area for surface cooling and wind forces to act upon (large L) or the possibility of the thermocline (the depth of maximum density gradient)

TABLE 2.1

RESERVOIR	LENGTH (m)	AVERAGE DEPTH (m)	DISCHARGE TO VOLUME RATIO (sec^{-1})	F_r	CLASS
Hungary Horse[1]	$4.7x10^4$	70	$1.2x10^{-8}$	0.0026	Deep
Fontana[2]	$4.6x10^4$	107	$2.5x10^{-8}$	0.0029	Deep
Detroit[2]	$1.5x10^4$	56	$3.5x10^{-8}$	0.0030	Deep
Lake-Roosevelt[3]	$2.0x10^5$	70	$5.0x10^{-7}$	0.46	Weakly-Stratified
Priest Rapids[4]	$2.9x10^4$	18	$4.6x10^{-6}$	2.4	Completely Mixed
Wells[4]	$4.6x10^4$	26	$6.7x10^{-6}$	3.8	Completely Mixed

1 Montana

2 TVA System

3 Montana

4 River run dams on the Columbia River below Grand Coulee Dam

TABLE 2.1 RESERVOIR STRATIFICATION CRITERIA

reaching the reservoir surface (small d).

However the inclusion of the ratio $\sqrt{\rho_o/g\beta_o}$ is questionable. β_o is defined as an average density gradient for which Orlob arbitrarily assigns the value 10^{-3} K g m^{-4}. Firstly, in the case of a completely mixed reservoir, $\frac{\partial \rho}{\partial y} = 0$ and β should also equal zero. Secondly, as a predictive tool to determine the shape of the reservoir isotherms, β_o would not be a known parameter as opposed to Q, $\forall_Q$, $\forall_r$, L and d which could be determined from the proposed reservoir geometry and inflowing stream hydrographs. Since a constant value is assumed for this ratio, the results obtained by Orlob are presented. However it is felt that the ratio, $\sqrt{\frac{\rho_o}{g\beta_o}}$, could be omitted from the reservoir criteria to avoid the unnecessary choice of arbitrary values.

2.3 Approximations to the Full Set of Equations

2.3.1 Marker and Cell Technique

Daly and Pract (10) and Slotta (43) have presented methods for solving the equations of motion numerically for the case of laminar flow in a density stratified fluid. The procedure, in two dimensions, consists basically of "flagging" or marking particles in rectangular cells of length δx and height δy according to set schemes. For example, Slotta calls EMP a cell containing no fluid particles, FULL, a cell containing particles with no adjacent EMP cell, OUT, a cell defining an outlet, etc. The Navier Stokes equations are written in a finite difference form and an algorithm is presented for their solution.

The fundamental problem that arises when trying to adopt this method to a thermally stratified reservoir is the complete neglect of

the temperature field on density variations. New densities are calculated in the algorithm by averaging the densities of the particles in a given cell. Since the thermal structure of a reservoir is continuously varying with time, the temperature field must be determined at each successive time step in order to correctly determine the density field. This involves the solution of the equations of motion, continuity, the equation of state and the conservation of heat equation which poses a formidable, if not impossible, programing and computer storage problem.

For very simple problems, such as withdrawal from a two layered system and flow over a submerged ridge in a two layered system, Slotta reports a storage requirement of 65,000 locations for a grid containing 800 cells and 3,000 particles. Using a time step near the maximum allowable by the stability conditions, one time cycle took seven seconds on a CDC 6600. A typical run of 200 cycles took twenty-three minutes. Slotta felt that this size and running times were nearly minimal.

Considering the added complexity of solving both the complete equations of motion, the equations of state, continuity, and the conservation of heat equation for a reservoir, an alternate approach, which would simplify the governing equations, seems to be called for.

2.3.2 The Boussinesq Approximation

A common assumption in phenomena governed by small density differences is that the equations of motion can be simplified by considering density variations only in the buoyancy term. Consider the case of a reservoir with horizontal isotherms in which the density can be

represented as

$$\rho(y) = \rho_o + \Delta\rho(y) \tag{2-10}$$

where

$$\frac{\Delta\rho}{\rho_o} << 1 \tag{2-11}$$

Since the vertical accelerations in a reservoir will be much less than the free fall acceleration, g, the density fluctuation, $\Delta\rho$, is neglected in the vertical acceleration term but included in the buoyancy term. The Boussinesq approximation is presented in Equation 2-12.

$$(\rho_o)\left[\frac{\partial v}{\partial t} + u\frac{\partial v}{\partial x} + v\frac{\partial v}{\partial y} + w\frac{\partial v}{\partial z}\right] = -(\rho_o + \Delta\rho)g - \frac{\partial p}{\partial y} + \mu\left[\frac{\partial^2 v}{\partial x^2} + \frac{\partial^2 v}{\partial y^2} + \frac{\partial^2 v}{\partial z^2}\right] \tag{2-12}$$

Unfortunately, the Boussinesq approximation does not sufficiently simplify the problem since $\Delta\rho$ is a function of y and 7 nonlinear simultaneous partial differential equations remain to be solved.

2.3.3 Solutions for Various Systems by Means of a Dispersion Coefficient

A widely used approach in arriving at concentration predictions for phenomena, in which the internal flow pattern is not well understood, involves a modified one-dimensional representation of the conservation of mass Equation 2-5. For example, if it is assumed that the phenomena is basically affected by longitudinal variations, Equation 2-5 would be written for the x direction:

$$\frac{\partial \bar{c}}{\partial t} + \bar{U}\frac{\partial \bar{c}}{\partial x} = \frac{1}{A}\frac{\partial}{\partial x}\left[D_p A \frac{\partial c}{\partial x}\right] + \frac{\text{sources}_m}{\rho} - \frac{\text{sinks}_m}{\rho} \qquad (2\text{-}13)$$

where

$\bar{c} = \bar{c}(x,t)$ = average concentration over the depth

$\bar{U} = \bar{U}(x,t)$ = average horizontal velocity over the depth

$A = A(x,t)$ = cross-sectional area normal to $\bar{U}$

D_p = longitudinal dispersion coefficient

Two fundamental differences appear between Equation 2-13 and a precise one-dimensional representation of Equation 2-5. The first is the omission of the turbulent fluctuation terms $u'c'$ and the second is the replacing of the molecular diffusion coefficient, D_m, by a dispersion coefficient, D_p. The basic philosophy of this one-dimensional dispersion model is to assume that all the parameters in Equation 2-13 are uniform over the depth and width (y and z directions). A very simple velocity field representation is assumed, i.e. $\bar{U} = Q/A$ where Q is the volumetric rate of flow. The longitudinal dispersion coefficient, D_p, is used to account for any non-uniformities which may exist in the actual velocity distribution. This method has been used extensively by chemical engineers to treat complex flow patterns which may exist in process equipment as is illustrated in Figure 2.3. Levenspiel and Bishoff (29) present a detailed discussion of various solutions to Equation 2-13. In different phenomena, the dispersion coefficient may be considered to be a constant, a function of space or time or some combination of these. In all cases, D_p must be empirically determined. Three examples follow.

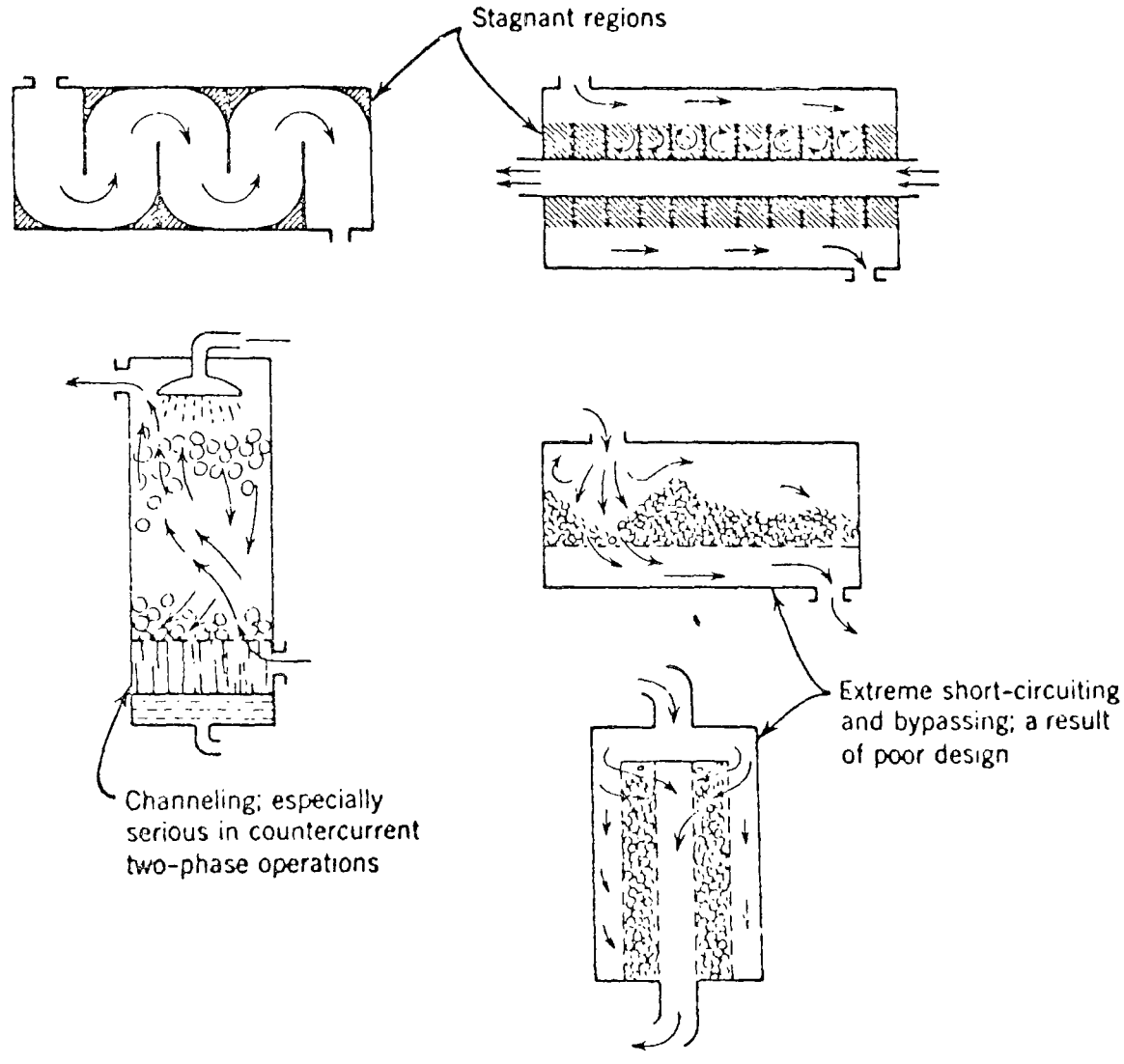

FIGURE 2.3 FLOW IN CHEMICAL ENGINEERING PROCESS EQUIPMENT

2.3.3.1 Constant Longitudinal Dispersion Coefficient

Consider a steady uniform turbulent flow in a long conduit of constant cross-sectional area, A (9). At time t = 0, tracer fluid E is injected into fluid B as a pulse input at x = 0. The flow rate, Q, is constant and it is desired to determine the spatial and temporal concentration distribution of the tracer.

Since there are no external sources or sinks of mass and A is a constant equation 2-13 reduces to

$$\frac{\partial c_E}{\partial t} + \bar{U} \frac{\partial c_E}{\partial x} = D_p \frac{\partial^2 c_E}{\partial x^2} \qquad (2\text{-}14)$$

The initial conditon is

$$c_E (x,0) = (M/\rho A) \ \delta(x) \qquad (2\text{-}15)$$

where M = mass of tracer E introduced

$\delta(x)$ = Dirac delta function

The conservation of mass consideration yields the further condition that

$$\int_{-\infty}^{+\infty} c_E (x,t) \, dx = M/\rho A \int_{-\infty}^{+\infty} \delta (x) \, dx = M/\rho A \qquad (2\text{-}16)$$

The boundary condition on x is obtained by stating that the concentration at $x = \pm \infty$ remains unchanged with time

$$c_E (\pm \infty, t) = 0 \qquad (2\text{-}17)$$

The solution to Equation 2-14 with these initial and boundary conditions is

$$c_E = \frac{M}{\rho A \sqrt{4\pi D_p t}} e^{-(x-ut)^2/4D_p t} \qquad (2\text{-}18)$$

This is the equation of a Gaussian curve. The value of the dispersion coefficient, however, is yet to be determined. Taylor (47) has demonstrated that for uniform turbulent flow in a straight conduit

$$D_p = 10.1\ r_o\sqrt{\tau_o/\rho} \qquad (2\text{-}19)$$

where r_o = pipe radius

τ_o = shear stress at the wall.

D_p can be either calculated from Equation 2-19 by modifying r_o to be the hydraulic radius of the channel or it can be determined empirically by fitting experimental data. The actual values for c_E in Equation 2-18 will depend on what is assumed for D_p. The larger the value of D_p the more rapidly the flow is dispersed. This is represented schematically in Figure 2-4.

2.3.3.2 The Dispersion Coefficient as a Function of Time

Holly (16) considers the solution to the problem of a pollutant undergoing first order decay while flowing in a constant area channel in which the average cross-sectional velocity is allowed to be a function of time. The longitudinal dispersion coefficient is assumed to be a function of time but independent of x. For this case Equation 2-13 can be written as:

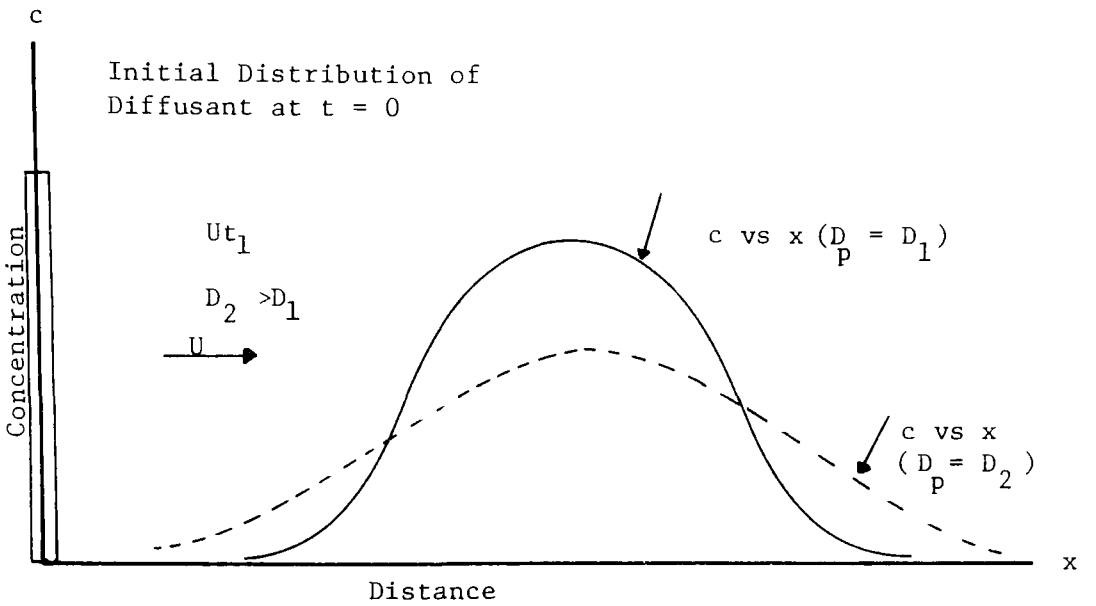

FIGURE 2.4a CONCENTRATION VARIATION AS A FUNCTION OF DISTANCE AT $t = t_1$ FOR VARIOUS LONGITUDINAL DISPERSION COEFFICIENTS

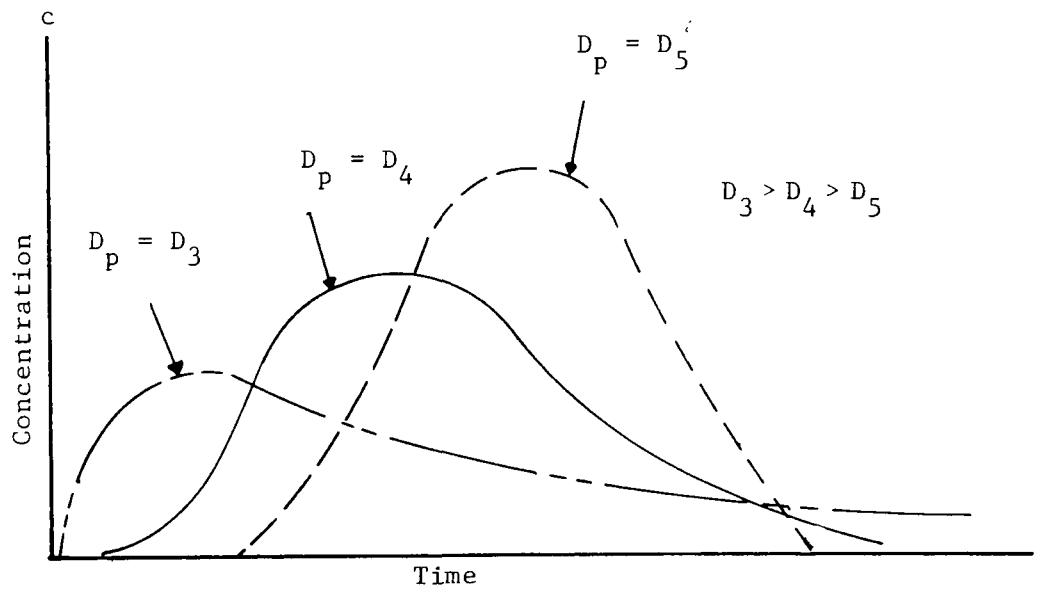

FIGURE 2.4b CONCENTRATION VARIATION WITH TIME AT $x = x_1$ FOR VARIOUS LONGITUDINAL DISPERSION COEFFICIENTS

FIGURE 2.4 CONSTANT LONGITUDINAL DISPERSION COEFFICIENT MODEL

$$\frac{\partial \bar{c}}{\partial t} + \bar{U}(t) \frac{\partial \bar{c}}{\partial x} = D_p(t) \frac{\partial^2 \bar{c}}{\partial x^2} - K_1 \bar{c} \qquad (2\text{-}20)$$

where K_1 = first order decay constant.

This is equivalent to the conservation of BOD equation, neglecting sources, for a stream.

Through the substitutions:

$$c = \lambda e^{-(K_1(t-\tau))} \qquad (2\text{-}21a)$$

$$\alpha = x - \int_{\tau}^{t} U(t)\, dt \qquad (2\text{-}21b)$$

$$\theta = \int_{\tau}^{T} \frac{D_p(t)}{D_o} dt \qquad (2\text{-}21c)$$

where τ = the reference time for which $c(x,\tau)$ is known

D_o = a reference dispersion value

Equation 2-20 is reduced to

$$\frac{\partial \lambda}{\partial \theta} = D_o \frac{\partial^2 \lambda}{\partial \alpha^2} \qquad (2\text{-}22)$$

For an instantaneous release at time $\theta = 0$ (i.e. $t = \tau$) at $\alpha = 0$, the solution is

$$\lambda = \frac{W_L}{\gamma A \sqrt{4\pi D_o \theta}} e^{-\left[\frac{\alpha^2}{4D_o\theta}\right]} \qquad (2\text{-}23)$$

where W_L = pounds of pollutant released

γ = specific weight of the fluid

A = flow area.

One must again turn either to a modified form of Taylor's equation or empirical data for the determination of D_o and D(t).

2.3.3.3 The Dispersion Coefficient as an Eddy Diffusivity

Morris and Thackston (48) treat the problem of the spread of a pulse injection of dye input at the inlet of a reservoir as a two-dimensional problem governed by two dispersion equations. In the longitudinal direction:

$$\frac{\partial c}{\partial t} + \bar{U} \frac{\partial c}{\partial x} = D_L \frac{\partial^2 c}{\partial x^2} \qquad (2\text{-}24)$$

and in the vertical direction

$$\frac{\partial c}{\partial t} = D_v \frac{\partial^2 c}{\partial y^2} \qquad (2\text{-}25)$$

where D_L = longitudinal dispersion coefficient

$D_v = D_v(y,t)$ = vertical eddy diffusivity.

Equation 2-24 is treated in exactly the same manner as the problem discussed in Section 2.3.3.1; with the solution given by Equation 2-18. D_L is determined by a fit of Equation 2-18 to field data.

Equation 2-25 is written in finite difference form and the solution for $D_v(y,t)$ also arrived at by comparison with field data.

The treatment of Equation 2-24 as the governing equation for the horizontal spread of the incoming water may give insight into this complicated phenomena. Perhaps a modification of Equation 2-24 would be to include the variation of vertical cross-sectional area and solve

Equation 2-24 by finite difference means. In the case of surface entrance $\bar{U}$ could be related to the inflowing stream rate. However, for subsurface entrance, care must be taken due to the superposition of the outflow velocity field on the flow in a given layer. By comparing Equation 2-25 with Equation 2-13 the lack of any attempt to represent the vertical velocity field should be noted. Also, since $D_v = D_v(y,t)$ Equation 2-25 should be written as:

$$\frac{\partial c}{\partial t} = \frac{\partial}{\partial y}\left[D_v \frac{\partial c}{\partial y} \right] \qquad (2\text{-}26)$$

The lack of a vertical convection term precludes any method of vertical transport except through dispersion. This places quite an empirical burden on this term which can only be determined by comparison with field data. The order of magnitude of D_v calculated by Morris and Thackston varied between 5×10^{-2} and 10^{-1} $cm^2/sec.$ whereas the value of the molecular diffusivity is 10^{-5} $cm^2/sec.$

In dye tests carried out in a reservoir, the investigators report that "there appeared to be very little vertical diffusion downward from the dye cloud and only slight diffusion upward". Because the stratified reservoir flow pattern is governed by the transient density field which is generated, vertical velocities will always be present if the inflow horizontal velocity profile is different from the outflow horizontal velocity profile as is usually the case. Thus, the large magnitude of the vertical eddy diffusivity does not necessarily reflect vertical turbulence.

2.3.3.4 Evaluation of the Dispersion Coefficient Approach

Relying on a dispersion coefficient to solve all but the most simple flow problems involves lumping all ignorance of a complicated flow field into some empirical value or function for D_p. The concept has practical value in cases where the flow field is governed by the geometry of the vessel in which the fluid is flowing. In these cases, a dispersion coefficient will uniquely describe the mixing characteristics of the vessel. When one considers the flow complexity of a thermally stratified reservoir, the weaknesses of this procedure become clear. The thermal structure and flow field of a reservoir are not only a function of its geometry but also a function of the yearly meteorological cycles, the inflowing stream flow rates and temperature and the operation of the discharge through the dam. Even if one were to empirically determine a functional relationship for D_p which satisfied one yearly cycle of reservoir operation, it would be doubtful that this would be of any use in calculating the next year's pollutant concentrations. Its use on other reservoirs and as a predictive tool for future reservoirs would be even more suspect. This leads to the conclusion that a model for predicting concentration of a pollutant in a reservoir must be linked with temperature predictions as is discussed in the next section.

2.3.4 A Solution Involving the Temperature Equation

Several attempts (4), (18), (54), have been made to solve the thermal stratification prediction problem (Equations 2-1 - 2-4) in a reservoir. Whatever the method, a velocity field, based on certain

assumptions, must be calculated. This derived internal current structure can subsequently be used in predictions of the convective and dispersive process acting on a substance introduced into the reservoir.

Before one can intelligently treat the problem of a non-conservative pollutant, such as DO, one should be fairly certain that a simplified form of the conservation of mass equation , 2-5, can reasonably predict the behavior of a conservative substance.

To follow the development of the proposed concentration prediction model, the assumptions involved in the determination of the velocity and temperature field must be completely understood. The velocity field used in the proposed model is a byproduct of the thermal stratification prediction method developed by Huber and Harleman. This is briefly summarized in the following section and the reader is referred to (18) for details of the development.

2.4 The Temperature Model

2.4.1 The Governing Equations

The basic assumption underlying the temperature model is the existence of horizontal isotherms. This will be a reasonable assumption in the case of reservoirs with a low discharge to volume ratio, and reservoir Froude number.

The governing differential equation can be derived by considering a horizontal slice through the reservoir as schematized in Figure 2.5. This finite control volume is of height Δy and width $B(y)$ with horizontal inflow and outflow rates $Q_i(y)$ and $Q_o(y)$ respectively. The vertical flow rate $Q_v(y)$, through the horizontal surface area $A(y)$, will

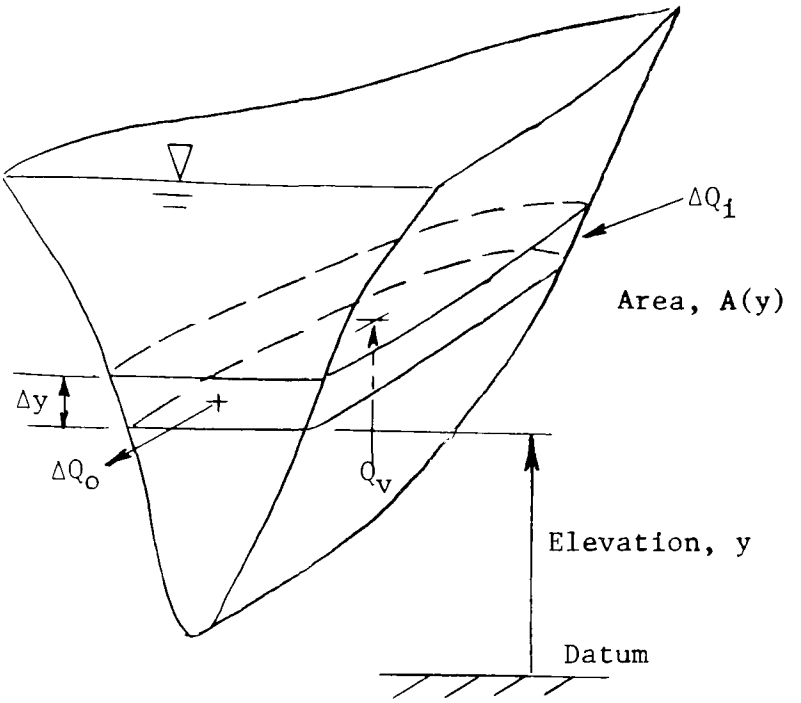

(a) Reservoir and Control Volume Illustrating Mass Continuity

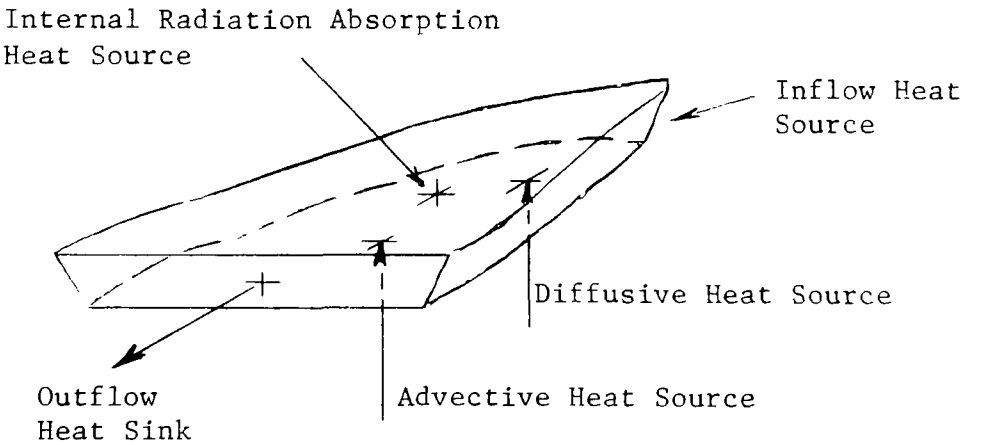

(b) Control Volume Illustrating Heat Conservation

FIGURE 2.5 CONTROL VOLUMES ILLUSTRATING CONSERVATION OF MASS AND ENERGY IN A STRATIFIED RESERVOIR

be assumed to be uniform over the length of the element. The governing equation for the distribution T(y,t) is then formulated from conservation of heat and volume considerations for this element, and extended to the entire reservoir.

Considering the element in Figure 2.5a to be always filled with water and applying the conservation of volume principle yields:

$$Q_o(y) - Q_i(y) = Q_v - (Q_v + \frac{\partial Q_v}{\partial y} \Delta y) \tag{2-27}$$

Defining q_o and q_i as the outflow and inflow rates per unit vertical distance reduces Equation 2-27 to:

$$q_i - q_o = \frac{\partial Q_v}{\partial y} \tag{2-28}$$

Treating the element in Figure 2.5b in a similar manner, the conservation of heat equation is derived. Heat is advected into the element by the incoming water q_i and away from the element by the outflowing water q_o as described in Equation 2-29 amd 2-30.

$$\text{Heat advected in} = \rho c_p q_i T_i \Delta y \tag{2-29}$$

$$\text{Heat advected out} = \rho c_p q_o T_o \Delta y \tag{2-30}$$

The heat advected in at the bottom of the element is

$$\rho c_p Q_v T$$

where Q_v is assumed positive upward.

The diffusive heat flux is

$$-\rho c A \, (D_T + E) \, \frac{\partial T}{\partial y}$$

where D_T = molecular diffusivity of heat

E = turbulent diffusivity of heat

The heat flux per unit area due to transmission of radiation can be represented as

$$\phi_b = - (1-\beta) \, \phi_o \, e^{-\eta(y_s - y)} \tag{2-31}$$

where β = fraction of radiation absorbed at the surface

η = solar radiation absorption coefficient

$\phi_o = \phi_o(t)$ = net solar radiation reaching the water surface

$y_s = y_s(t)$ = water surface elevation

Equation 2-31 is obtained from the assumption that of the solar insolation reaching the water surface, a certain percentage, β, is absorbed at the surface, and the remaining heat flux is distributed vertically as an exponential decay (Figure 2.6).

Finally, there is the possibility of heat flux losses through the sides of the reservoir ϕ_m, which are expressed as

$$\phi_m P \, \Delta y$$

where $P = P(y)$ = perimeter of the control volume.

Assuming that the density and specific heat of water are constant over the temperature ranges considered, conservation of heat

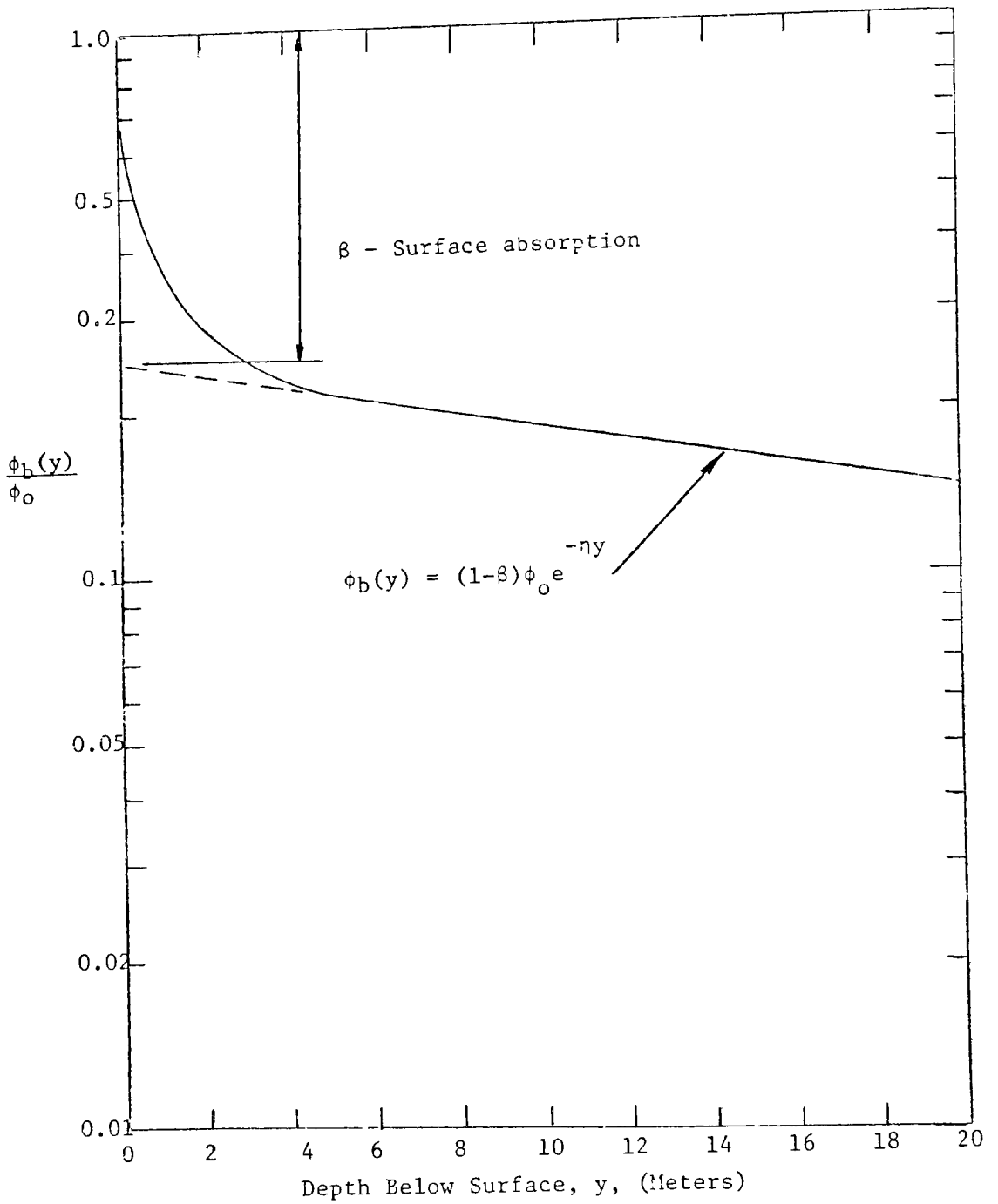

FIGURE 2.6 PENETRATION OF RADIATION INTO A RESERVOIR

energy applied to the control volume in 2.5a yields

$$\rho c_p A \Delta y \frac{\partial T}{\partial t} = \rho c_p Q_v T - \left[\rho c_p Q_v T + \left[\frac{\partial}{\partial y} (\rho c_p Q_v T) \right] \Delta y \right]$$

$$-\rho c_p A (D_M + E) \frac{\partial T}{\partial y} - \left[-\rho c_p A (D_M + E) \frac{\partial T}{\partial y} - \frac{\partial}{\partial y} \left[\rho c_p A (D_M + E) \frac{\partial T}{\partial y} \right] \Delta y \right]$$

$$+ \rho c_p q_i T_i \Delta y - \rho c_p q_o T \Delta y - P \Delta y \phi_m$$

$$+ A \phi_b - \left[A \phi_b + \frac{\partial}{\partial y} (A \phi_b) \Delta y \right] \qquad (2\text{-}32)$$

In Equation 2-32 it has been assumed that no solar insolation flux reaches the reservoir bottom.

Simplifying Equation 2-32 and combining it with the continuity Equation 2-28 results in:

$$\frac{\partial T}{\partial t} + \frac{Q_v}{A} \frac{\partial T}{\partial y} = \frac{1}{A} \frac{\partial}{\partial y} \left[A (D_M + E) \frac{\partial T}{\partial y} \right] + q_i \left[\frac{T_i - T}{A} \right]$$

$$- \frac{P \phi_m}{\rho c_p A} - \frac{1}{A \rho c_p} \frac{\partial \phi_b A)}{\partial y} \qquad (2\text{-}33)$$

Since Q_v has been assumed to be uniform over the horizontal cross-sectional area of the element, an average vertical velocity can now be defined as

$$v (y,t) = \frac{Q_v(y,t)}{A(y)} \qquad (2\text{-}34)$$

where v is positive upward.

Substituting the expression for ϕ_b and Equation 2-34 into Equation 2-33 yields

$$\frac{\partial T}{\partial t} + v\frac{\partial T}{\partial y} = \frac{1}{A}\frac{\partial}{\partial y}\left[A\,(D_M + E)\frac{\partial T}{\partial y}\right] + q_i\left[\frac{T_i - T}{A}\right]$$

$$- \frac{P\phi_m}{\rho c_p A} - \frac{-1}{\rho c_p A}(1-\beta)\phi_o e^{-\eta(y_s - y)}\left(-\eta A + \frac{\partial A}{\partial y}\right) \qquad (2\text{-}35)$$

This equation is basically the same equation derived by Huber and Harleman (18). In order to formulate a solution two boundary conditions are needed in y, and an initial condition in t.

The initial condition is provided by the isothermal state of a reservoir in the spring. Thus at t = 0 (spring):

$$T = T_o \text{ at } t = 0 \text{ for all } y \qquad (2\text{-}36)$$

At the reservoir surface, the heat absorbed due to the incoming radiation ϕ_o and atmospheric radiation ϕ_a minus surface losses, ϕ_L, must equal the amount of heat diffused into the reservoir from the water surface.

Thus at the surface $y = y_s$

$$\rho c_p\,(D_M + E)\left.\frac{\partial T}{\partial y}\right|_{y = y_s} = \beta\phi_o + \phi_a - \phi_L \qquad (2\text{-}37)$$

The details of the derivation of the expression for ϕ_a and ϕ_L are given in (18) and only the results will be presented here.

For laboratory conditions:

$$\phi_a = \varepsilon\sigma T_a^{\,4} \qquad (2\text{-}38)$$

where ε = emissivity of the radiating surface (ε= 0.97 in the laboratory)

σ = Stephan, Boltzman constant = 8.132×10^{-11} cal/cm^2 min°K^4

T_a = absolute air temperature

$$\phi_L = \phi_E + \phi_c + \phi_r \qquad (2\text{-}39)$$

where ϕ_E = evaporative heat flux

ϕ_c = conductive heat flux

ϕ_r = heat flux due to long wave radiation from the water surface to the atmosphere.

$$\phi_E + \phi_c = a_\rho \, (\varepsilon_s - \psi\varepsilon_a)\left[L + c_p T_s + 269.1 \, \frac{(T_s - T_a)}{(\varepsilon_s - \psi\varepsilon_a)} \right] \qquad (2\text{-}40)$$

ϕ_E, ϕ_c in cal/cm^2 - min

a = 5×10^{-5} cm/min - mm Hg

ε_s = saturated water vapor pressure at the water surface temperature in mm Hg

ε_a = saturated water vapor pressure at the air temperature in mm Hg

ψ = relative humidity in the laboratory

L = heat of vaporization of water = 595.9 - 0.54 T_s in cal/gm

T_s = water surface temperature in °C

T_a = air temperature in °C

and

$$\phi_r = \varepsilon \sigma T_s^4 \tag{2-41}$$

For field conditions (56)

$$\phi_a - \phi_r = 0.97 \times 0.937 \times 10^{-5} \ \sigma T_{a2}^6 \ (1.0 + 0.17C^2)$$

$$- 0.97 \ \sigma T_s^4 \tag{2-42}$$

where C is the cloudiness, as a fraction of the sky covered.

T_{a2} = absolute air temperature measured 2 meters above the water surface.

Many evaporation formula exist; the majority have the form of Equation 2-40, with different constants and an additional term to account for the increase in the rate of evaporation with wind speed. The two used in this study are after Rohwer (39).

$$\phi_E + \phi_c = (0.000308 + 0.000185w) \ \rho(\varepsilon_s - \psi\varepsilon_a)$$

$$\left[L + c_p T_s + 269.1 \ \frac{(T_s - T_a)}{\varepsilon_s - \psi\varepsilon_a} \right] \tag{2-43}$$

where ϕ_E, ϕ_c is in kcal/m^2 - day

w = wind speed in m/sec (measured six inches above the surface) and all the other terms are as defined in Equation 2-41 with centimeters replaced by meters, calories replaced by kilocalories etc. and Kohler's formula (84)

$$\phi_E + \phi_o = 0.000135 \; w\rho \; (\varepsilon_s - \psi\varepsilon_a) \left[L + c_p T_s + 372 \frac{T_s - T_a}{\varepsilon_s - \psi\varepsilon_a} \right] \quad (2\text{-}44)$$

where w is in m/sec (not less than 0.05 m/sec) and measured two meters above the water surface

ε_s, ε_a in millibars

T_a is measured two meters above the water surface.

The second boundary condition will be at the reservoir bottom $y = y_b$ where the temperature changes very little during the year. There are several ways of stating this mathematically:

$$T = T_o \text{ at } y = y_b \text{ for all } t \quad (2\text{-}45a)$$

$$\frac{\partial T}{\partial y} = 0 \text{ at } y = y_b \text{ for all } t \quad (2\text{-}45b)$$

$$\frac{\partial^2 T}{\partial y^2} = 0 \text{ at } y = y_b \text{ for all } t \quad (2\text{-}45c)$$

The condition to be applied depends on the scheme used to solve Equation 2-35. In this study Equation 2-45b was used.

In order to solve Equation 2-35, the velocity field must be determined. This is done by first assuming a form for the inflow and outflow velocity distributions. The vertical velocities are calculated using Equation 2-28 as described in the next section.

2.4.2 Reservoir Schematization and the Velocity Field

For any reservoir, the variation of horizontal cross-sectional area, with depth A(y), is assumed to be known. Since we are dealing

with a one-dimensional model in y for the temperature field, it will be assumed that at any reservoir elevation (as illustrated in Figure 2.7) the width B(y) is constant and equal to

$$B(y) = \frac{A(y)}{L(y)} \tag{2-46}$$

where $L(y)$ is the length of the reservoir at elevation y.

With B(y) thus defined, the inflow and outflow rates per unit depth as a function of y can be described as

$$q_i(y,t) = U_i(y,t)\ B(y) \tag{2-47a}$$

$$q_o(y,t) = U_o(y,t)\ B(y) \tag{2-47b}$$

where $U_i(y,t)$ = the inflow velocity at elevation y

$U_o(y,t)$ = the outflow velocity at elevation y.

The withdrawal velocity distribution is assumed to be governed by an equation derived by Koh (23) for viscous, diffusive, steady flow toward a line sink located at x = 0 (Figure 2.8).

The assumptions underlying his solution are:

1. Steady, two-dimensional flow in the infinite half plane. $x \geq 0$.
2. Small stratification, $\Delta\rho/\rho \ll 1$ in the flow field.
3. The fluid viscosity is μ and the molecular diffusion coefficient for heat or dissolved mass is D.
4. The density is a linear function of temperature or salt concentration.

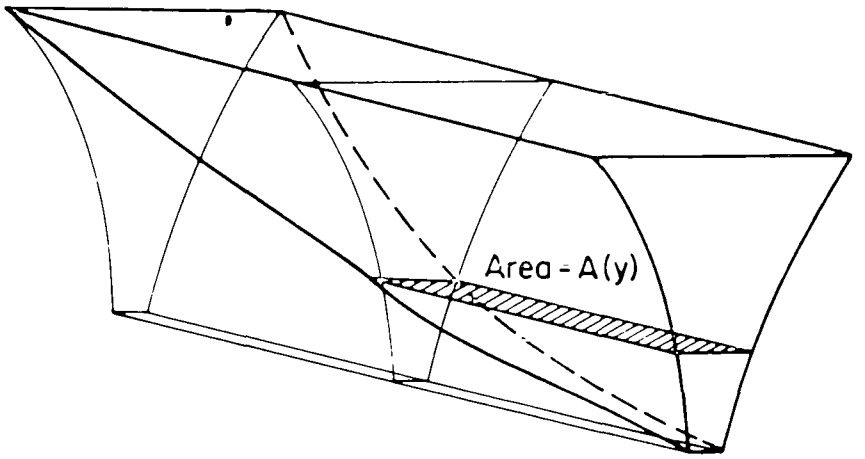

(a) Three Dimensional View

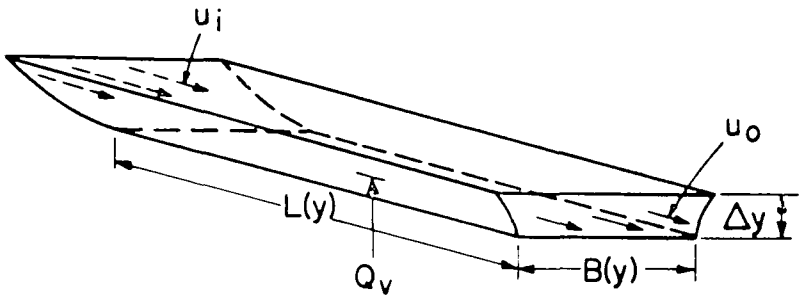

(b) Control Volume Slice

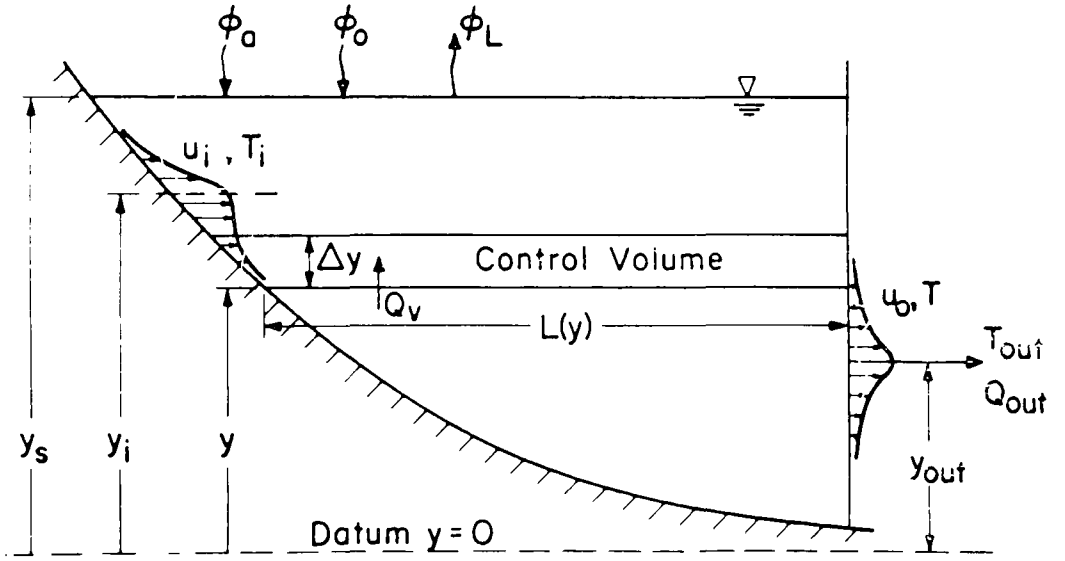

(c) Side Elevation

FIGURE 2.7 CONTROL VOLUME AND SCHEMATIZATION FOR MATHEMATICAL MODEL OF AN IDEALIZED RESERVOIR

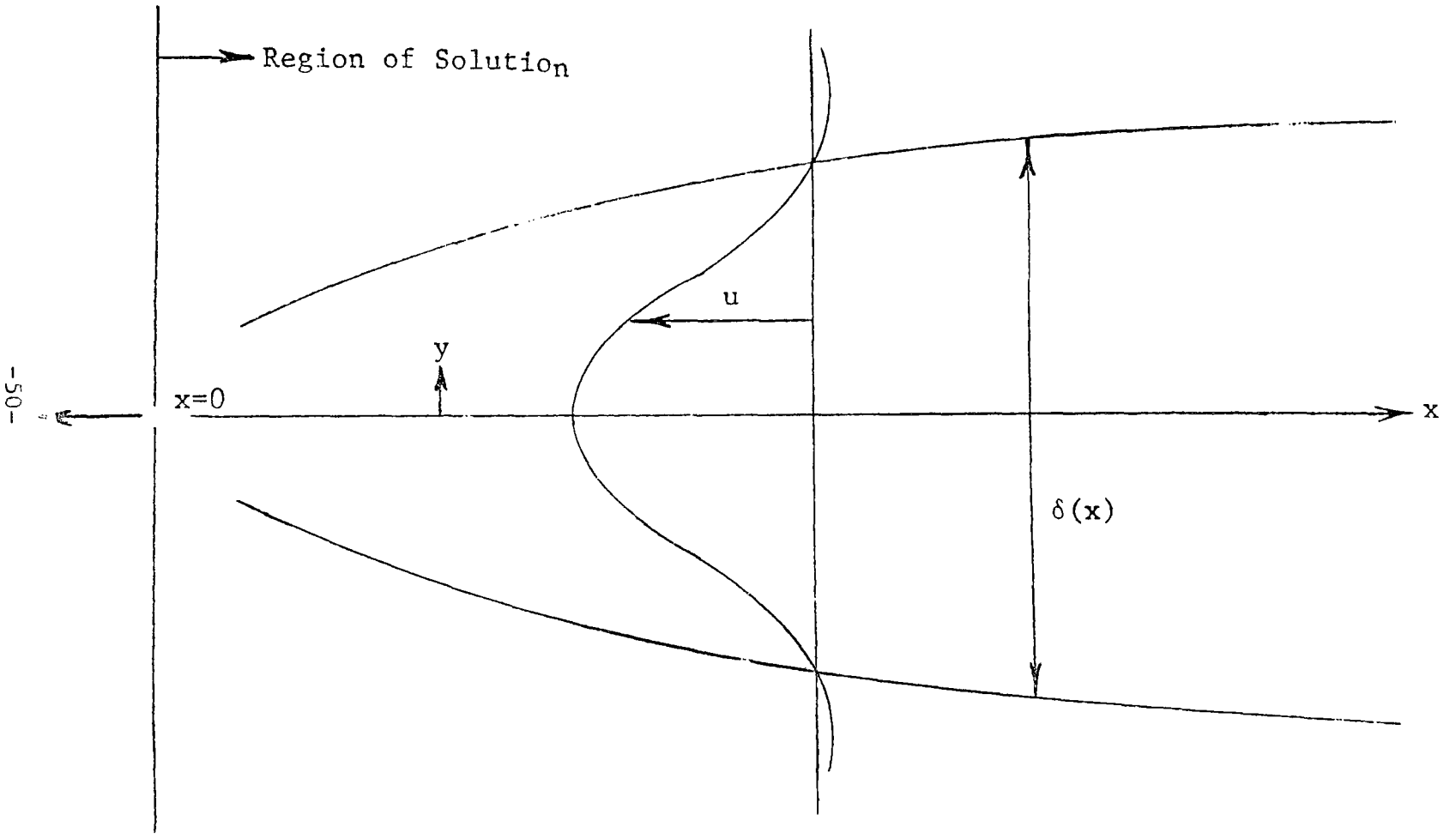

FIGURE 2.8 LAMINAR FLOW TOWARDS A LINE SINK (23)

5. The flowing depth is small compared to x, so that the usual boundary layer assumptions are made.

6. Stratification is linear far from the sink (i.e., $d\rho/dy$ = constant).

7. Non-linear terms are dropped and the solution is thus limited to laminar flow.

The velocity field which results can be approximated by a Gaussian curve

$$U_o = U_{o\ max}\, e^{-\frac{(y-y_{out})^2}{2\sigma_o^2}} \tag{2-48}$$

where $U_{o\ max}$ = the velocity at $y = y_{out}$ = the outlet centerline

σ_o = the standard deviation of the outflow velocity distribution.

The thickness of the withdrawal layer, δ, is given by Koh as

$$\delta = \frac{7.14\ x^{1/3}}{(\varepsilon g/D_T \nu)^{1/6}} \tag{2-49}$$

where x = horizontal distance from the outlet

g = gravitational acceleration

D_T = diffusion coefficient of temperature

ν = kinematic viscosity

ε = density gradient = $\frac{1}{\rho}\ \frac{d\rho}{dy}$

Once the thickness of the withdrawal layer is known, the standard deviation can be chosen in such a way that a certain percentage of the flow will be contained within the withdrawal layer. For example, if 95% of the flow is to be contained within $y_{out} - \delta/2 \leq y \leq y_{out} + \delta/2$,

the outflow standard deviation will be

$$\sigma_o = \frac{\delta/2}{1.96} \tag{2-50}$$

This is illustrated graphically in Figure 2.9.

It must be emphasized here that Equation 2-48 is only an approximation of what the withdrawal velocity field might look like in a stratified reservoir. Density profiles in reservoirs are not linear and velocity profiles are not necessarily symmetrical about the outlet. As yet no satisfactory theory exists for selective withdrawal under the influence of non-linear density gradients. It is assumed that the gradient of the density profile at the outlet is determined and Koh's theory is applied as if this gradient were constant throughout the depth of the reservoir. If the withdrawal layer is thin, this assumption will be a good one. However, if the density gradient at the outlet is small, this would dictate a very large withdrawal layer which could lead to serious errors. This will be discussed more fully with the experimental results (Chapter 4).

No work similar to Koh's has been done on the inflow velocity distributions. Here, different assumptions will be made depending on whether the water is entering at the surface or sinking to its own density level. As was discussed in Section 2.2, vertical motion in a stratified fluid is suppressed. Thus, it might be reasonable to assume that if the water which is entering from a turbulent stream of depth d_s is warmer than the reservoir surface water, it would tend to enter the

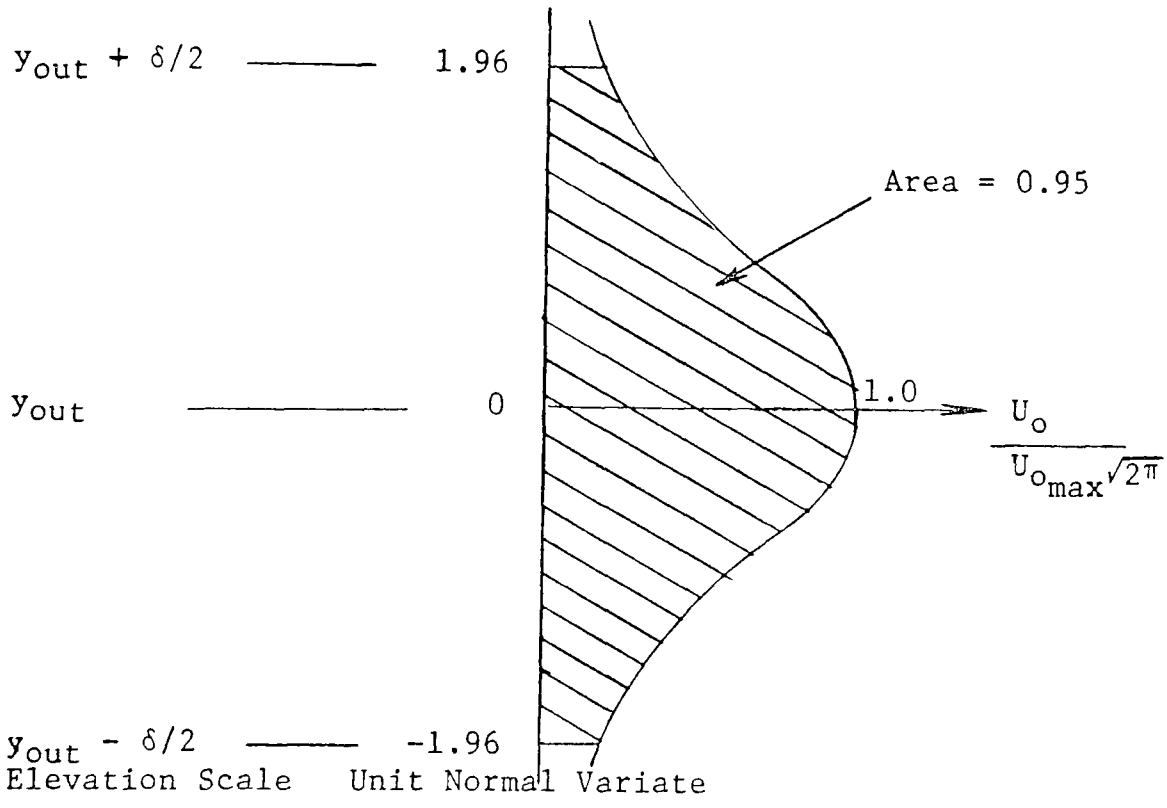

FIGURE 2.9 DETERMINATION OF THE OUTFLOW STANDARD DEVIATION

reservoir at the surface in a layer thickness of order d_s. However, if the entering water was cooler than the surface water it will sink to its own density level. In the process of sinking there will be a certain amount of entrainment and the mixture will begin to move horizontally at a higher elevation. In addition, the momentum of the incoming density current might carry some of this incoming water past the density level it was seeking and end up being entrained in still higher density water. With reference to Figure 2.10 the assumptions will be made that if the water is sinking, it will be distributed vertically in a Gaussian manner (after Huber and Harleman (18)) described as

$$U_i = U_{i\,max}\, e^{-\frac{(y-y_{in})^2}{2\sigma_i^2}} \qquad (2\text{-}51)$$

where $U_{i\,max}$ = the maximum inflow velocity

y_{in} = the depth at which the reservoir density is the same as that of the incoming water

σ_i = the inflow standard deviation. This will either have to be measured, or assumed.

If the water is entering at the surface, it is assumed that it will enter uniformly over a thickness equal to the depth of the entering stream. (Huber and Harleman treated surface and subsurface inflow as governed by Equation 2-51.)

The determination of the maximum velocities $U_{o\,max}$ and $U_{i\,max}$ is accomplished by equating the total discharge to the integral of the discharge per unit area, over the depth of the reservoir:

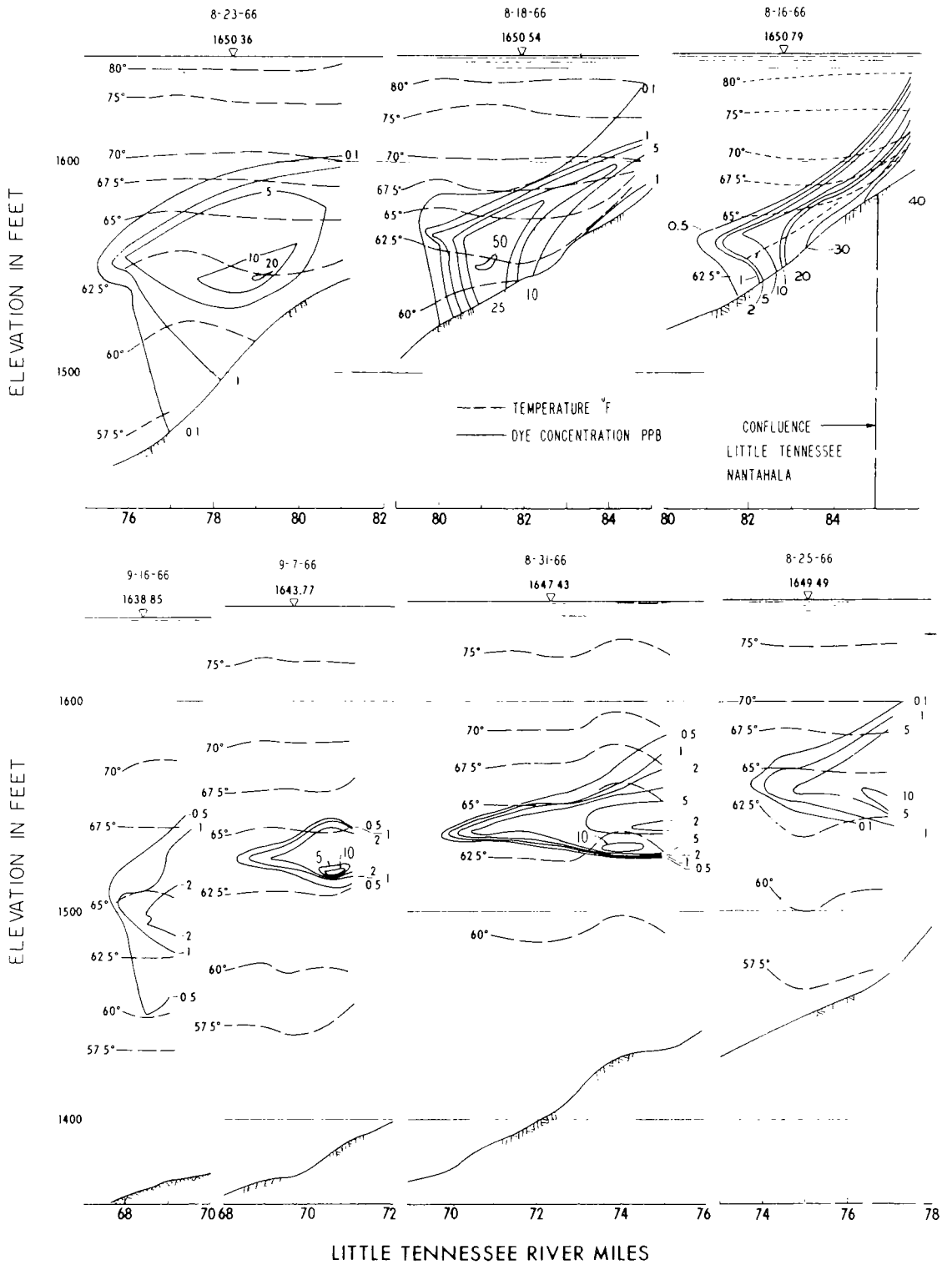

FIGURE 2.10 DYE CONCENTRATION PROFILES IN FONTANA RESERVOIR

$$Q_o(t) = U_{o\,max} \int_{y_b}^{y_s} B(y)\, e^{-\frac{(y-y_{out})^2}{2\sigma_i^2}}\, dy \qquad (2\text{-}52)$$

If the inflow water is sinking

$$Q_i(t) = U_{i\,max} \int_{y_b}^{y_s} B(y)\, e^{-\frac{(y-y_{in})^2}{2\sigma_i^2}}\, dy \qquad (2\text{-}53a)$$

and if the inflow water enters at the reservoir surface

$$Q_i(t) = U_{i\,max} \int_{y_s-d_s}^{y_s} B(y)\, dy \qquad (2\text{-}53b)$$

Once the horizontal velocity fields are known the vertical velocity v, and the vertical flow rate, Q_v, can be determined from

$$Q_v(y,t) = \int_{y_b}^{y} B(y)\ U_i\ (y,t)\ dy\ - \int_{y_b}^{y} B(y)\ U_o\ (y,t)\ dy$$

$$= v(y,t)\ A(y) \qquad (2\text{-}54)$$

2.4.3 Mixing at the Reservoir Entrance

As an inflowing stream enters a reservoir there will be a certain amount of mixing and entrainment of the stream and reservoir waters. The rate of entrainment, Q_m, is specified in terms of a fraction, r_m, of the incoming water Q_i and is expressed as

$$Q_m = r_m Q_i \qquad (2\text{-}55)$$

Using this definition the effective inflow rate, Q_i', is

$$Q_i' = Q_m + Q_i = (1 + r_m)\, Q_i \tag{2-56}$$

and the mixed inflow temperature is

$$T_{in}' = \frac{Q_m T_m + Q_i T_{in}}{Q_m + Q_i} = \frac{r_m T_m + T_{in}}{1 + r_m} \tag{2-57}$$

where T_m is the average temperature over the depth from which Q_m is withdrawn.

In order to account for Q_m in the velocity field there must be a backflow in the layers from which Q_m is being drawn. The velocity induced by this backflow, U_m is

$$U_m = \frac{Q_m}{B_{av}\, d_m} \tag{2-58}$$

where B_{av} is the average width of the backflow layer of thickness d_m. This is represented graphically in Figure 2.11.

Huber and Harleman assumed that no matter where the water entered the reservoir, the entrainment would always be coming from a surface layer of arbitrary thickness d_m. It was felt that this assumption needed testing. A complete discussion of the effect of changing the assumption of where the entrained water is coming from is given with the experimental results.

The value of r_m may be arrived at experimentally in the laboratory but for the field only limited data exists. Results to date

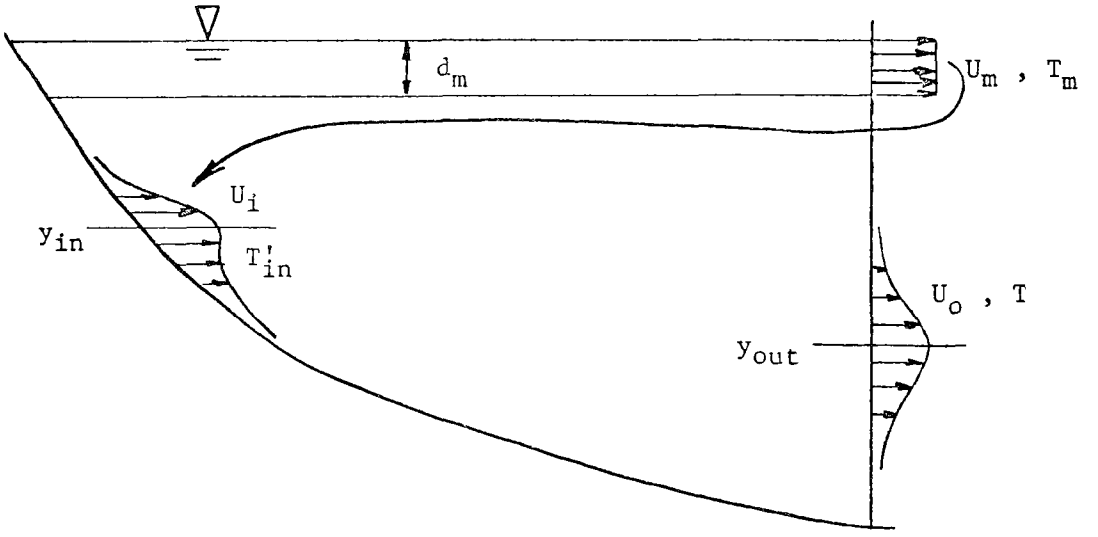

FIGURE 2.11 SCHEMATIC REPRESENTATION OF ENTRANCE MIXING

indicate that, for the field, a value of $r_m = 1$ is satisfactory.

2.4.4 Lag Time Determination

The equation developed in the preceeding sections are sufficient for determining the temperature distribution in reservoirs if the assumption is made that the entering water immediately reaches its own density level and spreads instantaneously along the entire length of the reservoir at that particular depth. However, it is not realistic to assume that this process takes place instantaneously. If the water is sinking into the reservoir, it will take a finite amount of time for it to reach its own density level. Once it has reached this depth, it may still be many miles from the dam. Huber and Harleman did not incorporate a lag time (for the entering water to reach the dam face) in their model. However, they concluded that its inclusion could significantly improve predicted outflow temperatures during the late autumn.

A method for accounting for lag time in the temperature model is developed in the next two sections.

2.4.4.1 The Time for the Incoming Water to Reach Its Own Density Level

As an approximation to the actual phenomena, the first part of the lag time will be treated as a two-layer flow problem governed by the average density difference between the mixed inflow water at temperature T_{in}' and the surface water at temperature T_s. With reference to Figure 2.12 the surface water is of density ρ_s and the sinking water of density $\rho_s + \Delta\rho$. Assuming that the flow is parallel to the reservoir bottom (the s direction), steady and of constant thickness d

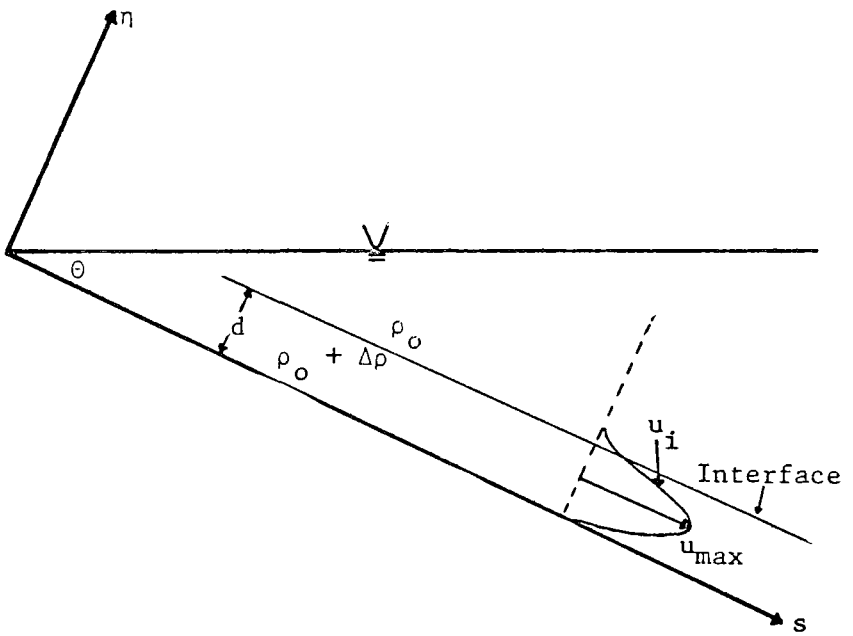

FIGURE 2.12 TWO LAYERED FLOW SCHEMATIZATION FOR SINKING FLOW

(i.e. no entrainment after the initial entrainment at the reservoir entrance), the equations governing the motion in the lower and upper layers are

$$0 = -\frac{\partial p}{\partial s} + \rho g_s + \mu \frac{d^2 u}{dn^2} \qquad \text{(s component)} \tag{2-59a}$$

$$0 = -\frac{\partial p}{\partial n} + \rho\, g_n \qquad \text{(n component)} \tag{2-59b}$$

where n is normal to the reservoir bottom.

Since

$$g_s = g \sin \theta \tag{2-60a}$$

$$g_n = -\, g \cos \theta \tag{2-60b}$$

and in the upper layers $\rho = \rho_s$, Equation 2-59b can be integrated to yield

$$p = -\, \rho_s\, g(\cos \theta) n + c(s) \tag{2-61}$$

At the free surface, $n = s \tan \theta$, $p = 0$, therefore

$$p = -\, (\rho_s\, g(\cos \theta) n + \rho_s\, g\, s \tan \theta) \tag{2-62}$$

Differentiating Equation 2-62 with respect to s and making the substitution

$$S = \sin \theta \tag{2-63}$$

Equation 2-59a reduces to:

$$0 = - \rho_o g S + (\rho_s + \Delta\rho)\, g S + \mu \frac{d^2 u}{dn^2} \tag{2-64}$$

or

$$\mu \frac{d^2 u}{dn^2} = - \Delta\rho g S \tag{2-65}$$

Equation 2-65 is the s equation of motion for the bottom layer. Integrating Equation 2-65 twice yields:

$$u = - \frac{\Delta\rho g S}{2\mu} n^2 + c_1 n + c_2 \tag{2-66}$$

The boundary conditions for the bottom layer are

$$u = 0 \text{ at } n = 0 \tag{2-67a}$$

$$u = u_i = \text{interfacial velocity at } n = d \tag{2-67b}$$

Substituting into Equation 2-66 results in:

$$u = \frac{\Delta\rho g S}{2\mu} (nd - n^2) + u_i \frac{n}{d} \tag{2-68}$$

Equation 2-68 may be expressed in terms of the maximum velocity in the lower layer u_{max}, by observing that

$$\frac{du}{dn} = 0 \rightarrow u = u_{max},\ n = n \text{ max} \tag{2-69}$$

Thus

$$\frac{u_{max}}{u_i} = \frac{\Delta\rho g S}{2\mu} \frac{d^2}{u_i} \left[\frac{n_{max}}{d} - \frac{n_{max}^2}{d^2} \right] + \frac{n_{max}}{d} \qquad (2\text{-}70)$$

Keulegan (22) has shown that

$$\frac{u_i}{u_{max}} = 0.59 \qquad (2\text{-}71)$$

Making this substitution

$$\frac{\Delta\rho g S d^2}{2\mu} = G \qquad (2\text{-}72)$$

and introducing Equation 2-71 into 2-70

$$\frac{1}{0.59} = \frac{G}{u_i} \left[\frac{n_{max}}{d} - \frac{n_{max}^2}{d^2} \right] + \frac{n_{max}}{d} \qquad (2\text{-}73)$$

From Equation 2-68, 2-69 and 2-72 it can be determined that

$$n_{max} = \frac{d}{2} \left[1 + \frac{u_i}{G} \right] \qquad (2\text{-}74)$$

Using this and the substitution

$$\frac{u_i}{G} = \psi \qquad (2\text{-}75)$$

in Equation 2-73 yields:

$$\frac{1}{\psi} \left[\frac{1}{2} (1 + \psi) - \frac{1}{4} (1 + \psi)^2 \right] + \frac{1}{2} (1 + \psi) = \frac{1}{0.59} \qquad (2\text{-}76)$$

Rearranging

$$\frac{(1+\psi)^2}{\psi} = \frac{4}{0.59} \tag{2-77}$$

Equation 2-77 has the solutions

$$\psi_1 = 4.44 = u_i/G \tag{2-78a}$$

$$\psi_2 = 0.23 = u_i/G \tag{2-78b}$$

The average velocity of the lower layer, $\bar{u}$, can be expressed as

$$\bar{u} = \frac{1}{d}\int_0^d u\, dn \tag{2-79}$$

Substituting Equation 2-68 into 2-79 and integrating yields:

$$\bar{u} = \frac{G}{6} + \frac{u_i}{2} \tag{2-80}$$

Referring to Equation 2-74 for u_{max} to be contained within the lower layer

$$\frac{u_i}{G} \leq 1 \tag{2-81}$$

Therefore, for $\psi_2 = \frac{u_i}{G} = 0.23$

$$\bar{u} = 0.281\ G \tag{2-82}$$

$$\bar{u} = 0.1405\ \frac{\Delta\rho g S d^2}{\mu} \tag{2-83}$$

Further, substituting an average Reynolds number, R

$$R = \bar{u} \frac{d(\rho_o + \Delta\rho)}{\mu} \tag{2-84}$$

into Equation 2-83 yields:

$$\bar{u} = 0.1405 \ (\Delta\rho g S d^2) \ \frac{12}{\bar{u} \ d \ (\rho_o + \Delta\rho)} \tag{2-85}$$

With the assumption that:

$$\frac{\Delta\rho}{\rho} << 1 \tag{2-86}$$

and introducing the modified gravity g'

$$g' = \frac{\Delta\rho}{\rho} g \tag{2-87}$$

Equation 2-85 reduces to:

$$\bar{u} = 0.375 \ (g' S d)^{1/2} \ R^{1/2} \tag{2-88}$$

Defining q as the discharge per unit width

$$q = \bar{u} \ d \tag{2-89}$$

and, introducing Equation 2-89 into 2-88 and rearranging

$$d = 1.92 \left[\frac{q \ \nu}{g' S}\right]^{1/3} \tag{2-90}$$

Thus, knowing q, the depth of the density current and the average velocity of the sinking water can be determined from Equations 2-89 and 2-90. With this velocity known and the distance to be traveled, the lag time for the sinking water to reach its own density level, t_{Ly}, can be approximated.

$$t_{Ly} = \frac{(y_s - y_i)d}{S\, q_i} \tag{2-91}$$

2.4.4.2 Horizontal Travel Time

Once the water has reached its own density level it will take a finite amount of time to travel the distance to the dam face. This time will depend on q_i and the thickness of the flowing layer, Δh. It is assumed here that there is no entrainment as the water flows horizontally and that the thickness of this layer remains constant as the water traverses the reservoir. Thus the horizontal travel time can be calculated as

$$t_{LH} = \frac{L' \Delta h}{q} \tag{2-92}$$

where

L' = average horizontal length the water has to travel.

The value of Δh can either be determined by dye tests or assigned some typical value as the depth of the entering stream or determined indirectly from temperature measurements. The third method will be discussed more fully in Chapter 5.

2.4.5 Surface Instabilities and Surface Mixing

In the late summer, the cooling of the reservoir surface begins a process through which the lake eventually becomes isothermal. Due to increased evaporative cooling, the surface water becomes denser than the warmer water below it. This is an unstable situation and the surface water begins to sink. As it sinks, it mixes with the water beneath it,

lowering the temperature of that water. By this process an isothermal layer extending down from the surface is generated. The mixing process will continue until a stable situation has been reached. The thickness of the mixed, isothermal layer increases as fall turns to winter until, at the start of spring, the stratification process begins anew.

The mixed layer thickness and isothermal temperature can be calculated through an iterative procedure since one is dependent on the other. If the surface water is cooler than the water beneath it a depth of mixing, y_{mix}, must be assumed and a mixed temperature, T_{mix}, calculated from

$$T_{mix} = \frac{\int_{y_{mix}}^{y_s} T(y)\, A(y)\, dy}{\int_{y_{mix}}^{y_s} A(y)\, dy} \qquad (2\text{-}93)$$

If T_{mix} is less than the temperature immediately beneath it y_{mix} has been assumed too small and a larger value must be tried. If T_{mix} is greater than the temperature immediately below y_{mix}, a stable condition has been reached and the water will stop sinking. However, this is not a guarantee that y_{mix} is the minimum depth for which a stable situation exists. Therefore, $y_s - y_{mix}$ should be continuously decreased until the thickness of the isothermal layer has been determined within the desired accuracy. In this manner the important process by which turbulent mixing gradually produces an isothermal reservoir can be accounted for without specifying the actual form of the turbulent diffusivity. The advantage of this method over some empirical method involving a vertical eddy diffusivity should be apparent.

2.5 The Method of Solution of the Temperature Model

There is no analytical way of solving Equation 2-35 subject to the prescribed initial and boundary conditions. Huber and Harleman discuss various techniques of numerical solutions and conclude that an implicit, finite difference approach based on the Stone and Brian method is appropriate.

Any finite difference scheme, whether explicit or implicit, is a way of taking a continuous equation and representing the continuous functions by numerical approximations. It should be noted that the continuous equation was originally derived from a finite control volume representation of the phenomena. Therefore, it is concluded that a finite element schematization is a logical way to approach the problem.

2.5.1 The Finite Element Approach

With reference to Figure 2-5 it is seen that all of the terms in Equation 2-35 come from considering the changes in advection, convection, and diffusion between the sides of a control volume and heat source inside the element. The finite element form of the equations for calculating the temperature field derives from Equation 2-32, the control volume equation, and not Equation 2-35, the continuous equation. For ease of understanding, Equation 2-32 is presented below with the terms numbered to facilitate discussion.

$$\overbrace{\rho c_p \bar{A} \Delta y \frac{\partial T}{\partial t}}^{[1]} = \overbrace{\rho c_p Q_v T - \left[\rho c_p Q_v T + \left[\frac{\partial}{\partial y} (\rho c_p Q_v T) \right] \Delta y \right]}^{[2]}$$

$$\overbrace{- \rho c_p A (D_M + E) \frac{\partial T}{\partial y} - \left[- \rho c_p A (D_M + E) \frac{\partial T}{\partial y} - \frac{\partial}{\partial y}\left[\rho c_p A (D_M + E) \frac{\partial T}{\partial y} \right] \Delta y \right]}^{[3]}$$

$$\overbrace{+ \rho c_p q_i T_i \Delta y}^{[4]} \quad \overbrace{- \rho c_p q_o T_o \Delta y}^{[5]} \quad \overbrace{- p \Delta y \phi_m + A\phi_b - \left[A\phi_b + \frac{\partial (\phi_b A)}{\partial y} \Delta y \right]}^{[6]} \qquad (2\text{-}32)$$

Term 2 represents the net amount of heat convected into the control volume of Figure 2-5. An equivalent representation is

$$(\rho c_p Q_v T)\Big|_1 - (\rho c_p Q_v T)\Big|_2 \qquad (2\text{-}94)$$

where the point of evaluation of these terms is represented schematically in Figure 2-13.

Since longitudinal uniformity has been assumed:

$$Q_v\Big|_1 = vA\Big|_1 \qquad (2\text{-}95a)$$

$$Q_v\Big|_2 = vA\Big|_2 \qquad (2\text{-}95b)$$

where $v = v(y,t)$ = vertical velocity

$A = A(y)$ = the longitudinal cross section area.

From Figure 2-13, since there will be elements both above and below element I, the temperature to be assigned to the convective transport will depend on the direction of the vertical velocity. Thus, if v_1 is positive, T_1 will be the temperature of element III. If v_1 is negative,

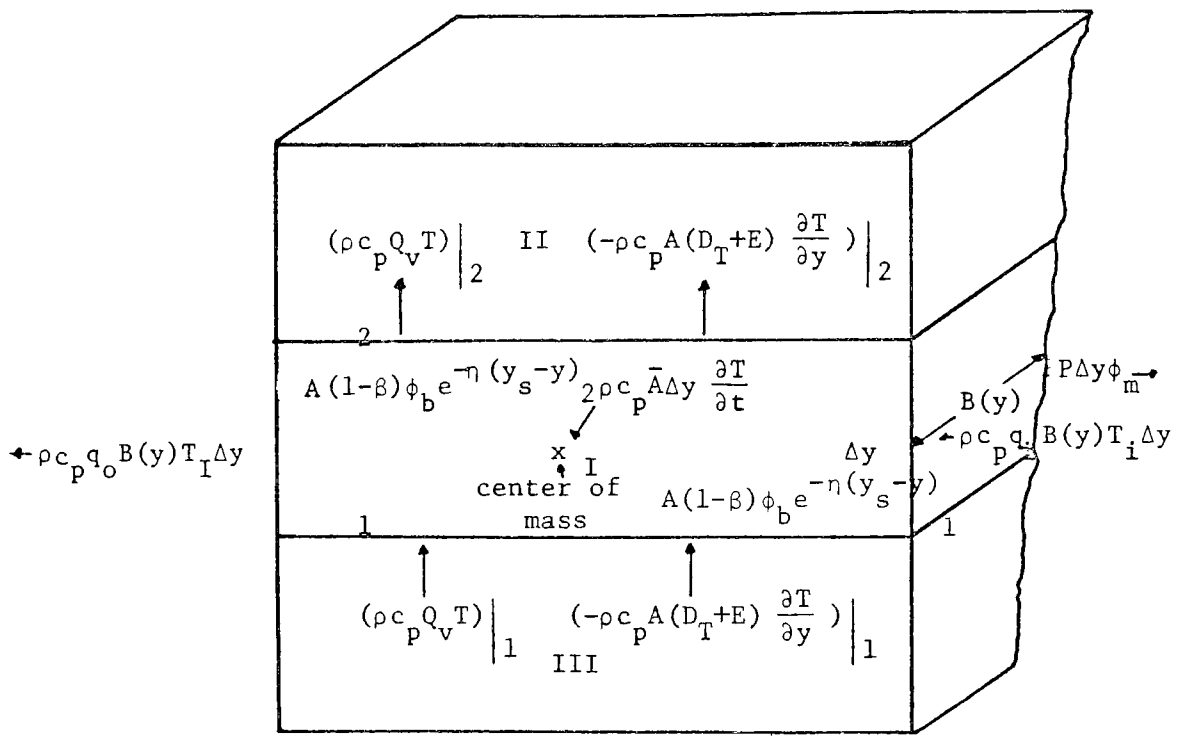

FIGURE 2.13 POINTS OF EVALUATION OF EQUATION 2-32

T_1 will be the temperature of element I. Similarly, a positive v_2 is matched with T of element I and a negative v_2 with T of element II.

An analogous representation applies to expression 3 of Equation 2-32.

Since expressions [4] and [5] are independent of y and are in fact already in a finite element representation they remain unchanged.

Expression [1] and [6] pertain to changes occurring within the element and should therefore be evaluated at the center of mass of the element.

With these modifications Equation 2-32 can be represented as:

$$\rho c_p \bar{A}\, \Delta y \left.\frac{\partial T}{\partial t}\right|_I = \left. \rho c_p vAT \right|_1 - \left. \rho c_p vAT \right|_2$$

$$- \left. \rho c_p A\, (\nu_M + E) \frac{\partial T}{\partial y} \right|_1 + \left. \rho c_p A\, (D_M + E) \frac{\partial T}{\partial y} \right|_2$$

$$+ \left. \rho c_p (q_i T_i - q_o T)\, \Delta y - p \Delta y \phi_m + (1-\beta)\phi_o e^{-\eta(y_s-y)} A \right|_1$$

$$- \left. (1-\beta)\phi_o e^{-\eta(y_s-y)} A \right|_2 \qquad (2\text{-}96)$$

It should be explained here that Huber and Harleman's choice of an implicit scheme was partly based on the consideration that the Stone and Brian procedure is unconditionally stable. However, physical instabilities were noted in their results. In order to locate the cause of the physical instabilities the solution technique was changed to an explicit scheme which has the advantage of being a much easier representation in which to follow the physical processes which are occurring. It was found

Huber and Harleman had neglected the important point of assigning the temperature to the convective flux term based on the direction of the vertical velocity. With this corrected, no advantage was seen in returning to an implicit scheme and an explicit solution was used.

Equation 2-96 involves only first order derivatives whose finite difference representation is

$$\frac{\partial T}{\partial t} = \frac{T(t + \Delta t) - T(t)}{\Delta t} \tag{2-97a}$$

$$\frac{\partial T}{\partial y} = \frac{T(y + \Delta y) - T(y)}{\Delta y} \tag{2-97b}$$

What remains to be determined is how the lag time will be incorporated into the model. Since the model is uniform with x, water which has entered at a certain time is assumed to have spread out over the entire length of the reservoir. From the lag time Equations 2-91, 2-92, the total time, t_L, necessary for the water to traverse the reservoir is

$$t_L = t_{Ly} + t_{LH} \tag{2-98}$$

Thus, if a flow entered the reservoir at time t, the time at which it will have traversed the reservoir to the dam face is $t + t_L$. For each physical input to the reservoir at time t (the amount of flow which would enter in one day for example), t_L is calculated. This flow is then input to the mathematical model a time t_L past the time that it physically entered the reservoir. By "lagging" the inflows in this

manner the assumption that the inflow enters uniformly, longitudinally dispersed is consistent with the time that it is input to the mathematical model.

2.5.2 Stability of the Explicit Scheme-Numerical Dispersion

A difficulty caused by choosing an explicit over an implicit method of solution is the limitation imposed on the choice of Δt and Δy by stability criteria. The first of these criteria is

$$\frac{v\Delta t}{\Delta y} < 1 \qquad (2\text{-}99)$$

This expresses mathematically that the vertical distance traveled by a particle of water in the time interval Δt is not greater than one length step, Δy. For a typical Δt of 1 day, and Δy of 2 meters, the maximum allowable vertical velocity would be 2 m/day. It is conceivable that vertical velocities would be greater than this. There are two possible ways of coping with this problem. (1) Use a larger Δy; (2) use a smaller Δt. Ideally, one would like Δy and Δt to be as small as possible so alternative (2) should be used. At the beginning of the mathematical run values for Δy and Δt are assumed. Since it is possible that the choice of Δy and Δt may lead to violation of Equation 2-99 it is first necessary to calculate the vertical velocities before the next temperature iteration is attempted. If condition 2-99 has not been violated the temperature iteration is allowed to proceed with the values of Δt and Δy originally chosen. If inequality 2-99 has not been met the value of Δt necessary to satisfy this condition, Δt_{max}, is calculated from:

$$\Delta t_{max} = \frac{\Delta y}{v_{max}} \tag{2-100}$$

where

v_{max} = the maximum vertical velocity in time step Δt.

Based on Equation 2-100, the time step Δt is divided into an integer, n, number of time steps, Δt_n so that

$$\Delta t_n < \Delta t_{max} \tag{2-101a}$$

and

$$n\Delta t_n = \Delta t \tag{2-101b}$$

Once $n\Delta t_n$ has been completed the time step reverts back to Δt until condition 2-99 dictates that it be reduced again. If it is necessary to go through this procedure too many times it is an indication that the original choice of Δt or Δy was a poor one.

A second problem inherent in the numerical scheme is that of numerical dispersion, D_p. Consider a volume of fluid at temperature T located at elevation J at time t, in a stratified reservoir as represented schematically in Figure 2-14a. Due to convection this slug of fluid will be physically transferred to a new position at time $t + \Delta t$ as shown by the dotted rectangle in Figure 2.14b. However, because the finite element scheme represents values at specific points, the numerical representation of the new location of the slug would be that of the solid lines in Figure 2.14b. The difference between the dotted and

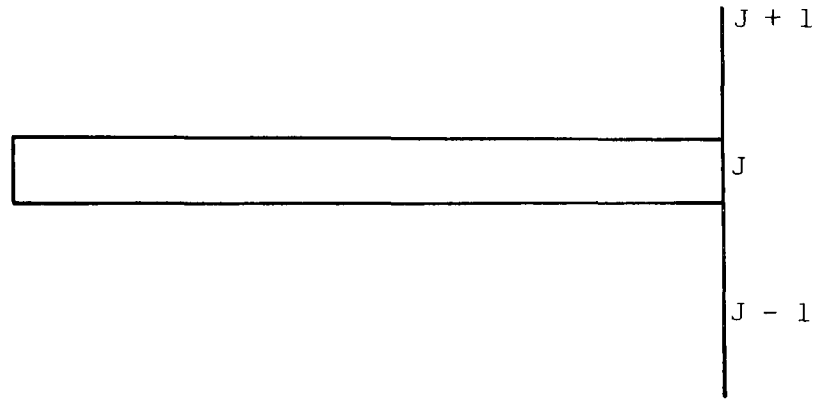

FIGURE 2.14a A VOLUME OF WATER AT TIME t

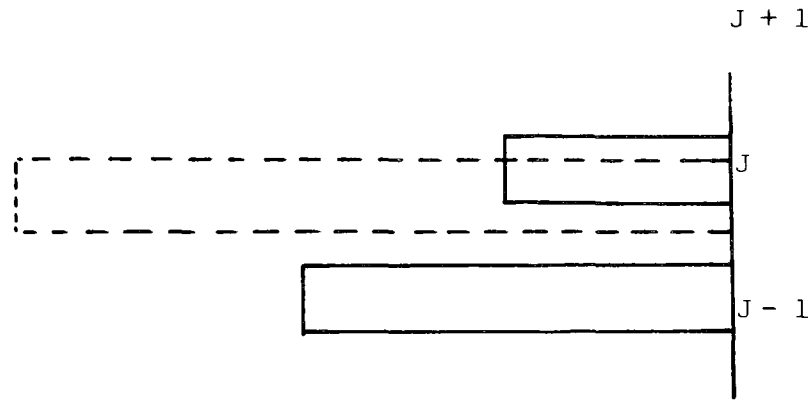

FIGURE 2.14b THE VOLUME AT TIME t + Δt

FIGURE 2.14 NUMERICAL DISPERSION

solid figure in 2.14b is termed numerical dispersion.

Bella (2) has presented an expression for evaluating numerical dispersion for a variable area transport equation:

$$D_p = \frac{v}{2}\left[\Delta y - \frac{vA(n - 1/2,t)\ \Delta t}{A(n,t + \Delta t)}\right] \qquad (2\text{-}102)$$

The effect of D_p is to increase the value of the dispersion coefficient in Equation 2-35 from D_m to $D_m + D_p$. If D_p is the same order of magnitude or larger than the assumed value of D_m, serious problems could result unless the entire dispersion expression is insignificant compared with the other terms in the heat balance equation. This will be discussed more fully in Chapters 4 and 5.

CHAPTER 3. THE WATER QUALITY MODEL

3.1 The Water Quality Model

3.1.1 Introduction

The concentration distribution of a single water quality parameter within a reservoir is governed by the three-dimensional mass transport Equation (2-5). The difficulties of utilizing this equation in a stratified reservoir are exactly the same as the difficulties of the three-dimensional heat transport Equation (2-3). The basic philosophy of the temperature distribution model described in Chapter 2, which is applicable to reservoirs maintaining horizontal isotherms, is the simplification of the governing heat transport equation to the one-dimensional form in which temperature is a function of vertical elevation and time. The objective of this chapter, and the primary objective of this investigation, is to develop a mathematical water quality model based on the one-dimensional mass transport equation to be used in conjunction with the temperature distribution model for horizontally stratified reservoirs.

The temperature distribution model considers a horizontal layer extending over the entire reservoir, of vertical thickness Δy, located at an arbitrary elevation within the reservoir. At any instant of time this layer may receive, at its upstream end, a portion of the water entering the reservoir and it may lose, at its downstream end, a portion of the water being discharged through the reservoir outlet. The proportions, of the total water entering and leaving the reservoir, which are received and lost by a given layer, depend upon the instantaneous temperature-density structure within the reservoir and on the tempera-

ture and initial mixing of the entering water. The continuity equation specifies the vertical convection of water through the layer which is necessary to maintain a volumetric balance. Finally, the one-dimensional heat transport equation, with appropriate heat sources and sinks, determines the instantaneous temperature of the layer.

The above summary is given in order to emphasize that the internal flow pattern in the reservoir is governed by the assumptions of the temperature distribution model. The concentration distribution of any water quality parameter such as conservative dye tracers or non-conservative substances such as biochemical oxygen demand or dissolved oxygen will be governed by the same internal flow pattern. The instantaneous concentration of an arbitrary layer will be determined by the one-dimensional mass transport equation, with source and decay terms appropriate to the water quality parameter.

The one-dimensional water quality model is developed in the following sections. A general method of solution is presented, with specific examples given for a pulse injection of a conservative tracer and the continuous injection of non-conservative substances such as B.O.D. and D.O.

3.2 Literature Review

Though much work has been done on predicting dissolved oxygen concentration in streams, very little work has been done on the development of methods for predicting the effects of a thermally stratified reservoir on water quality. The earliest attempts at D.O. prediction in reservoirs show the natural tendency to apply to an impoundment the

methods developed for stream D.O. prediction.

O'Connell et. al. (33) suggested that the dynamics of dissolved oxygen in the euphotic zone of impoundments, when sedimentation is not important, could be represented by

$$\frac{\partial D}{\partial t} = k_1 \ell_a e^{-k_1 t} - k_2(D) + (R-P) \qquad (3\text{-}1)$$

where

D = D.O. deficit at any time

t = time

k_1 = deoxygenation rate constant

ℓ_a = total organic B.O.D. at t = 0

k_2 = reoxygenation rate constant

R = rate of oxygen demand by algae

P = rate of oxygen prediction by algae

This equation is a statement that the rate of change of oxygen in the euphotic zone is equal to the net rate of demand of oxygen by the surface water. Since this method does not consider any advection of B.O.D. by the inflow to the reservoir or any variation of D.O. in the vertical direction it can at best be thought of as the governing equation of a well mixed lake with no inflow or outflow or the governing equation for a B.O.D. bottle test in the presence of sunlight (photosynthesis).

An alternate method of D.O. prediction is a statistical approach. Churchill and Nicholas (8) suggested that D.O. concentration in the

outflow of a reservoir be expressed as a function of retention time (measured from April 1), the temperature of the outflow, and some factor which considers reservoir operation. The governing mathematical expression, obtained through a multiple regression analysis, is

$$y = a + b_1x_1 + b_2x_2 + b_3x_3 + b_4x_1^2 + b_5x_2^2 + b_6x_3^2 \qquad (3\text{-}2)$$

in which

y = decrease in D.O. concentration in the outflow (mg/ℓ) between April 1 and the date for which D.O. prediction is desired.

$a, b_1, b_2, b_3, b_4, b_5, b_6$ are constants developed from the regression analysis.

$$x_1 = t/10 \qquad (3\text{-}3)$$

where

t = the number of days from April 1

$$x_2 = \sum_{i=1}^{n} (t/10)_i \, \Delta Te_i \qquad (3\text{-}4)$$

where

n = number of 10-day time increments after April 1

ΔTe = increase in temperature of the outflow, in °C, between April 1 and the day at which a D.O. prediction is desired.

$$x_3 = \sum_{i=1}^{n} \frac{t}{10H_i} \qquad (3\text{-}5)$$

where

H = distance, in feet, above the center line of the reservoir outlet at which the April 1 inflow exists on the date of interest, assuming no mixing in the pool and that water is drawn from the pool at the elevation of the outlet only.

The above definition indicates that this equation might be suitable for a reservoir already in existence for which several years data are available and no change of the B.O.D. level of the incoming waters occurs from year to year. However, as a predictive tool this method would be highly questionable unless a reservoir similar to the one proposed exists nearby.

Wunderlich (57) developed a graphical D.O. model which, like that of Churchill and Nicholas, considered the D.O. concentration to be a function of residence time of the water in the reservoir. Since any reservoir water quality prediction model should be related to the changing temperature field in a stratified reservoir, he also developed a graphical temperature prediction model. This is the most recent work on D.O. prediction in reservoirs; a detailed description of the graphical D.O. method of Wunderlich follows.

The following assumptions were made: (1) the inflowing water at the upstream end of the reservoir immediately spread out along the entire horizontal area corresponding to its own temperature level (2) there is no mixing of the inflow at the entrance of the reservoir and (3) the temperature in the outlet corresponds to the temperature at the level of the outlet. These assumptions are suspect in light of the

discussion in Section 2.4.2, 2.4.3 and 2.4.4.

The basic philosophy of Wunderlich's method is that the change of D.O. concentration can be directly related to residence time of the water in the reservoir. The residence time, t_d, is a variable, which for a given day's input is determined from a graphical temperature prediction method as discussed below.

Referring to Figure 3.1a, mean monthly values of inflow and reservoir surface temperatures are plotted at the middle of each month and connected by a continuous curve.

Wunderlich assumes that the reservoir surface temperature can be calculated from meteorological data by assuming that the surface temperature is equal to the equilibrium temperature. The equilibrium temperature is defined as the temperature at which the net rate of heat transfer at the surface is equal to zero.

As shown in Figure 3.1b a cumulative inflow volume curve is drawn with the initial value on January 1 being equal to the volume of the reservoir above the intake, V_{it}. On the same graph the outflow volume band is plotted. The thickness of this band corresponds to the reservoir volume between the invert and the top of the intake on January 1. Since it has been assumed that the withdrawal layer corresponds to the height of the outlet opening, no water below the outlet is ever withdrawn. Thus, the amount of time necessary to discharge V_{it} is shown by the horizontal distance, t_{it}, in Figure 3.1b. During this time the outflow temperature corresponds to the initial isothermal temperature in the reservoir on January 1. The outflow temperature after this time is

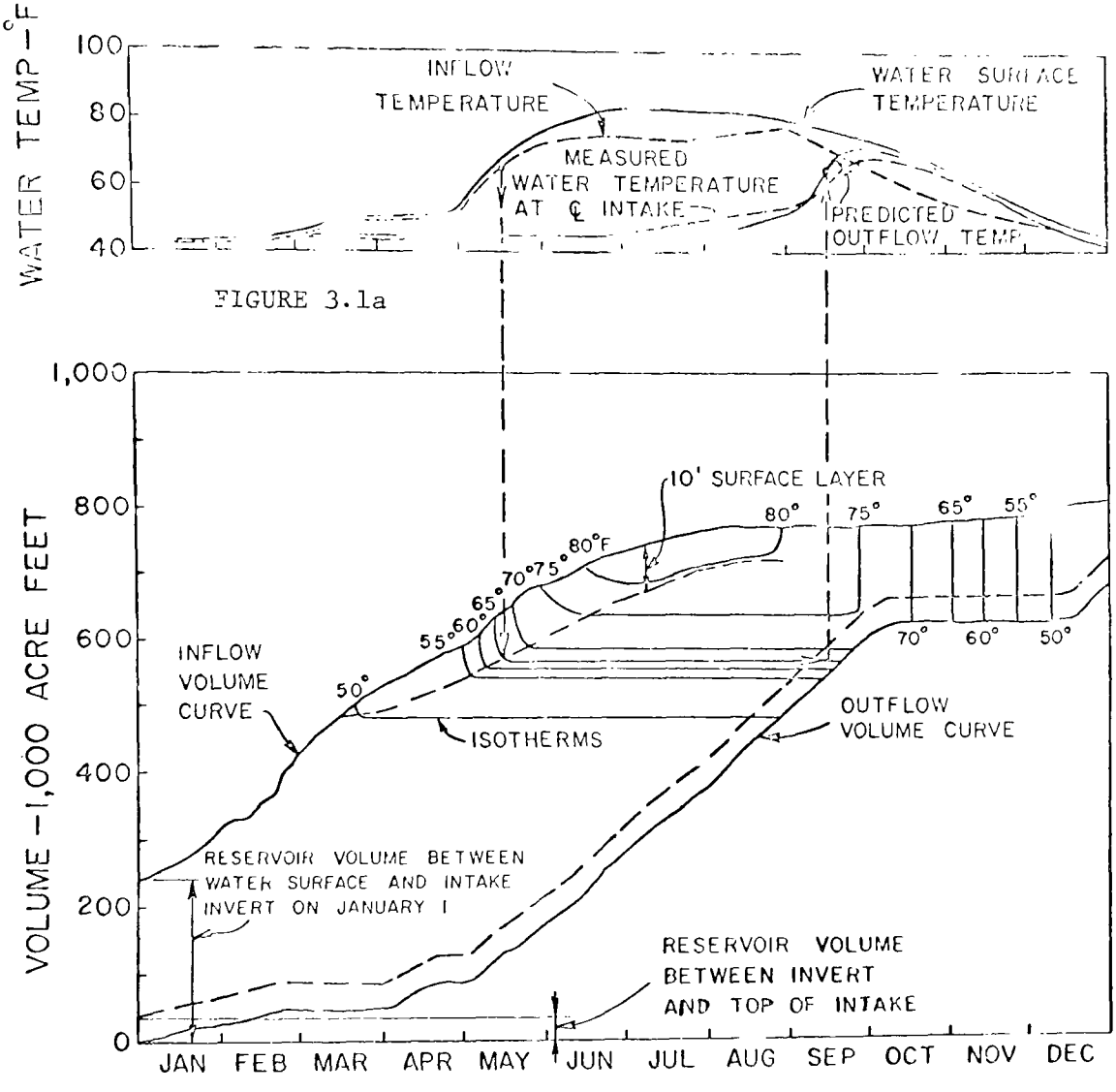

FIGURE 3.1a

FIGURE 3.1b

FIGURE 3.1 THE GRAPHICAL TEMPERATURE PREDICTION MODEL OF WUNDERLICH

assumed to correspond to the value of the isotherm intersecting the centerline of the outflow volume band and the bottom of an assumed 10' thick uniform surface layer. These predicted outflow temperatures are projected upward and plotted in Figure 3.1a.

The residence time for a selected input is defined by Wunderlich as the time period between which a given input temperature appears on the inflow volume curve and the time at which this temperature appears at the center of the outflow volume band. These are evaluated graphically from the horizontal distances in Figure 3.1b. The residence time varies for different input temperatures, thus reflecting the thermal characteristics of the reservoir.

Wunderlich notes that the rate of D.O. decay in a reservoir is a function of the water quality of the inflow and the complicated interplay of surface and bottom D.O. and B.O.D. production and consumption. Thus, the rate of D.O. decay cannot readily be generalized. However, Wunderlich assumed that the D.O. in the outlet could be calculated from

$$c = c_o \, e^{-k(t_d)} \tag{3-6}$$

where

c_o = the initial D.O. concentration for the inflow

c = D.O. concentration in the outlet

t_d = residence time in days of that inflow

$k = k(T)$ = bulk depletion factor for D.O.

The bulk D.O. depletion factor for a given inflow temperature

was determined from a plot of the measured D.O. in the layer corresponding to this temperature vs. time, Figure 3.2. With k(T) thus calculated, "predictions" are made from Equation 3-6 and shown graphically in Figure 3.3. The value of k is seen to vary from 5.5×10^{-3} day^{-1} at 60°F to 1.6×10^{-2} day^{-1} at 75°F.

It would seem that "predictions" made in this manner are merely a check that the plot of measured D.O. vs. time has been fitted correctly for a given temperature. Whether the bulk depletion coefficient is actually reflecting the B.O.D. in the incoming water, or the assumptions of no mixing and a simplified withdrawal profile, is questionable. If, for example, the B.O.D. in the inflowing water increased new bulk depletion factors would have to be calculated for the same inflow temperatures. Therefore, this method as a predictive tool is very weak. In addition, if the bulk depletion factor must be determined empirically from internal reservoir measurements, the D.O. in the outlet could be much more easily measured than predicted by the graphical method.

In Chapter 5 the graphical model of Wunderlich will be discussed again in order to investigate the concept of detention time as applied to a reservoir. The remainder of this chapter is devoted to the development of a one dimensional model for water quality prediction and appropriate methods of solution.

3.3 The Governing Equation for the Water Quality Model

Following the assumptions made in the temperature model, the conservation of mass equation will be treated as a one dimensional problem in the vertical direction, y. Thus, the governing equation is:

FIGURE 3.2 EVALUATION OF THE BULK DEPLETION FACTOR(57)

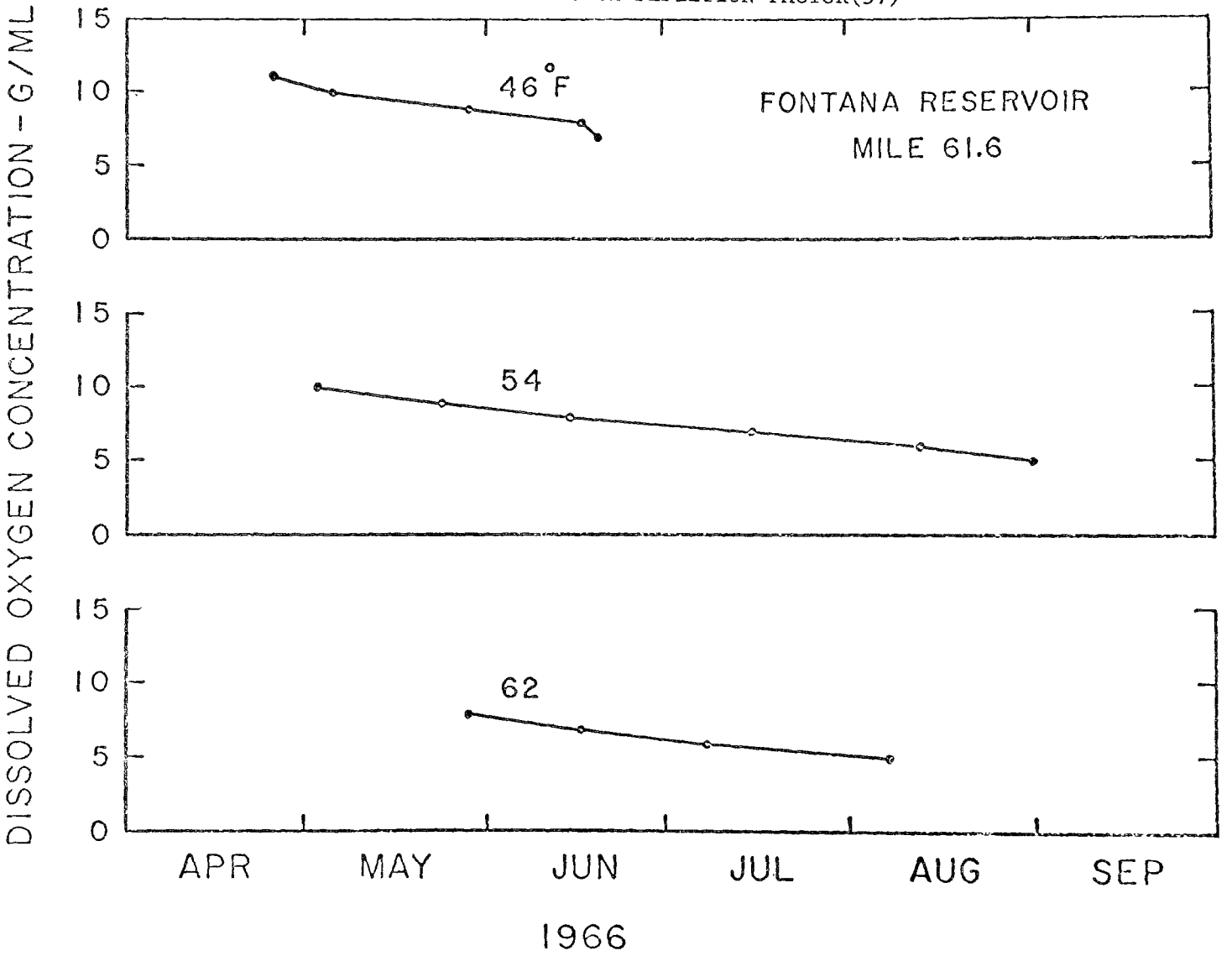

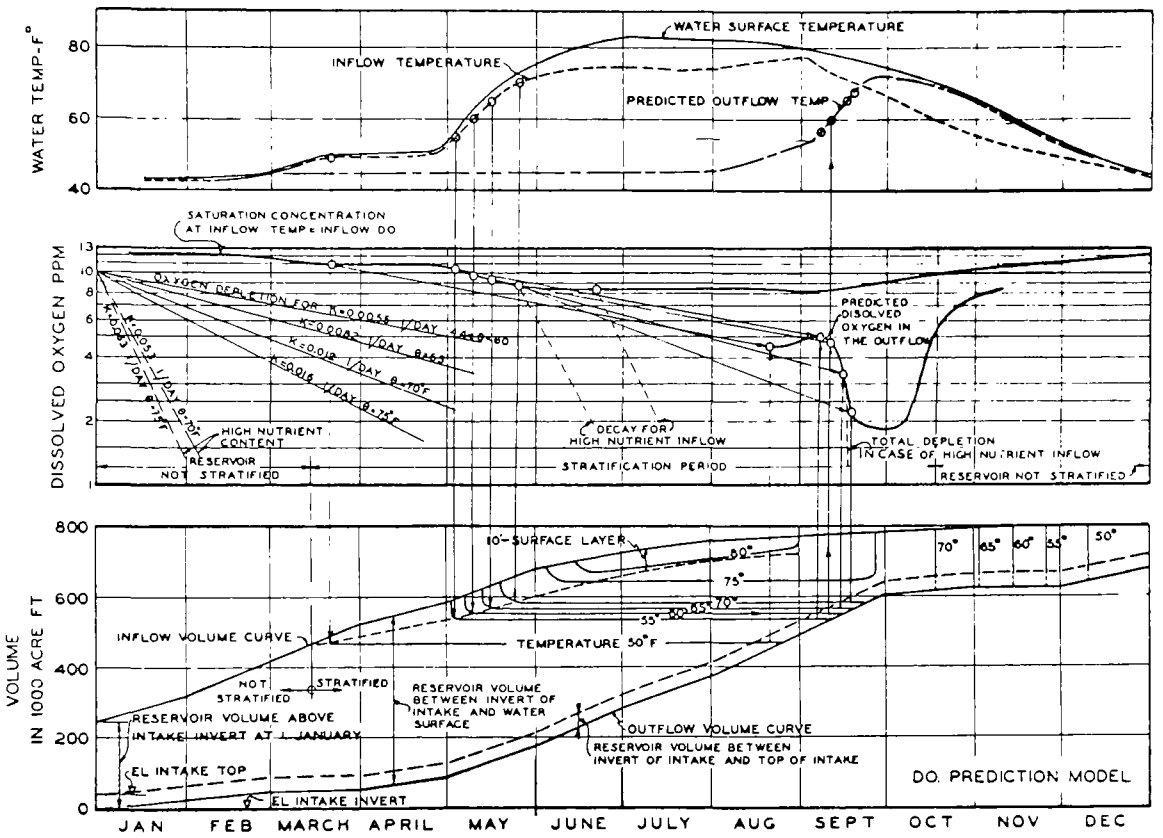

FIGURE 3.3 THE GRAPHICAL D.O. PREDICTION METHOD OF WUNDERLICH

$$\frac{\partial c}{\partial t} + v \frac{\partial c}{\partial y} = \frac{1}{A(y)} \frac{\partial}{\partial y}\left[D_M A(y) \frac{\partial c}{\partial y}\right] + \frac{\text{sources}_m}{\rho} - \frac{\text{sinks}_m}{\rho} \qquad (3\text{-}7)$$

where the source and sink terms have the units of mass/volume/time.

If the assumption is made that the changes in density caused by various pollutants are minimal compared to those caused by the temperature field, the method developed in Chapter 2 for calculating the velocity field in the reservoir remains unchanged.

It is possible that the concentration of one pollutant will depend on the concentration of another pollutant present. If this occurs, Equation 3-7 must be written for each pollutant and the equation solved simultaneously with coupling through the source and sink terms. For example, if one pollutant was undergoing a first order decay and the second pollutant was also undergoing a first order decay proportional to the amount of the first pollutant present, Equation 3-7 would be written twice:

$$\frac{\partial c_1}{\partial t} + v \frac{\partial c_1}{\partial y} = \frac{1}{A(y)} \frac{\partial}{\partial y}\left[D_M A(y) \frac{\partial c_1}{\partial y}\right] - Kc_1 + \frac{\text{sources}_1}{\rho} - \frac{\text{sinks}_1}{\rho} \qquad (3\text{-}7a)$$

$$\frac{\partial c_2}{\partial t} + v \frac{\partial c_2}{\partial y} = \frac{1}{A(y)} \frac{\partial}{\partial y}\left[D_M A(y) \frac{\partial c_2}{\partial y}\right] - Kc_1 + \frac{\text{sources}_2}{\rho} - \frac{\text{sinks}_2}{\rho} \qquad (3\text{-}7b)$$

where

K = first order decay constant

The sources and sinks of substances 1 and 2 are due to (1) the advection of mass by the inflow and outflow velocity distribution (2) internal production or consumption not accounted for by the first order decay term. The advective sources and sinks are directly analogous to the advective sources and sinks of temperature discussed in Section 2.4.1. Other sources and sinks will be discussed in Section 3.4.2.1.

It is also possible that the reaction rates would be temperature dependent. In this case information gained from the temperature field determination could be used in a relation expressing the functional dependence of the reaction coefficient with temperature.

Equation 3-7 can be simplified if the diffusion term is neglected. The Prandtl number P_r for water is

$$P_r = \frac{\nu}{D_T} \simeq 10 \tag{3-8}$$

where ν = kinematic viscosity of water

D_T = molecular diffusivity of heat

The Schmidt number, S_c, for water is

$$S_c = \frac{\nu}{D_M} \simeq 1000 \tag{3-9}$$

where

D_M = molecular diffusivity of mass

Therefore, the ratio of the molecular diffusivity of mass and that of heat for water is

$$\frac{D_M}{D_T} = \frac{P_r}{S_c} \simeq \frac{1}{100} \tag{3-10}$$

Since the molecular diffusion of heat has not been found to be significant in the temperature prediction it is felt that the molecular diffusivity of mass which is two orders of magnitude smaller, can be neglected.

The convective velocity field v(y,t) in Equation 3-7 is determined from Equation 2-54. Thus, in order to solve Equation 3-7, initial and boundary conditions must be stated. In addition to the advective sources and sinks, a mathematical representation of the internal and surface source and sink terms must be made.

3.4 Examples

3.4.1 The Dissolved Oxygen and B.O.D. Model

3.4.1.1 Governing Equations

The conservation of B.O.D. and D.O. equations are exactly the same as Equation 3-7 with c in one case representing B.O.D. and the other case, D.O. As discussed in Section 3.3, the diffusion term will be neglected. It remains to define the non-advective source and sink terms and the initial and boundary conditions.

The usual assumption is that B.O.D. can be represented by a first order decay process, i.e. the rate of change of B.O.D. is pro-

portional to the amount of B.O.D. present. This is represented as

$$\frac{\partial \ell}{\partial t} = - K \ell \tag{3-11}$$

or

$$\ell = \ell_o e^{-K(t-\tau)} \tag{3-12}$$

where

ℓ_o = the B.O.D. at time τ

ℓ = the B.O.D. at time t

K = B.O.D. decay rate constant

The values of K and ℓ_o are traditionally determined from 5 day B.O.D. tests with K being the order of 0.1 per day and a function of temperature.

In dealing with a reservoir, where water can be retained from several days to several years, five day B.O.D. values generally are not indicative of the total B.O.D. in the incoming water. It is generally agreed that the B.O.D. decay process is composed of two stages, carbonaceous and nitrogenous demand. The first stage proceeds fairly rapidly and usually starts as soon as waste is introduced into a body of water. At first there is a small population of aerobic bacteria. After the waste has been input, the population builds up to a new level, characteristic of the concentration of waste and the available oxygen. This is the carbonaceous stage. In the presence of other bacteria,

the second stage, nitrification, may occur. Here ammonia type nitrogen is oxidized to the nitrite ion and subsequently to nitrate. In many cases, nitrification occurs several days after the carbonaceous stage and at a much slower rate. If the initial population of a nitrifying bacteria is small, it may be a long time before nitrification is observed.

Churchill (8) presents data showing that the inflow to the Cherokee Reservoir (in the TVA system) in 1952 had a 5 day B.O.D. of about 2 mg/ℓ and a 30 day B.O.D. of about 8 mg/ℓ while the reservoir outflow had a 5 day B.O.D. of 1 mg/ℓ and a 30 day B.O.D. of about 3 mg/ℓ. Thus, although the 5 day B.O.D. decreased by only 1 mg/ℓ, the 30 day B.O.D. decreased by 5 mg/ℓ. If the water had remained in the reservoir for 30 days, a decrease of 5 mg/ℓ of oxygen, neglecting surface reaeration and oxygen production by photosynthesis would have occurred.

Churchill also reports that in the summer of 1945 the inflow to Douglas Reservoir (in the TVA system) contained about 7 mg/ℓ of oxygen and about 2 mg/ℓ of 5 day B.O.D. while the outflow contained about 1 mg/ℓ of oxygen.

Therefore, for reservoir use, long term B.O.D. studies should be made, yielding values of 10, 30 and even 50 day B.O.D. These data are rarely available. The representation of the complete B.O.D. cycle in one mathematical function has not been satisfactorily accomplished. Dougal and Bowmann (11) attempt to represent this by an expression of the form

$$\ell = \frac{t}{a + bt} \tag{3-13}$$

where

a and b are constants

They report, however, that this expression failed to predict the experimental long term B.O.D. values.

For simplicity, the complete B.O.D. cycle will be represented as a first order decay.

$$\ell = \ell_o e^{-Kt} \tag{3-14}$$

Since the overall rate of decay will be slower than 0.1 day^{-1} for a long term process, K will be assumed to be a constant of the order of 0.01 day^{-1}. Also, since the ultimate B.O.D. value will be larger than that calculated from a 5 day B.O.D. test, a larger value for ℓ_o will be assumed.

There are also two sources of B.O.D. within the reservoir. The first is the bottom demand, which is found in new reservoirs. This is due to the amount of oxygen needed to oxidize the organic material originally present on the reservoir bottom. Krenkel et. al. (26) states that "the oxygen demand due to organic deposit generally decreases with time after the first few years as the organic matter is slowly oxidized or leached into solution and discharged". In this study, bottom demand will be neglected since there is, at present, no satisfactory way to quantify it and, as a general rule, it is exhausted after several years of reservoir life.

In the surface layers of a reservoir there is the possibility of oxygen production by photosynthesis. Also, if the surface water is not saturated with oxygen, there will be a transfer of oxygen from the atmosphere to the surface waters. An additional surface phenomenon is the production of B.O.D. due to algae death and oxygen consumption by plant respiration. Verduin (51) estimated that in the euphotic zone (defined as the depth by which 99 percent of the incident light is observed), photosynthetic production is about equal to the respiration of the total biota and that mean algae respiration is about 12 percent of maximum photosynthesis. Pritchard and Carpenter (37a), however, reported that the rate of oxygen production by photosynthesis was double the rate of consumption in Roanoke Rapids Reservoir.

In the absence of conclusive information, two different assumptions will be tested. The first is that in the entire euphotic zone, the rate of production of oxygen by photosynthesis and atmospheric reaeration is sufficient to cause D.O. saturation. The second is that there is oxygen saturation down to some arbitrary depth d_{sat}, above the limit of the euphotic zone. Additionally, in the euphotic zone, the rate of B.O.D. production and consumption will be assumed to be equal.

Following the form of Equation 3-7, the governing equations based on the previous assumptions are directly analogous to the temperature Equation, 2-35, with redefinition of the source and sink terms:

$$\frac{\partial \ell}{\partial t} + v \frac{\partial \ell}{\partial x} = - K\ell + (u_i \ell_i - u \ell) \frac{B(y)}{A(y)} \qquad (3\text{-}15)$$

$$\frac{\partial c}{\partial t} + v \frac{\partial c}{\partial y} = - K\ell + (u_i c_i - u_i c) \frac{B(y)}{A(y)} \tag{3-16}$$

where

ℓ = B.O.D.

c = dissolved oxygen

The surface has been assumed to be D.O. saturated. Additionally it has been assumed that there is no net production of B.O.D. in the euphotic zone and at the surface. Thus, there can be no transfer of B.O.D. across the free surface and the surface boundary conditions are:

$$\frac{\partial \ell}{\partial y} = 0 \quad \text{at} \quad y = y_s \tag{3-17a}$$

$$c = c_{sat} \quad \text{at} \quad y = y_s \tag{3-17b}$$

where

c_{sat} = D.O. saturation at the temperature of the water surface.

Since there is assumed to be no transfer of mass across the reservoir bottom, the bottom boundary conditions are:

$$\frac{\partial \ell}{\partial y} = 0 \quad \text{at} \quad y = y_b \tag{3-18a}$$

$$\frac{\partial c}{\partial y} = 0 \quad \text{at} \quad y = y_b \tag{3-18b}$$

The initial condition must be stated in terms of the initial B.O.D. and D.O. in the reservoir at time $t = t_i$, the start of the D.O. and B.O.D. calculations.

Since Equations 3-15 and 3-16 are solved simultaneously along with the one-dimensional temperature Equation 2-35, it is helpful to discuss the relationship between the time scale of the two models.

The initial condition in the temperature equation is that

$$T = T_o \quad \text{at} \quad t = 0 \tag{3-19}$$

In other words, time, t, in the temperature model is measured from $t = 0$, the time at which the reservoir is assumed to be isothermal. Consequently, the velocity field $v(y,t)$ is referred to $t = 0$.

In the water quality model, times are also referred to $t = 0$, the isothermal condition. No calculations need to be made for Equations 3-15 and 3-16 until $t = t_i$ the time at which the initial B.O.D. and D.O. profiles are known. However, temperature calculations must be made from $t = 0$ in order to determine $v(y,t)$ which depends on the temperature field.

The saturation level of D.O. in water is a function of temperature, Figure 3.4. A least squares parabola for this relationship is

$$D.O._s = 14.48 - 0.36T + 0.0043T^2 \tag{3-20}$$

where

$D.O._s$ = the saturated D.O. value (ppm)

T = temperature in °C.

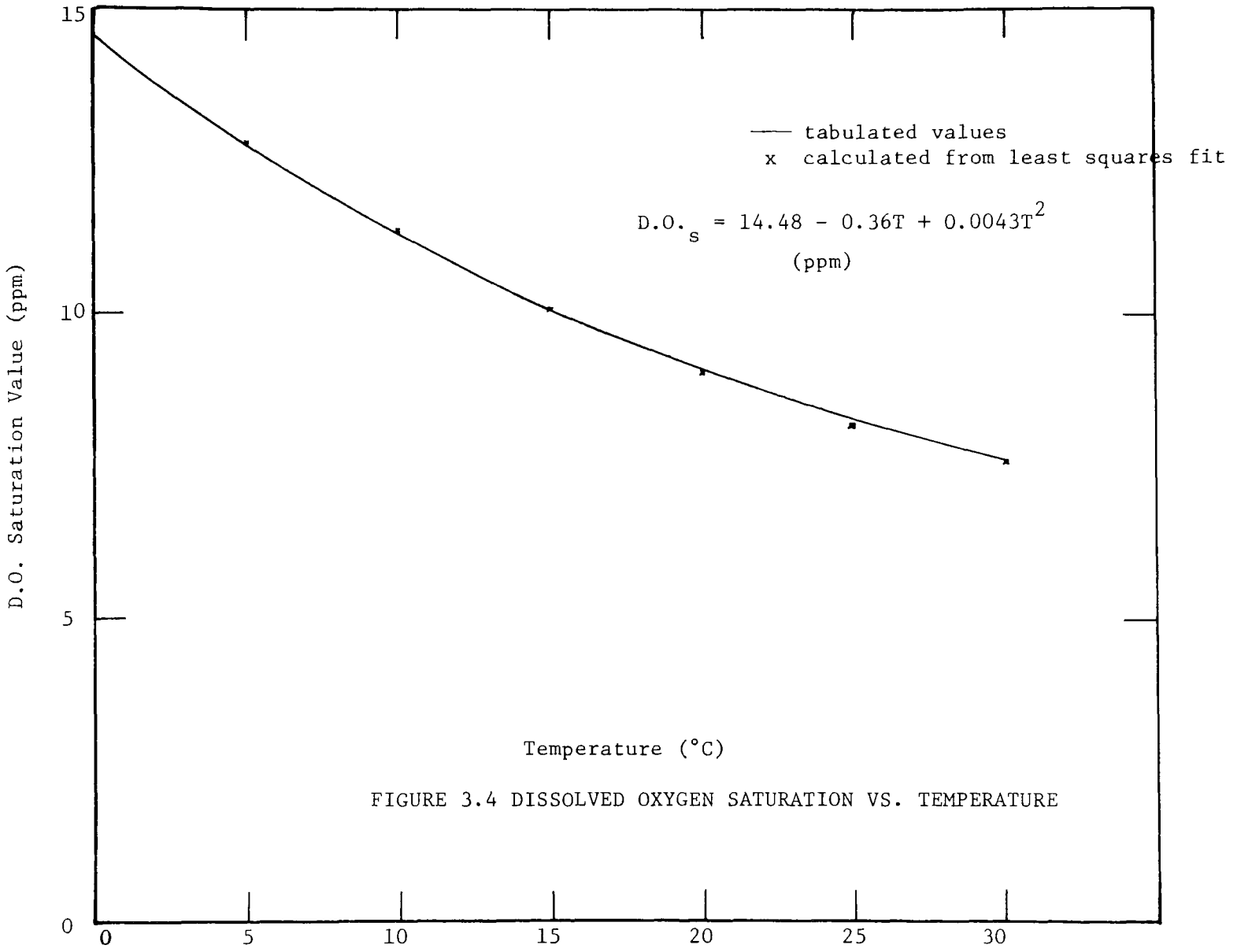

FIGURE 3.4 DISSOLVED OXYGEN SATURATION VS. TEMPERATURE

The added restriction is that the D.O. value calculated at a depth y in the reservoir cannot exceed the saturated value for this depth. If calculations show that D.O.(y) exceeds $D.O._s$ calculated at that depth, D.O.(y) will be replaced by $D.O._s$.

The method of solution is discussed in the following section.

3.4.1.2 Formulation of the Numerical Solution

Mixing at the reservoir entrance and surface mixing due to evaporative cooling will be treated in a manner similar to that used in the temperature model. The finite volume representation of Equations 3-15, 3-16, is derived by considering the control volume in Figure 3.5.

$$\frac{\Delta \ell}{\Delta t} \bar{A} \Delta y = v_1 A_1 \ell_1 B_1 - v_2 A_2 \ell_2 B_2 + (u_i \ell_i - u_o \ell_o) \bar{B}(y) \Delta y - K \ell \bar{A} \Delta y \quad (3\text{-}21)$$

$$\frac{\partial c}{\Delta t} \bar{A} \Delta y = v_1 A_1 c_1 B_1 - v_2 A_2 c_2 B_2 + (u_i c_i - u_o c_o) \bar{B}(y) \Delta y - K \ell \bar{A} \Delta y \quad (3\text{-}22)$$

where

the subscript i refers to inflow

the subscript o refers to outflow

The point of evaluation of c_1 and c_2 will depend (as in Section 2.5.1) on the sign of the convective velocities v_1, v_2. For example,

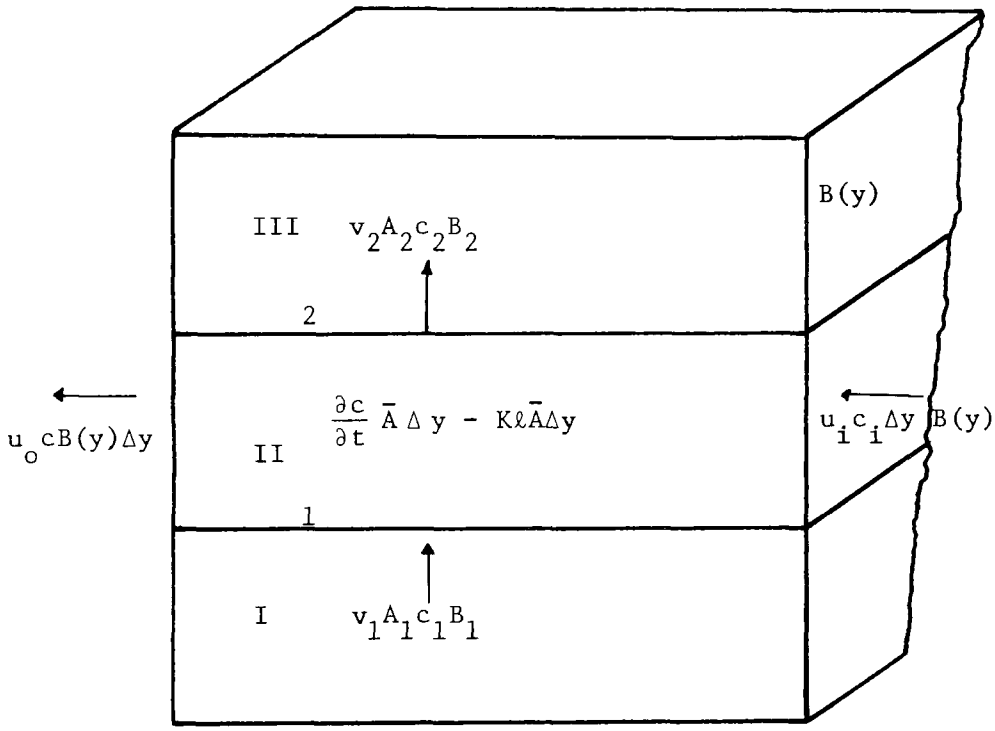

(c can be replaced by ℓ with no other changes necessary)

FIGURE 3.5 CONTROL VOLUME FOR THE WATER QUALITY MODEL

if v_1 is positive, c_1 refers to the concentration in element I (Figure 3.5). If v_1 is negative c_1 refers to the concentration in element II. A similar rule applies for c_2. This also applies to ℓ_1 and ℓ_2.

The surface boundary condition for B.O.D. can be formulated from a conservation of mass consideration. With reference to Figure 3.6a, since it has been assumed that there is no net consumption of B.O.D. in the euphotic zone K is zero in this region. In addition, there can be no transfer across the free surface. The resulting B.O.D. surface boundary condition is

$$\frac{\Delta \ell}{\Delta t} \bar{A} \Delta y = (u_i \ell_i - u_o \ell_o) \Delta y \, B(y) + v\ell A \Big|_{y_s - \Delta y} \text{ at } y = y_s \qquad (3\text{-}23a)$$

The bottom boundary condition for B.O.D. is similarly formulated from Figure 3.6b.

$$\frac{\Delta \ell}{\Delta t} \bar{A} \Delta y = (u_i \ell_i - u_o \ell_o) \Delta y \, B(y) - v\ell A \Big|_{y_b + \Delta y} - K\ell \qquad (3\text{-}23b)$$

The bottom boundary condition for D.O. is arrived at in an analogous manner and is

$$\frac{\Delta c}{\Delta y} \bar{A} \Delta y = (u_i c_i - u_o c_o) \Delta y \, B(y) - vcA \Big|_{y_b + \Delta y} - K\ell \qquad (3\text{-}24a)$$

The surface D.O. boundary condition as discussed in Section 3.4.1.1 is

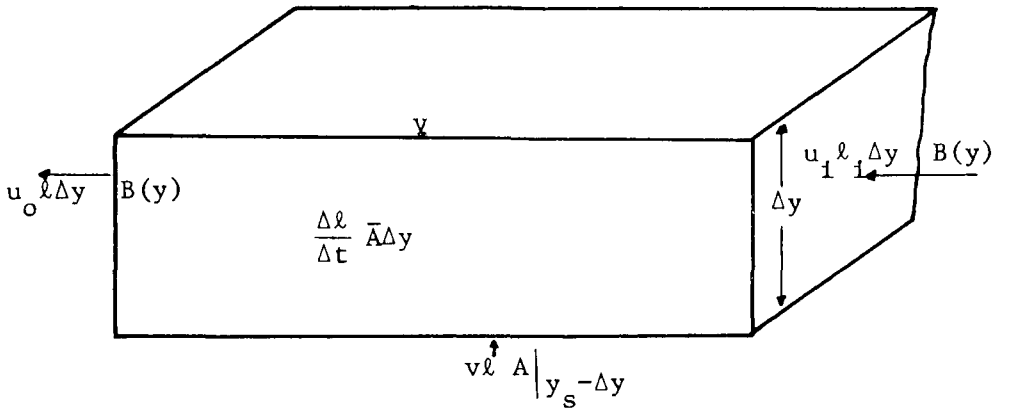

FIGURE 3.6a SURFACE BOUNDARY CONDITION

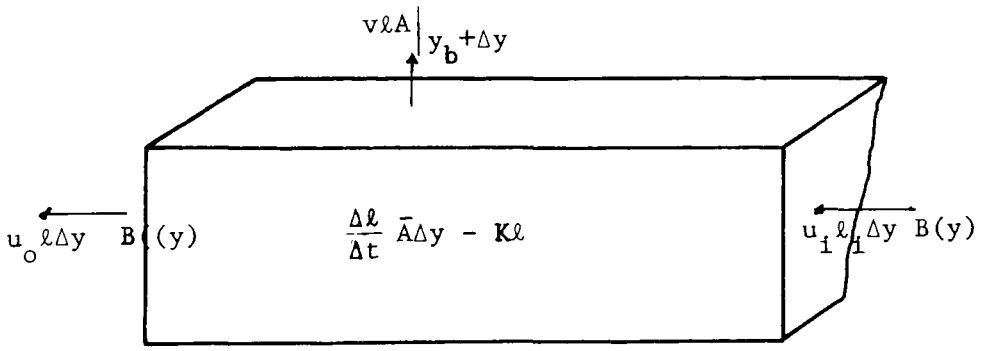

FIGURE 3.6b BOTTOM BOUNDARY CONDITION

FIGURE 3.6 BOUNDARY CONDITIONS FOR D.O. AND B.O.D. IN THE NUMERICAL SCHEME

$$c = c_{sat} \text{ at } y = y_s \tag{3-24b}$$

In addition, as discussed in Section 3.4.1.1, it has been assumed that to some arbitrary depth, d_{sat} within the euphotic zone, the water is saturated. Thus

$$c = c_{sat} \text{ for } d_{sat} < y < y_s \tag{3-24c}$$

This will be assumed to apply before any convective mixing due to surface cooling occurs. Thus, the surface layers become a source of highly oxygenated water in the convective mixing depth when surface cooling occurs.

As discussed in Section 2.4.4, the amount of time necessary for the incoming water to reach its own density level and to traverse the remaining length of the reservoir is the lag time t_L (Equation 2-98). To be consistent with the one-dimensional model assumption that the incoming water is uniformly dispersed horizontally, the actual time at which the inflowing water at time τ is input to the mathematical water quality model is t_i', defined by:

$$t_i' = \tau + t_L \tag{3-25}$$

At time $t = t_i'$, the water which physically entered the reservoir at time τ is considered to be distributed vertically according to the velocity field which exists mathematically at time t_i' (Figure 3.7). The amount of D.O. and B.O.D. in the incoming water will depend on the

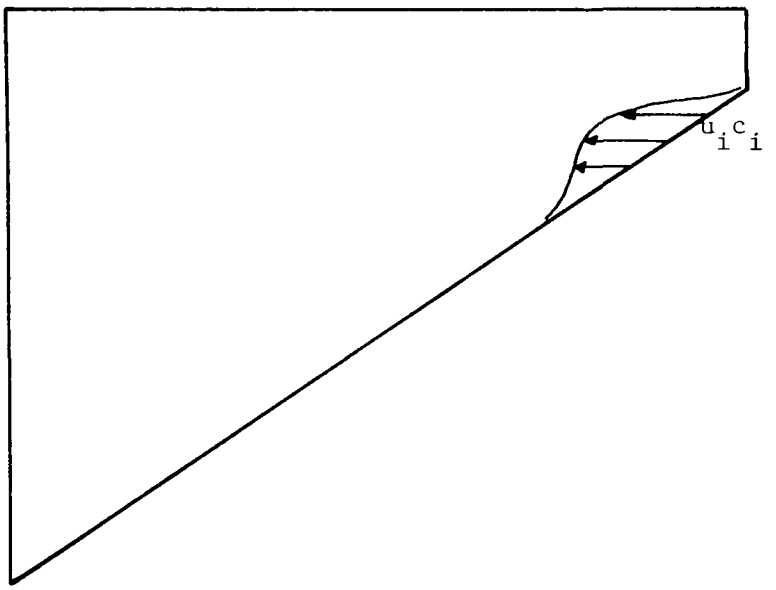

FIGURE 3.7 THE DISTRIBUTION OF AN INPUT UNDER STRATIFIED CONDITIONS

amount of mixing at the reservoir entrance (calculated in a directly analogous manner to the mixed inflow temperature, Equation 2-54) and on the following assumptions:

(1) If the water is cooler than the reservoir surface water, and entering below the euphotic zone, the incoming D.O. and B.O.D. begin to undergo decay immediately upon physical entrance into the reservoir.

(2) If the water is entering in the euphotic zone, there is no net B.O.D. consumption and the consumption of oxygen is assumed to be balanced by reaeration and photosynthetic production during the time of traverse, t_L, of the reservoir surface.

These assumptions are introduced into Equations 3-21 and 3-22 through ℓ_i and c_i, the incoming B.O.D. and D.O. in each time step Δt. For surface entrance

$$c_i\Big|_t = c_i\Big|_{t-t_L} \tag{3-26a}$$

$$\ell_i\Big|_t = \ell_i\Big|_{t-t_L} \tag{3-26b}$$

For subsurface entrance

$$c_i\Big|_t = c_i\Big|_{t-t_L} - \ell_o\Big|_{t-t_L} \quad 1 - e^{-(Kt_L)} \tag{3-26c}$$

$$\ell_i\Big|_t = \ell_o\Big|_{t-t_L} \quad e^{-(Kt_L)} \tag{3-26d}$$

When convective mixing occurs, due to cooling of the reservoir surface (as was discussed in Section 2.4.5) the D.O. and B.O.D. located in the mixing layers will be redistributed. Since complete mixing is assumed to occur, the new concentration of D.O. in this mixed layer c_{mix} can be determined from

$$c_{mix} = \frac{\int_{y_{mix}}^{y_s} c(y)\ A(y)dy}{\int_{y_{mix}}^{y_s} A(y)dy} \tag{3-27}$$

An analogous equation applies to ℓ_{mix}.

One special point of interest is the reservoir outlet. The concentration of D.O. in the outflow $D.O._{out}(t)$ at a given time t, can be calculated from the integral over the depth of the D.O. being advected out by the outflow velocity distribution divided by the outflow rate, Equation 3-28.

$$D.O._{out}(t) = \frac{\int_{y_b}^{y_s} \rho\ D.O.(y,t)\ u_o(y,t)\ B(y)dy}{\rho Q_o(t)} \tag{3-28}$$

If the B.O.D. and D.O. profiles in the reservoir are known at some time, (the initial condition) preferably at the start of the stratification phenomena, t = 0, Equations 3-15 and 3-16 can be simultaneously explicitly solved in time steps Δt where the B.O.D. value, ℓ, used in the D.O. calculation is ℓ at the beginning of the time step.

All that remains is to evaluate the depth of what has been called the euphotic zone. This has been chosen to be the depth below which only 1% of the incoming solar radiation penetrates. Below this depth there is assumed to be no photosynthesis. If the surface water is turbid, the depth of the surface layer will be small. Hence, any assumption relating to the thickness of the surface layer is not very critical. However, in a clear reservoir the surface layer could be quite deep. The depth of the euphotic zone d_e, can be calculated by setting

$$\frac{\phi}{\phi_o} = 0.01 \tag{3-29}$$

in Equation 2-31. This dictates that

$$y_s - y = d_e = \frac{4.6}{\eta} \tag{3-30}$$

where

η = radiation extinction coefficient (Equation 2-31).

3.4.1.3 Required Inputs to the D.O. and B.O.D. Prediction Model

Those parameters which can be measured directly are

1) Reservoir geometry

2) Initial isothermal reservoir temperature

3) Inflow temperatures

4) Air temperatures

5) Relative humidities

6) Atmospheric radiation

7) Inflow rates

8) Outflow rates

9) Surface elevation

10) Inflow D.O.

11) Inflow B.O.D. (long term) and decay rate, K, Equation (3-14)

12) Initial B.O.D. and D.O. profiles

Other factors which must be chosen are:

1) Values for absorption coefficient, η, and surface absorption fraction, β (Equation 2-31).

2) Inflow standard deviation, σ_j (Equation 2-51) and uniform surface entrance depth d_s (Equation 2-53b).

3) Entrance mixing ratio r_m and mixing depth, d_m (Equation 2-55)

4) Thickness for lag time determination, Δh (Equation 2-92).

5) Thickness of the saturated surface layer, d_{sat}, (Equation 3-24c)

6) Evaluation of the withdrawal thickness (Equation 2-49).

3.4.2.1. Application of the Water Quality Model to a Pulse Injection of a Conservative Tracer

In this section it is desired to solve Equation 3-7 for a pulse injection of dye at time $t = \tau$ into a stratified reservoir.

The governing equation is the same as 3-21, with K = 0. The boundary conditions are stated in terms of no transfer across the free surface or the bottom and thus

$$\frac{\partial c}{\partial y} = 0 \quad \text{at } y = y_s,\ y_b \tag{3-31}$$

At $t = \tau$ a pulse of dye is physically injected into the water entering the reservoir. As explained in Section 3.4.1.2, the amount of time necessary for the dye to reach its own density level and to traverse the remaining horizontal length of the reservoir is the lag time t_L calculated from Equation 2-98. To be consistent with the assumption that the dye is uniformly dispersed horizontally, the actual time at which the dye is input to the mathematical model, t_i, is

$$t_i = \tau + t_L \tag{3-32}$$

At time t_i, the initial mass, M, of the conservative tracer is considered to be distributed vertically according to the velocity field which exists mathematically at time t_i (Figure 3.7). Therefore, the initial condition becomes

$$c(y,t) = 0 \text{ at } t < t_i \tag{3-32a}$$

$$c(y,t_i) = \frac{M}{\rho A(y)dy} \quad \frac{u_i(y,t_i)\ B(y)dy}{Q_i'\ (t_i)} \quad \text{at } t = t_i \tag{3-32b}$$

where

$Q'(t_i)$ = the mixed inflow rate at time t_i (Eq. 2-56)

ρ = the density of water

In the formulation of the numerical solution of this problem Equation 3-21 applies with K = 0. The boundary conditions are Equations

3-23a and 3-23b with K = 0.

As a check that the initial condition (Equation 3-32b) is observed, it can be noted in the time interval that $t = t_i - \Delta t$ and $t = t_i$. Equation 3-21 reduces to

$$c = \Delta c = \frac{u_i c_i \bar{B}(y)\, \Delta y \Delta t}{\bar{A}\, \Delta y} \tag{3-33}$$

Δc is the change in concentration (from a value of zero in this case) in the element in time step Δt.

The concentration of tracer in the incoming water at time $t = t_i$ is given by

$$c_i = \frac{M}{\rho Q_i'(t_i) \Delta t} \tag{3-34}$$

Q_i' is evaluated at time t_i because it is this flow which is mathematically entering the reservoir at time $t = t_i = \tau + t_L$. For this same reason u_i is also evaluated from the inflow rate at time t_i.

Equation 3-33 and 3-34 yield

$$c(y,t_i) = \Delta c = \frac{M}{\rho A(y) \Delta y} \frac{u_i(y,t_i)\, B(y) \Delta y}{Q_i'(t_i)} \tag{3-35}$$

which is identical to Equation 3-32b.

After the initial pulse has entered the reservoir c_i will be equal to the mass of tracer entrained by the inflow water at time t, divided by the total mass inflow including entrainment. This is expressed as

$$c_i(t) = \frac{\sum_{\text{mixing depth}} u_m(y)\ c(y)\ B(y)\ \Delta y}{(1 + r_m)\ Q_{in}(t)} \qquad (3\text{-}36)$$

where

u_m = the backflow velocity due to mixing (Equation 2-58)

r_m = mixing ratio (Equation 2-55)

From Equation 3-36 it is seen that the amount of tracer entrained depends both on the mixing ratio, r_m, and the definition of the mixing depth. As discussed in Section 2.4.3 Huber and Harleman defined the mixing depth as an arbitrary thickness, d_m, extending down from the reservoir surface. For the case of surface inflow it is certainly possible that the entrainment is coming from beneath the surface layer (28). This will be further discussed in Chapter 4 in connection with the experimental results.

3.4.2.2 Inputs to the Pulse Injection Model

The inputs to this mathematical model are the same as those discussed in Section 3.4.1.3 with the obvious exception that no B.O.D. or D.O. data is required. In addition the time of input of one or more pulse injections is needed. The model is capable of handling up to 20 pulse injection solutions simultaneously.

3.4.2.3 Discussion of the Pulse Injection Solution

By means of the method discussed in the previous section, the concentration distribution of a conservative tracer c(y,t) can be calculated. Thus, if attention is fixed at one particular elevation within the reservoir, a concentration time curve for that depth

can be determined. In addition, a cumulative mass curve, defined as the total mass of tracer which has passed a given depth at a given time, divided by the initial mass input vs. time can be determined.

The point of measurement of concentration in the laboratory experiment will be the reservoir outlet. The concentration of tracer in the outlet, cout(t) can be calculated from an equation analogous to Equation 3-28.

$$\text{cout}(t) = \frac{\int_{y_b}^{y_s} \rho c(y,t)\, u_o(y,t)\, B(y)\, dy}{\rho Q_o(t)} \qquad (3\text{-}37)$$

A typical plot of cout(t) vs. time is found in Figure 3.8a.

Integrating, with respect to time, the instantaneous amount of mass advected out of the reservoir from time $t = t_i$ to time t and dividing by the mass of tracer input one can determine the total percentage of tracer, tracot, which has left the reservoir:

$$\text{tracot} = \frac{\sum_{t=t_i}^{t=t} \rho Q_o(t)\, \text{cout}(t)\, dt}{\text{mass of tracer input}} \qquad (3\text{-}38)$$

This curve is shown graphically in Figure 3.8b. This will be referred to as the cumulative mass out curve.

In summary, the method developed in this section gives a prediction of both the time variation of the outflow concentration and the total mass which has passed through the reservoir as a result of a pulse injection of a conservative tracer. The validity of the combined temperature and water quality model will be tested in a laboratory reservoir using pulse injections. It should be noted that verification of

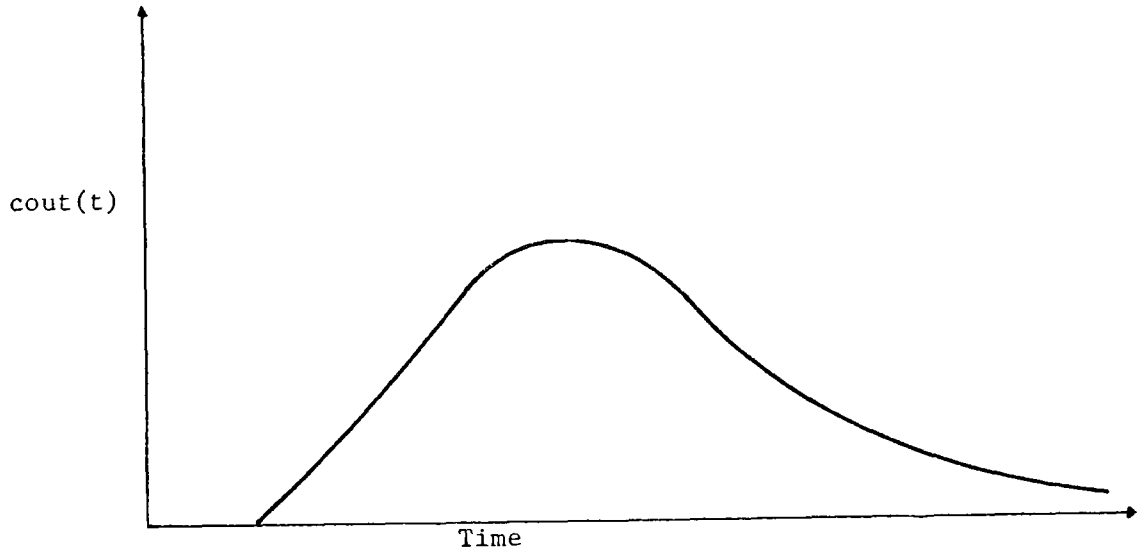

FIGURE 3.7a CONCENTRATION IN THE OUTLET VS. TIME (SCHEMATIC)

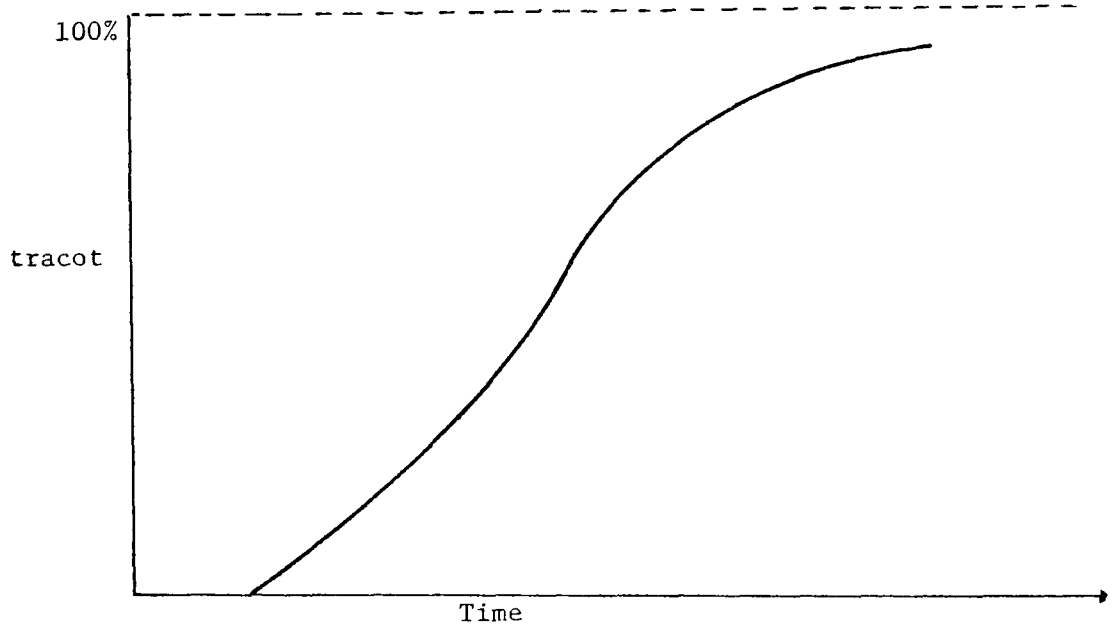

FIGURE 3.8b CUMULATIVE MASS OUT CURVE (SCHEMATIC)

FIGURE 3.8 SCHEMATIC CURVES PREDICTED FOR THE PULSE INJECTION SOLUTION

both temperature and tracer concentration is a much more stringent test of the ability to simulate the internal flow pattern in a reservoir than is temperature alone.

3.5 Review of the Mathematical Models

In the field case, there does not appear to be any available data on outflow concentrations due to pulse injections of tracers. However, recent measurements have been made on dissolved oxygen concentrations in reservoirs. Unfortunately, the data is not complete and additional assumptions must be made in order to predict D.O. concentration. The verification of some of these assumptions is more in the hands of biologists than engineers. Nevertheless, the model includes the effects of advective inflows and outflow and convective transport, selective withdrawal, entrance mixing, lag time, and first order decay. The mathematical model for concentration prediction (Equations 3-15 and 3-16) is first applied to a pulse injection of a conservative substance into a stratified laboratory flume. In Chapter 5, the D.O. prediction model is tested on Fontana Reservoir in the TVA system. It is hoped the assumptions found on the D.O. prediction model will show where additional research in this area should be directed.

CHAPTER 4. LABORATORY EXPERIMENTS

4.1 Laboratory Equipment

In the Hydrodynamics Laboratory of the Massachusetts Institute of Technology experiments were conducted in a laboratory flume having the shape of an idealized reservoir. The flume is not intended to be a physical model of an existing or proposed reservoir, but rather to be a physical system for verifying the mathematical models developed for temperature and concentration predictions in chapters 2 and 3. Most of the basic phenomena involved in reservoir stratification and dilution process are present in the laboratory system, except wind and wave forces and precipitation. The mathematical models require, as input, meteorological hydrolical and water quality data along with the reservoir geometry and operation scheme. The laboratory simulation has the advantage of being a controlled system in which the effects of different variables can be isolated from one another along with a time scale measured in minutes instead of days.

The laboratory reservoir is basically the same as that used by Huber and Harleman and is shown in Figure 4.1. The main section of the flume is thirty-six feet long, one foot wide and of rectangular cross section. The depth varies linearly from four and one-half (4–1/2) inches at the upstream entrance section 4 feet long, 1 foot wide and four

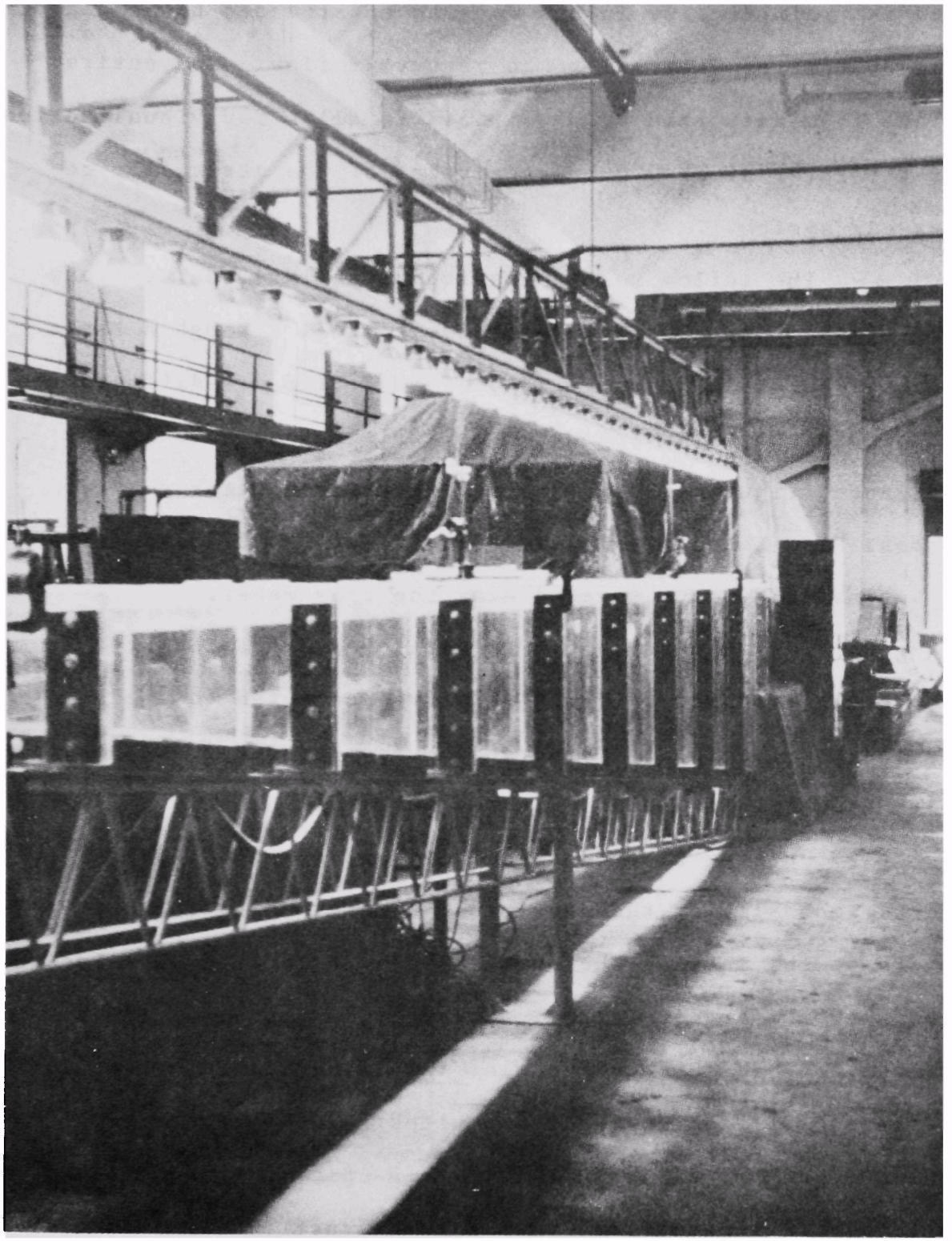

FIGURE 4.1 THE LABORATORY FLUME

and one-half (4 1/2) inches deep as constructed to simulate the transition from stream to reservoir flow. The entire flume is constructed of plexiglass to allow for visualization of the internal flow characteristics of the stratified reservoir system.

The inflow to the reservoir was into the upstream end of the four foot long entrance channel through a three quarter (3/4) inch hose. The incoming flow was diffused through a short section of gravel filter located near the entrance (Figure 4.2). The flow rate was monitored by a Brooks Flow Meter (Tube 4-9M-25-3, Float 9RS-87) and varied by means of a valve located near the flow meter.

The incoming water temperature was varied by adjusting a temperature mixing valve connected to a heat exchanger. The inflow temperature was measured continuously with a thermistor located in the entrance channel.

Outflow from the reservoir was through a one-eighth (1/8) inch slot in the downstream end extending the entire width of the model. The outlet slot was located 22.4 inches above the reservoir bottom. The flow, which was gravity driven, passed through the slot into a semicircular section (Figure 4.3) from which it was withdrawn through three three-eighth (3/8) inch pipes. These pipes, approximately 2 inches in length, lead into a three quarter (3/4) inch rubber hose in which a thermistor was located to monitor

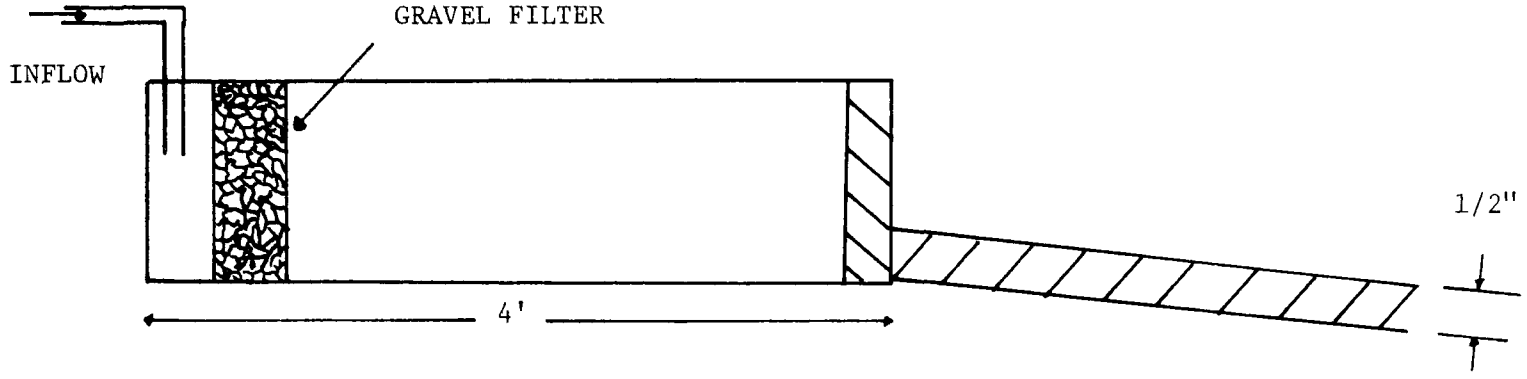

FIGURE 4.2 ELEVATION VIEW OF RESERVOIR INLET

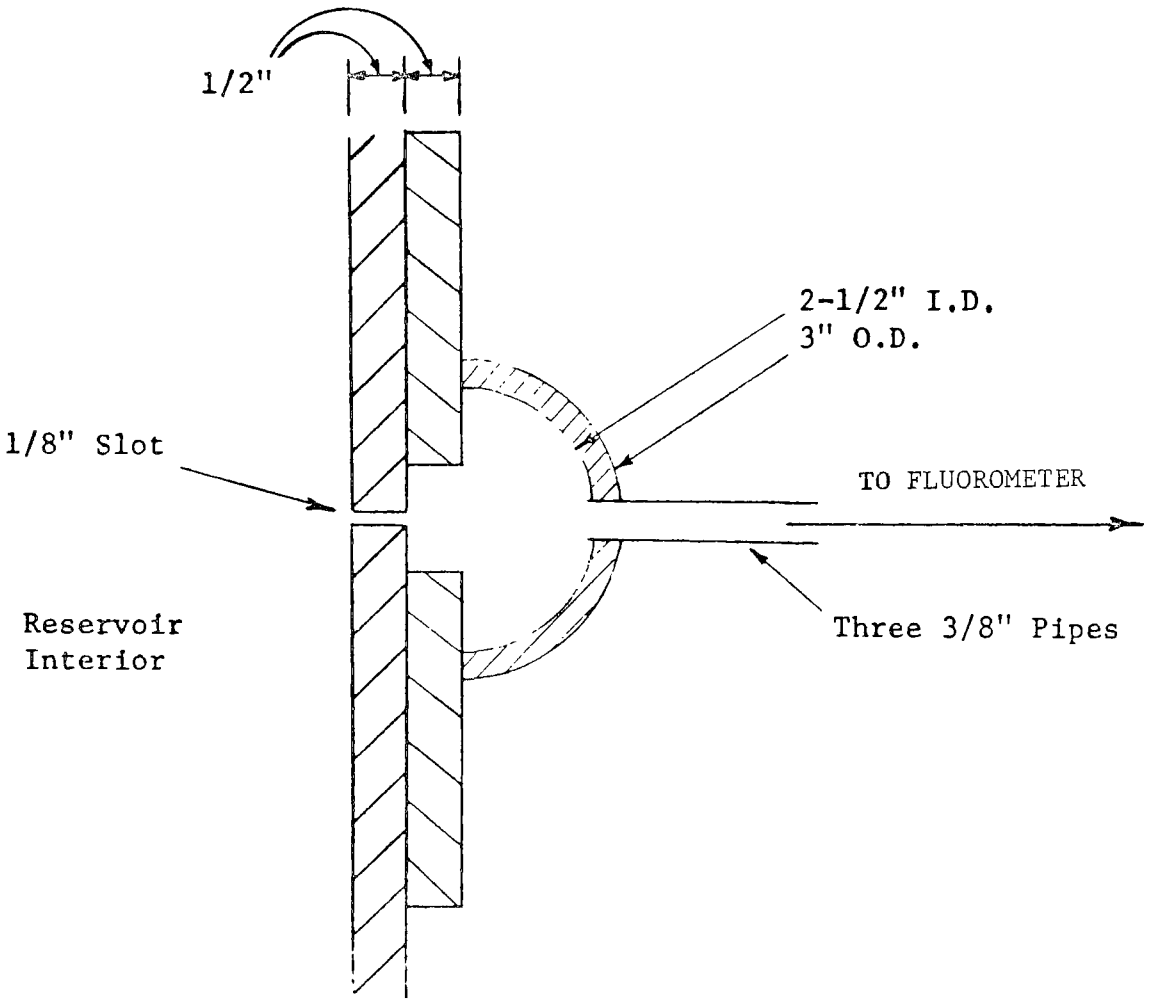

FIGURE 4.3 THE OUTLET SECTION

the outlet temperature. The flow then passed through a Tuner Model 111 Fluorometer with a flow through cell attachment (VT 110-880) to detect the concentration of any fluorescent dye, which was used as a tracer, in the outlet water. The outflow passed through a Brooks Flow Meter identical to that at the inflow end and was controlled by a valve.

The Fluorimeter, which has four different sensitivity ranges was calibrated in the laboratory against samples of known dye concentration. A log-log plot of Fluorometer dial reading vs. concentration for three of the sensitivities (Figure 4.4) produced a straight line from which a calibration equation was obtained. The Fluorometer dial reading was continuously monitored with a Sanborn recorder (Figure 4.5). The Sanborn recorder deflection was calibrated against the Fluorometer dial reading. A log-log plot (Figure 4.6) produced a straight line from which the relationship between the two was determined. Since the Fluorometer is also temperature sensitive a calibration for temperature was also made (Figure 4.7).

Temperature measurements in the flume were made with thermistor probes (Fenwal Electronics GA51SM2). The thermistor has a fast response time, 0.35 seconds to 98% of change in temperature. Thermistors were attached to two movable probes shown schematically in Figure 4.8. The probes

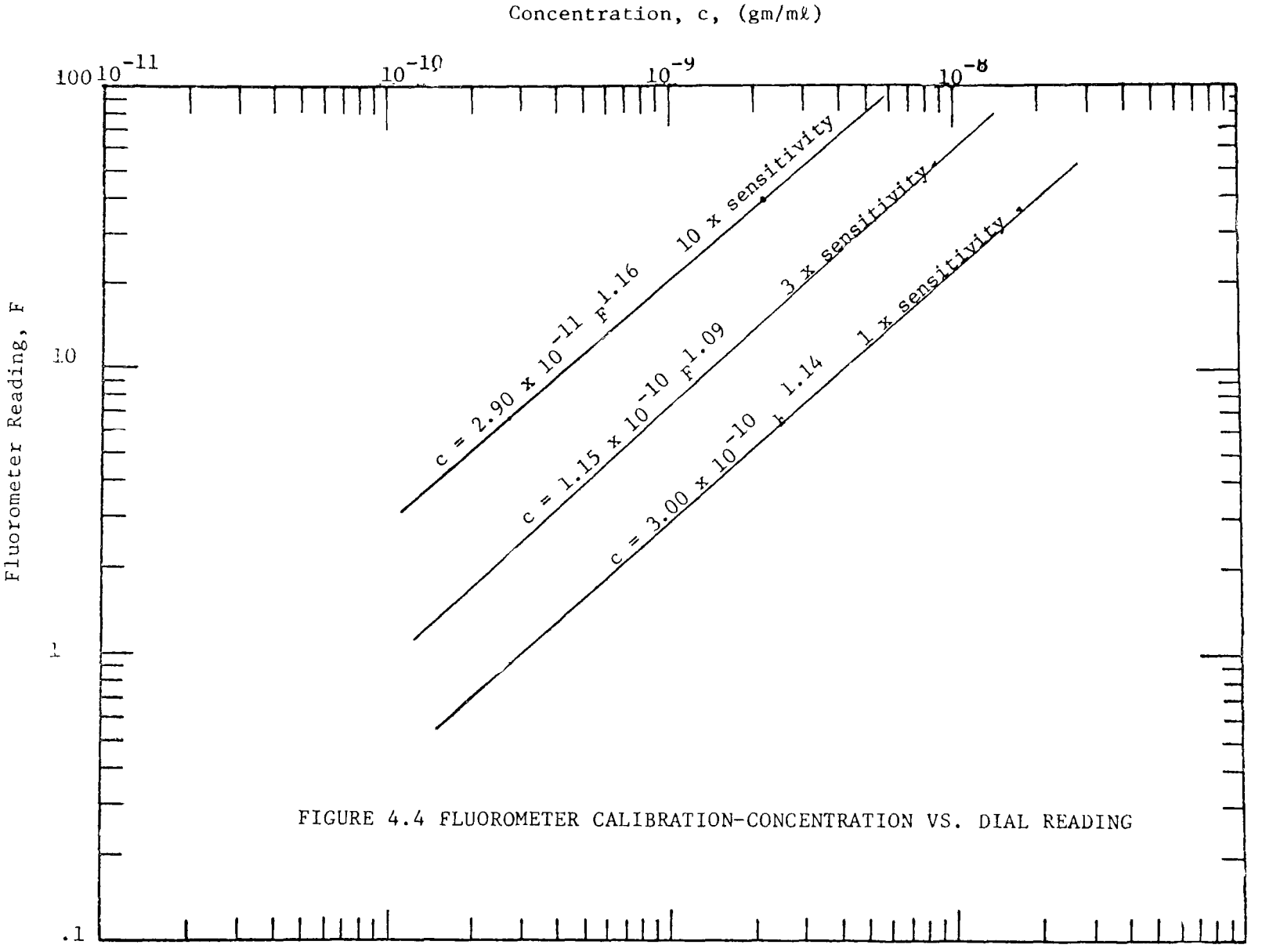

FIGURE 4.4 FLUOROMETER CALIBRATION-CONCENTRATION VS. DIAL READING

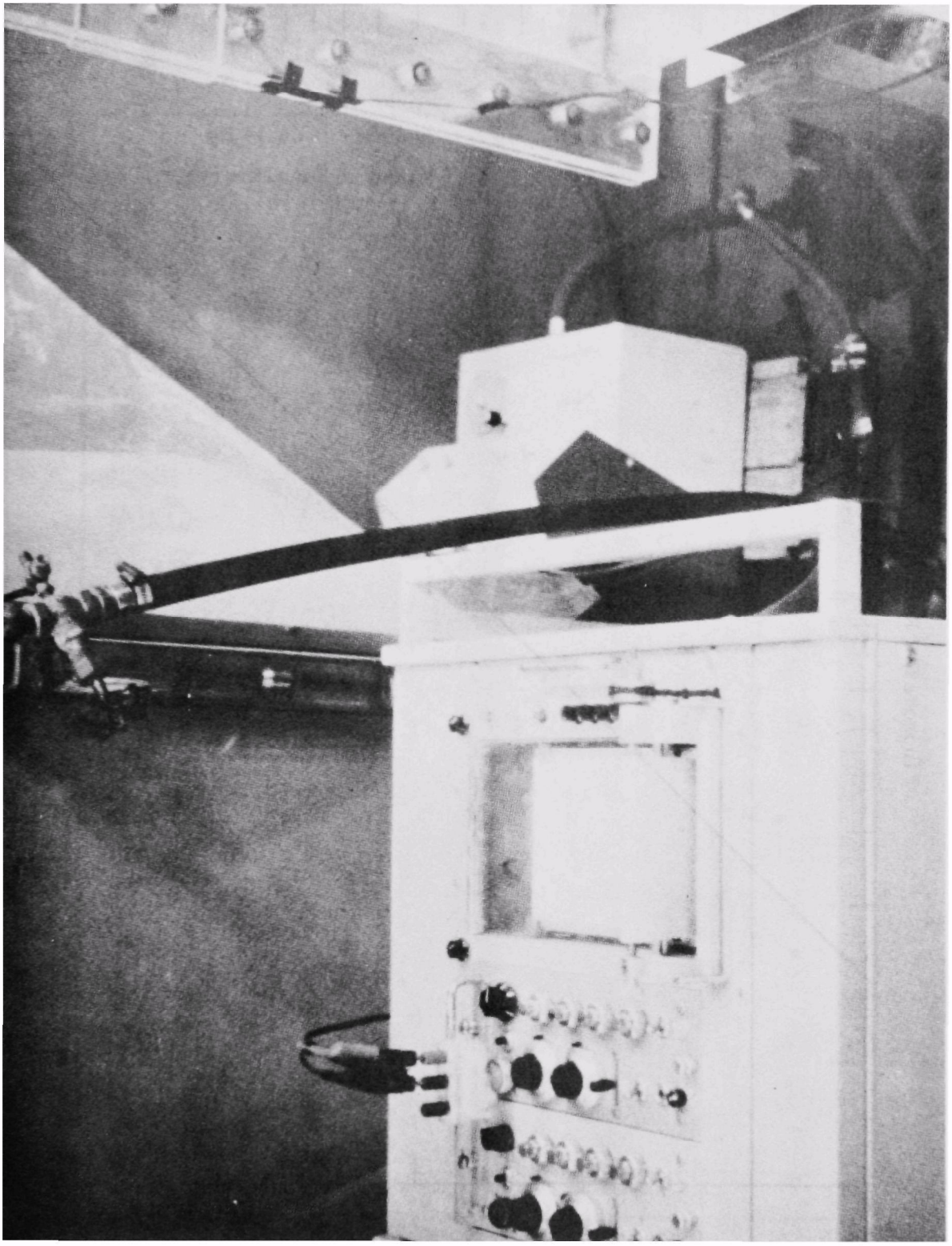

FIGURE 4.5 MONITORING OF FLUOROMETER READING WITH A SANBORN RECORDER

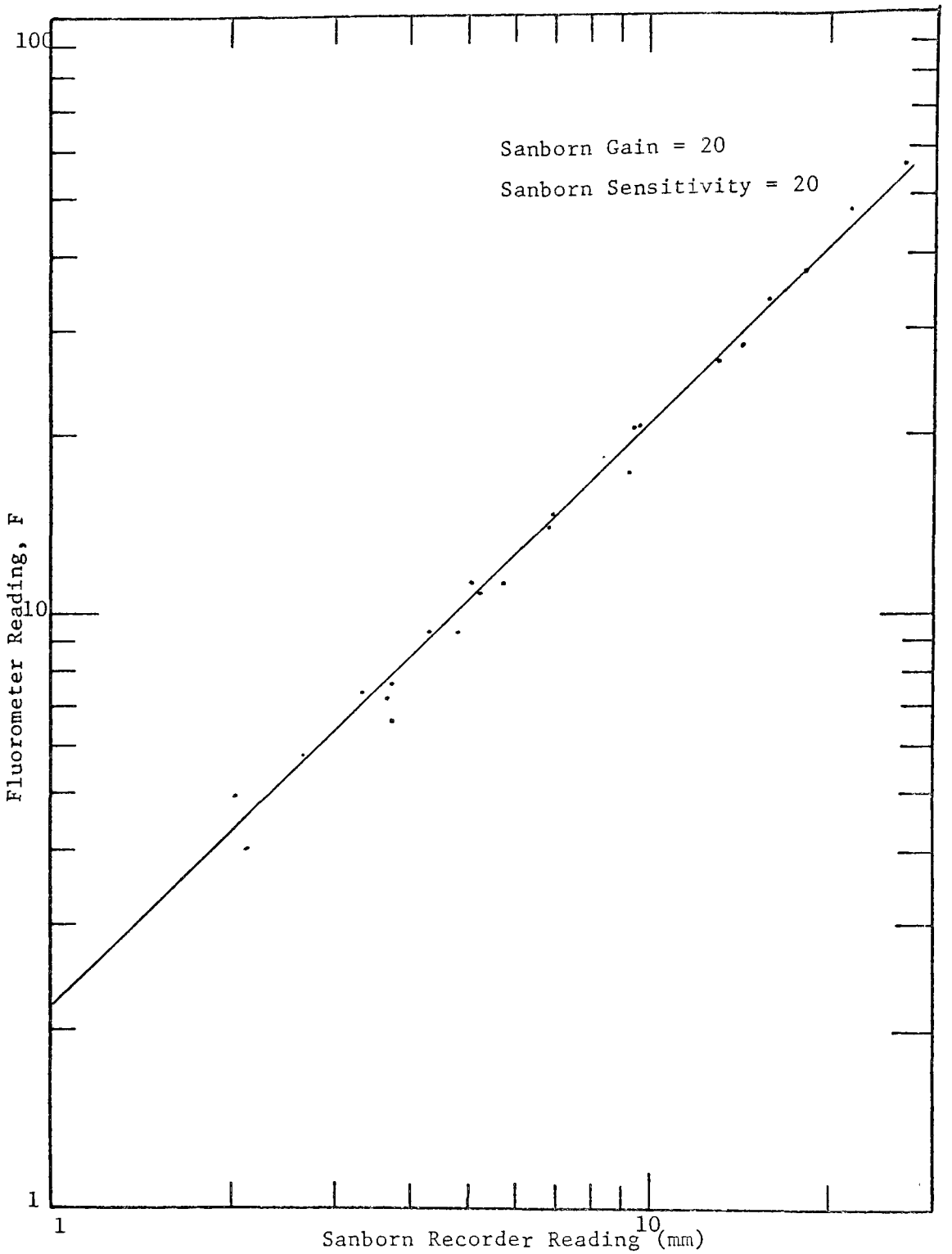

FIGURE 4.6 FLUOROMETER CALIBRATION-DIAL READING VS. SANBORN DEFLECTION

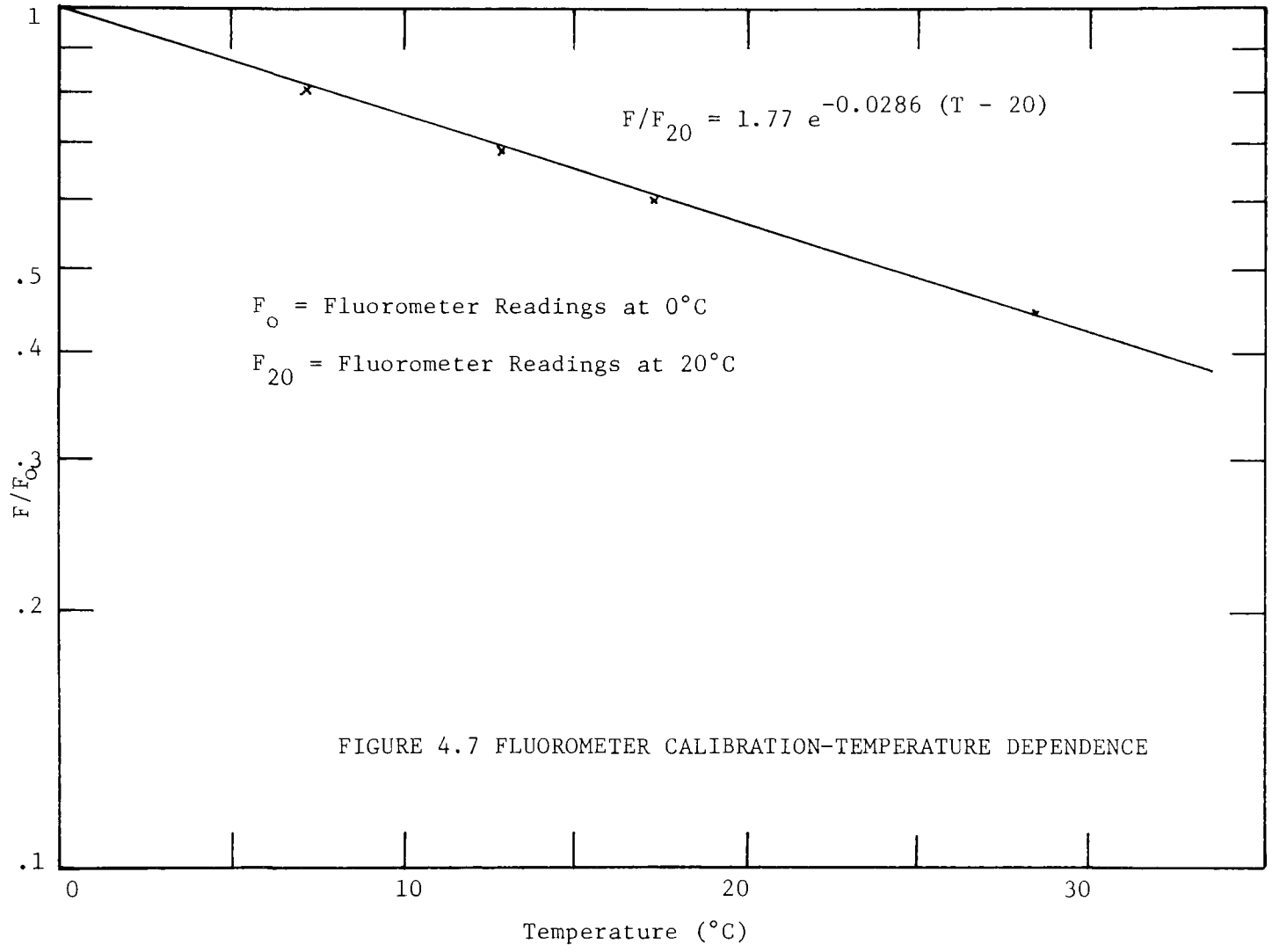

FIGURE 4.7 FLUOROMETER CALIBRATION-TEMPERATURE DEPENDENCE

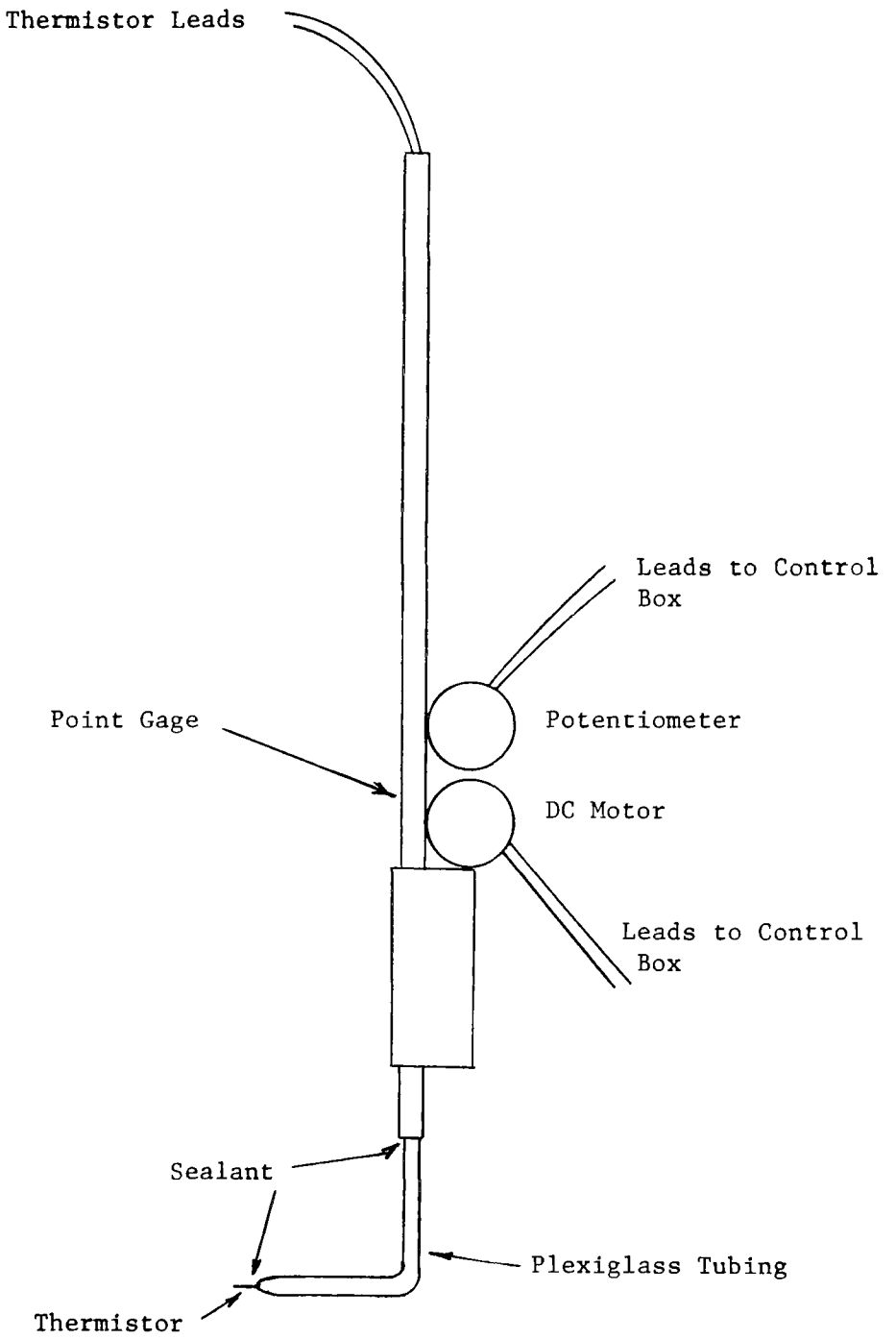

FIGURE 4.8 MOVABLE PROBE WITH THERMISTOR FOR TEMPERATURE MEASUREMENTS

were driven by a small remote controlled motor, geared to the point gage rod and a ten-turn potentiometer. The output from the potentiometer circuit was connected to the vertical axis of an x-y plotter (Bolt, Berenek and Neuman). The thermistor was connected through a switching box to a Wheatstore bridge circuit, the output of which was connected to the horizontal axis of the x-y plotter. As the movable probe made a vertical traverse, a direct plot of depth versus the millivolt output of the thermistor was obtained. The vertical traversing rate could be controlled to a maximum speed of about one and one-half feet per minute.

Artificial insolation for the laboratory reservoir was provided by thirty-six heat lamps (250 watt quartz iodine lamps GE Q250-PAR-38FL) one foot on center mounted on a joist suspended from the ceiling. The joist height could be varied by means of winches connecting the supporting cables to the joist. The intensity of the lamps could be varied to simulate the solar insolation intensities of different periods of the year. The reasons for choosing this type of lamp and the method of calibration is discussed in detail by Huber. Only the results are presented here in a plot of the average surface intensity vs. lamp height and voltage is presented in Figure 4.9.

The relative humidity, ψ, was measured with a Bacharod Industrial Instrument Co. #45715 Psychrometer.

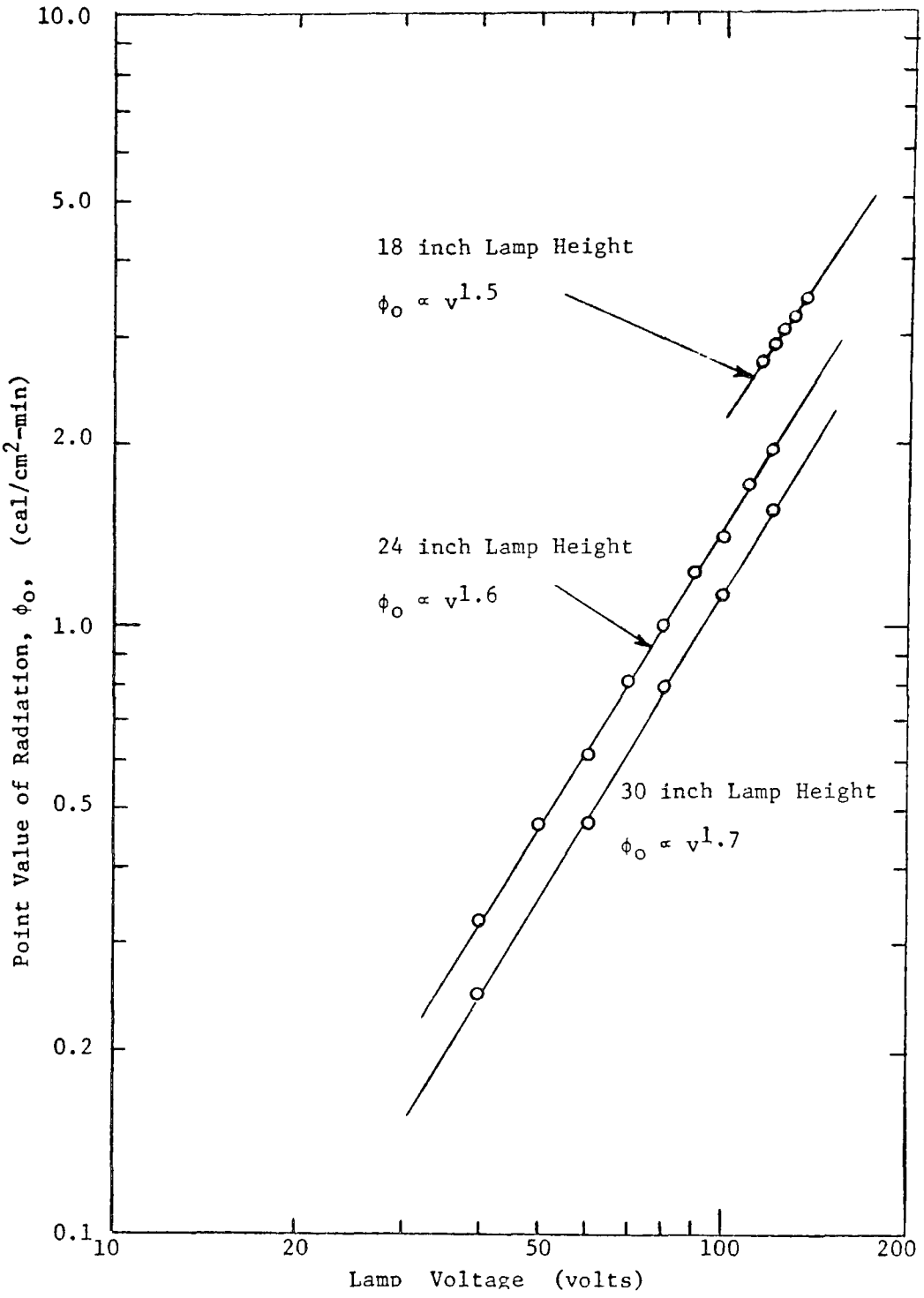

FIGURE 4.9 LABORATORY INSOLATION CALIBRATION

Surface elevations were measured with a point gage located on top of the reservoir.

4.2 Experimental Procedures

Three different types of experiments were conducted.

1. Constant inflow and outflow, no insolation
2. Variable inflow and outflow, variable insolation, constant surface elevation
3. Variable inflow and outflow, variable insolation, variable surface elevation

All of the tests were run for approximately 6 hours. At the start of a run the reservoir was isothermal at room temperatures. The inflow temperature was varied continuously in a sinusoidal manner simulating the type of distribution found in nature (53). The incoming insolation was provided by the overhead lamps varied in a stepwise manner simulating the variation of solar intensity changes through the year.

At a certain time in each experiment a known amount of Rhodamine B dye was "instantaneously" injected at the upstream end of the four foot entrance channel, downstream of the gravel filter. The outlet dye concentration was monitored continuously by the Fluorimeter. No concentration measurements were made within the flume but visual evidence (Figure 4.10) showed that each dye trace spread out

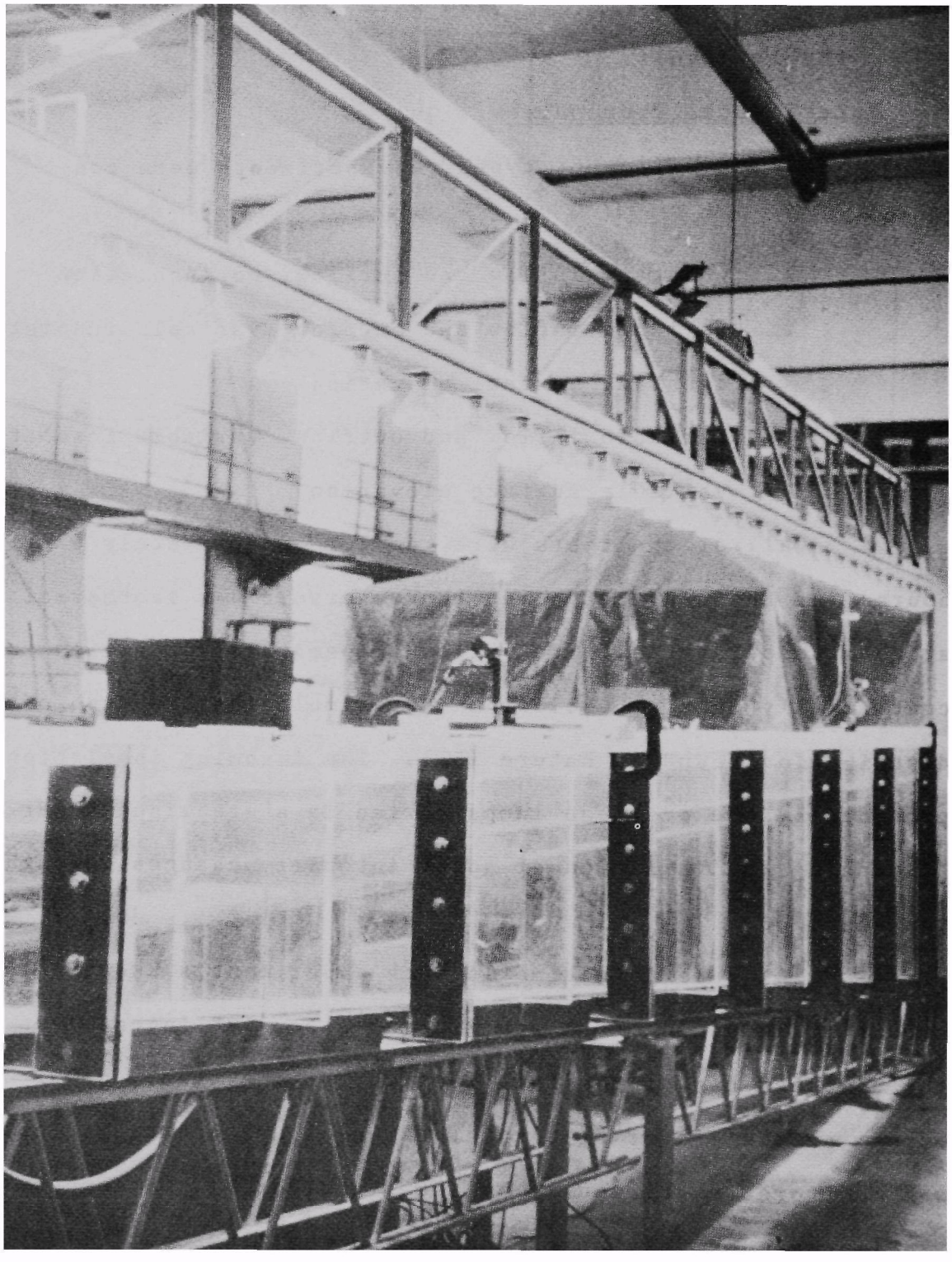

FIGURE 4.10 DYE TRACE IN A LABORATORY FLUME (3 TRACES)

horizontally along the entire length of the flume and that there was no visible turbulence in the reservoir except at the entrance section. It was possible to make more than one dye injection during an experiment if the previous tracers were seen to have passed through the reservoir or to be at an elevation where they would not interfere with an additional injection.

Temperature measurements of the inflow and outflow were made at 5 minute intervals, while temperature profiles in the flume were taken at approximately half-hour intervals. The air temperature and relative humidity were monitored about once an hour.

In the tests involving variable inflow and outflow, flow changes were made in a stepwise manner since no continuous means of varying the flow rate was available.

4.3 Inputs to the Mathematical Model

In addition to the parameters discussed in the previous section, other parameters remain to be determined. These are:

1. Side heat loss flux, ϕ_m
2. Evaporation constant a (Equation 2-40)
3. Values of the absorption coefficient, η, and the surface absorption fraction, β (Equation 2-31)

4. Thickness of the outflow withdrawal layer, δ, (Equation 2-49)

5. A cutoff criteria for the limit of the withdrawal layer when no density gradient exists at the outlet (Section 2.4.2)

6. Thickness of the inflowing layers, Δh, both for surface and subsurface entrance (Equation 2-92)

7. Inflow standard deviation, σ_i (Equation 2-51) and the assumption of a uniform flow for surface entrance over a thickness d_s (Equation 2-53b)

8. Mixing ratio, r_m and the mixing depth d_m (Equation 2-55 and 2-58)

9. The effect of numerical dispersion D_p (Equation 2-102)

The first three parameters were evaluated for the laboratory reservoir by Huber and Harleman. Only the results are presented.

$$\phi_m = 0.97\sigma \quad (T_w(y)^4 - T_a^4) \tag{4-1}$$

where

$T_w = T_w(y,t)$ = water temperature (°C)

$T_a = T_a(t)$ = air temperature (°C)

σ = Stephan-Boltzman constant = 8.132×10^{-11} cal/cm^2- min-°K^4

and $a = 0.00003$ (4-2a)

$\eta = 0.03\ cm^{-1}$ (4-2b)

$\beta = 0.70$ (4-2c)

4.3.1 Evaluation of the Outflow Withdrawal Layer Thickness

The outflow withdrawal layer thickness, δ, was calculated from Koh's Equation 2-49.

$$\delta = \frac{7.14\ x^{1/3}\varepsilon^{-1/6}}{\left[\frac{D\nu}{g}\right]^{1/6}} = \frac{7.14\ x^{1/3}}{\alpha_o} \qquad (4\text{-}3)$$

where

$D = 0.00144\ cm^2/sec$ (molecular diffusivity of heat)

$\nu = 0.01\ cm^2/sec$

$g = 980\ cm/sec^2$

Equation 4-3 was evaluated at an x chosen at about the midpoint of a horizontal line between the outlet and the reservoir bottom, so that x=240cm.

Substituting the above values in Equation 4-3 results in

$$\delta = 2.2\ \varepsilon^{-1/6} \qquad (4\text{-}4a)$$

or

$$\delta = \text{const}\left[\frac{1}{\rho}\ \frac{d\rho}{dy}\right]^{-1/6} \qquad (4\text{-}4b)$$

The density gradient can be related to the temperature gradient through the expression

$$\frac{d\rho}{dy} = \frac{d\rho}{dT}\frac{dT}{dy} \tag{4-5}$$

A least squares fit of density vs. temperature for the ranges of T = 4°C to T = 26°C, Figure 4.11, yielded

$$\rho = 1.0 - 6.63 \times 10^{-6} (T - 4)^2 \text{ gm/cm}^2 \tag{4-6}$$

Thus

$$\varepsilon = \frac{1}{\rho}\frac{d\rho}{dy} = \frac{2(T - 4)}{151000 - (T-4)^2}\frac{dT}{dy} \quad (\text{cm}^{-1} \text{ or } \text{m}^{-1}) \tag{4-7}$$

Equation 4-7 was used in both the laboratory and field study.

The validity of Equation 4-3 is based on a small perturbation parameter, ω, which imposes the restriction

$$\omega = \frac{q}{D\alpha_o x^{2/3}} << 1 \tag{4-7a}$$

Koh has presented an empirical relationship to extend Equation 4-3 when Equation 4-7a is violated

$$\frac{\alpha}{\alpha_o} = 3.5 \frac{q}{D\alpha_o x^{2/3}}^{-1/6} = 3.5\omega^{-1/6} \quad \text{for } 0.3<\omega<c \tag{4-8}$$

where c = 25 for thermal stratification and 1000 for salinity stratification and α replaces α_o in Equation 4-3.

The maximum flow rate, Q_o used in the laboratory was 7500 cm^3/min. This is equivalent to a flow per unit width, q_o, of 248cm^2/min. For a typical valve of ε of

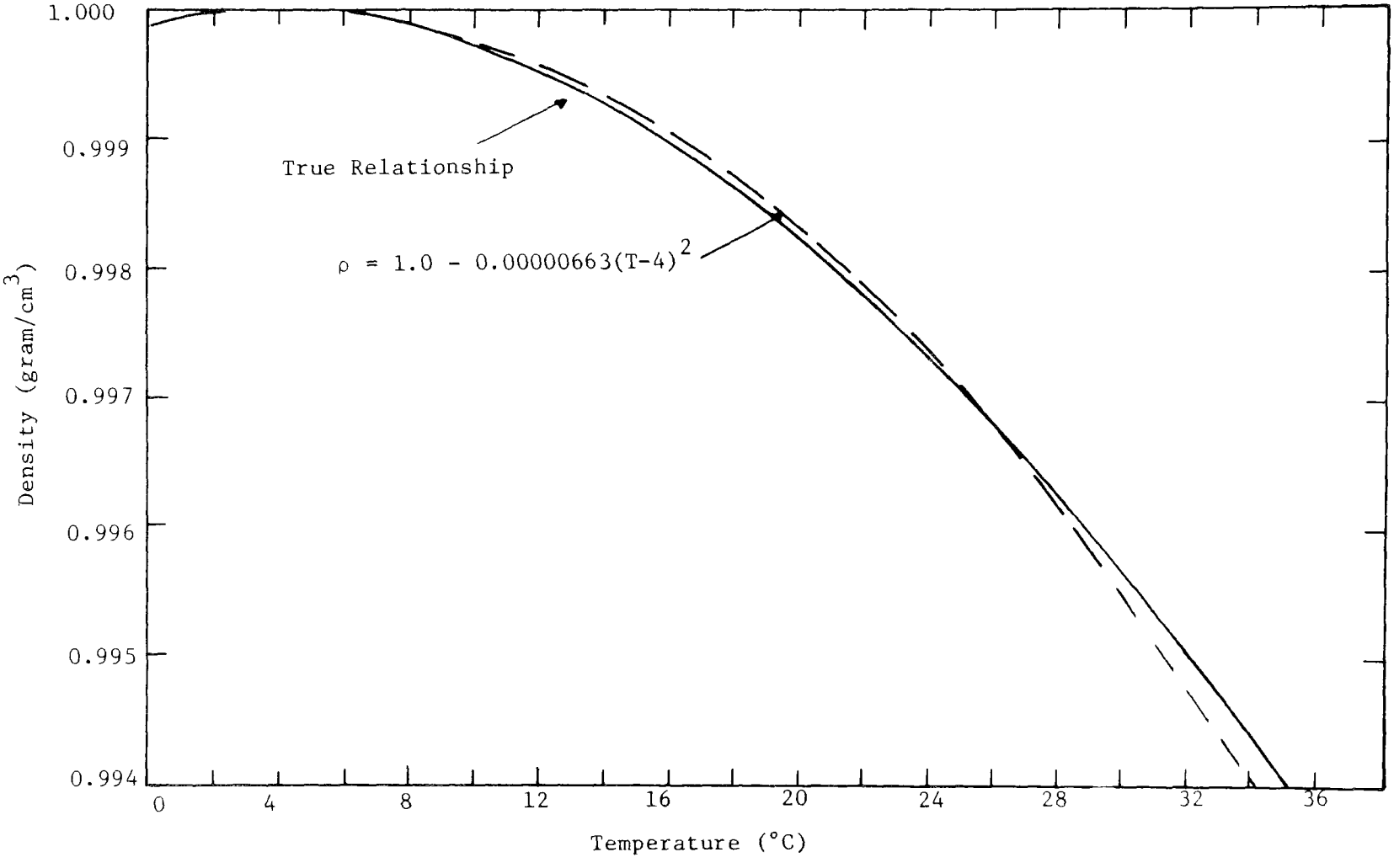

FIGURE 4.11 WATER TEMPERATURE VS. DENSITY

3×10^{-5} cm^{-1} ($\frac{dT}{dy} \simeq 0.1$ °C/cm^{-1}) the value of ω is 28. However, the effect of the correction for this higher value of ω is minor and Equation 4-3 was used.

For high stratification ($\frac{dT}{dy} \simeq 0.3$ °C/cm) measured values from dye traces of δ agreed well with the values of the order of 10cm calculated from Equations 4-4a. Therefore, Equation 4-4a was assumed to be valid.

4.3.2 Thickness of the Inflowing Layers, Δh, for Lagtime Determination

The thicknesses Δh for lagtime determination were found from observation to be approximately 5cm for surface flow and 4cm for subsurface flow. A typical depth of water in the inlet section is 5cm and this is an indication that Δh can be related to the depth of the inflowing stream. The remaining parameters were evaluated from the experiments and are discussed with the results.

4.4 Experimental Results

4.4.1 Runs with Variable Insolation and Flow Rates, Constant Surface Elevation

Two experiments were conducted in this series. Since the temperature model had been verified previously by Huber and Harleman in the experiments conducted in the same flume, the main objective was to investigate the validity of the water quality model. Therefore, the input temperature, insolation and flow rates were kept as

identical as possible between the two runs. Thus, it is felt that the dye tests taken in the two runs can be directly compared.

First, the final predicted results will be presented, using an inflow standard deviation, $\sigma_i = 5$ cm (for sinking flow) an entrance mixing ratio and depth, $r_m = 0.2$, $d_m = 5$ cm, and a depth for uniform su face entrance, $d_s = 5$ cm. Then the sensitivity of both the temperature and water quality models to various parameters will be discussed.

The typical inflow temperature variation flow rates and insolation values for this set of experiments are found in Figure 4.12 along with measured and predicted outflow temperatures. Before the peak temperature is reached the predicted outlet temperatures are slightly higher than those measured. After the peak temperature, the predicted values fall off more quickly than the measured values. However, the measured and predicted temperatures are all within 1°C.

Predicted and measured vertical temperature profiles are given in Figure 4.12a. The predicted profiles, though generally slightly lower than those measured, agree within 1°C in all cases.

Three dye tests, with injections at 10,33 and 329 minutes after the start of the test were made. In each

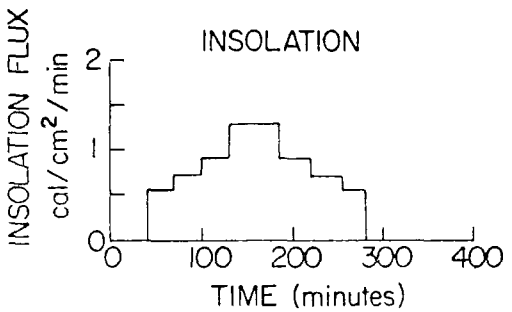

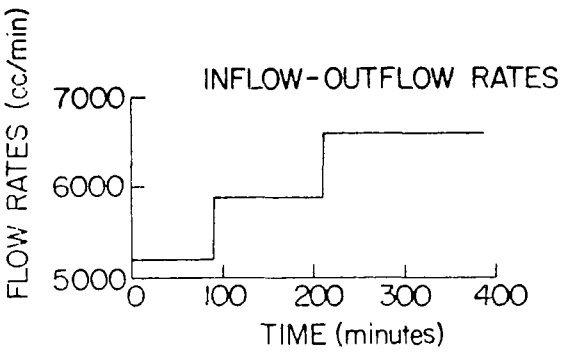

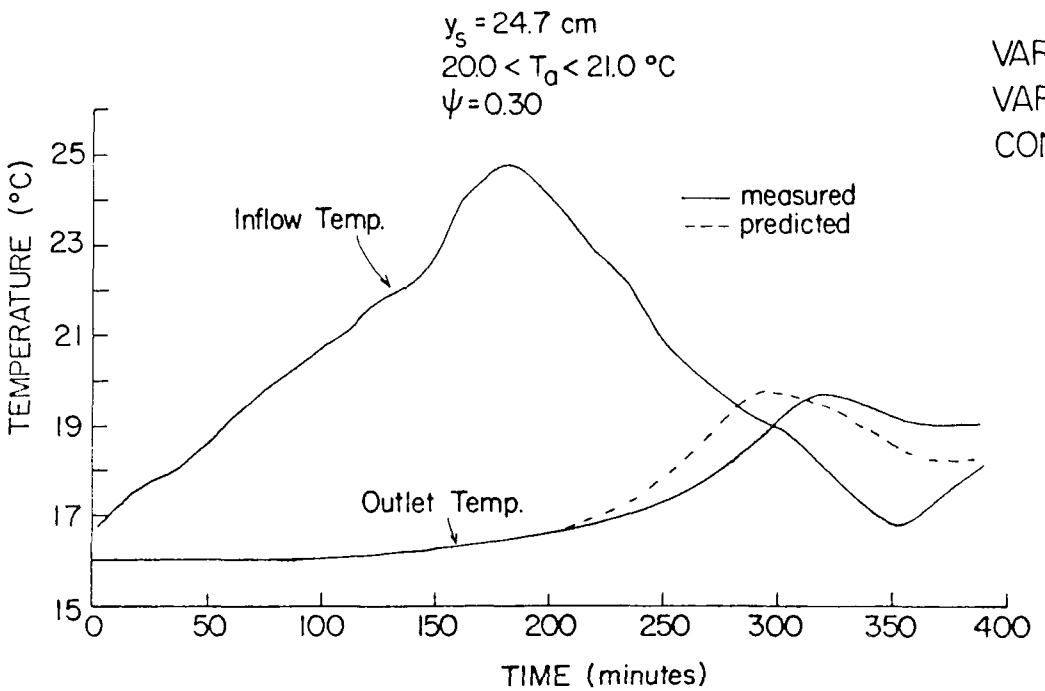

VARIABLE INFLOW-OUTFLOW
VARIABLE INSOLATION
CONSTANT SURFACE ELEVATION

FIGURE 4.12 INPUTS TO THE VARIABLE INFLOW-OUTFLOW, VARIABLE INSOLATION, CONSTANT SURFACE ELEVATION EXPERIMENTS

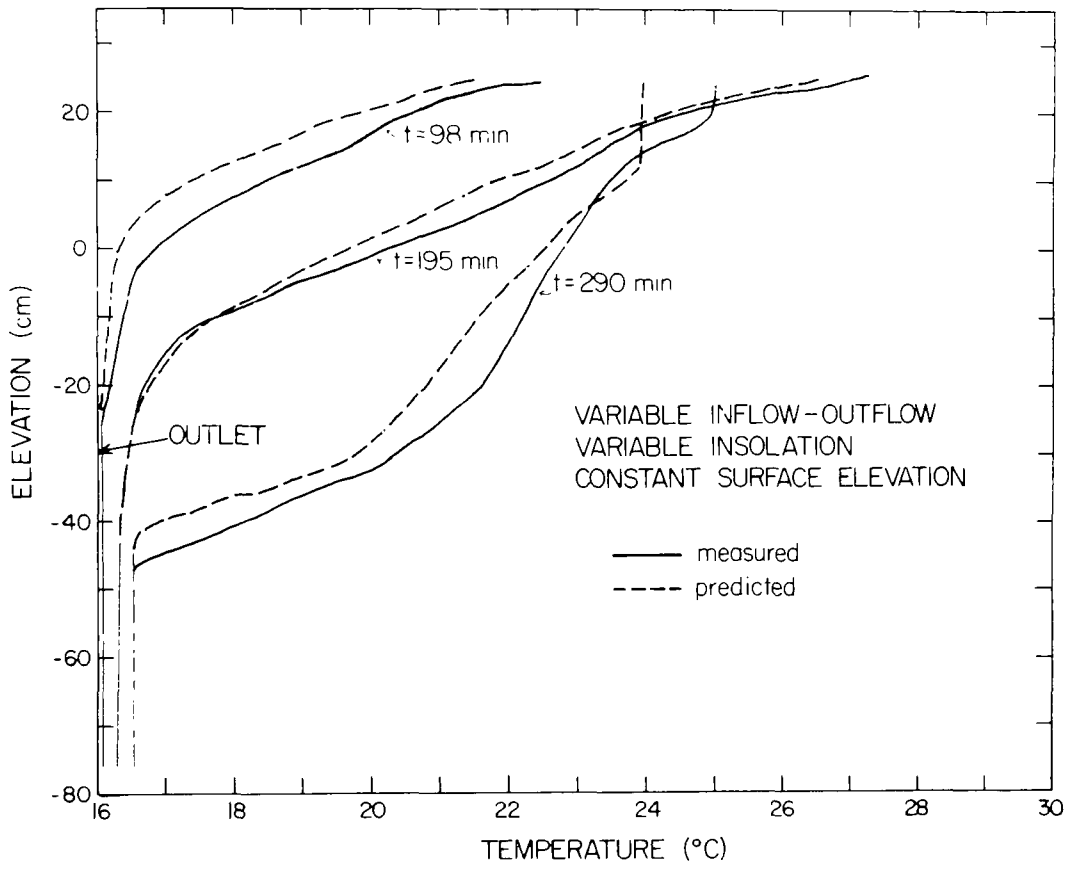

FIGURE 4.12a TEMPERATURE PROFILES

test, 10^{-2} gm of tracer was injected. The results are presented in Figures 4.13 and 4.14 in terms of concentration measured at the outlet divided by the mass injected vs. time. In Figure 4.15, the results are presented in terms of the total percentage of tracer which had passed through the flume (tracot, Equation 3-38) vs. time.

From Figures 4.13, 4.14, it can be seen that the order of magnitude of the concentrations predicted in the outlet is in reasonably good agreement with the measured values. The measured and predicted arrival time of the peak concentration and the peak concentration divided by the mass injected are presented in Table 4.1.

It is noted that the peak concentrations are in very good agreement with measured values, differing at most by 2.48×10^{-6} gm^{-1}. The time of the peak outlet concentration is also reasonably well predicted.

For the 10 and 33 minute dye injections, the predicted start of the outlet concentration curve, Figures 4.13, 4.14, is somewhat early. This may be partially due to frictional affects which are not accounted for in the mathematical model.

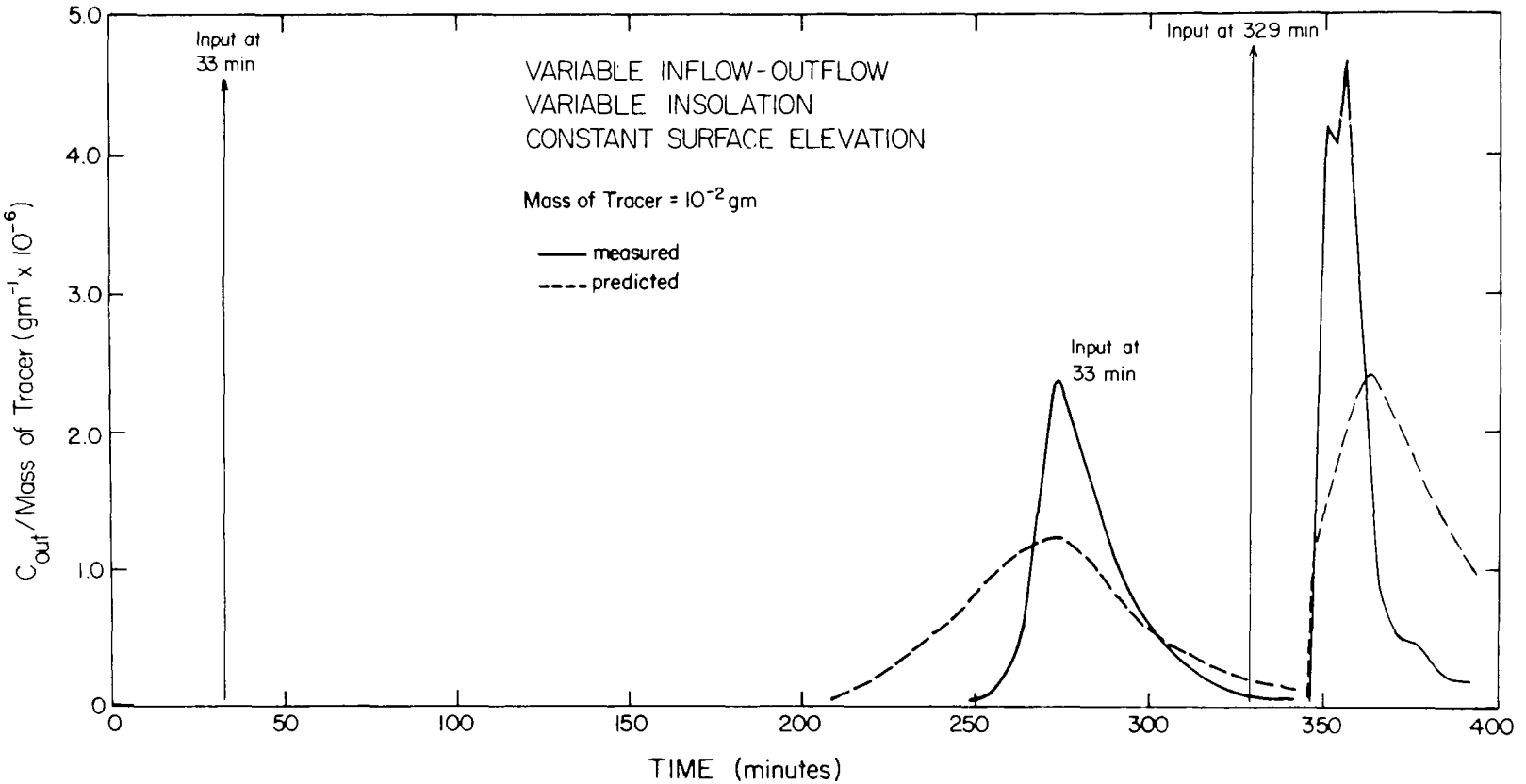

FIGURE 4.13 CONCENTRATION PREDICTIONS

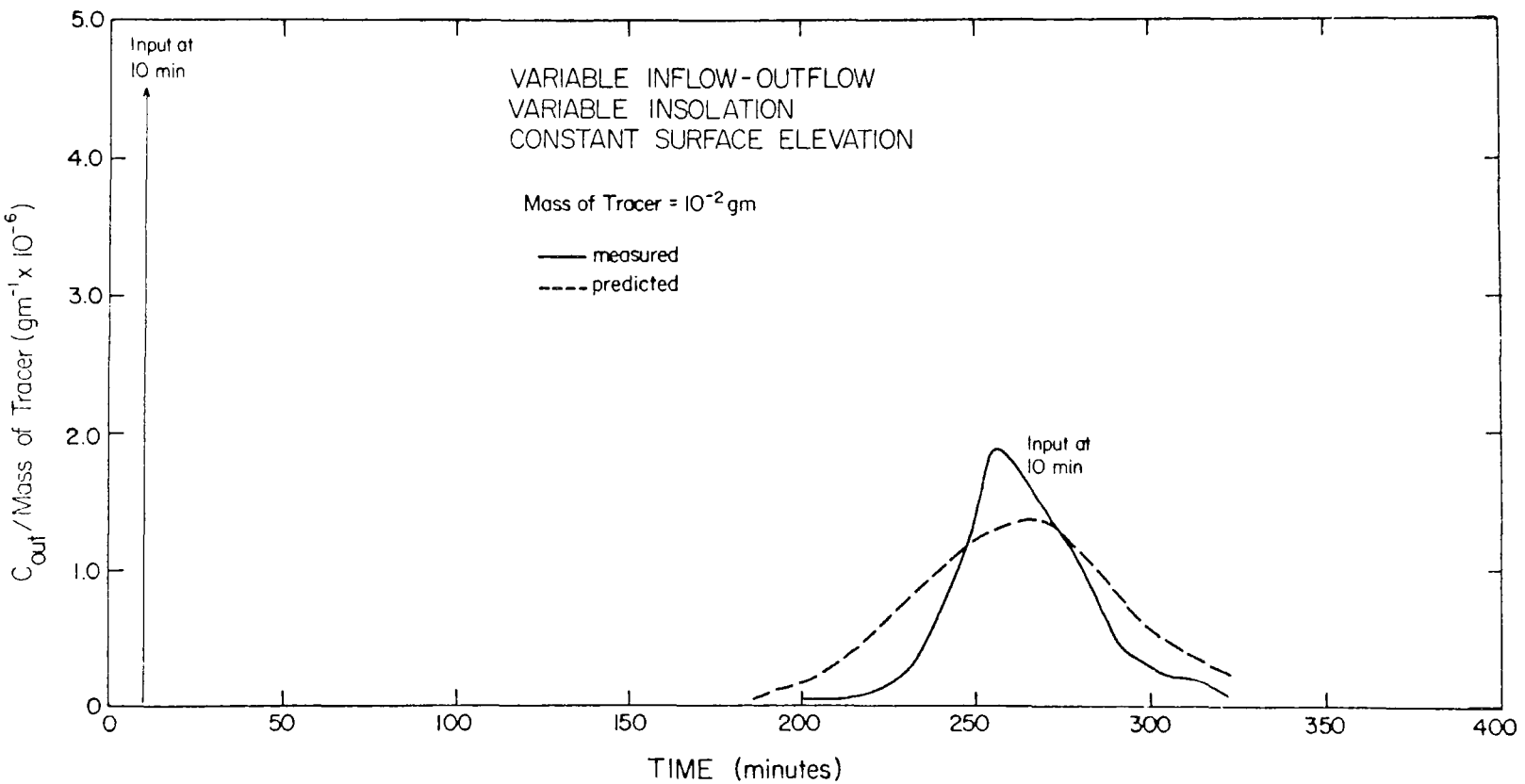

FIGURE 4.14 CONCENTRATION PREDICTIONS

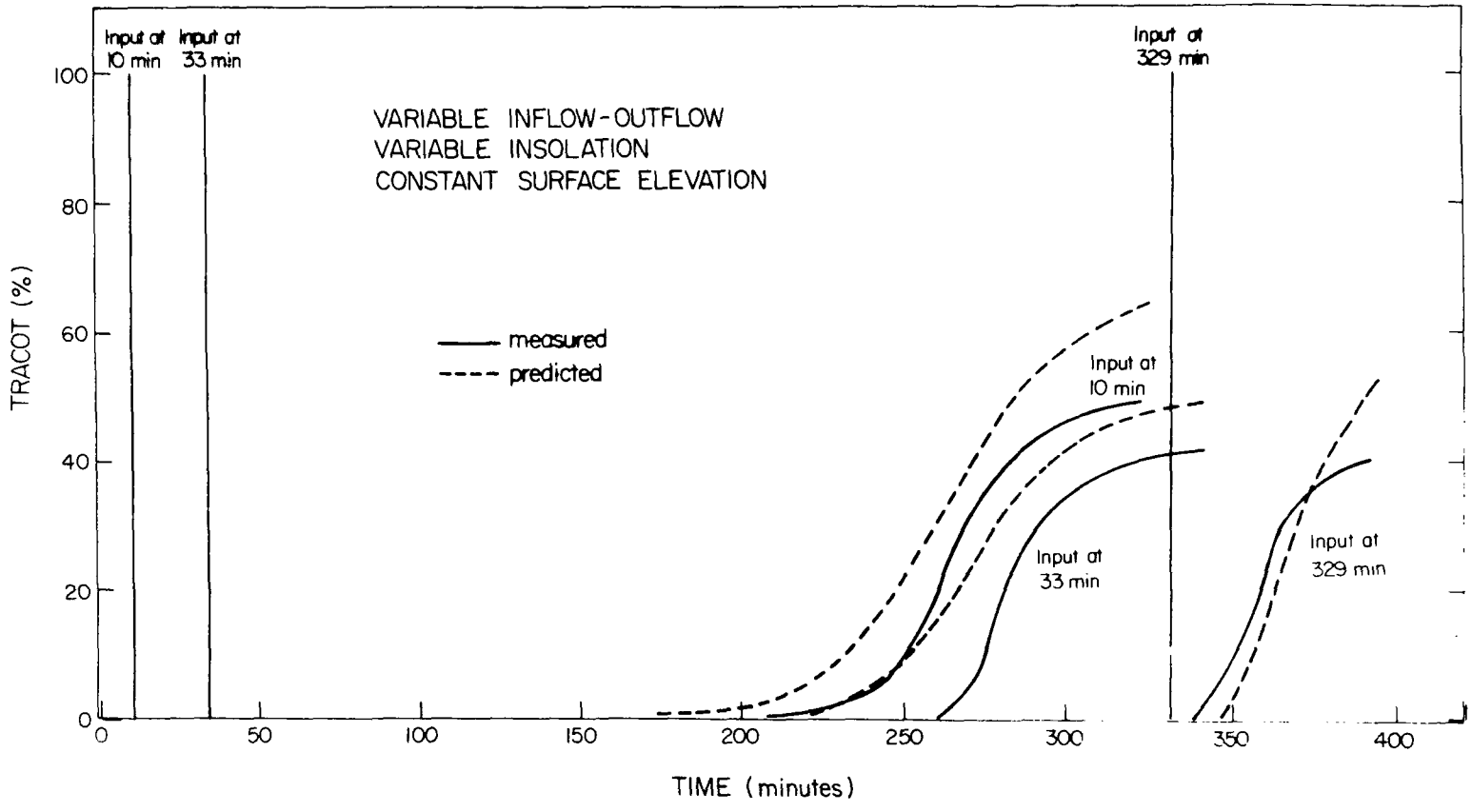

FIGURE 4.15 CUMULATIVE MASS OUT PREDICTIONS

TABLE 4.1

TRACE (MIN)	PEAK CONCENTRATION/MASS INJECTED (gm^{-1})		PEAK ARRIVAL TIME (MIN)	
	MEASURED	PREDICTED	MEASURED	PREDICTED
10	1.86×10^{-6}	1.35×10^{-6}	255	265.0
33	2.35×10^{-6}	1.21×10^{-6}	273	272.5
329	4.88×10^{-6}	2.40×10^{-6}	355	362.5

TABLE 4.1 PEAK CONCENTRATION AND ARRIVAL TIMES-VARIABLE INFLOW-OUTFLOW AND INSOLATION, CONSTANT SURFACE ELEVATION

This may also account for the lower predicted rate of fall off from the peak concentration. As can be seen in Figure 4.15, both of these effects tend to cause the total predicted percentage of traces passing through the reservoir to be higher than that measured.

A sensitivity analysis for parameters 5, 7, 8 and 9 in Section 4.3 follows.

4.4.1.1 Sensitivity to a Cutoff Criterion for the Upper Limit of the Withdrawal Layer When No Density Gradient Exists at the Outlet

When no density gradient exists at the outlet, the thickness of the withdrawal layer, δ , (Equation 2-49) is theoretically infinite. In practice, δ would equal the total depth of water in the reservoir. This corresponds to the early portion of an experiment when the incoming warmer water has not yet reached the outlet and the temperature in the vicinity of the outlet is the initial isothermal reservoir temperature. As the stratification begins to form, although no density gradient exists at the outlet, a gradient will exist near the surface. The depth at which the density gradient becomes zero increases with time until a gradient eventually exists at elevation of the outlet (Figure 4.16a). Though the mathematical model would not "sense" a density gradient if none existed at the outlet, the physical system tends to withdraw water mainly from the

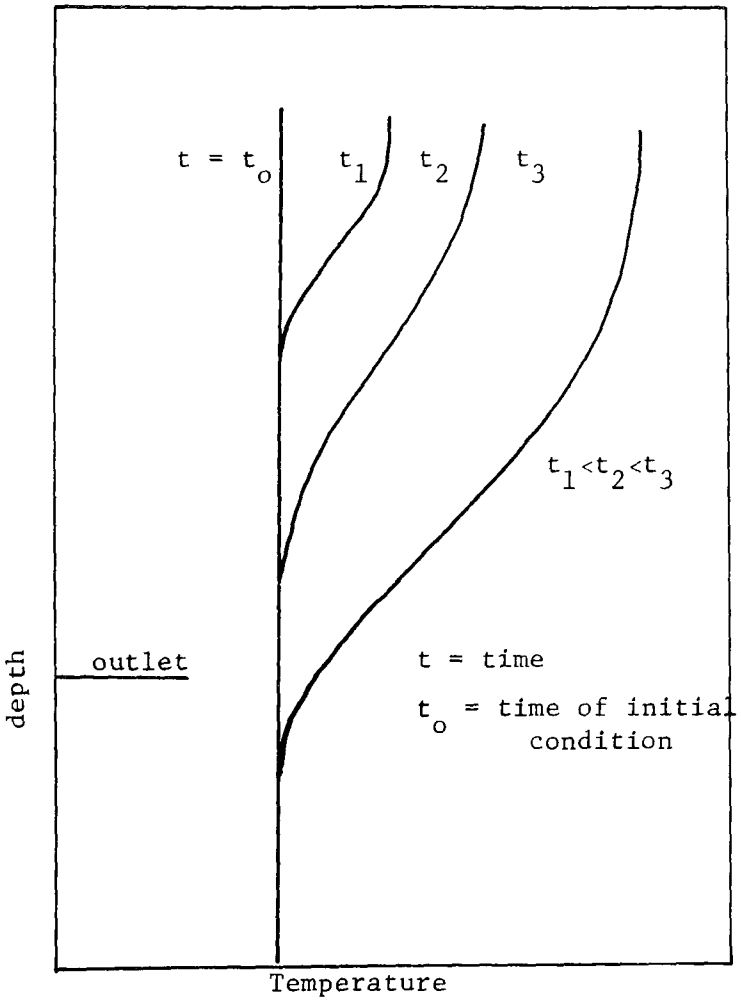

FIGURE 4.16a

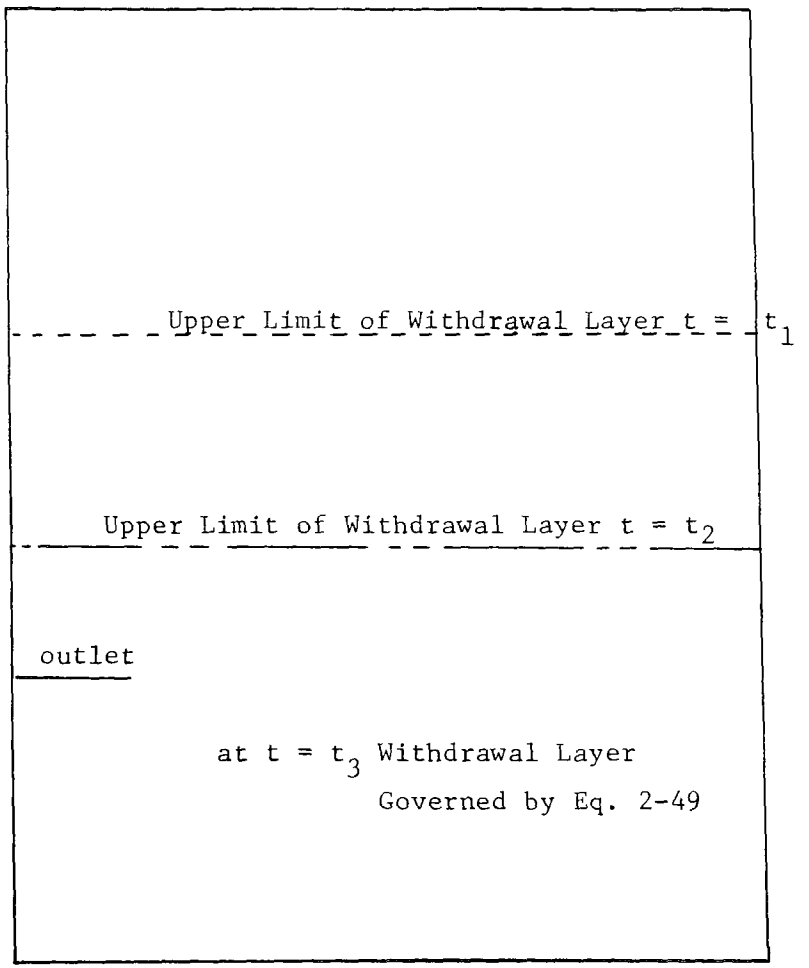

FIGURE 4.16b

FIGURE 4.16 CUT OFF CRITERIA FOR THE WITHDRAWAL LAYER

isothermal region (Figure 4.16b). Thus a criterion was needed for the magnitude of the temperature gradient, $(\Delta T/\Delta y)_c$, which would dictate the upper limit of the withdrawal layer in the case of zero density gradient at the outlet.

Two values were tested, $(\Delta T/\Delta y)_c$ of 0.01 and 0.001 $^{\circ}$ c/cm for the laboratory. Temperature predictions were minimally effected. However, the dye tests showed that a criteria was definitely needed. In Table 4.2 it is seen that the earlier the dye traces the more sensitive to $(\Delta T/\Delta y)_c$ the prediction of the start of the arrival of the trace are. However, it should be also noted that although significant improvement was seen in the time at which 1% of the tracer was predicted to have passed through the reservoir, less change occurred in the 5 and 10 percent cases and the arrival time of the peak concentration remained unchanged. This is because the cutoff criterion is in effect only as long as there is no density gradient at the outlet. When the stratification begins to effect the density gradient at the outlet Equation 4-4a governs the withdrawal layer phenomena. Changing the cutoff criteria

TABLE 4.2

($\sigma_i = 2.5 \quad r_m = 0.2$)

Cut Off Criteria	Flow Through Time (min.) 1%	5%	10%	Peak	Trace Input
$(\Delta T/\Delta y)_c \leq 0.01$	47.5	202.5	220.0	270.0	10 min.
$(\Delta T/\Delta y)_c \geq 0.001$	202.5	225.0	237.5	270.0	
Measured	220.	240.	248.	255.	
$(\Delta T/\Delta y)_c \leq 0.01$	200.0	227.5	242.5	277.5	33 min.
$(\Delta T/\Delta y)_c \geq 0.001$	225.0	245.0	255.0	277.5	
Measured	260.	268.	273.	273.	

TABLE 4.2 CUT OFF CRITERION

has little effect on the prediction of the peak time.

4.4.1.2 Sensitivity to a Guassian Vs. Uniform Surface Distribution and the Inflow Standard Deviation, σ_i, for Subsurface Inflow

The effect of assuming a Gaussian distribution with σ_i = 3cm vs. a uniform distribution d_s = 5cm for the surface inflow velocity profile was found to have no effect on the temperature prediction early in the run. However, in Figures 4.17 and 4.18 the Gaussian assumption is seen to predict slightly higher temperatures. A Gaussian assumption also raises the predicted outflow temperatures (Figure 4.19), but lowers the predicted percentage mass out (Figure 4.20, 4.21). A Gaussian assumption for the surface inflow distribution inputs water in such a way as to add to the stratification near the surface. Since the thicknesses of the inflow layers are comparable (5 m for uniform inflow and 6 m for Gaussian) the Gaussian distribution results in warmer surface temperatures.

The higher percentage mass out prediction under the uniform surface input distribution is due to the original input being concentrated uniformly in the surface layers rather than being diluted as in the Gaussian distribution. This produces higher concentration in the outflow and consequently higher percentage mass out prediction.

No effect of varying σ_i from 2.5 to 5.0 for sinking flow with d_s = 5 cm was noted in temperature prediction.

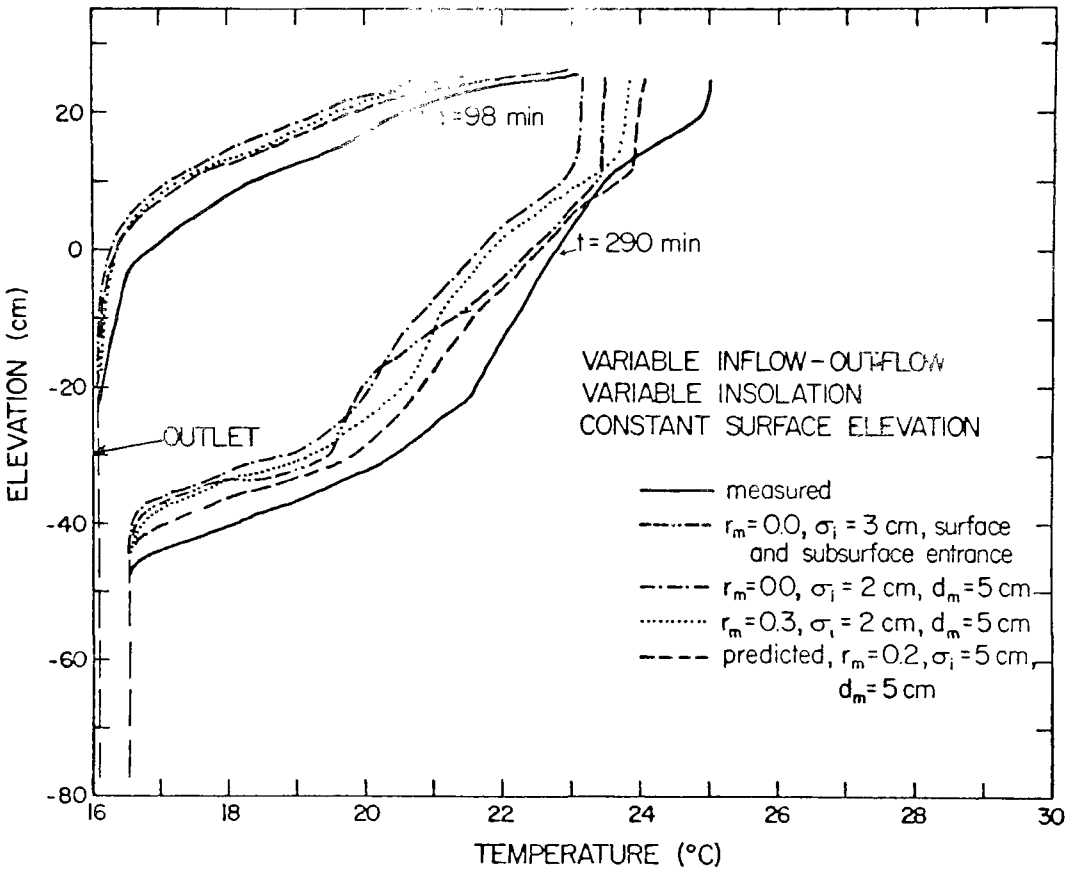

FIGURE 4.17 TEMPERATURE PROFILE PREDICTIONS - SENSITIVITY ANALYSIS

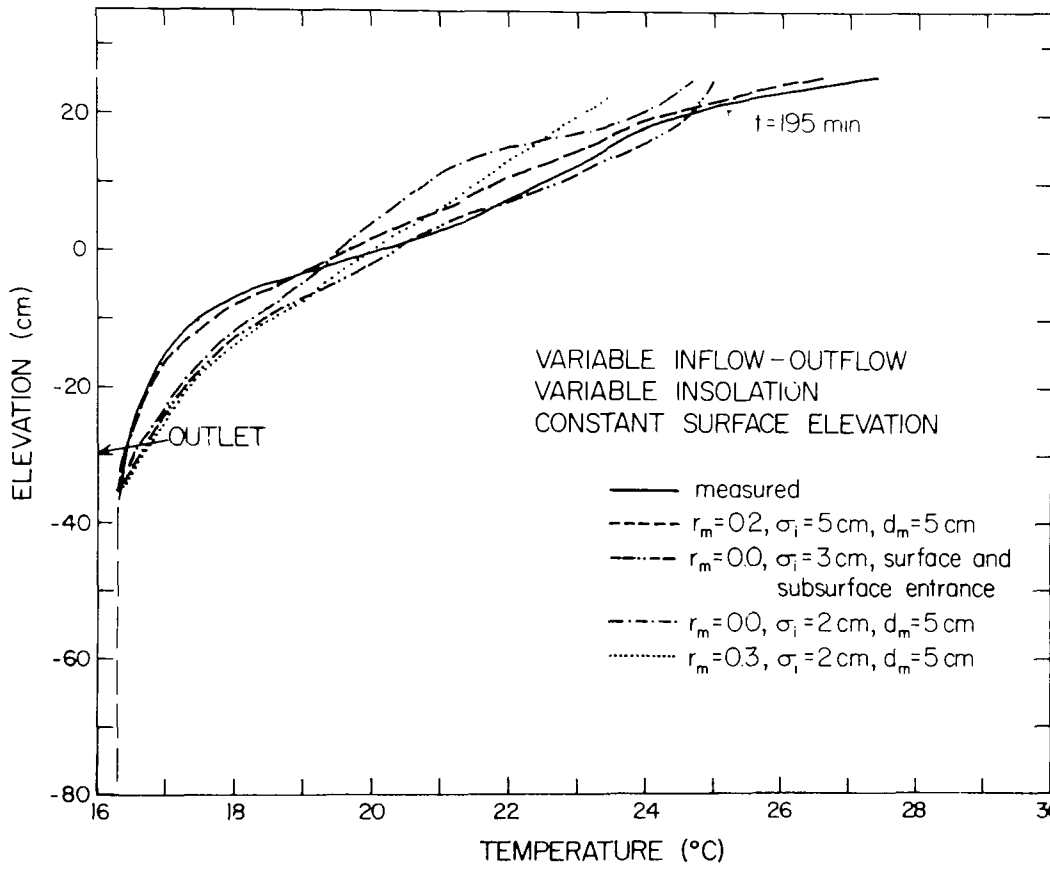

FIGURE 4.18 TEMPERATURE PROFILE PREDICTIONS - SENSITIVITY ANALYSIS

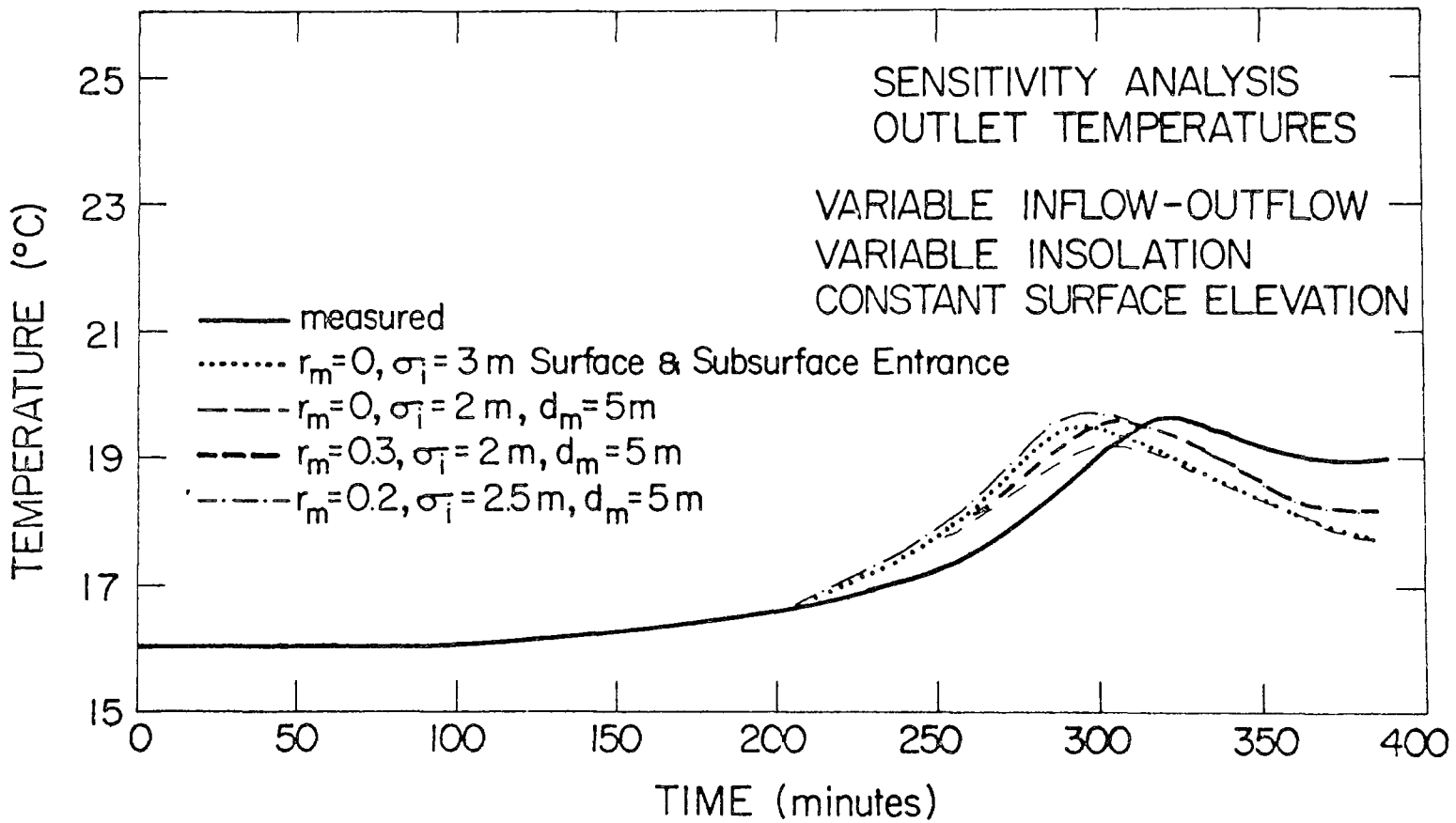

FIGURE 4.19 OUTLET TEMPERATURE PREDICTIONS - SENSITIVITY ANALYSIS

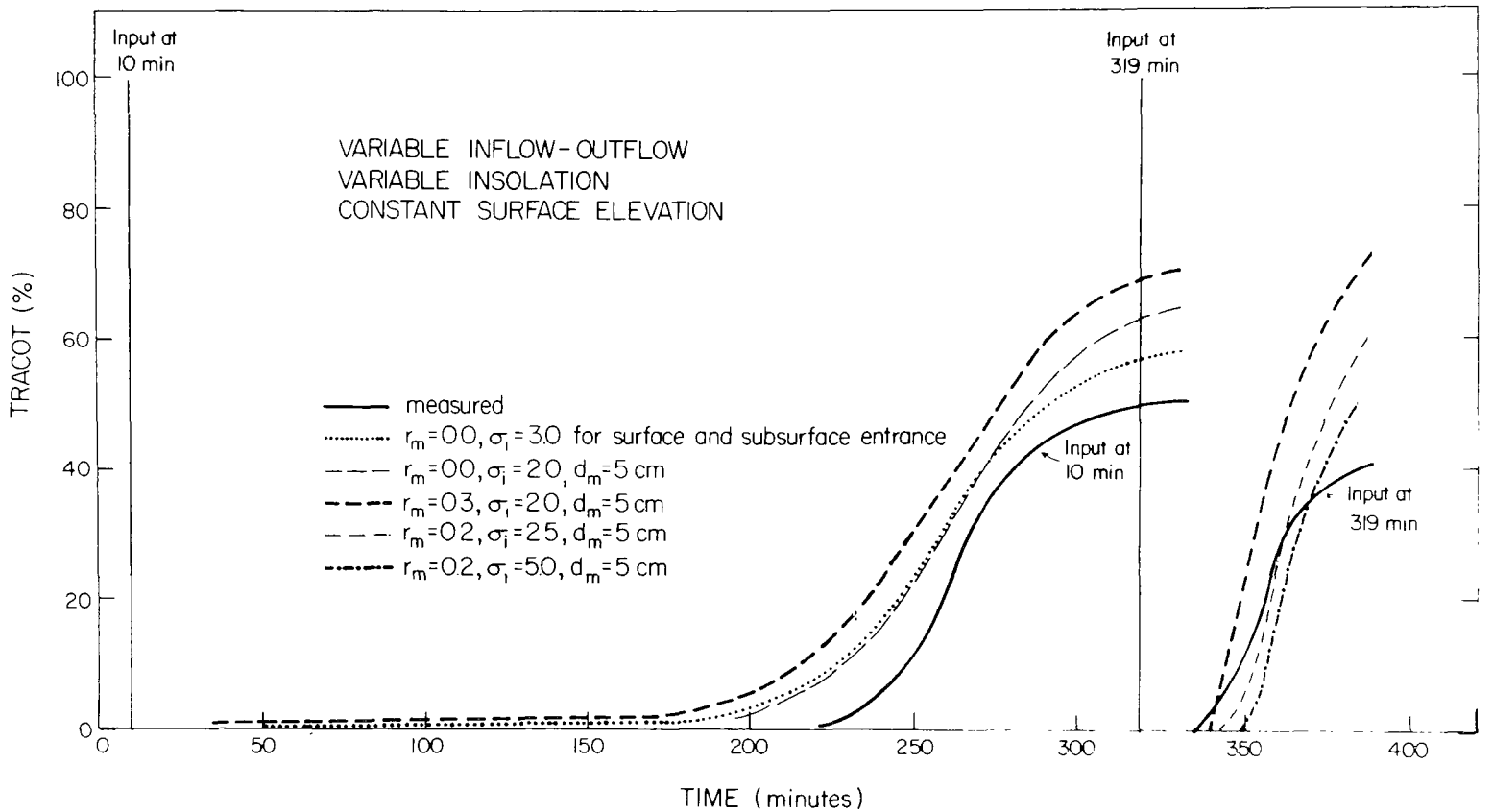

FIGURE 4.20 CUMULATIVE MASS OUT PREDICTIONS - SENSITIVITY ANALYSIS

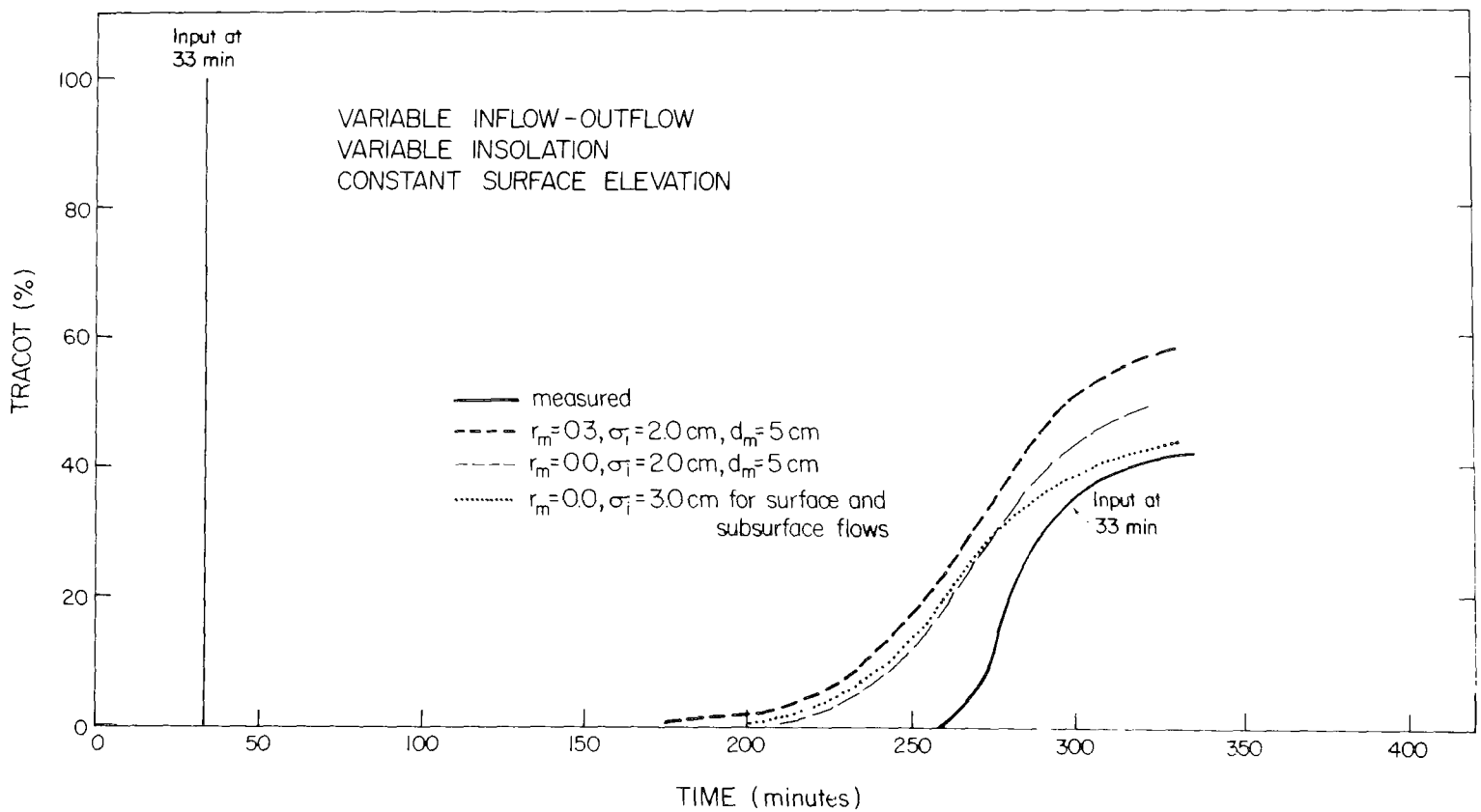

FIGURE 4.21 CUMULATIVE MASS OUT PREDICTIONS - SENSITIVITY ANALYSIS

However, from Figure 4.20 it is seen that increasing σ_i had the effect of reducing concentration for the input at 319 min. This is expected in light of the larger spreading of inflow sinking water with increase σ_i and the strong stratification at the outlet which dictates a narrow withdrawal layer at late times. The very high sensitivity of the late traces to σ_i make predictions difficult unless can be accurately determined. It was found that a value of 5 cm produced much better results than a value of 2.5 cm. Since 5 cm was the order of the depth of flow in the inlet channel, it is believed that σ_i can be related to this depth if no other information is available.

4.4.1.3 Sensitivity to the Entrance Mixing Ratio, r_m

From Figures 4.17 and 4.18 it can be seen that increasing r_m from a value of 0 to 0.3 has the effect of raising the predicted temperatures. This is because the entrained water was assumed to come from a surface layer of thickness d_m (Equation 2-58) equal to 5 cm. At early times (the 98 minute profile, Figure 4.17), the water enters at the surface and would tend to be cooled slightly through the entrainment process. However, this also reduces evaporative heat loses and the effects tend to cancel. However, water entering below the surface, as would be occurring after the peak inflow temperature (180 minutes) would tend to be heated by the mixing process. A similar trend, of warmer

outlet temperatures for higher r_m can be noted in the outlet temperature predictions.

The effect of increasing r_m on the cumulative mass out prediction (Figures 4.20, 4.21) is seen to have the general characteristic of increasing the amount of tracer material that reaches the outlet. This is related to the earlier arrival time of the traces at the outlet as r_m increases, due to the assumption of a constant layer thickness, Δh , for lagtime determinations independent of r_m. Since increasing r_m effectively increases the amount of flow input to this layer, it increases the velocity and decreases the lagtime. The inputs at late times (329 minutes) are most affected because these flows are sinking and in general tend to be withdrawn in a much shorter period of time than the earlier flows. Typical of these late inputs is the arrival of the peak concentration very close to the time that measurable concentrations are first observed, (Figure 4.14). Thus, the earlier arrival time of a late input (329 min.) means that the peak concentration arrives earlier along with higher predicted cumulative mass out values.

One advantage of working in the laboratory is the possibility of making independent observations of the mixing ratio. From dye tests on both surface and subsurface entrance an average value of 0.2 for r_m was arrived at.

For the field cases r_m can be estimated or deduced from the temperature prediction if temperature data are available. This will be further discussed in Chapter 5.

The assumption that all of the entrance mixing water comes from a surface layer of thickness d_m whether the flow is entering at the surface or not was investigated. It may not be reasonable to assume that the entrainment is coming from the surface if the flow is entering there. The following assumption was tested: if the flow enters at the surface in a layer 5 cm deep, the entrainment comes from a 10 cm thick layer beneath this depth. If the flow entered beneath the surface the original assumption was used. The results showed virtually no change in predicted temperatures and concentrations under this new assumption. To avoid arbitrarily assigning more than one mixing depth, the original assumption of d_m = 5 cm from the surface, for surface and subsurface entrance was retained.

4.4.1.4 Numerical Dispersion

The sensitivity of the numerical procedure to numerical dispersion was evaluated indirectly. From Equation 2-99 and 2-102, neglecting the area variation, it is seen that the numerical dispersion coefficient, D_p, is limited by

$$D_p < \frac{1}{2}\left[\frac{\Delta y^2}{\Delta T} - v\Delta y\right] \qquad (4\text{-}9)$$

where

$$v < \frac{\Delta y}{\Delta T} \qquad (4\text{-}10)$$

Thus, if Δy is varied while ΔT is kept constant, all other parameters being equal, the amount of numerical dispersion will change. Δy was changed from 2.5 to 1.5 cm while ΔT was kept at 2.5 min. From Equation 4-9 and 4-10, $D_p <$ 0.5 cm^2/min for $\Delta y = 2.5$ and $D_p <$ 0.2 cm^2/min for $\Delta y = 1.5$ cm. Under these two conditions insignificant changes occurred in the temperature and concentration prediction. It was concluded that doubling the maximum amount of numerical dispersion did not affect the results and further adjustments were not attempted.

4.4.2 Discussion of the Two Remaining Sets of Experiments

In order for any analytical method to be of much practical use it must be free of many empirical constants which change in some arbitrary fashion. Therefore, the values of σ_i, r_m and d_m used in arriving at predicted temperature and concentration curves (Figures 4.12 through 4.15) were kept constant in the analysis of the three different types of experiments performed. The ultimate importance of the values obtained for various parameters is that they may be useful in selecting values of these parameters for actual reservoir. Thus σ_i and d_m were chosen to be 5 cm, the depth of water in the inlet channel.

r_m was set at 0.2 as determined for independent experiments. Δh was found to be approximately 5 cm for surface entrance and 4 cm for subsurface entrance which is also the order of the depth in the inlet channel. The results for the experiments with variable inflow, outflow and insolation, constant surface elevation using the parameters noted above have been presented in Figures 4.12 through 4.15.

4.4.2.1 Constant Inflow and Outflow, No Insolation

Three experiments were conducted with constant inflow and outflow rates. As in the first set of experiments discussed, the input temperature variations were kept as identical as possible between the three runs. The flow rates for all three runs were constant and one dye injection was made in each run. In keeping the flow rates and temperature variation similar, dye tests taken in each of the three runs can be compared.

The temperatures of the inflow for a typical experiment in this series, along with the predicted outflow temperatures are presented in Figure 4.22. Measured and predicted vertical temperature profiles taken at different times in the run are compared in Figure 4.23.

The temperature predications are in very good agreement with measured values. The peak predicted temperatures, though slightly lower than that measured, occur at the same time as the measured value. All predicted tem-

FIGURE 4.22 INPUT TO CONSTANT INFLOW-OUTFLOW, NO INSOLATION EXPERIMENTS

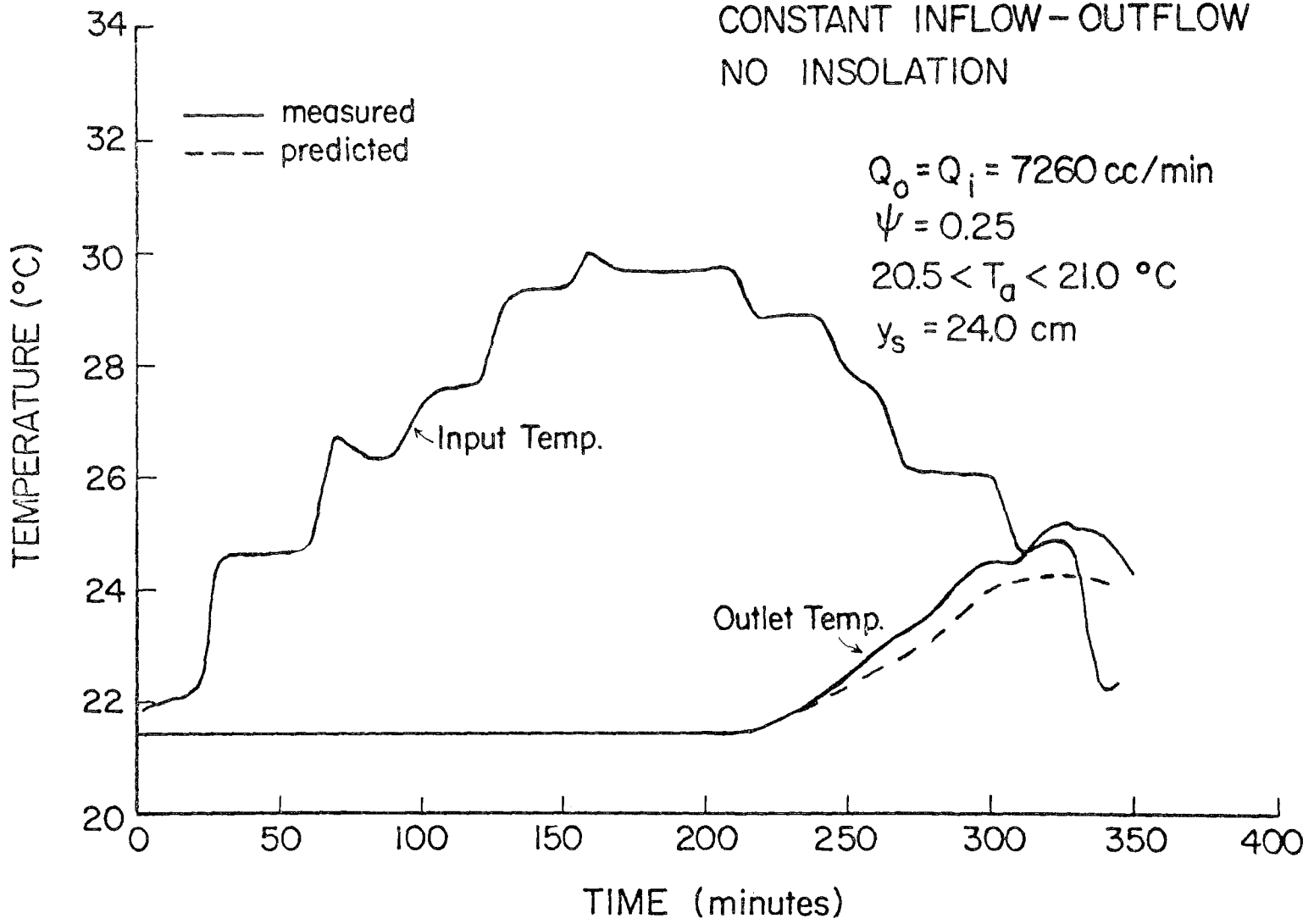

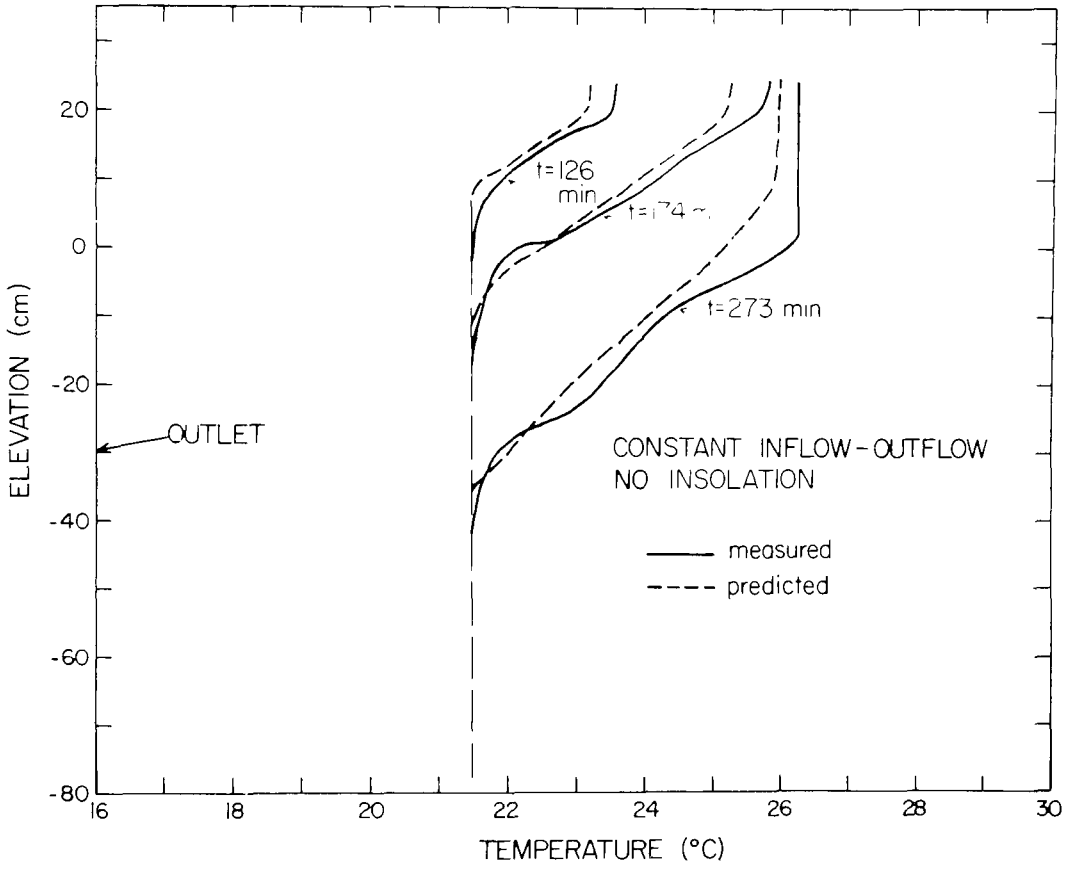

FIGURE 4.23 TEMPERATURE PROFILES

peratures are within 1°C of those measured.

Three dye tests, with injections at 33, 92 and 300 minutes respectively were performed. In each test 10^{-2} gm. of tracer was injected. The results are again presented in terms of concentrations measured at the outlet divided by the mass injected vs. time, and the cumulative mass out curve in Figures 4.24 through 4.27. From the first three curves, it is again seen that the order of magnitude of the concentrations predicted in the outlet is in reasonably good agreement with measured values. The measured arrival time and peak concentrations are presented in Table 4.3.

Trace	Peak Concentration/Mass In (gm^{-1})		Peak Arrival Time (min)	
	Measured	Predicted	Measured	Predicted
33	3.1×10^{-6}	1.40×10^{-6}	238	255
92	1.7×10^{-6}	1.45×10^{-6}	291	310
300	3.6×10^{-6}	2.75×10^{-6}	320	321

TABLE 4.3 PEAK CONCENTRATION CHARACTERISTICS

The absolute difference between measured and predicted peak concentration occurred in the test input at 33 and was 1.7×10^{-6} gm^{-1}. The predicted peak arrival times are in fairly good agreement with those measured.

All of the predicted curves follow the same

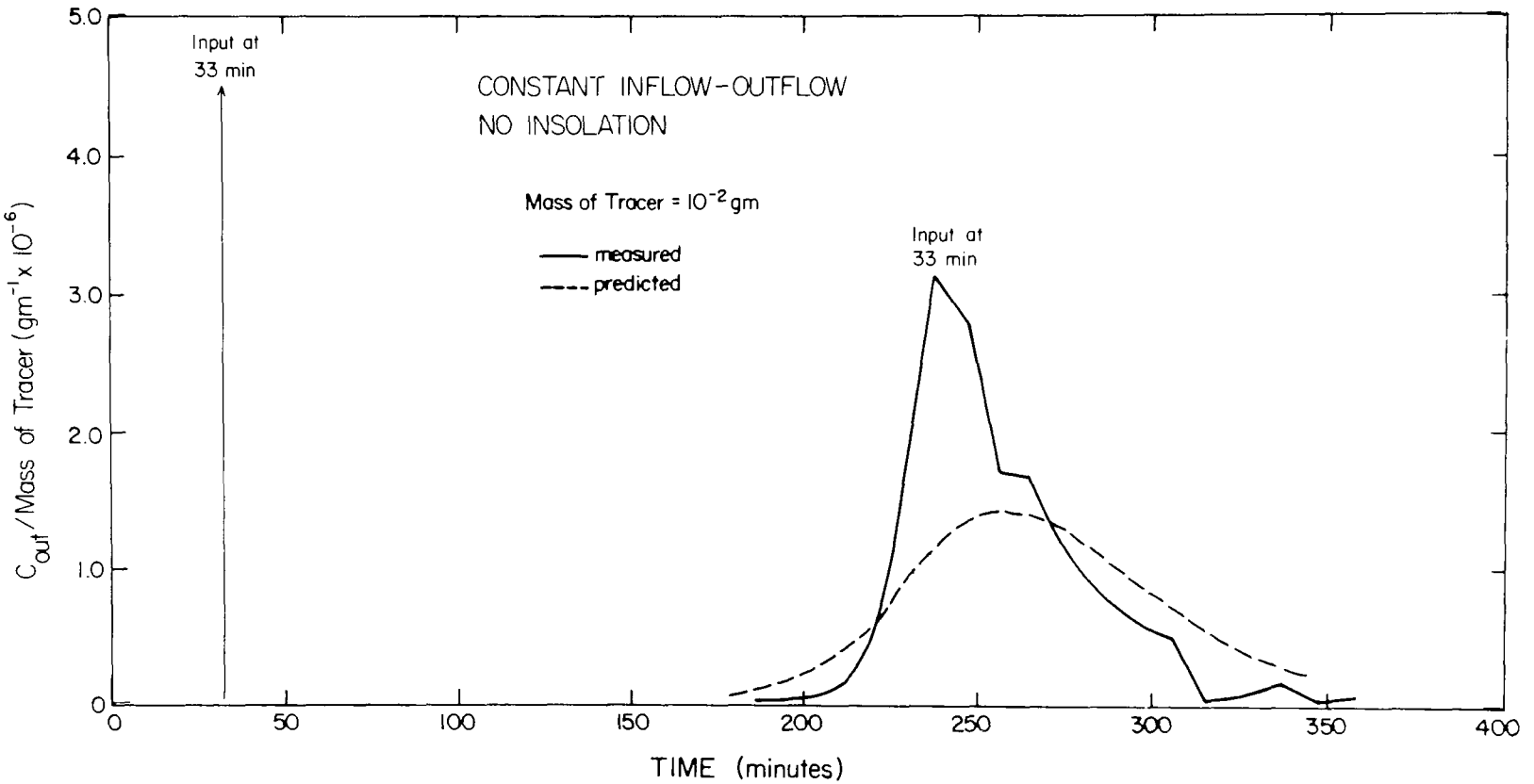

FIGURE 4.24 CONCENTRATION PREDICTION

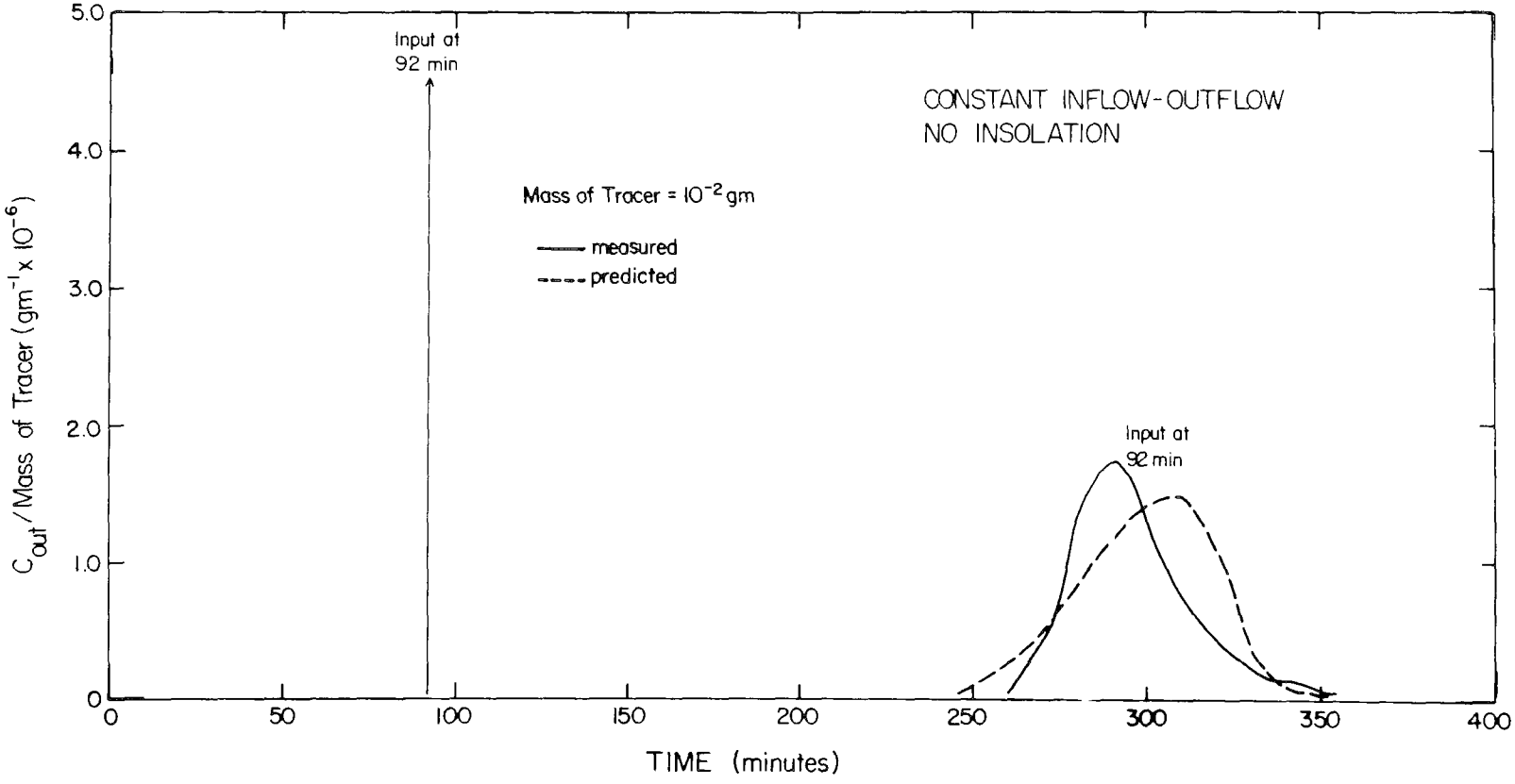

FIGURE 4.25 CONCENTRATION PREDICTION

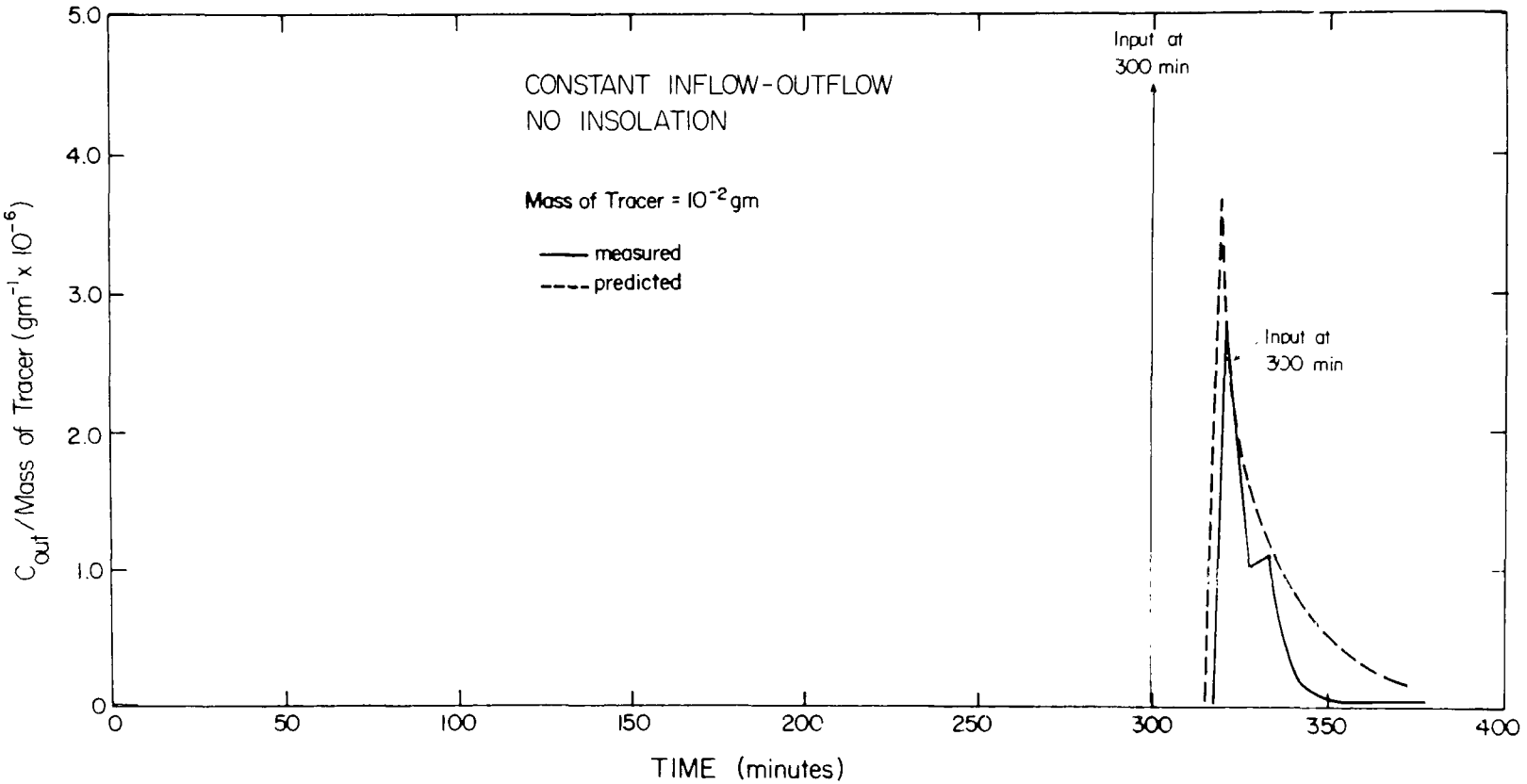

FIGURE 4.26 CONCENTRATION PREDICTION

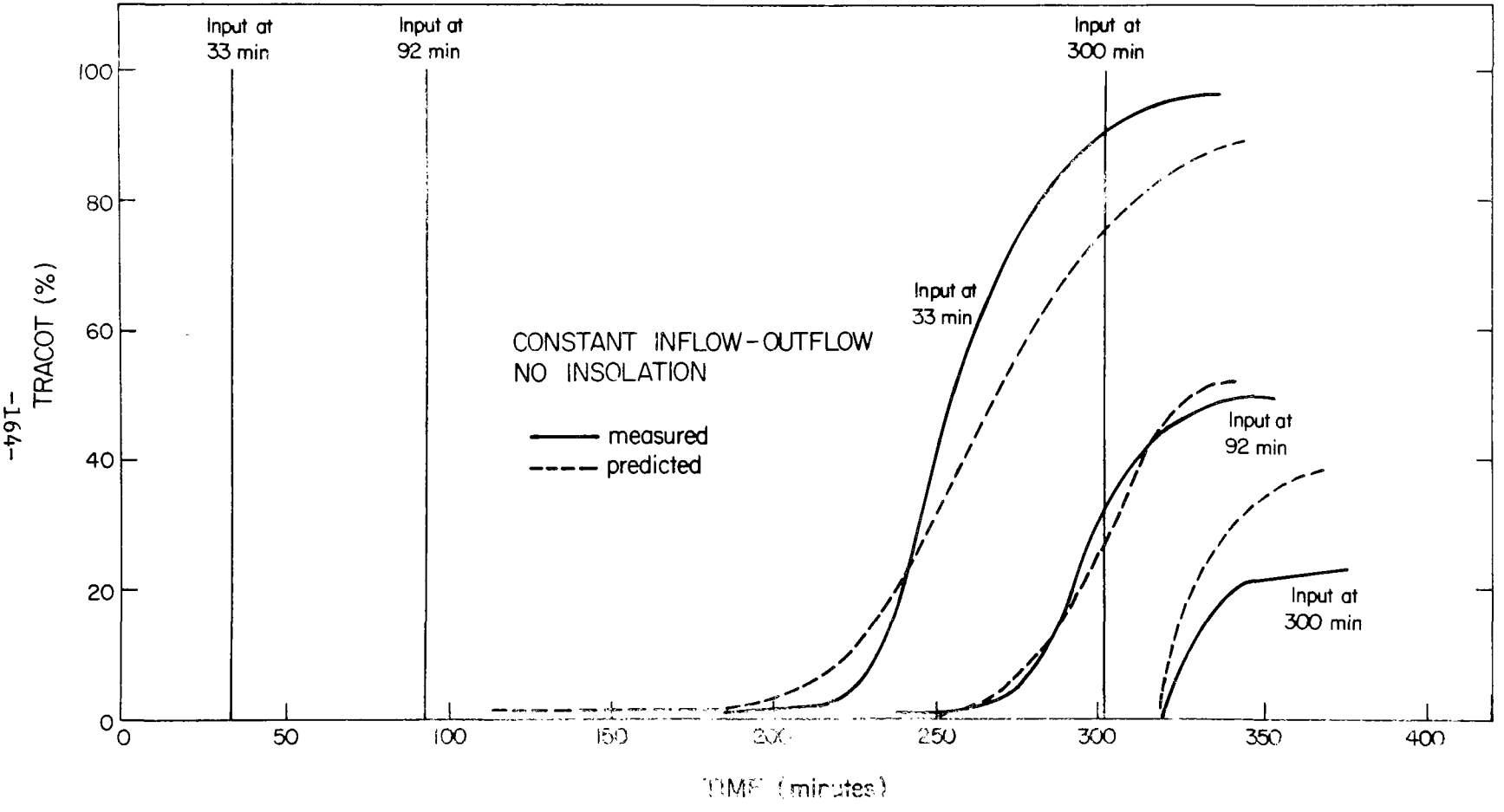

FIGURE 4.27 CUMULATIVE MASS OUT PREDICTIONS

general trend as those measured in the laboratory. It is interesting to note that the time interval between injection of the 33 and 92 minute traces is 59 minutes while that of their peaks is 53 minutes (measured) and 55 minutes (predicted). Between the 92 minute and 300 minute injections the peaks were separated by 29 minutes (measured) and 11 minutes (predicted) although the inputs were 208 minutes apart. This most important consequence of the internal thermal stratification is well predicted by the water quality model.

Discrepancies between the cumulative mass out predictions and measurements (Figure 4.27) for the input at 33 minutes is caused by a slightly earlier predicted arrival time of the traces and a slightly slower predicted fall from the peak concentration (Figure 4.24). Though the predicted and measured concentrations never differ by more than 0.75×10^{-8} gm and the curves appear quite similar, the apparent small discrepancies are magnified when the integrals of the concentration-time curves are taken.

4.4.2.2 Variable Inflow, Insolation and Surface Elevation

In this experiment three dye injections at 10,302 and 350 minutes were made. The input data and predicted outlet temperatures are given in Figure 4.28. Predicted and measured temperature profiles are in Figure 4.29. Again $\sigma_i = 5.0$ cm, $r_m = 0.2$, $d_m = 5$ cm, $\Delta h = 5$ cm for

FIGURE 4.28 INPUTS TO THE VARIABLE INFLOW-OUTFLOW, VARIABLE INSOLATION, VARIABLE SURFACE ELEVATION EXPERIMENTS

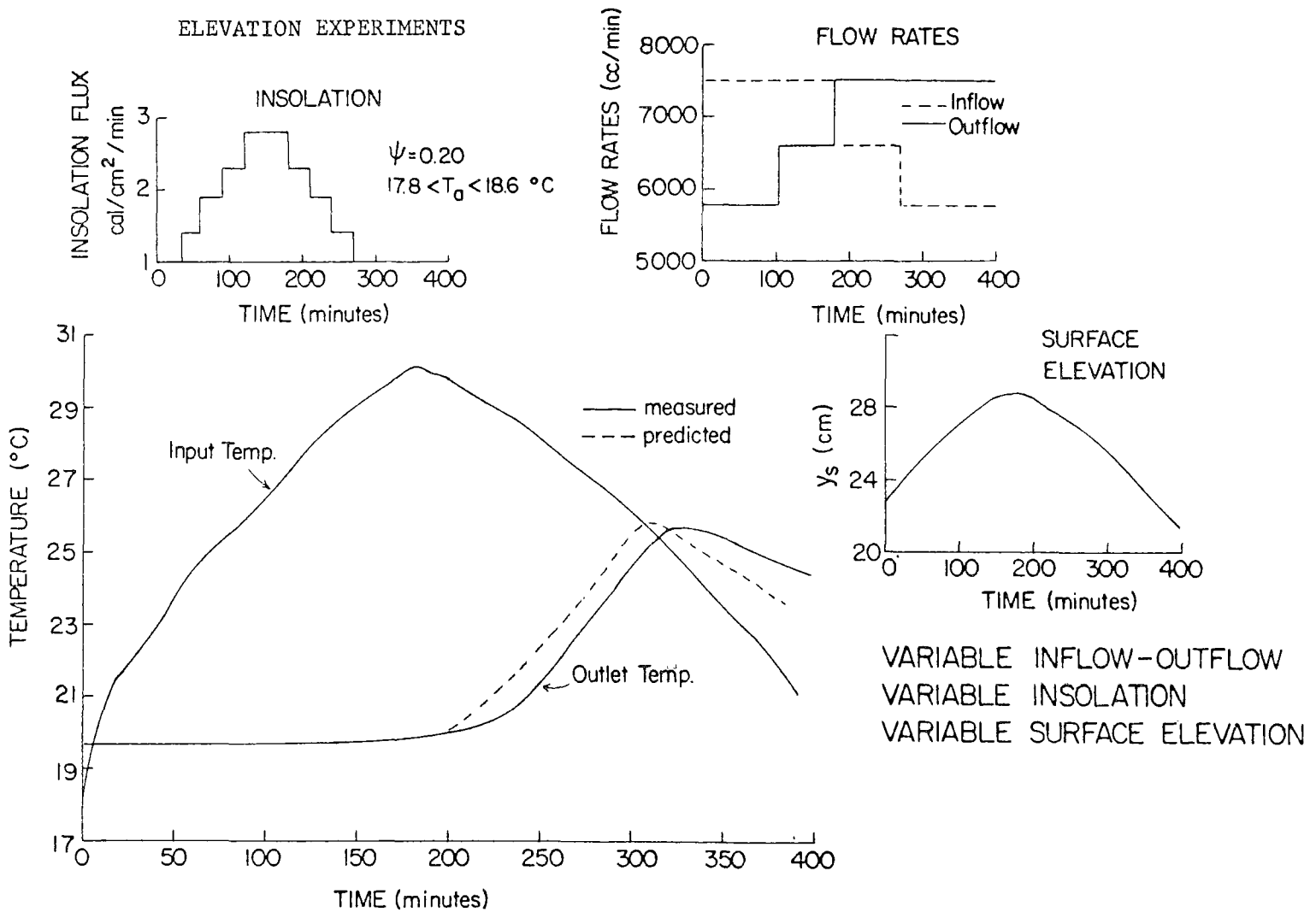

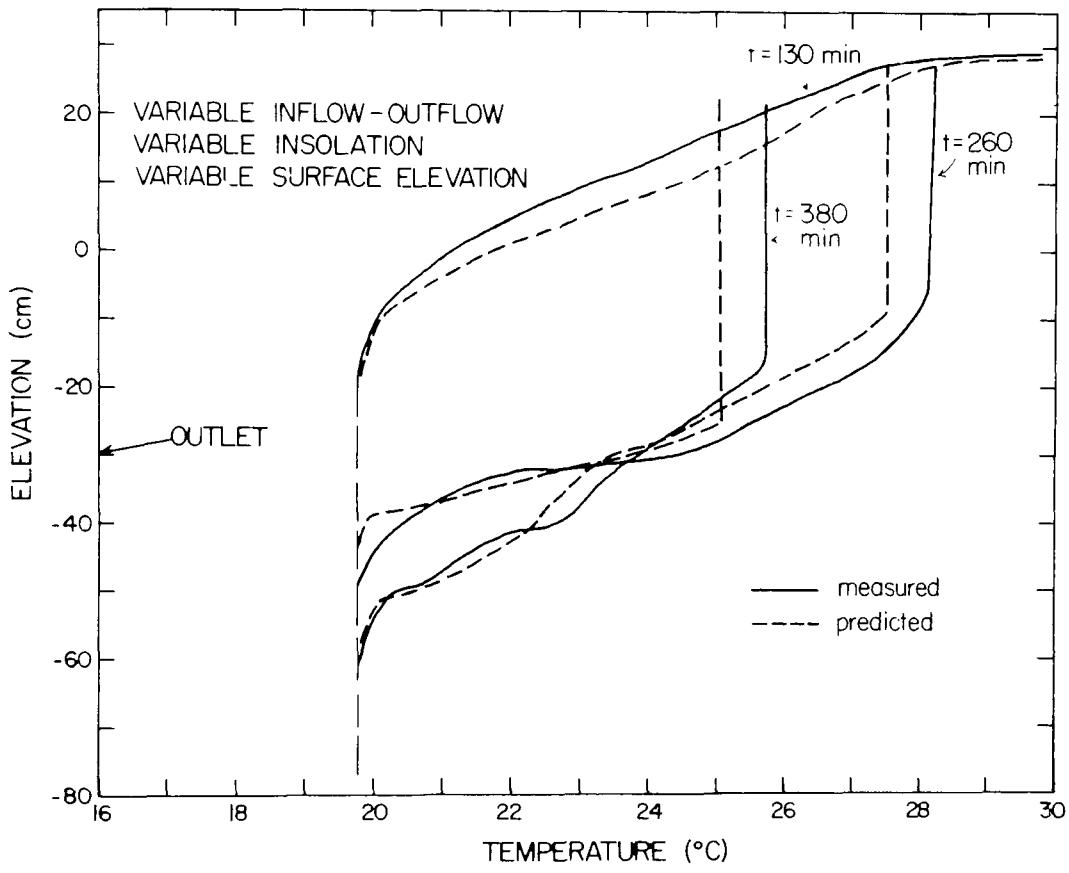

FIGURE 4.29 TEMPERATURE PROFILES

surface input and 4 cm for subsurface input. Excellent temperature predictions result.

Dye concentration predictions (Figure 4.30) are quite representative of the measured curves for the 10 and 302 minute traces. The 350 minute prediction, though beginning at approximately the same time as the measured curve, and of the same order of magnitude, is not very good. This is probably due to the large amount of short circuiting occurring at late times which magnifies discrepancies between assumed and actual values of σ_i , r_m and Δh

The cumulative mass out curves (Figure 4.31) show, for the 10 minute input, the effect of the earlier predicted arrival and slower reduction from the peak concentration. The 302 and 350 minute traces also reflect the slower predicted decline from the peak concentration values.

4.5 Summary of Experimental Results

In general, measured temperatures agreed very well with predicted values. Concentration predictions were better for traces input early in the stratification cycle than later when the inflowing water was sinking. However, the order of magnitude of the predicted concentration and the general trend of the measured curves could be predicted.

FIGURE 4.30 CONCENTRATION PREDICTIONS

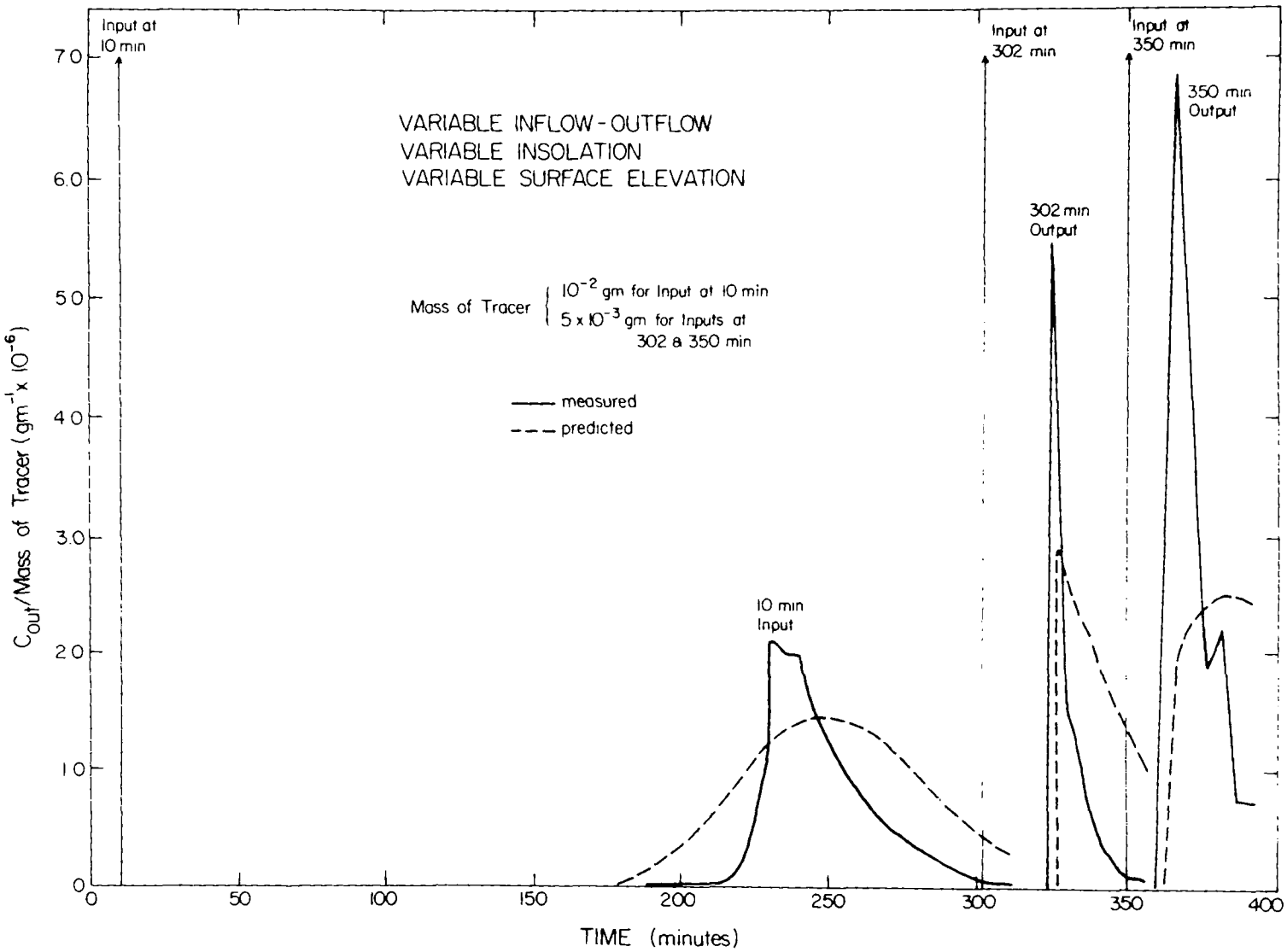

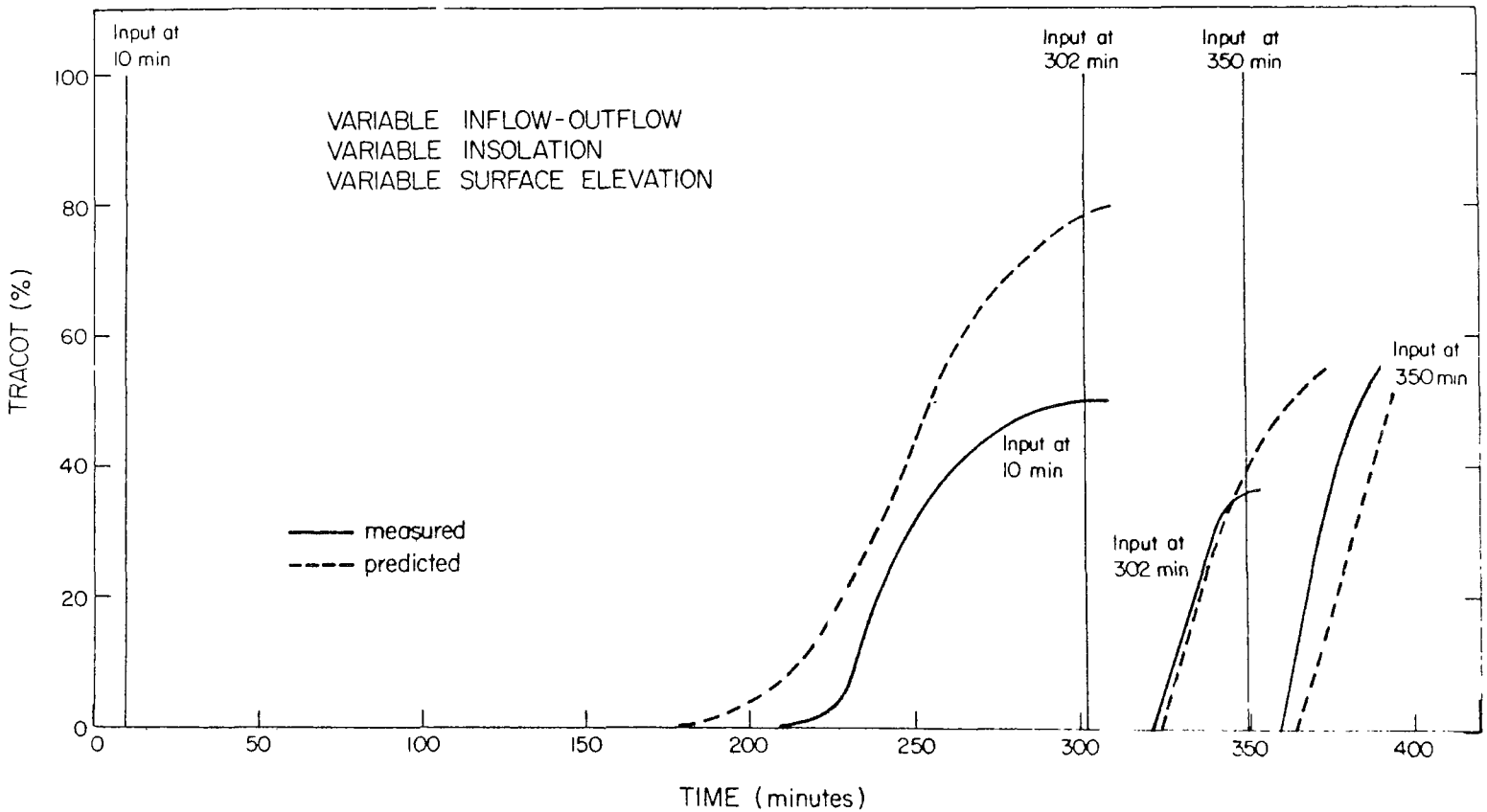

FIGURE 4.31 CUMULATIVE MASS OUT PREDICTIONS

Though three different types of experiments were run, and different flow rates used in each, an invarient set of parameters (σ_i, r_m, d_m Δh) was sufficient for prediction.

CHAPTER 5. APPLICATION OF THE WATER QUALITY AND TEMPERATURE MODELS TO FONTANA RESERVOIR

5.1 Introduction

In 1966 a detailed temperature and D.O. study was conducted on Fontana Reservoir by the T.V.A. Engineering Laboratory, Norris, Tennessee. The lake, formed by 400 foot high Fontana dam, is located on the Little Tennessee River in Western North Carolina. Three major streams, the Little Tennessee, Tuckaseegee and Nantahala, and several smaller streams, feed the 29 mile long reservoir (Figure 5.1).

The meterological, hydrological and temperature data obtained from the 1966 survey were used by Huber and Harleman to test their temperature model. In this chapter the same data will be used to compare the predicitions obtained from Huber and Harleman's model in the modified form developed in Chapter 2.

In addition, cumulative mass out predictions (Section 3.4.2.3) are presented for various conservative tracer dye injection tests even though such field tests have not as yet been carried out.

It is hoped that the method of analysis developed in Chapter 3, will motivate the undertaking of dye tests which will shed further light on the complicated flow field and dispersion characteristics of a stratified reservoir. The predicted curves are compared with detention times calculated by Wunderlich (57).

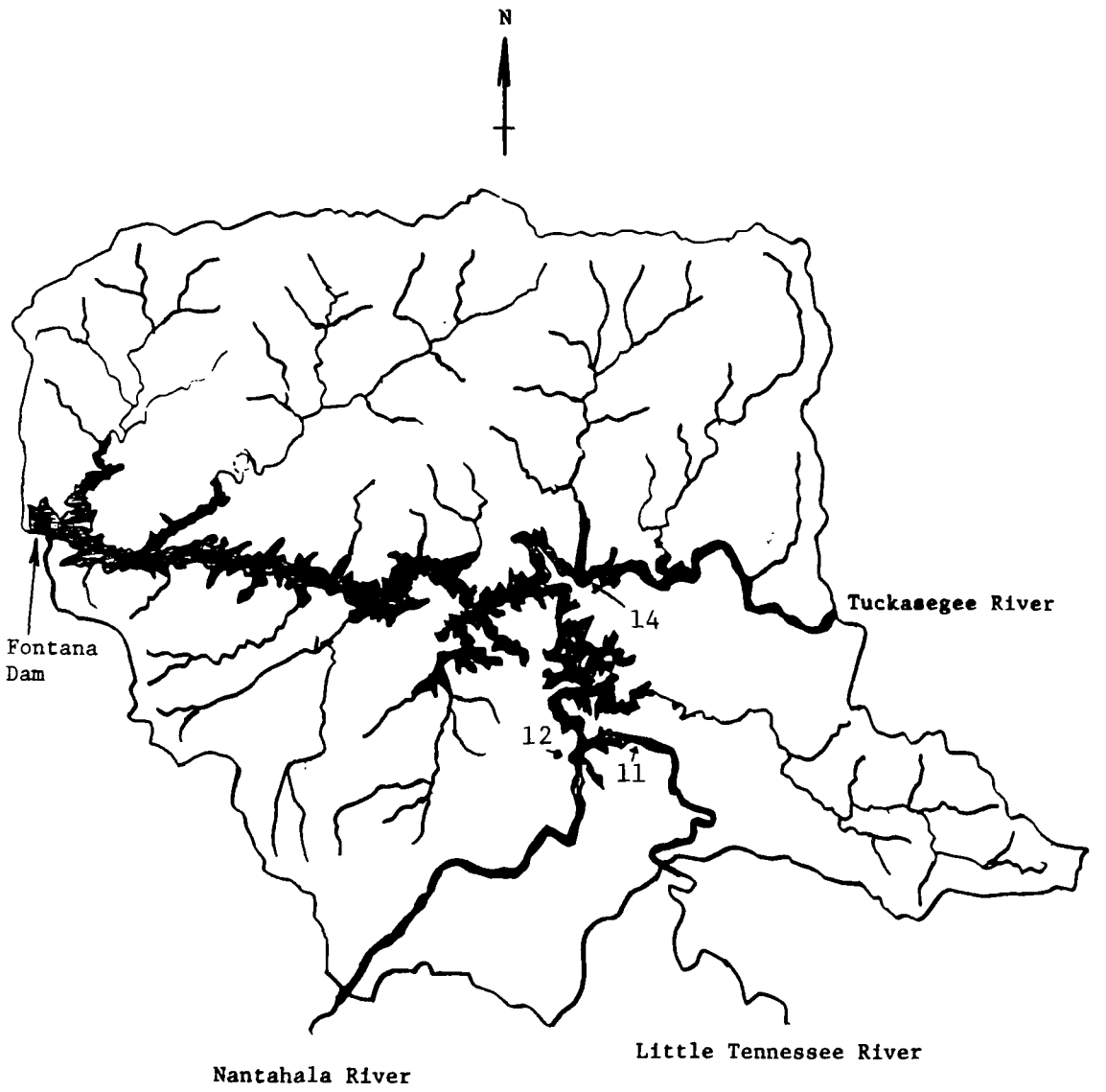

FIGURE 5.1 MAP OF FANTANA RESERVOIR AND WATERSHED

Detailed measurements of the D.O. of the incoming streams were made daily from February through December and D.O. profiles in the lake were measured periodically from April through December.

No corresponding B.O.D data exists. Therefore B.O.D. values had to be assumed. The D.O. data and the assumed B.O.D. input is applied to the D.O. and B.O.D. prediction models developed in Chapter 3.

5.2 Temperature Prediction

5.2.1 Inputs to the Temperature Model

The necessary inputs to the temperature model are tabulated in Section 3.4.1.3.

The hydrological and meterological data obtained by the T.V.A. were presented either on an hourly or daily basis. The computer program was run with a time step of one day and all hourly data were reduced to daily averages. The values for the various parameters discussed below are presented in Appendix III in the form of computer input.

5.2.1.1 Inflow and Outflow Rates and Temperatures

The mathematical model is designed to handle only one input stream to the reservoir. Inflow rates and temperatures of the five sources of water for the reservoir (the three streams previously mentioned and the runoff from the water sheds bordering the north and south shorelines) were available on a daily basis. The combined flow rate and

weighted average of their temperatures were used as input to the model.

The reservoir outflow rate and temperature were available on a daily basis. Since the power plant operates on a peaking power production schedule these average daily values may hide considerable variation in flow rates and temperatures.

5.2.1.2 Solar Insolation and Related Parameters

Due to the lack of direct radiation measurements being available the input solar radiation values were calculated from a modification of Kennedy's (1949) method. In this modification, developed by Wunderlich, variation in the surface reflection coefficient, β cloudiness, C, optical air mass, m, solar altitude α and the normalized radius vector of the earth about the sun, r, are accounted for. Huber and Harleman concluded that the radiation values calculated for Fontana, compared with unreduced pyroheliometer readings, should be increased by 15%. The resulting expression is:

$$\phi_o = 1.15 \frac{\phi_{sc} \sin}{r^2} \; a_t^{\,m} \; (1-\beta) \; (1-0.65C^2) \qquad (5\text{-}1)$$

ϕ_o = Incoming solar radiation flux penetrating the water surface (energy/area-time)

ϕ_{sc} = Solar constant = 1.94 cal/cm^2/min

a_t = Atmospheric transmission coefficient

The optical air mass, m, is defined as the ratio of the path length of the sun's rays through the atmosphere to their path length when the sun is directly overhead. The value of the atmospheric transmission coefficient, a_t, was determined from measurements at nearby areas and found to be 0.882.

The average surface absorbed fraction, β and the absorption coefficient, ε in Equation 2-31 were determined from measurements taken at different times of the year as shown in Figure 5.2. The value of ε used was 0.7 m^{-1} and a value of 0.5 was used for β.

5.2.1.3 Withdrawal Layer Thickness

Koh's Equation 2-49 forms the basis of the withdrawal layer calculation. This equation had to be extended in order to apply to the high flow rates encountered in the field. As mentioned in Section 4.3.1 Koh presents an empirical relationship:

$$\frac{\alpha}{\alpha_o} = 3.5 \left(\frac{q}{D\alpha_o x^{2/3}}\right)^{-0.133} \quad \text{for } 0.3 \leq \frac{q}{D\alpha_o x^{2/3}} \leq c \qquad (5\text{-}2)$$

Where c = 25 for thermal stratification and 1,000 for salinity stratification and suggests that α replace α_o in Equation 2-2-49.

An average outflow rate of 8 x 10^6 m^3 /day was assumed for a width at the outlet elevation of 310m. Thus, q = 8 x 10^6/310 = 2.58 x 10^4 m^2/day. Using molecular diffusion and viscosity and ε = 1 x $10^{-4} m^{-1}$,

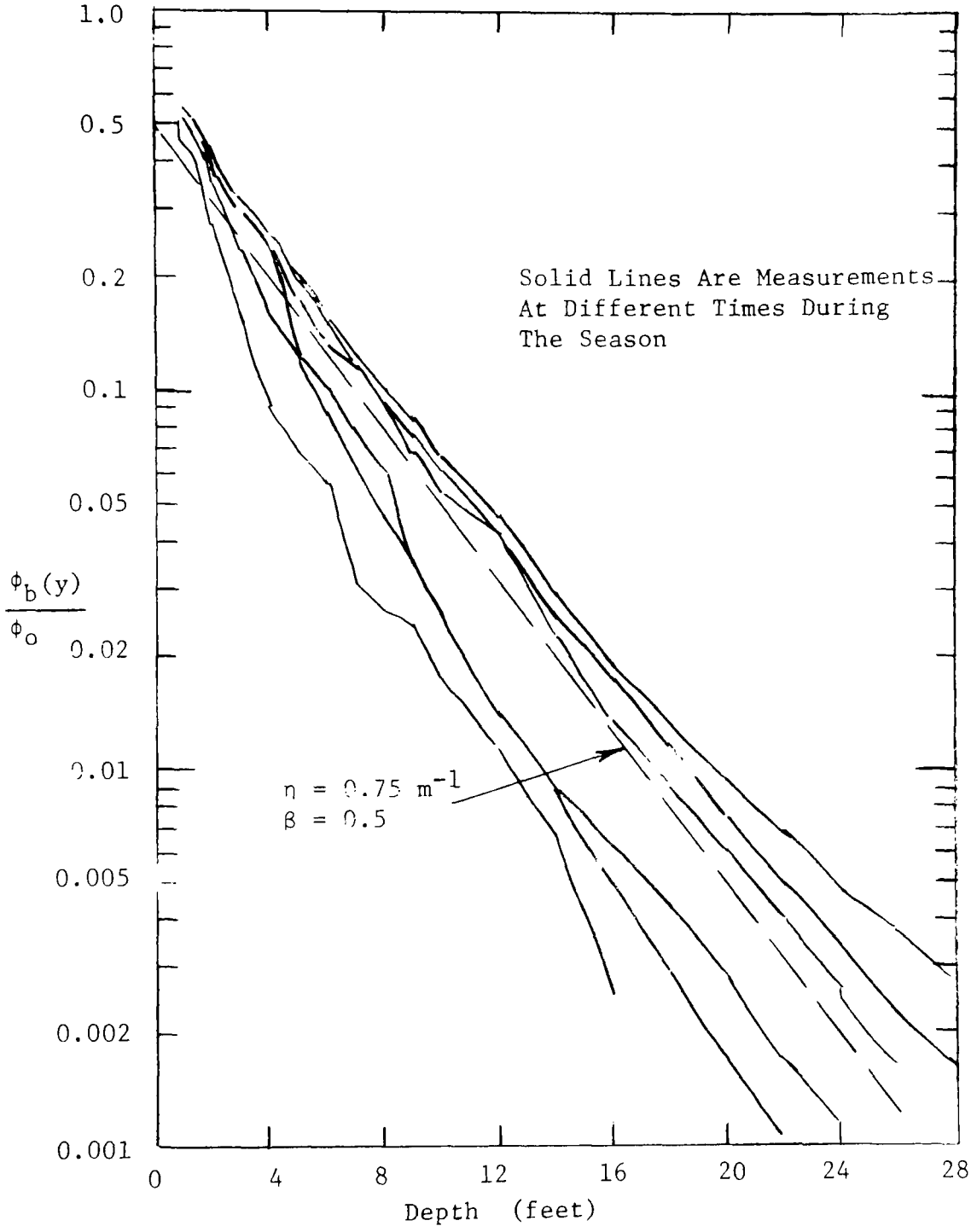

FIGURE 5.2 DETERMINATION OF ABSORPTION COEFFICIENT AND SURFACE ABSORBED FRACTION FOR FONTANA RESERVOIR

$$\alpha_o = 44 \text{ m}^{-2/3}$$

For $x = 1000$ m, $\dfrac{q}{D\alpha_o x^{2/3}} = 480$

and

$$\frac{\alpha}{\alpha_o} = \frac{1}{(3.5 \times 480)^{0.133}} = 0.385$$

Then

$$\delta = \frac{7.14 \times^{1/3}}{\alpha} = 1.0\ \varepsilon^{-1/6} \qquad (5\text{-}3)$$

As discussed by Huber and Harleman, during high stratification, Koh's Formula 5-3 predicts withdrawal thicknesses on the order of the diameter of the penstock opening (4 meters). This was felt to be unrealistic. Hence, the coefficient in Equation 5-3 was doubled, yielding the final form:

$$\delta = 2/\varepsilon^{1/6} \qquad (5\text{-}4)$$

The outflow standard deviation can then be calculated from Equation 2-50.

5.2.1.4 Other Parameters

The inflow standard deviation, σ_i was set at 4m. This value was estimated from the observed spread of a dye trace in the upstream region of the reservoir (Figure 2.10).

Air temperatures and relative humidities were available on an hourly basis and averaged to obtain daily values.

As was mentioned in Section 2.3.4, the evaporation formulae used in the field depend on where specific quantities are measured. Wind values were measured at a reservoir shore location. These were transferred to mid-lake values by an empirical correlation provided by the T.V.A. Engineering Laboratory and Rohwer's evaporation formula (Equation 2-43) was used.

The reservoir width was schematized according to Equation 2-46. The length of the reservoir at a given depth was measured along the Little Tennessee River. The results are tabulated in Table 5.1. Huber and Harleman have shown that if the width varies exponentially with depth the evaluation of Equation 2-52 is greatly simplified. A semi-log plot of width vs elevation, Figure 5-3, produced the relationship:

$$B = 0.885e^{0.0133y} \qquad (5\text{-}5)$$

Where

B = width in meters

y = elevation above sea level in meters

5.2.2 Temperature Predictions

In Figures 5.4-5.12 predicted outlet temperatures and temperature profiles are presented as calculated both by Huber and Harleman and from Equation 2-96. Five different cases are shown. The first two, calculated by Huber and Harleman are for:

1. Molecular diffusion, no entrance mixing, no lag time ($D = D_m = 0.0124 m^2/day$, $r_m = 0$)

TABLE 5.1

FONTANA RESERVOIR AREAS, LENGTHS AND WIDTHS

Elevation above sea level (ft)	(m)	Area (m^2)	Length (m)	Width (m)
1300	396	283,000	1,770	160
1350	411	1,700,000	10,863	157
1400	427	4,249,000	16,077	265
1450	442	7,244,000	23,480	308
1500	457	10,643,000	28,212	378
1550	472	14,488,000	34,553	420
1600	488	21,286,000	41,038	519
1650	503	30,028,000	43,259	694
1700	518	40,469,000	45,738	885

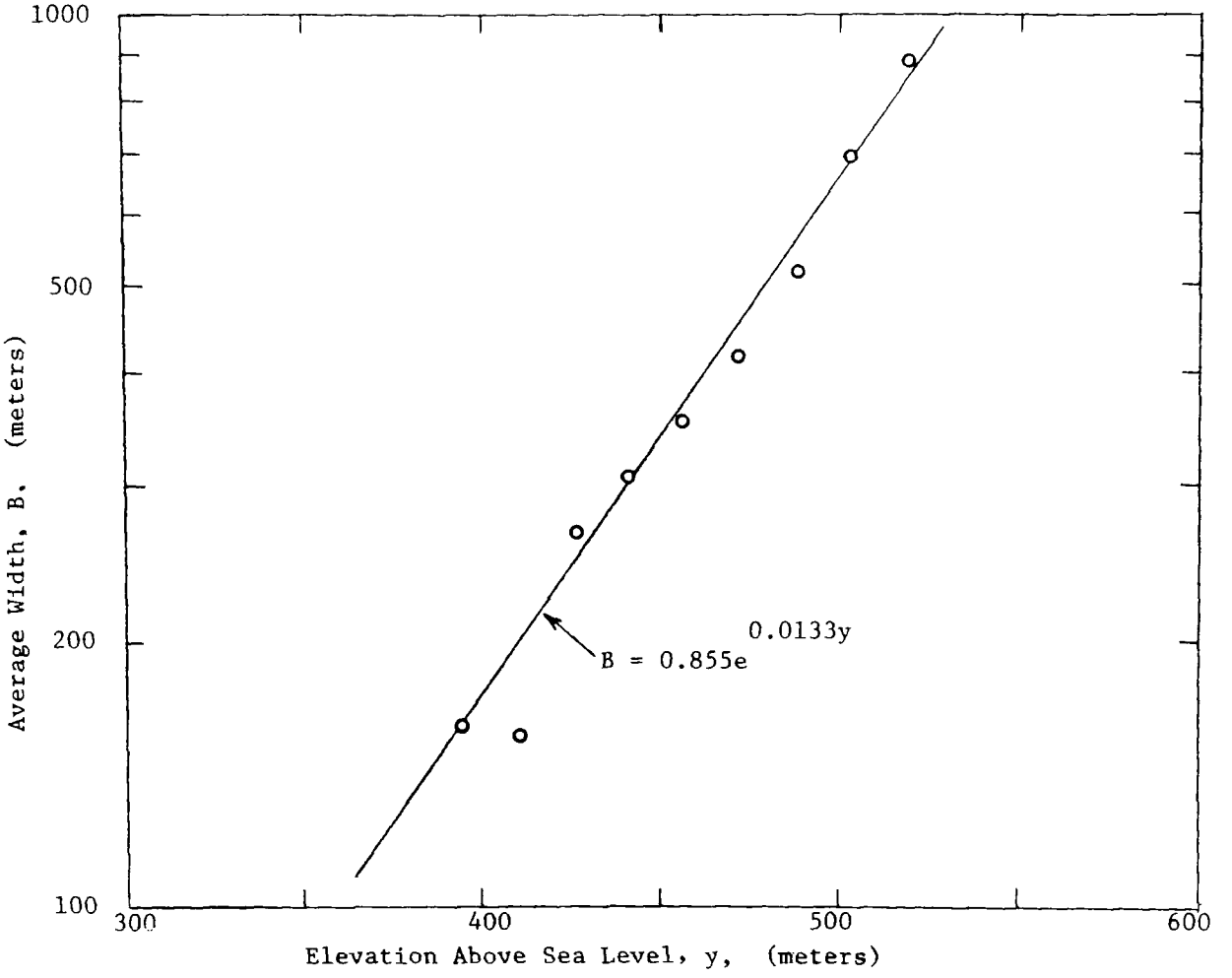

FIGURE 5.3 EXPONENTIAL WIDTH-ELEVATION RELATIONSHIP FOR FONTANA RESERVOIR

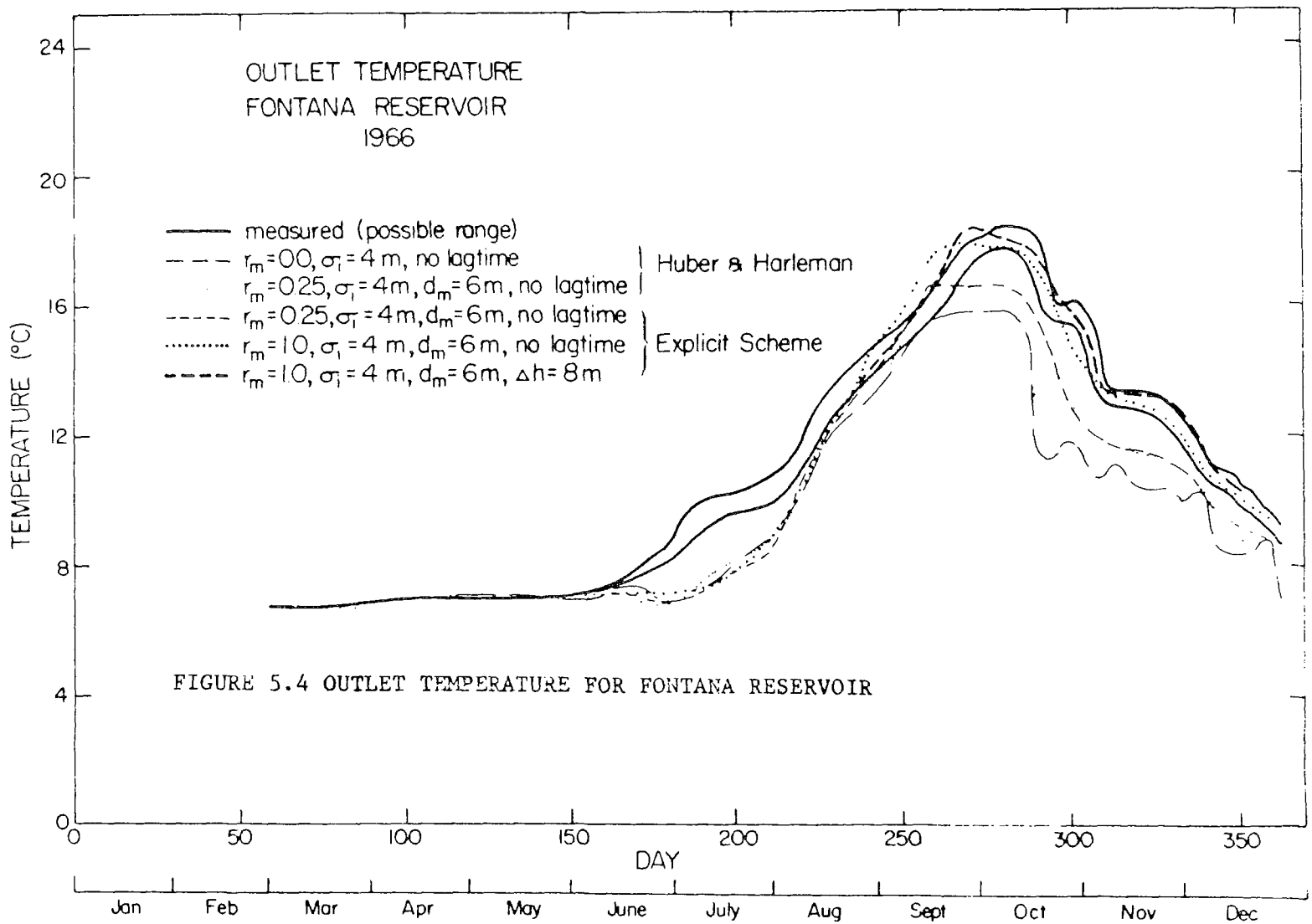

FIGURE 5.4 OUTLET TEMPERATURE FOR FONTANA RESERVOIR

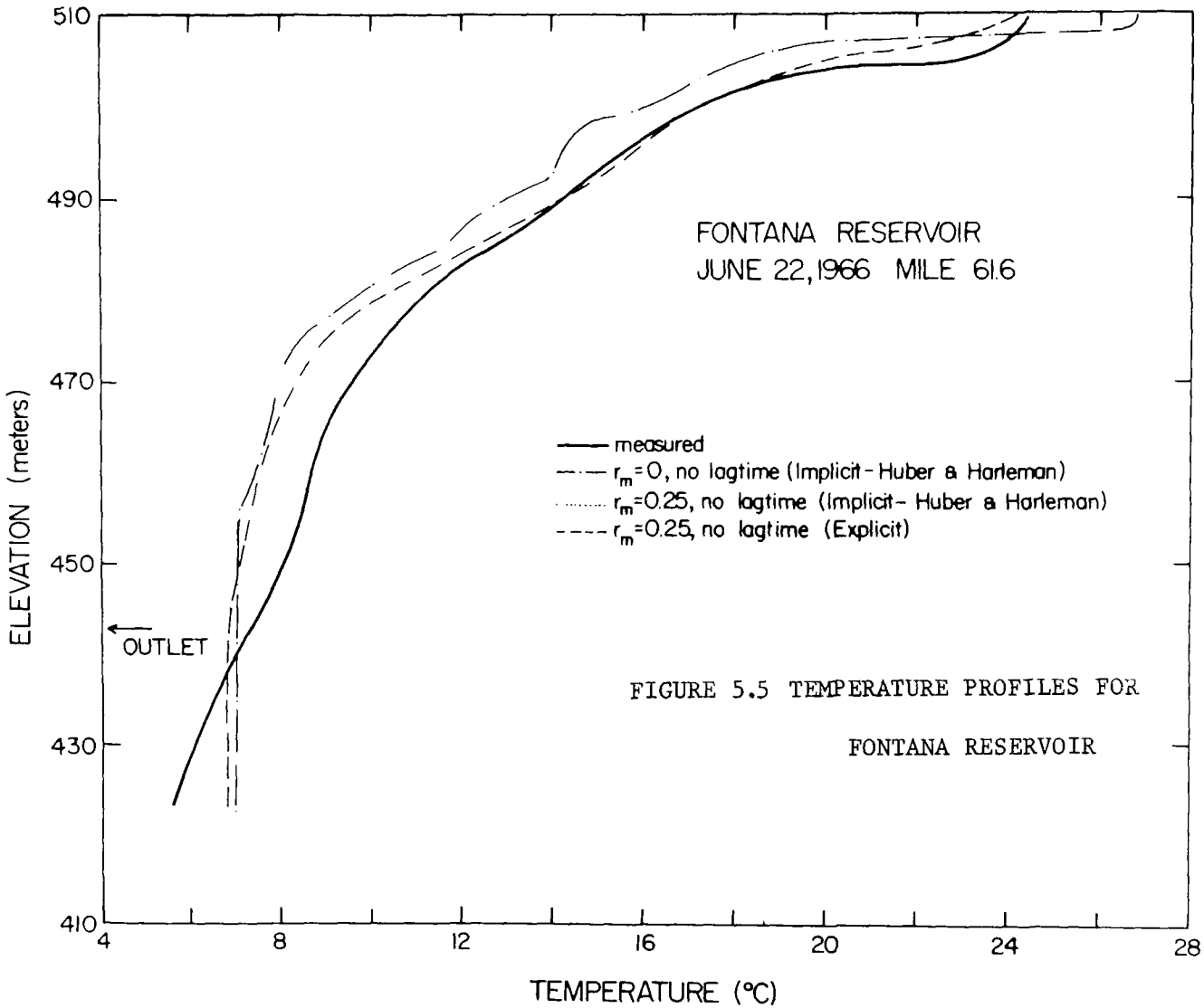

FIGURE 5.5 TEMPERATURE PROFILES FOR FONTANA RESERVOIR

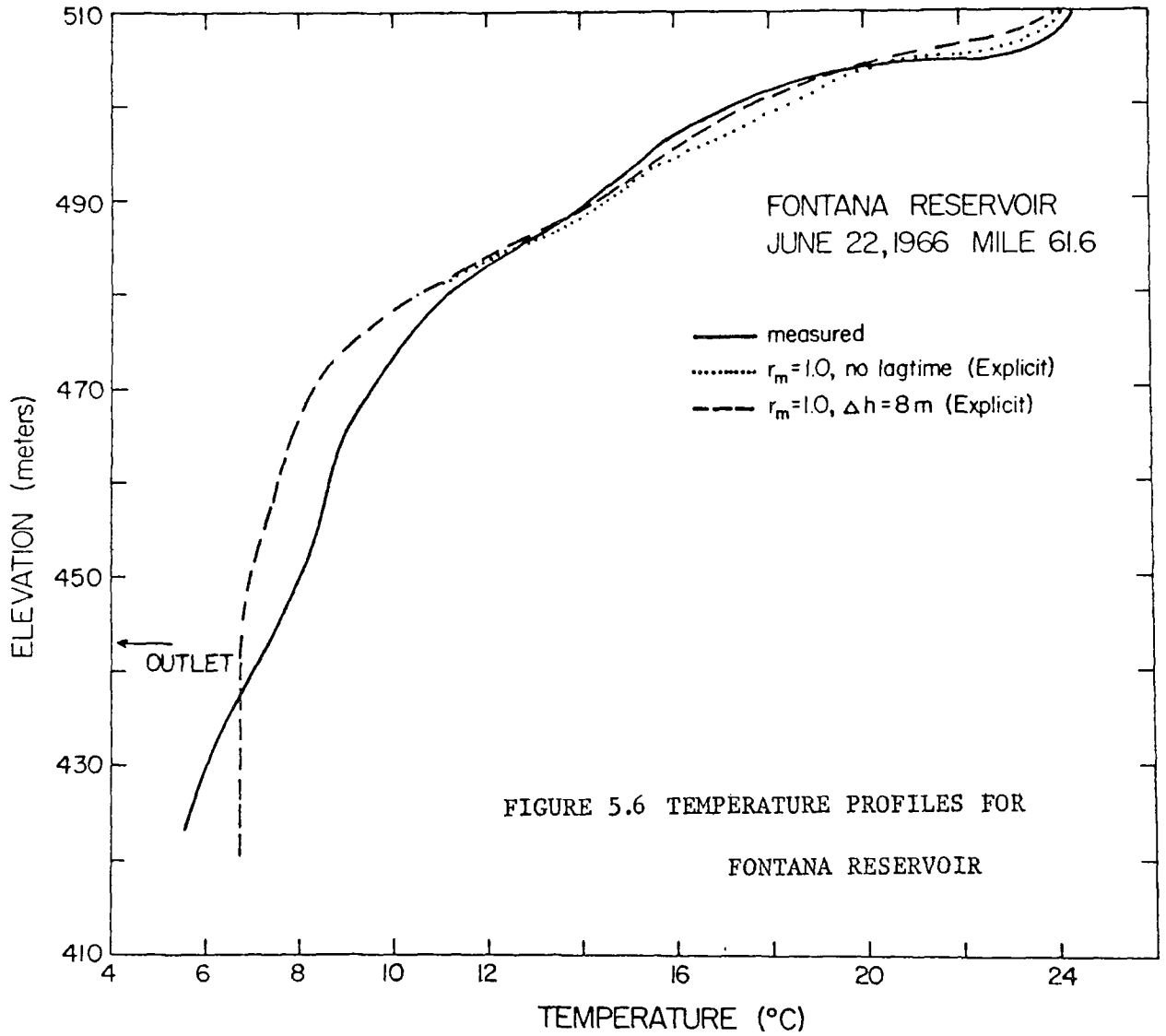

FIGURE 5.6 TEMPERATURE PROFILES FOR FONTANA RESERVOIR

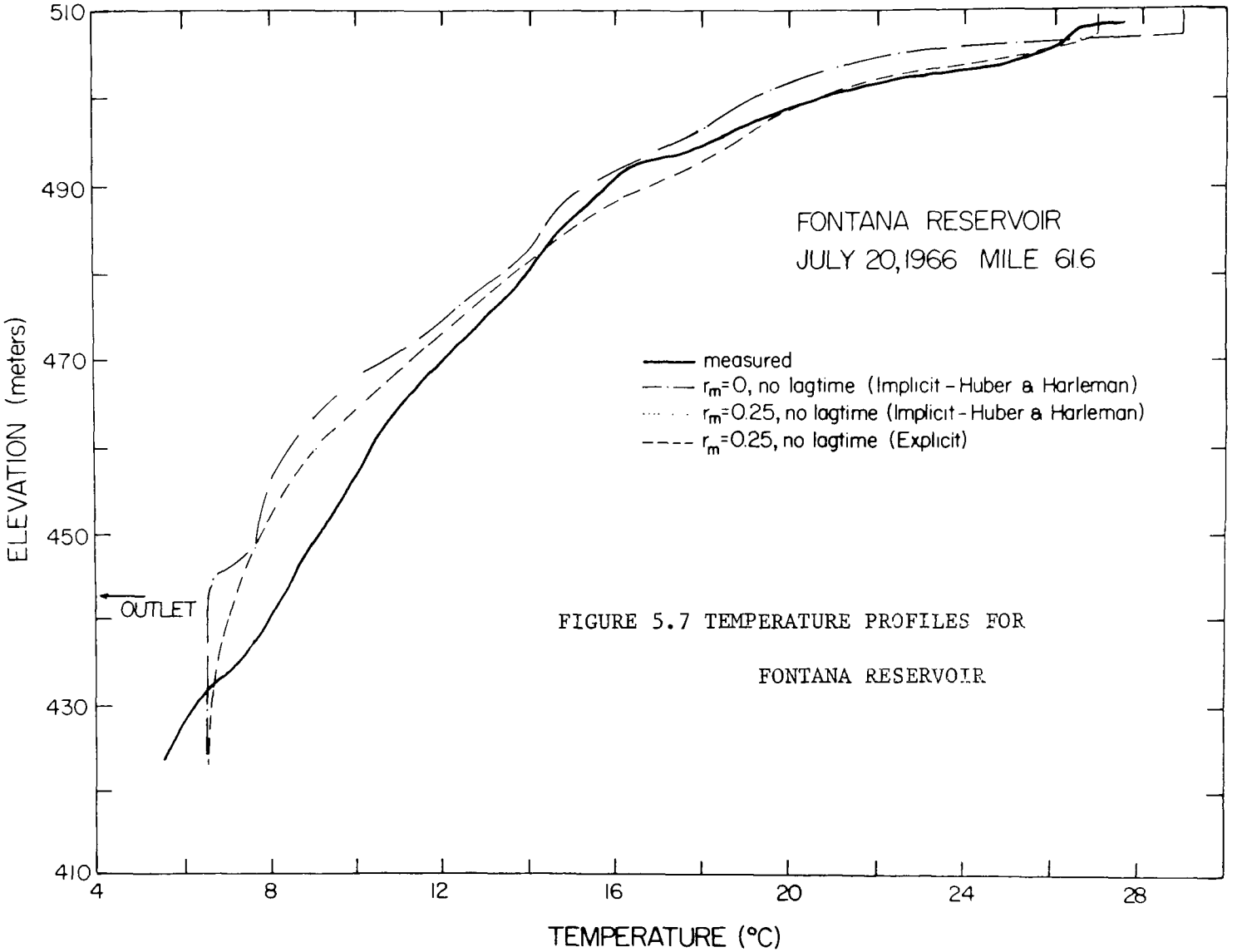

FIGURE 5.7 TEMPERATURE PROFILES FOR FONTANA RESERVOIR

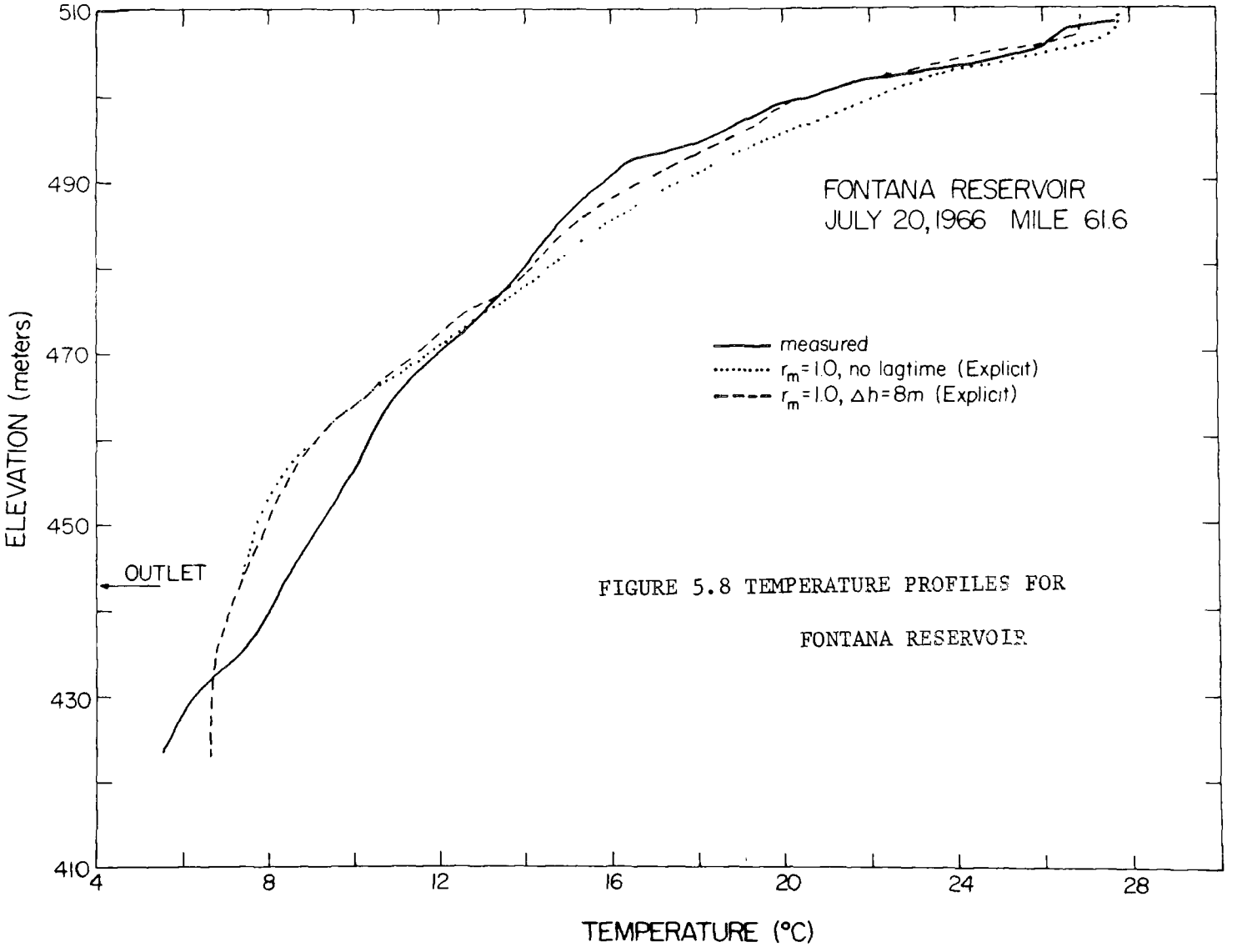

FIGURE 5.8 TEMPERATURE PROFILES FOR FONTANA RESERVOIR

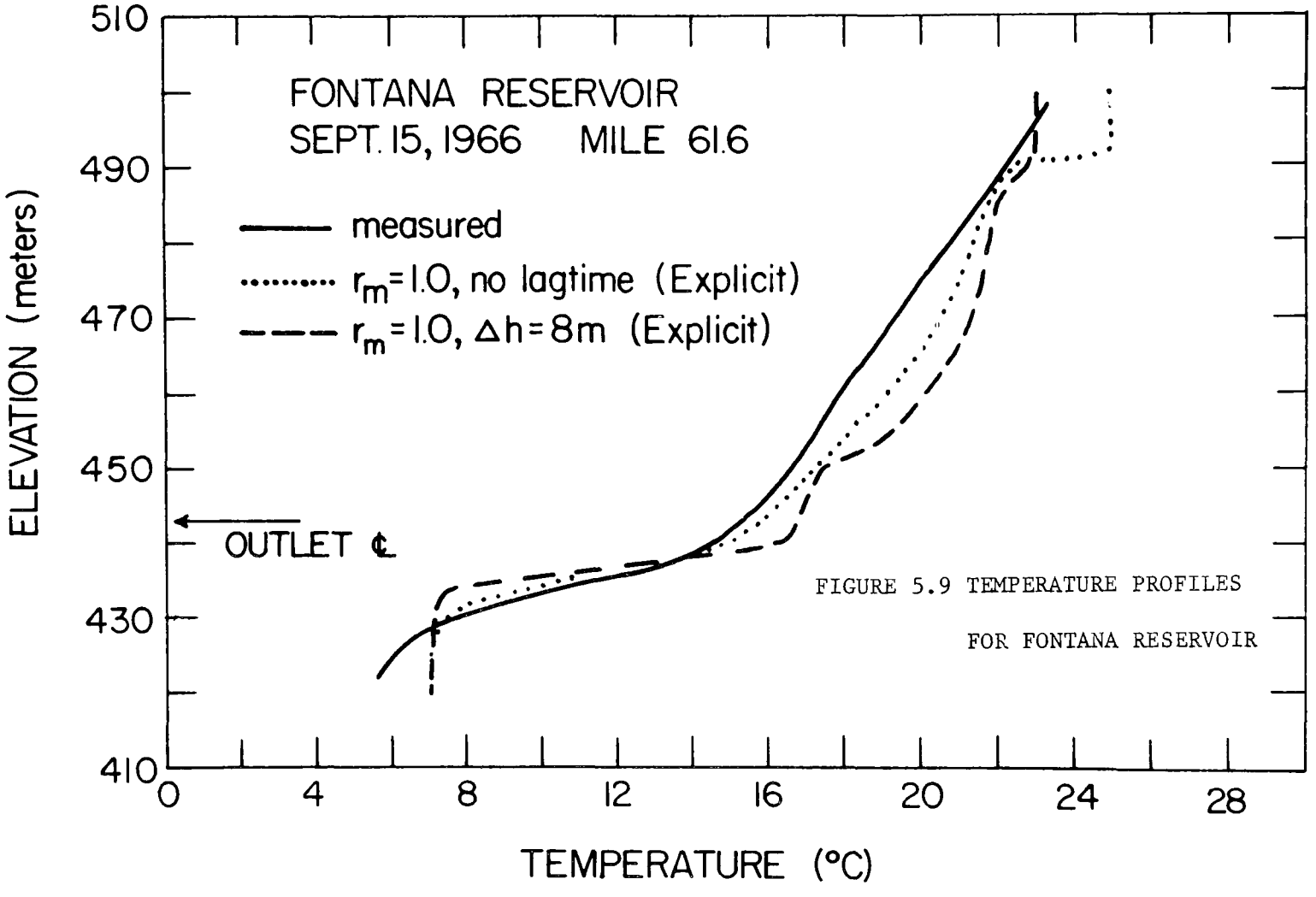

FIGURE 5.9 TEMPERATURE PROFILES FOR FONTANA RESERVOIR

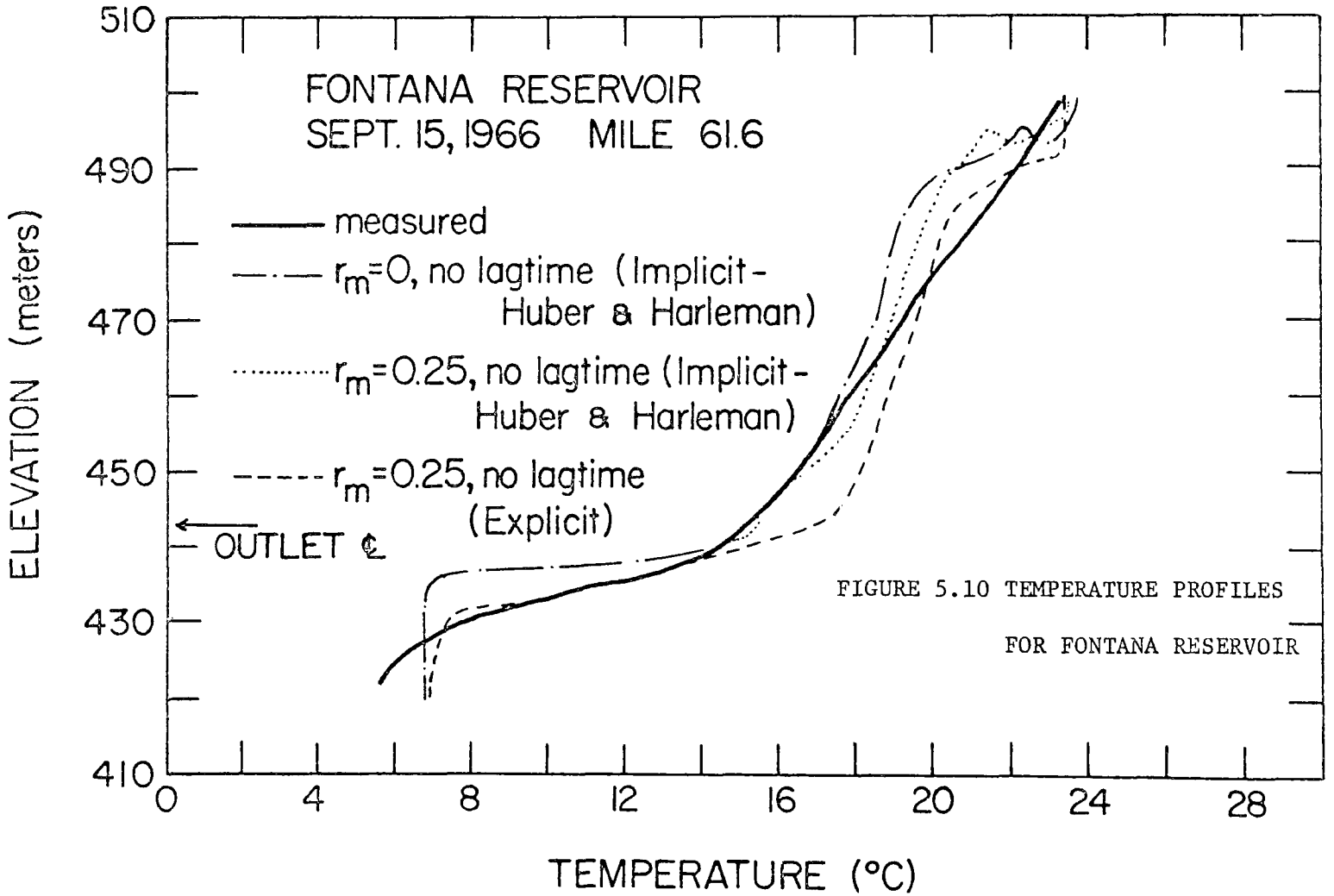

FIGURE 5.10 TEMPERATURE PROFILES FOR FONTANA RESERVOIR

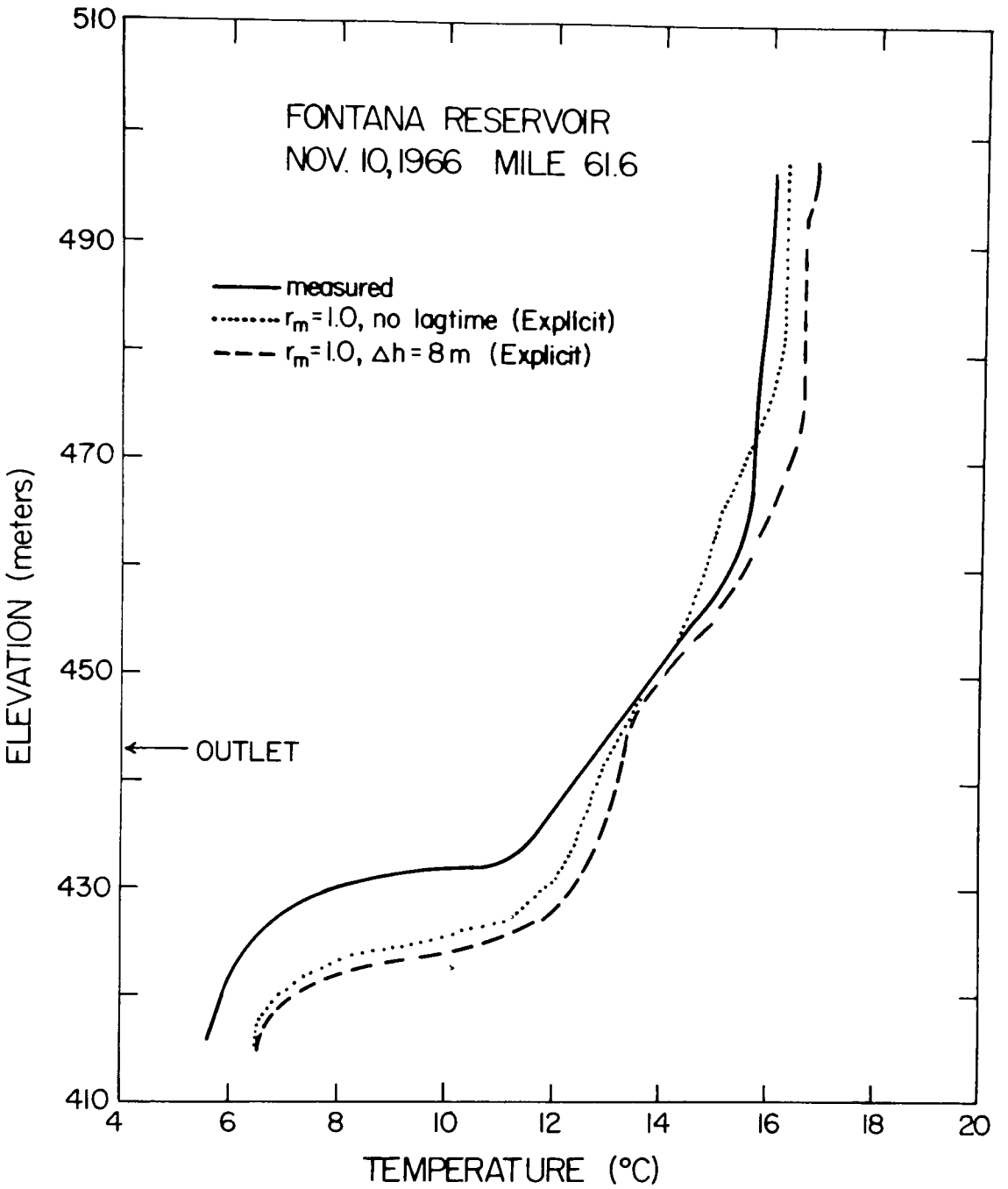

FIGURE 5.11 TEMPERATURE PROFILES FOR FONTANA RESERVOIR

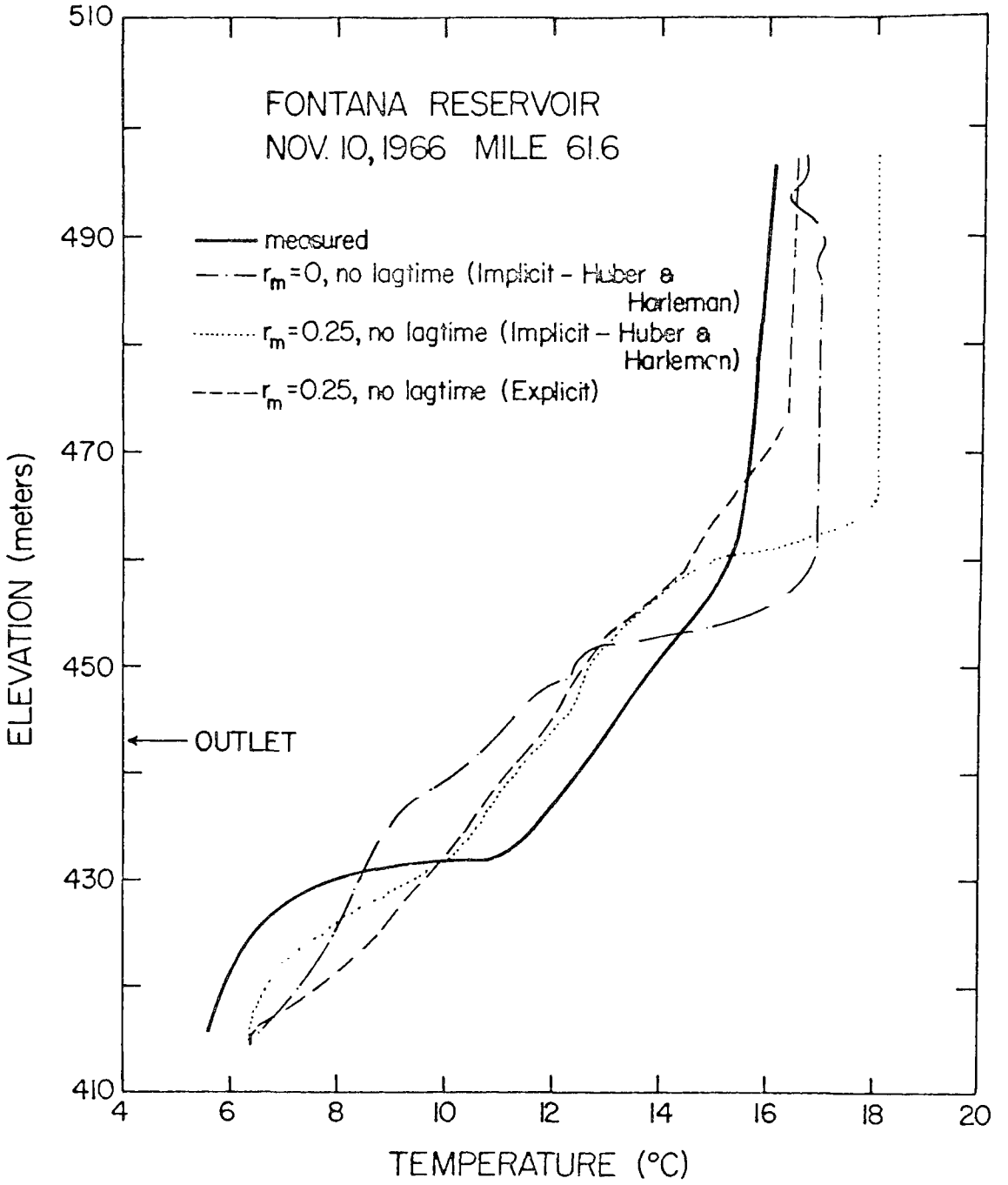

FIGURE 5.12 TEMPERATURE PROFILES FOR FONTANA RESERVOIR

2. Molecular diffusion, entrance mixing, no lag time

($D = D_m$, $r_m = 0.25$, $d_m = 6.0m$)

The remaining three cases were calculated from the modified explicit scheme developed in Chapter 2 and are for:

3. Molecular diffusion, entrance mixing, no lag time

($D = D_m$, $r_m = 0.25$, $d_m = 6.0m$)

4. Same as 3 but $r_m = 1.0$

5. Molecular diffusion, entrance mixing, lag time

($D = D_m$, $r_m = 1.0$, $d_m = 6.0$, $\Delta h = 8m$)

5.2.2.1 Results and Conclusions for the Temperature Model

For case 1, without any parameters which depend on observations within the reservoir, the general shape of the outlet temperature curve was reasonably reproduced. Predicted temperatures were consistently low, however, especially after the peak outlet temperature was reached. The low temperatures after the peak were attributed, by Huber and Harleman, to lack of a lag time consideration. The discrepancies before the peak were felt to be possibly due to inaccurate (low) values of solar radiation which would cause insufficient heat to be present in the outlet regions at early times.

The predicted vertical temperature profiles were in fairly good agreement with those measured. This is quite important since, for predictive purposes, values for r_m, d_m and Δh will, in general, not be known. Therefore, it can be concluded that, without modification, the predictive model of Huber and Harleman is quite sufficient for times before the peak temperature in the outlet

is reached. However, after the peak temperature the results become poorer with instabilities occuring in the temperature profiles near the surface (Figures 5.9,5.11).

The effect of mixing (r_m = 0.25) was found to be insignificant until the cooling cycle began. The effect, similar to the laboratory results (Section 4.4.1.3), was to raise predicted temperatures in the region of the outlet because the mixing was assumed to take place with the warmer surface water.

For comparison, the explicit numerical scheme was run with r_m = 0.25 as in case 2 of Huber and Harleman. The outlet temperature curve yields slightly higher values than those predicted by the implicit scheme. Though it is difficult to specify the exact cause, it is felt that this is due to the proper assignment of temperature to the convective velocity depending on the direction of the velocity (Section 2.5.1). Though the results using the explicit scheme are better before the peak temperature, they are almost identical to the implicit solution afterwards. As the outlet temperature reflects an average temperature over the withdrawal layer, more pronounced changes can be noted in the temperature profiles.

The effect of increasing r_m to a value of 1.0 is seen to generally increase predicted temperatures. Without any lag time consideration outlet temperatures are predicted within 1°C for the entire year. Vertical temperature profiles are also in excellent agreement and no instabilities are present.

The effect of including a lag time, $\Delta h = 8m$, chosen to be indicative of the total depth of the inflowing streams, is seen to shift the entire outlet temperature curve to the right, thus "lagging" the outflow temperatures. Temperatures before the peak are lower and after the peak higher than under identical conditions not including lag time. The same trend can be noted in the vertical temperature profiles.

It was found that increasing the values of the diffusion coefficient to 100 times the molecular values did not change the temperature predictions. From Equation 2-99 and 2-102 the maximum value of numerical dispersion, with $\Delta y = 2m$, $\Delta t = 1$ day is found to be approximately 50 times the molecular values. Thus it is concluded that neither molecular diffusion nor numerical dispersion are significant in this analysis.

5.3. Water Quality Prediction

5.3.1 Conservative Tracer

No long term dye tests were made in Fontana Reservoir. Predicted cumulative mass out curves, analogous to those for the pulse injection solution discussed in Chapter 4, were calculated. This was done to illustrate the mechanics of stratified reservoir flow and for comparison with the detention time predictions derived from the graphical method of Wunderlich,(Section 3.2).

For the cumulative mass out prediction the same parameters that gave the best fit of the outlet temperature curves were used ($r_m = 1.0$, $d_m = 6.0m$, $\sigma_i = 4m$, $\Delta h = 8m$). A hypothetical instan-

taneous injection was made every 60 days starting March 2. The volume of each dye injection was equal to the total volume of flow of a particular day. The cumulative mass out curves for a given input (Section 3.4.2.3) thus reflect the percentage of the days inflow which has passed through the reservoir as a function of time. For example, from Figure 5.13, by September 7 (250 days), 87% of the flow which entered on March 2 (day 61) and 30.5% of the flow which had entered on May 1 (day 121) had passed through the reservoir.

Figure 5.13 dramatically demonstrates the short circuiting characteristics of a stratified reservoir. The warm inflow of March 2 and May 1 entered at the reservoir surface 60 days apart. The outlet cumulative mass out curves are for the most part parallel, separated by approximately 60 days. This in indicative of convection being the major transport mechanism in the vertical direction. The cooler inflows of late summer and of the fall (August 31 and October 29, days 241 and 301) enter beneath the reservoir surface at their respective density levels. Once entered, the vertical distance to the outlet is reduced by the subsurface entrance, these inflows tend to reach the outlet relatively sooner than the spring inflows. For example it is predicted that ten per cent (10%) of the input of October 29 would have passed through the reservoir by November 7 (day 308), i.e., nine (9) days later. The corresponding time for the input of March 2 is ninety four (94) days.

FIGURE 5.13 FONTANA RESERVOIR SIMULATION OF VARIOUS PULSE INJECTIONS

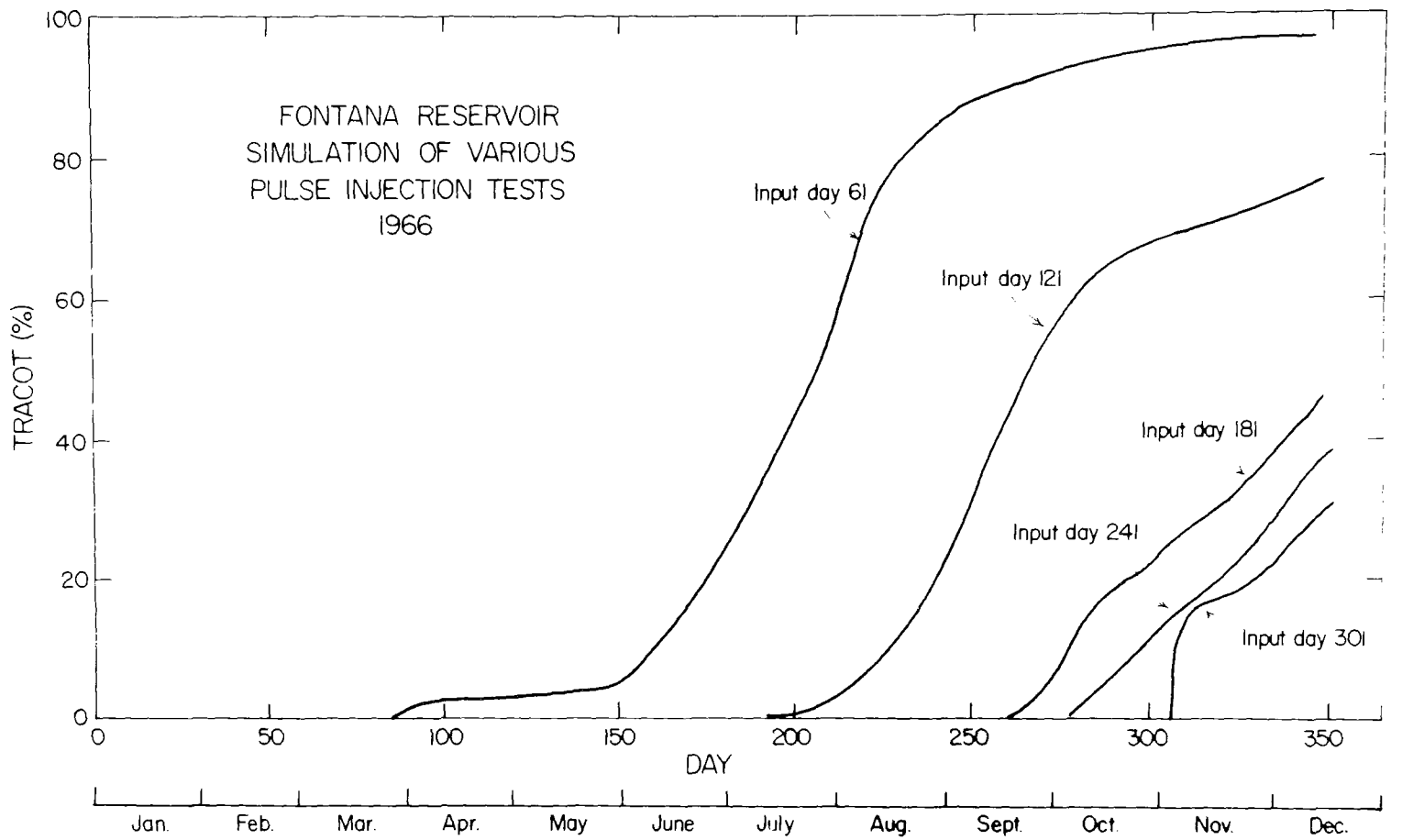

During the cooling cycle, inflows tend to enter below the surface of the reservoir. Each successivelycooler input tends to enter lower than the input which enters before it. This has the effect of raising the level of the withdrawal layer and preventing the complete withdrawal of a given day's input. For example, by December 21 (350 days) only seventy seven per cent (77%) of the flow which entered on May 1 had been withdrawn from the reservoir. Since the gradual process of surface mixing due to surface cooling is well advanced by late December, it is highly probable that all of the flow which entered on May 1 would not pass through the reservoir until the following spring or summer. For later inputs this effect becomes more pronounced. For example, only 52 per cent of the inflow of July 1 (day 181) had passed through the reservoir by December 21.

In view of the above discussion, it is clear that it is extremely difficult to define precisely what is meant by a detention time for a given reservoir input. Wunderlich, as stated in Chapter 3, defined the detention time, t_d, as the time span between a given input temperature and the time at which that temperature appeared in the outlet. In Table 5.2 the detention times are presented for inputs of every 60 days from March 2 as calculated by the graphical method of Wunderlich (Figure 3.1). For comparison, the corresponding percentages of these inputs which would have passed through the reservoir at the end of their respective "detention times" and by day 350 (December 21) from

Table 5.2

Input	Detention Times (t_d) Wunderlich (57) (Days)	Tracot after t (%) Equation 3.28	Tracot by December 21 (%)
March 3(Day 61)	0	___	96
May 1(Day 120)	123	25	77
July 1(Day 181)	___	___	47
August 31(Day 241)	___	___	39
October 29(Day 301)	20	18	31

Table 5.2 Comparison of Predicted Cumulative Mass Out Values with The Detention Times of Wunderlich.

Figure 5.13 are given.

The "detention times" calculated from Wunderlich's method do not correlate with the values calculated from Equation 3-38. Though Wunderlich calculates no outflow from the inputs of July 1 and August 31, Equation 3-38 predicts that 47% and 39% of these inputs, respectively, would have passed through the reservoir by December 21. Though the curves of Figures 5.13 have not been verified from field measurements they are indicative of the stratified reservoir flow through pattern since the results follow the trend verified in the laboratory. It can be generally concluded that the use of one "detention time" for a given input in an attempt to describe its flow through time in a stratified reservoir gives results which do not reflect the complicated short circuiting characteristics of a stratified reservoir.

5.3.2 Dissolved Oxygen Predictions for Fontana Reservoir

5.3.2.1 Input to the Mathematical Model

In addition to the inputs to the temperature model already discussed (section 5.2), several additional parameters need to be specified in order to solve the D.O. prediction problem. These are:

1. The D.O. and B.O.D. of the incoming streams and the long term B.O.D. decay rate, K (Equation 3-14)
2. The initial conditions for B.O.D. and D.O. in the reservoir at time $t = t_i$
3. A surface boundary condition which effectively accounts for the interplay between D.O. and B.O.D. production and

consumption at the reservoir surface (this was discussed in Section 3.4.1.1).

The D.O. of the incoming streams to Fontana reservoir was monitored daily from February through December of 1966 from random samples analyzed in the field using a simplified Winkler test kit. Daily weighted averages of the five incoming streams were used as inputs to the model.

The B.O.D. of the incoming streams was sporadically sampled in 1965. In the most polluted stream, Tuckaseegee, at most twelve tests were made at a given monitoring station. The results were presented in terms of five day B.O.D. with no long term B.O.D. reported. Typical D.O. and B.O.D. data is presented in Table 5.3. The station number refer to points along the various rivers as shown in Figure 5.1. A weighted average of the median values for the station closest to the reservoir produced a five day B.O.D. of about 1.5 ppm. As was discussed in section 3.4.1.1, long term B.O.D. values, due to nitrification, are higher than five day B.O.D. values. Lacking any long term data, a constant input value of 8 ppm of B.O.D. was assumed.

A value for the first order decay constant, K, also had to be assumed. Again, considering a slow, long term decay, two different values, 0.01 and 0.05 day^{-1} were tested. Though K is probably temperature dependent there was no basis for assuming the functional relationship. It was also felt that a constant value would more clearly illustrate the other

TABLE 5.3

STATION NO.		FLOW (cfs)	$B.O.D._5$ (mg/ℓ)	$B.O.D._{10}$ (mg/ℓ)	$B.O.D._{15}$ (mg/ℓ)
11	NO. Tests	0	5		
	Maximum		2.1		
	Minimum		0.9		
	Median		1.3		
12	NO. Tests	0	5		
	Maximum		1.2		
	Minimum		0.7		
	Median		0.8		
14	NO. Tests	---	7	2	1
	Maximum		7.0^+	7.0^+	7.4^+
	Minimum		1.5	3.5	7.4^+
	Median		1.7	3.5	7.4^+

TABLE 5.3 B.O.D. MEASUREMENTS IN FONTANA RESERVOIR INFLOWS

assumptions which had been made.

Unfortunately, there was no B.O.D. profile taken at the time that the first D.O. profile in the lake was made, (April 20, 1966). In fact, the only B.O.D. measurements taken in the reservoir were in July and August of 1965 at depths no greater than 20 meters. Therefore, initial conditions, $B.O.D._i$, for Equation 3-15 had to be assumed.

In order to illustrate the sensitivity of the results to the initial condition, calculations were carried out for a uniform $B.O.D._i$ of 3 ppm and for zero $B.O.D._i$ in the reservoir on March 1. (Table 5.4)

Since the reservoir was isothermal on March 1, it was assumed that the D.O. in the reservoir was uniform at that time. An inspection of the measured outlet D.O. in February and March indicated that a reasonable initial D.O. value would be 8 ppm on March 1. This differs from the saturated value of 12.2 ppm for the isothermal reservoir temperature of 6.7°C that one might be tempted to assume.

5.3.2.2 Comparison with D.O. Measurements in Fontana Reservoir

Predicted outlet D.O. concentrations and profiles for various days of the year for different initial and input B.O.D. condition and D.O. surface assumptionsare presented in Figures 5.14-5.23. The same parameters that were arrived at from the temperature model (r_m = 1.0, d_m = 6m, σ_i = 4m, Δh = 8m, Section 5.2) were used. The different trends which result from

Table 5.4

Run	D.O. Initial (ppm)	B.O.D. Initial (ppm)	K $(Day)^{-1}$	
1	8	0	0.01	
2	0	3	0.05	Entire Euphotic Zone Saturated
3	8	3	0.01	
4	8	3	0.05	
5	8ppm	3ppm	0.05	Top 3m Saturated

Table 5.4 The Various Initial Condition Tested in the D.O. Analysis.

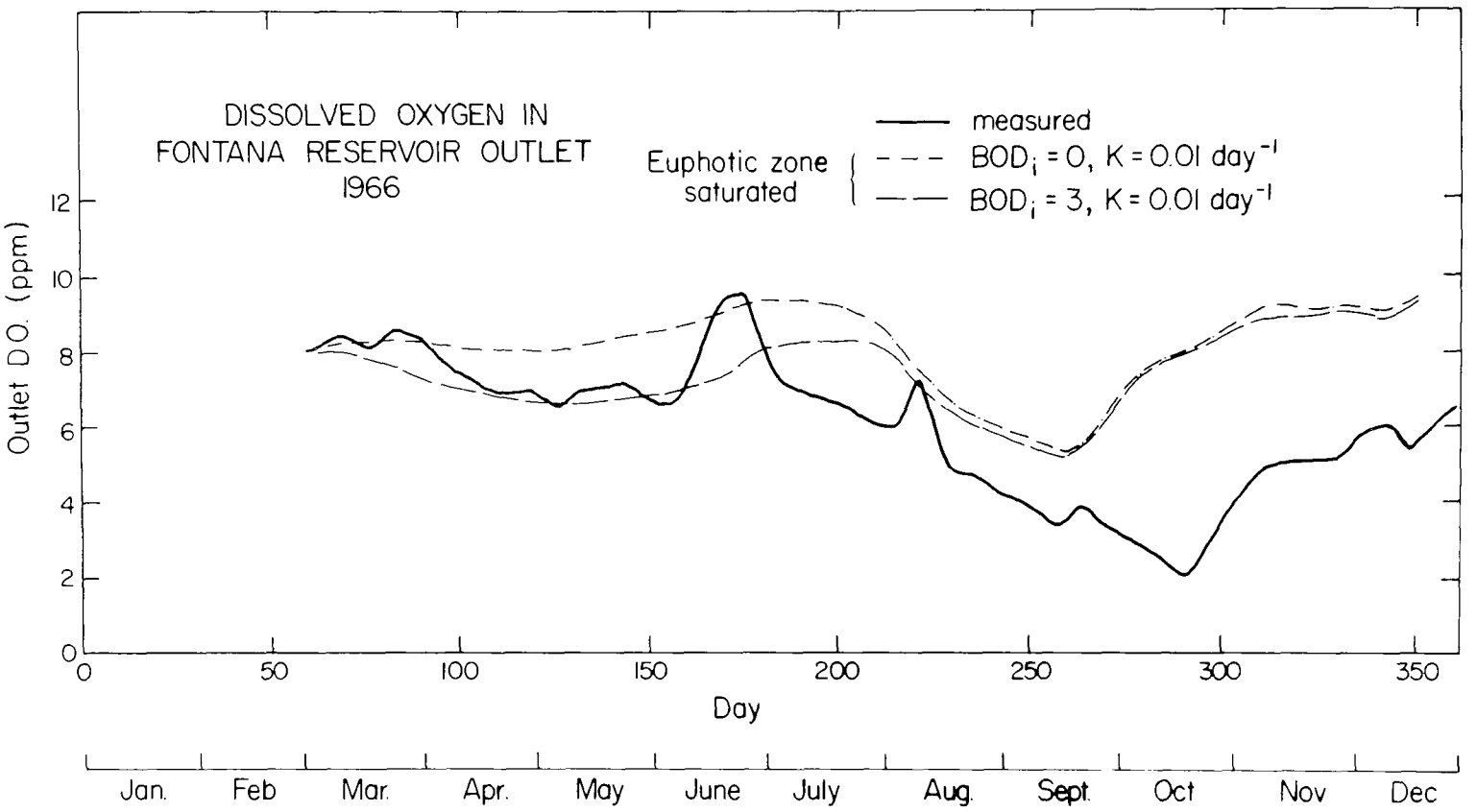

FIGURE 5.14 OUTLET D.O. CONCENTRATIONS FOR FONTANA RESERVOIR

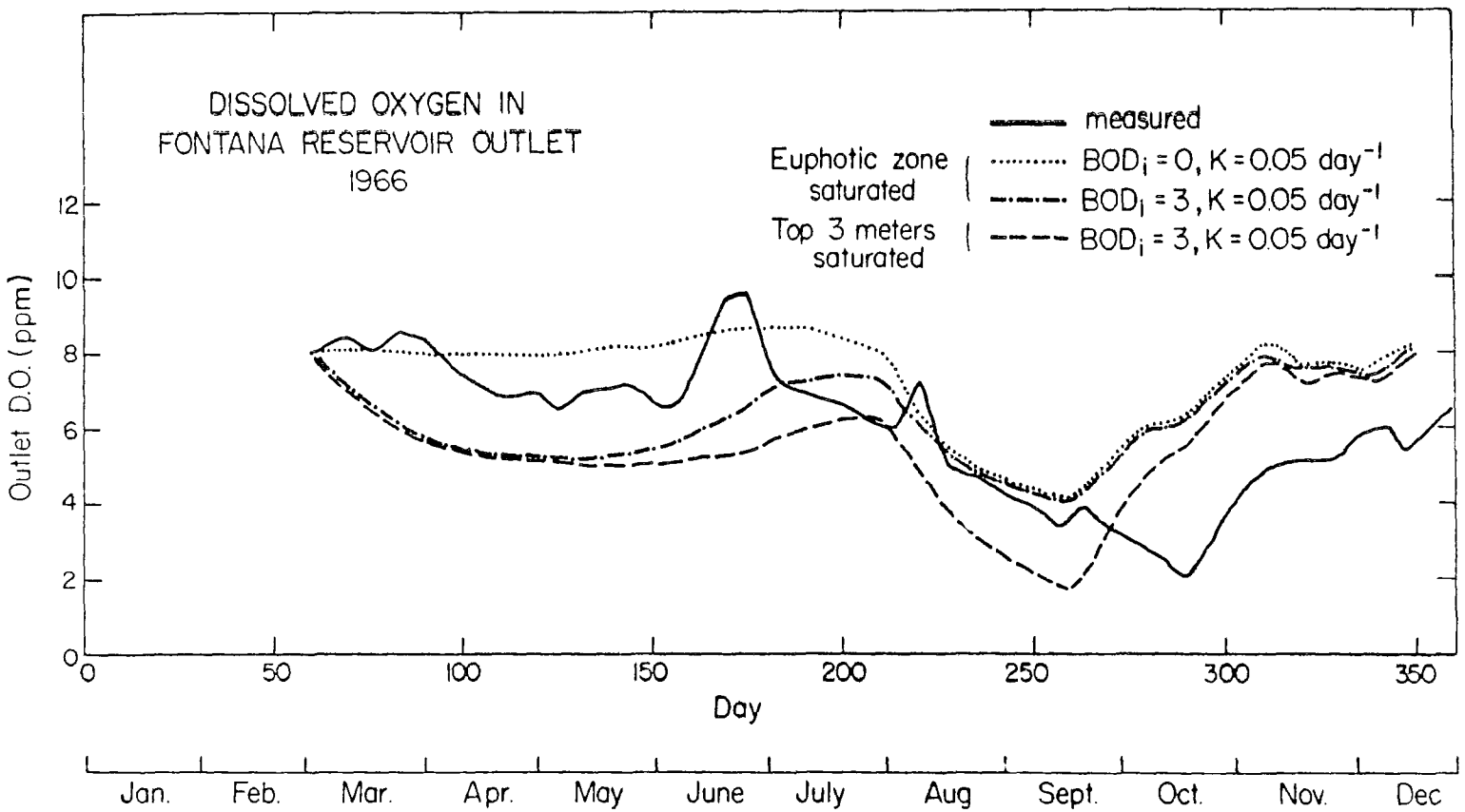

FIGURE 5.15 OUTLET D.O. CONCENTRATIONS FOR FONTANA RESERVOIR

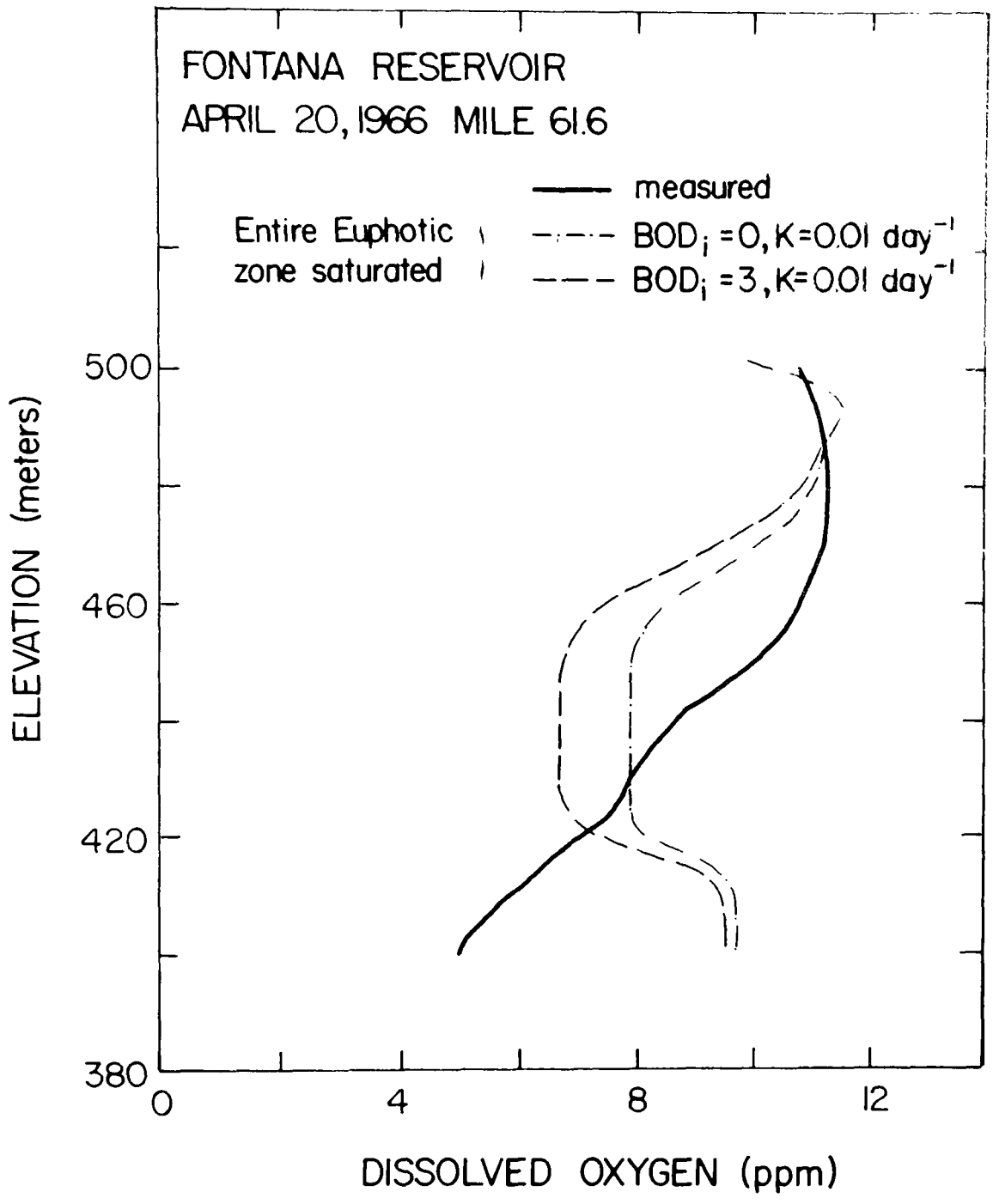

FIGURE 5.16 DISSOLVED OXYGEN PROFILES FOR FONTANA RESERVOIR

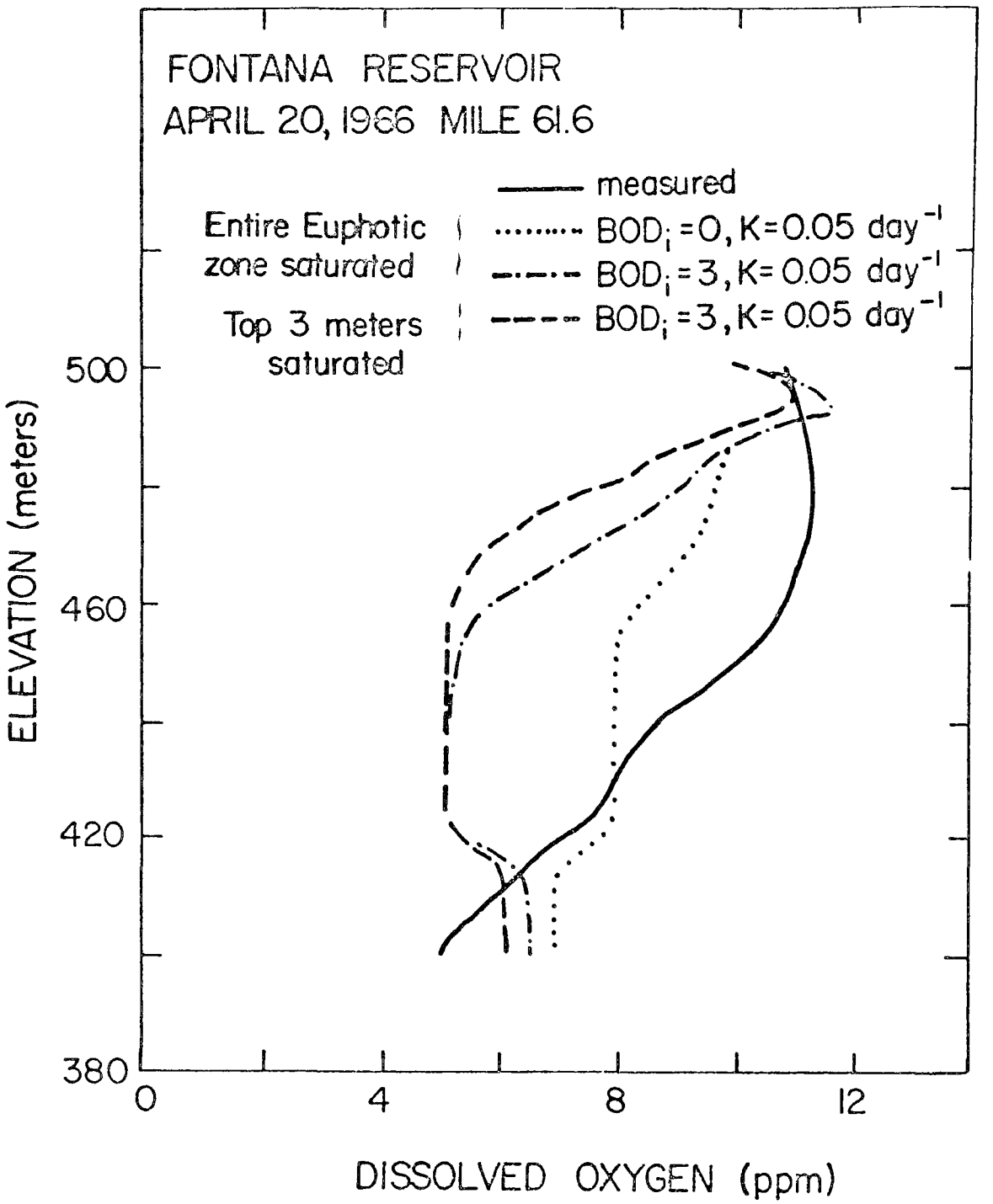

FIGURE 5.17 DISSOLVED OXYGEN PROFILES FOR FONTANA RESERVOIR

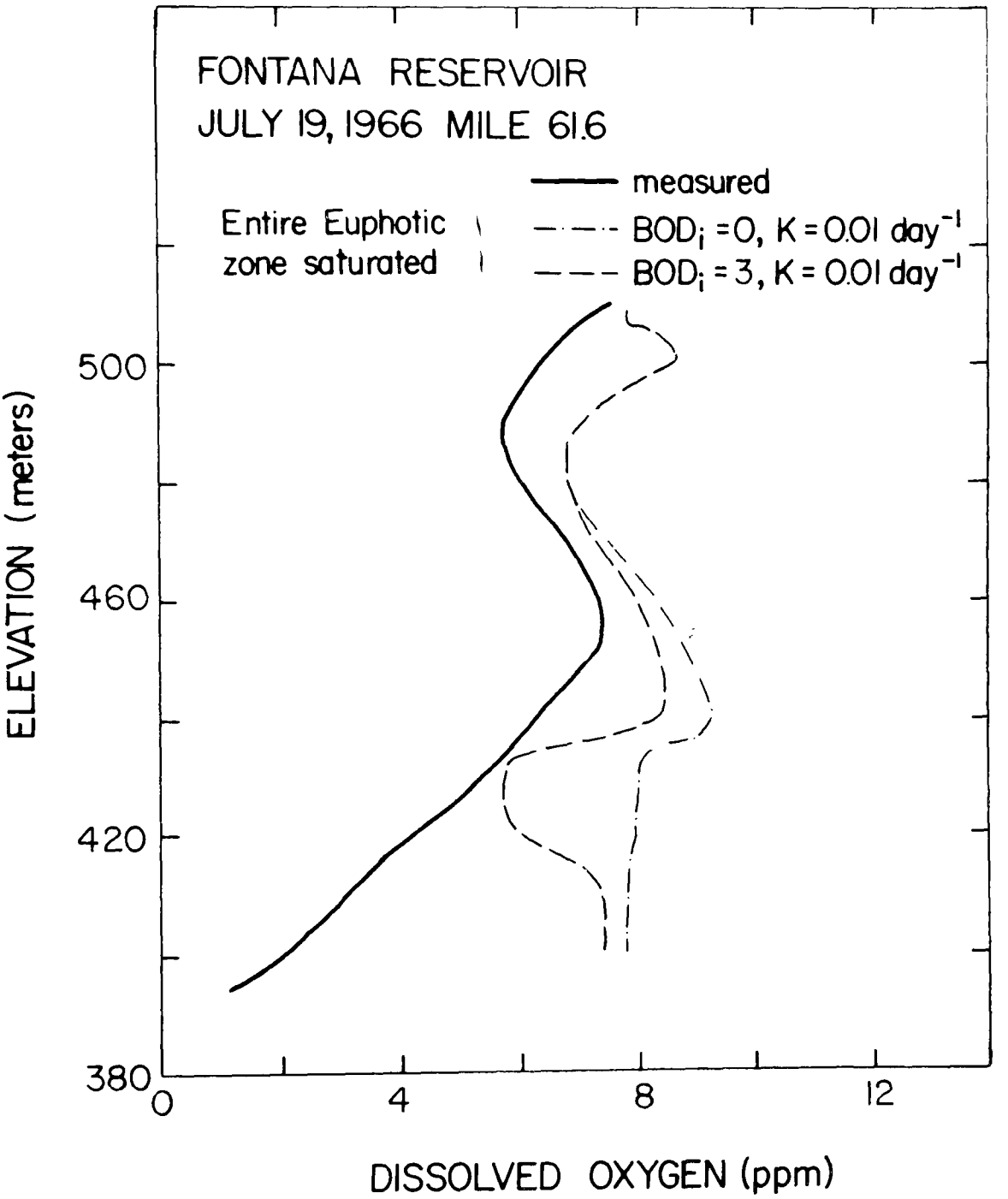

FIGURE 5.18 DISSOLVED OXYGEN PROFILES FOR FONTANA RESERVOIR

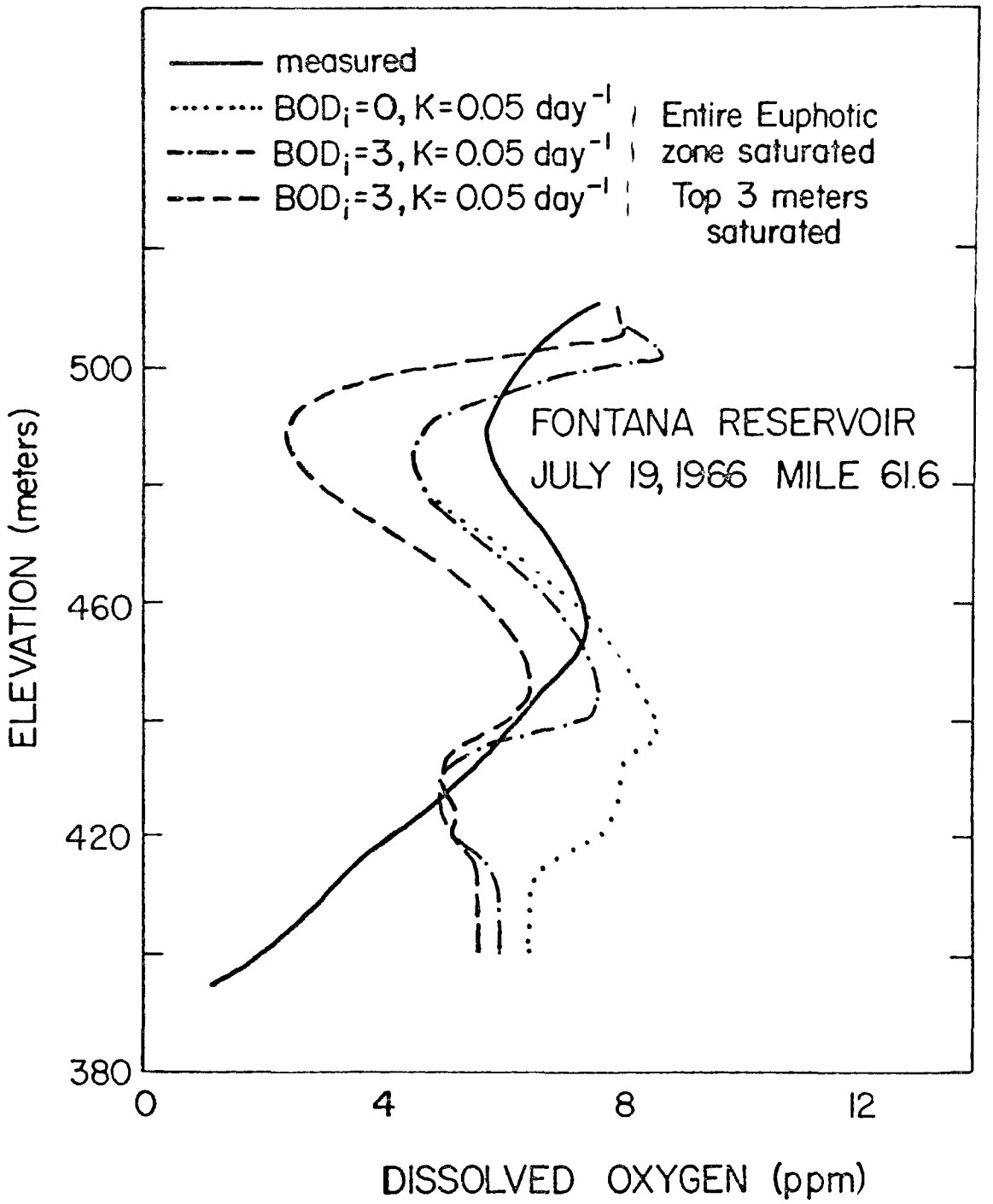

FIGURE 5.19 DISSOLVED OXYGEN PROFILES FOR FONTANA RESERVOIR

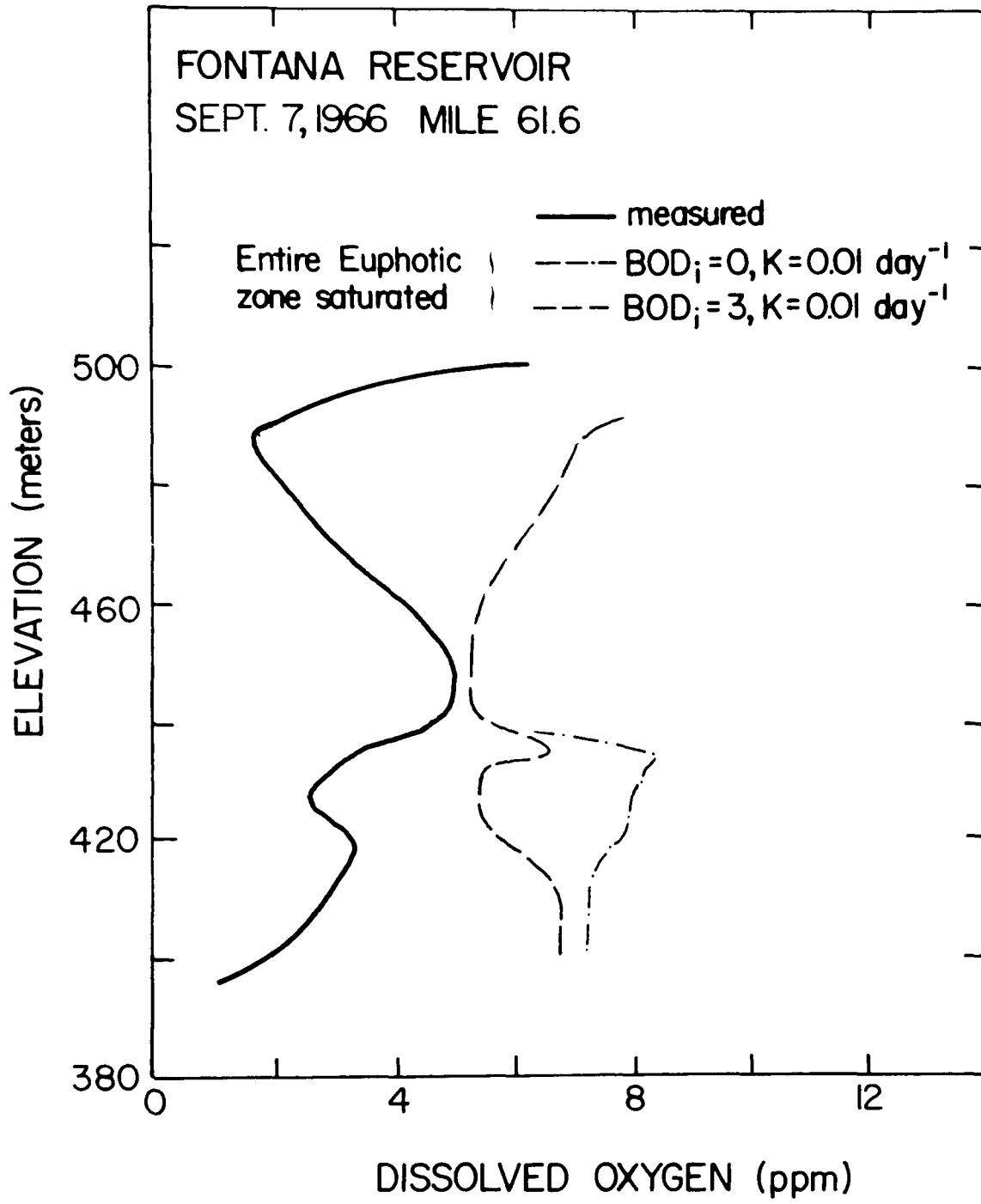

FIGURE 5.20 DISSOLVED OXYGEN PROFILES FOR FONTANA RESERVOIR

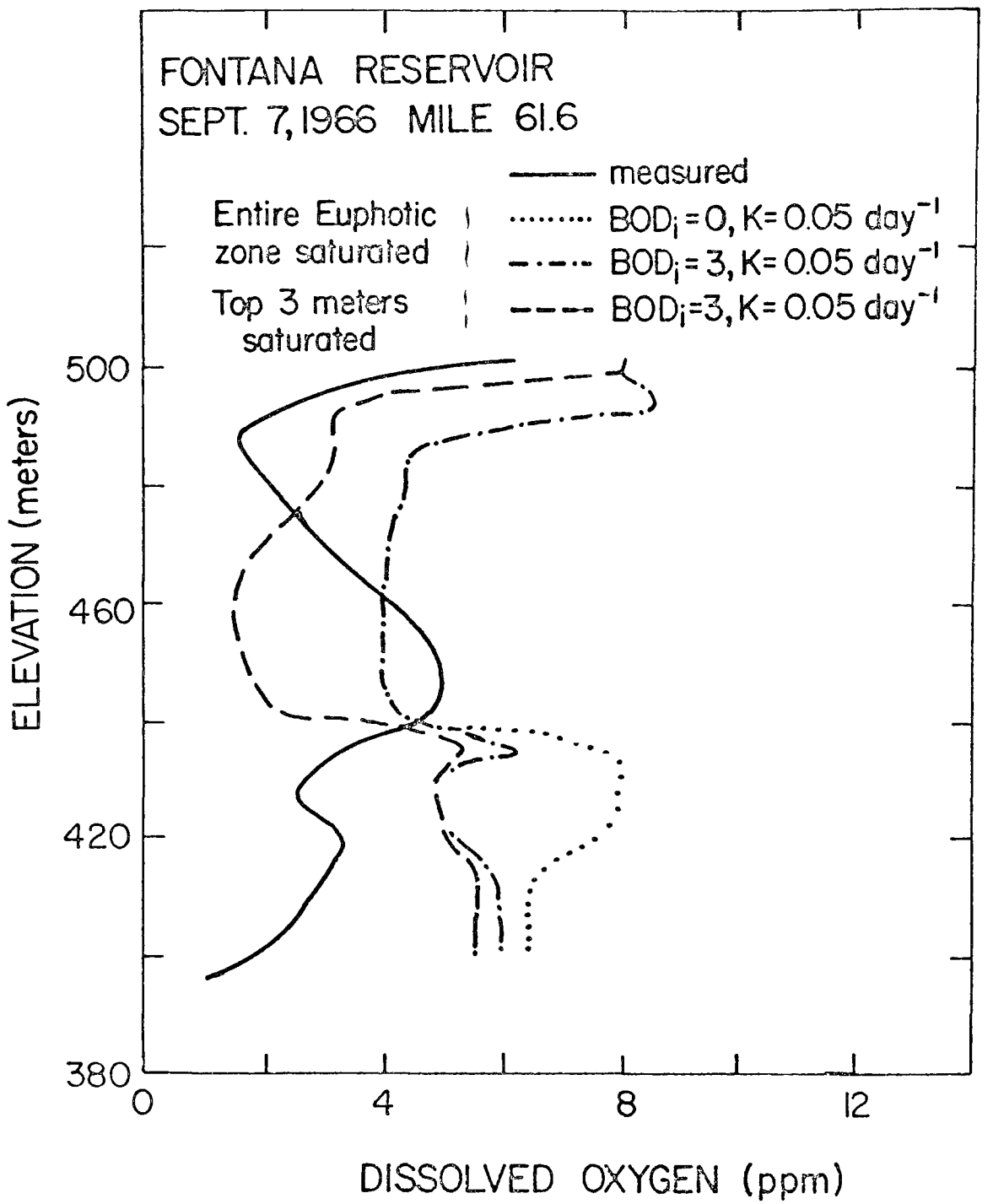

FIGURE 5.21 DISSOLVED OXYGEN PROFILES FOR FONTANA RESERVOIR

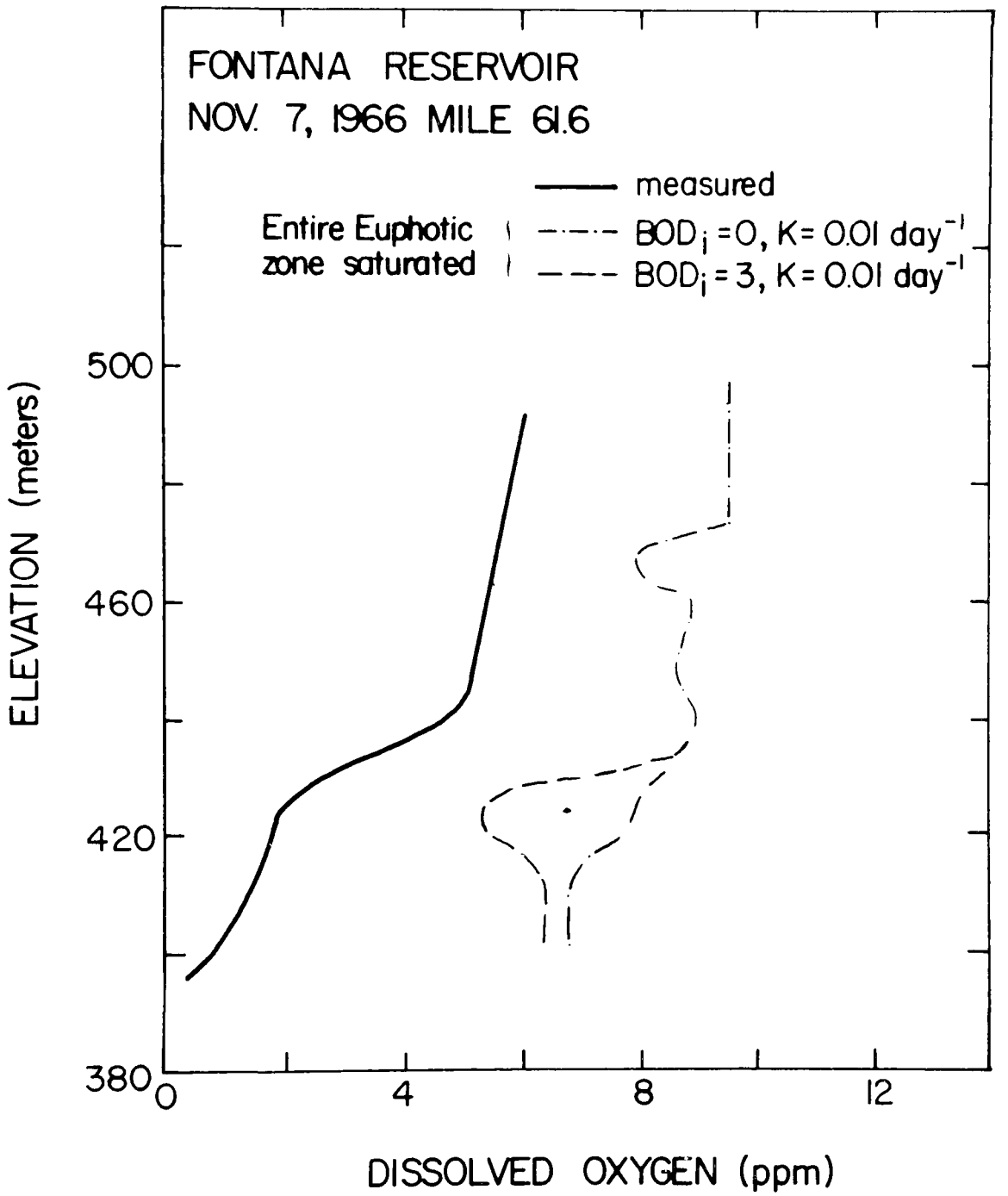

FIGURE 5.22 DISSOLVED OXYGEN PROFILES FOR FONTANA RESERVOIR

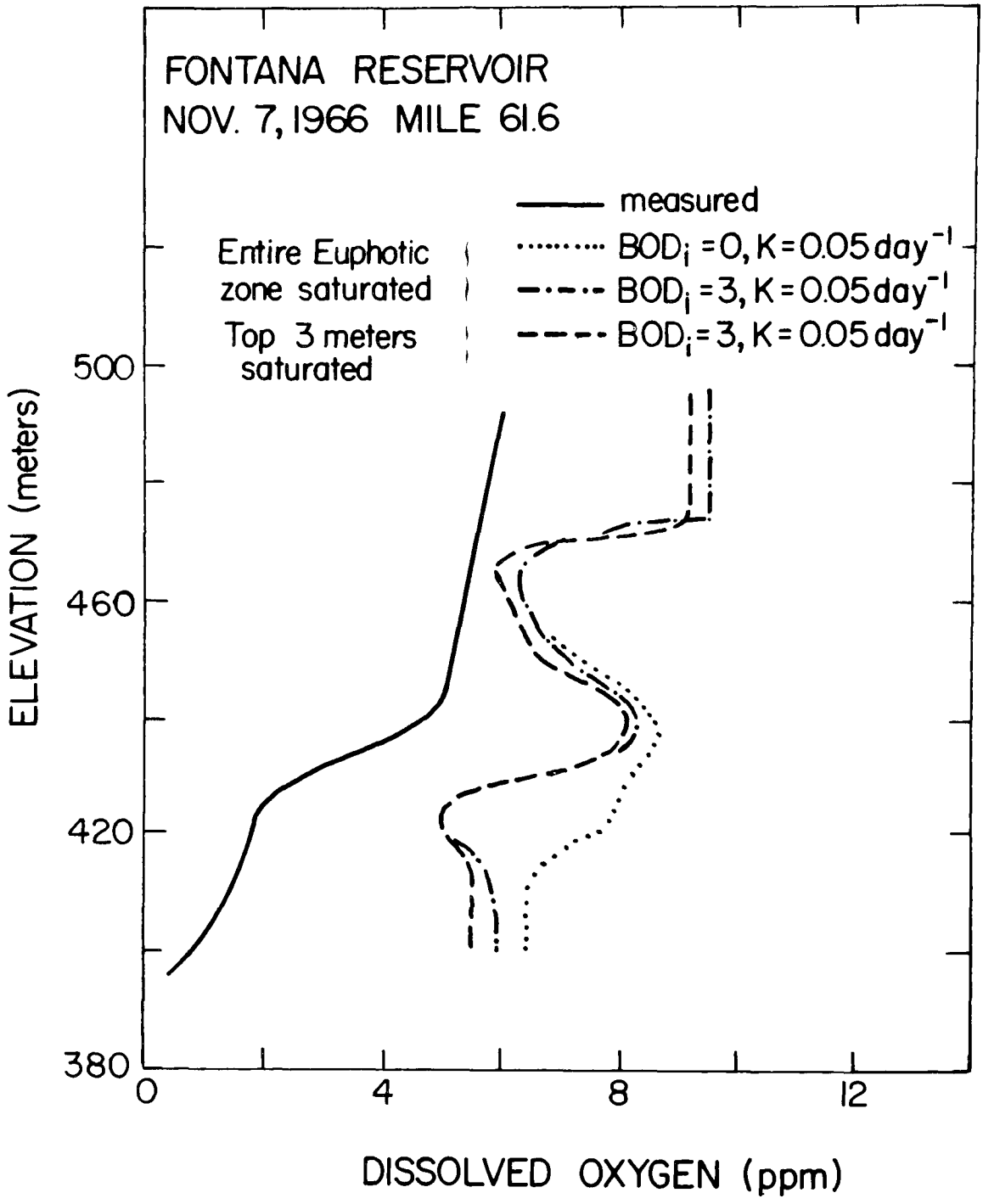

FIGURE 5.23 DISSOLVED OXYGEN PROFILES FOR FONTANA RESERVOIR

The different assumptions mentioned above help to illustrate the mechanics of the D.O. prediction model and its sensitivity to the various assumptions resulting from a lack of certain data.

From Figures 5.14 and 5.15 (considering for a moment the case where the entire euphotic zone (approximately 6m for Fontana) has been assumed to be saturated (Section 3.4.1.2)), it is seen that if K is constant, and the initial B.O.D. value is changed from 0 to 3.0 ppm, lower D.O. predictions result until about day 225 (August 13). This corresponds to the time at which the temperature in the outlet is beginning to rise (Figure 5.4) indicating that the warm inflow water of the previous months is reaching the outlet. Thus, the assumption for the initial B.O.D. in the reservoir tends to affect the outlet D.O. only as long as the major part of the water discharged is the water which was initially in the reservoir. The same trend is found in the predicted D.O. profiles.

The effect of increasing the decay rate, K, is to increase the rate of D.O. consumption within the reservoir. A value of K = 0.05 instead of 0.01 day^{-1} produces lower predicted D.O. values in all cases.

Changing the surface assumption for D.O. from saturation in the entire euphotic zone (6m) to saturation to a depth of 3m (initial B.O.D. = 3 ppm) is seen to result in generally lower D.O. predictions. This is due to two phenomena. The first is the obvious fact that less dissolved oxygen is being input to the model

in the surface region. The second is involved in the assumption that the inflowing water is mixing with the water over the top 6m of the reservoir. Because this entire depth is not saturated under the assumption of surface saturation to only 3m, less dissolved oxygen is entrained in the incoming water through the mixing process.

One curious point about all of the profiles is the prediction of a reversal near the bottom of the reservoir. This is due to the inflows of March 6-10 which were saturated with D.O. but colder than the initial isothermal temperature of 6.7°C. Therefore, in the mathematical model, high oxygenated water was brought to the bottom layer of the reservoir displacing the water which was originally there. Since no bottom oxygen demand was assumed, the only mechanism of D.O. consumption was the B.O.D. originally present in this water. Since a constant value of 8 ppm B.O.D. was assumed for all of the inflows, the maximum D.O. consumption was 8 ppm. Perhaps there was some residual B.O.D at the bottom or the incoming B.O.D. of the March 6-10 water was greater than 8 ppm. In the absence of detailed data, it is impossible to come to a definite conclusion.

CHAPTER 6. CONCLUSIONS AND RECOMMENDATIONS FOR FUTURE RESEARCH

6.1 The Thermal Stratification Phenomena

In reservoirs characterized by horizontal isotherms, water entering at the upstream end undergoes some initial mixing and enters the reservoir at an elevation corresponding to its own density. The water which enters at the beginning of the stratification season tends to enter at the reservoir surface and remain in the reservoir for a relatively longer time than the cooler water which enters late in the stratification cycle. The thickness of the internal withdrawal layer near the reservoir outlet depends on the vertical temperature gradient at the outlet, decreasing as the temperature gradient increases. The temperature and water quality in the outflow are average values for the water in the withdrawal layer. As summer turns to fall, evaporative cooling and the resulting surface instabilities tend to cause a mixed isothermal layer which eventually returns the reservoir to a completely isothermal state. During this mixing process the water quality of the reservoir also tends to become uniform.

6.2 Temperature Predictions

The temperature model of Huber and Harleman was modified to include an internal lagtime and a proper assignment of temperatures to the vertical convective term depending on the sign of the convective velocity. The horizontal advective velocities were determined from a selective withdrawal theory developed by Koh and assumptions about the shape of the inflow velocity distribution. Vertical convection was found to be the major mechanism for heat transport within the reservoir. No vertical turbulent diffusivities were introduced at any time

into the mathematical model. During the initial period of the year in which temperature profiles are stable with regard to vertical density distribution, the effect of vertical diffusion does not appear to be important. In later periods of potentially unstable vertical density distributions, the effect of vertical mixing is accounted for indirectly by the development of a uniformly mixed surface layer. In both laboratory and field cases excellent temperature predictions were obtained with the modified temperature model during the entire yearly stratification cycle. This is an improvement over the model of Huber and Harleman in which outlet temperature predictions after the time of the peak outflow temperature tended to be lower than observed values.

6.3 Concentration Predictions

6.3.1 Laboratory Experiments

Outlet concentration predictions for pulse injections of a conservative tracer in a laboratory reservoir agreed well with measured values. The predicted time at which measurable values of tracer first appeared in the outlet was usually somewhat earlier than measured values. However, the time of the peak outlet concentration was fairly well predicted. The concentration predictions were found to be more sensitive than temperature predictions to assumptions about the shape of the inflow velocity profile and the amount of mixing at the reservoir entrance. However, one set of parameters was sufficient to predict reasonable results for the three different types of experiments conducted. Difficulty was occasionally found with predicting outlet concentrations from pulse injection toward the end of the stratification

cycle. This is attributed to the high degree of short circuiting which occurs at late times and the resulting sensitivity to the choice of the various parameters in the mathematical model. Nevertheless, the laboratory tests illustrated that many of the parameters involved in the mathematical model can be related to the depth of the inflowing stream at the head of the reservoir.

6.3.2 Field Results

The simulations of pulse injection tests for an actual reservoir served to illustrate the flow through time characteristics of a stratified reservoir. The trends are similar to those found in the laboratory. Flows entering toward the latter part of the stratification cycle tend to reach the outlet much more quickly, relative to the time of inflow, than flows which enter in the spring. It is unfortunate that there are no long term pulse injection dye tests available for comparison with the predicted values.

In 1966 detailed temperature and D.O. measurements were made in Fontana reservoir and its inflowing streams. Though long term B.O.D. data was not available, the water quality mathematical model was tested using assumed values for initial B.O.D. and values for the B.O.D. of the inflowing streams. In addition, having no detailed information about the complicated oxygen balance in the surface regions, two different assumptions were tested. The resulting sensitivity analysis to the various assumptions made about the input B.O.D. data provided several interesting observations.

A first order decay rate was assumed for the long term B.O.D. process. Lower D.O. prediction resulted from higher values of the decay

constant.

Increasing the value assumed for the initial amount of B.O.D. in the reservoir decreases the amount of D.O. in the outlet until the temperature at the outlet begins to rise. After this time, the initial value assumed for the B.O.D. in the reservoir changed D.O. profiles and outlet D.O. concentrations very slightly. This indicated that the quality of the discharged water began to be determined by the quality of the water in the inflowing streams as the warm inflow began to reach the outlet.

Assuming the entire eupthotic zone to be saturated produced higher D.O. predictions than the assumption of D.O. saturation to only 3 meters.

The lack of sufficient input water quality data made it difficult to make a direct comparison of measured and predicted values except through a sensitivity analysis. The combination of the information gained from the pulse injection simulation and the D.O. predictions indicates that the use of a detention time approach for water quality prediction in a stratified reservoir tends to greatly oversimplify a very complex problem.

6.4 Recommendations for Future Research

6.4.1 Improvement of the Mathematical Model

1. The present model is capable of handling only one entering stream at the head of the reservoir. In the case of the T.V.A. Fontana data, the input temperature and water quality of the incoming streams were averaged to yield one value of T_i, Q_i, ℓ_i. This may not be representative of the actual inflow to the reservoir. It is possible

that one stream could be colder than another (for example, if one stream was the discharge from another reservoir) and thus it could enter the reservoir at a different depth without interacting. Therefore provision should be made to accommodate several input streams to the reservoir independently of one another.

Similarly provision should also be made to handle more than one outlet from the reservoir. For this case the outflow withdrawal velocity distribution could be considered to be the sum of the Gaussian distribution of the individual outlets.

2. At present observed water surface elevations are an input to the mathematical model. These could be computed from a continuity equation applied to the entire reservoir including precipitation and evaporative mass loss in addition to the inflow and outflow contributions.
3. The water quality model is oriented toward treating substances undergoing a first order decay. The decay rate has been assumed to be constant and independent of temperature. A more general model could be developed to treat other types of decay rates or water quality interactions including decay rates which are temperature dependent.

6.4.2 Laboratory and Field Research

1. Much work remains to be done on the determination of the inflow velocity distribution in a continuously stratified reservoir. A theoretical prediction of the spread of the

inflow layers is almost imperative if multiple inflows are to be incorporated into the model. This would also be beneficial in determining a proper thickness, Δh, for the lag time determination.

2. The time for the inflow to reach its own density level was based on a two-layered theory. A method which accounts for the continuous stratification in the reservoir would be a more rigorous approach.
3. Laboratory tests for a continuous injection of tracer would be another step toward verifying the model for conditions closer to those encountered in the field. Experiments using radioactive tracer with known decay rates would be a more stringent test of the mathematical model.
4. There is a need for long term water quality data in existing reservoirs. Included in this are (1) the initial reservoir water quality at the beginning of the stratification cycle, (2) long term B.O.D. and chemical oxygen demand (C.O.D.) tests on the water in the inflowing streams and the effects of temperature on these processes and (3) evaluation of the complicated D.O. balance in the euphotic zone.

It is hoped that the development of a method for analyzing D.O. and other water quality parameters in a stratified reservoir will provide the incentive for field data collection programs to be used in further tests of the mathematical model.

CHAPTER 7. BIBLIOGRAPHY

1. Austin, Garry H., Gray, Donald A., and Swain, Donald A., Report on Multilevel Outlet Works at Four Existing Reservoirs, Bureau of Reclamation, U. S. Department of the Interior, Denver, Colorado, August 1968.

2. Bella, David A., Finite-Difference Modelling of River and Estuary Pollution, Ph.D. Thesis, New York University, New York, April 3, 1967.

3. Bohan, J. P. and Grace, J. L., "Mechanics of Flow from Stratified Reservoirs in the Interest of Water Quality", U. S. Army Engineering Waterways Experiment Station, Corps of Engineers, Vicksburg, Miss., 1969.

4. Burt, W. C., "Preliminary Study of the Predicted Water Changes at the Lower Snake River Due to the Effects of Projected Dams and Reservoirs", Water Research Associates, Corvalis, Oregon, November 1963.

5. Camp, T. R., Water and Its Impurities, Reinhold Publishing Company, New York, 1963.

6. Carslaw, H. S. and Jaeger, J. C., Operational Methods in Applied Mathematics, Dover Publications, Inc., New York, 1963.

7. Cederwall, Klas and Hansen, Jens, Tracer Studies on Dilution and Residence Time Distribution in Receiving Waters, Water Research, Vol. 2, No. 4, June 1868, pp. 297-310.

8. Churchill, M. A. and Nicholas, W. R., Effects of Impoundments on Water Quality, A.S.C.E., SA6, December 1967.

9. Daily, J. W. and Harleman, D. R. F., Fluid Dynamics, Addison Wesley Publishing Company, Inc., Reading, Mass., 1966.

10. Daly, B. J. and Pracht, W. E., A Numerical Study of Density Current Surges, Los Alamos Scientific Laboratory of the University of California, Los Alamos, New Mexico, 1968.

11. Dougal, M. D. and Baumann, E. R., Mathematical Models for Expressing the B.O.D. in Water Quality Studies, Proc. 3rd Annual Am. Water Research Conference, San Francisco, November 1967.

12. Fenerstein, D. L. and Selleck, R. E., Fluorescent Tracers for Dispersion Measurements, A.S.C.E., SA4, August 1963.

13. Gannon, J. J., River and Laboratory B.O.D. Rate Considerations, A.S.C.E., SA1, February 1966.

14. Harleman, D. R. F. and Abraham, G., One-Dimensional Analysis of Salinity Intrusion in the Rotterdam Waterway, Delft Hydraulics Laboratory, Publication No. 44, October 1966.

15. Harleman, D. R. F. and Stolzenbach, K. D., "A Model Study of Thermal Stratification Produced by Condenser Water Discharge", M.I.T. Hydrodynamics Laboratory Technical Report No. 107, October 1967.

16. Holley, E. R., Discussion of Difference Modeling of Stream Pollution, by David A. Bella and William E. Dobbins, Proc. A.S.C.E., Vol. 94, No. SA5, Paper 6192, October 1968.

17. Holley, E. R. and Harleman, D. R. F., "Dispersion of Pollutants in Estuary Type Flows", M.I.T. Hydrodynamics Laboratory Technical Report No. 74, January 1965.

18. Huber, W. C. and Harleman, D. R. F., "Laboratory and Analytical Studies of the Thermal Stratification of Reservoirs", M.I.T. Hydrodynamics Laboratory Technical Report No. 112, October 1968.

19. Ingols, Robert S., Discussion of Some Effects of Water Management on Biological Production in Missouri River Main Stem Reservoirs, Proceedings of the Specialty Conference on Current Research into the Effects of Reservoirs on Water Quality, Vanderbilt University, Nashville, Tennessee, 1968.

20. Jaske, R. T. and Spurgeon, J. L., A Special Case, Thermal Digital Simulation of Waste Heat Discharge, Water Research, Vol. 2, No. 11, November 1968.

21. Kennedy, R. E., "Computation of Daily Insolation Energy", Bulletin, American Met. Society, Vol. 30, No. 6, pp.208-213, June 1949.

22. Keulegan, G. H., Laminar Flow at the Interface of Two Liquids, Journal of Research for the National Bureau of Standards, Vol. 32, June 1944.

23. Koh, R.C.Y., "Viscous Stratified Flow Towards a Line Sink", W. M. Keck Laboratory Report, KH-R-6, California Institute of Technology, 1964.

24. Kohler, M. A., "Lake and Pan Evaporation" in Water Loss Investigation, Lake Hefner Studies, Technical Report, U.S.G.S. Professional Paper 269, 1954.

25. Krenkel, P. A., Cawley, W. A. and Minch, V. A., The Effects of Impoundments on River Waste Assimilative Capacity, Journal of the Water Pollution Control Federation, 37, 9, September 1965.

26. Krenkel, P. A., Thackston, E. L. and Parker, F. L., The Influence of Impoundments on Waste Assimilation Capacity, Proc. of the Specialty Conference on Current Research into the Effects of Reservoirs on Water Quality, Vanderbilt University, Nashville, Tennessee, TR 17, 1968.

27. Krenkel, P. A., Thackston, E. L. and Parker, F. L., Impoundment and Temperature Effect on Waste Assimilation, Proc. A.S.C.E., SA1, Feb. 1969.

28. Lean, G. H. and Whillock, A. Z., The Behavior of a Warm Water Layer Flowing Over Still Water, International Association for Hydraulic Research, 11th International Congress, Leningrad, 1965.

29. Levenspiel, O. and Bischoff, K. B., Patterns of Flow in Chemical Process Vessels, Advances in Chemical Engineering, Vol. 4, New York, 1963.

30. Miyauchi, T., "Residence Time Curves", Chemical Engineering (Japan) Vol. 17, p. 382, 1953.

31. Murphy, K. L. and Timpany, P. L., Design and Analysis of Mixing for an Aeration Tank, A.S.C.E., SA5, October 1967.

32. O'Connell, R. L., Thomas, N. A., Godsil, P. J. and Hearth, C. R., Report of Survey of the Trucker River, U. S. Public Health, 1963.

33. O'Connell, R. L. and Thomas, N. A., Effect of Benthic Algae on Stream Dissolved Oxygen, Proc. A.S.C.E. Journal of the Sanitary Engineering Division, SA3, 1965.

34. O'Connor, D. J. and DiToro, D. M., The Solution of the Continuity Equation in Cylindrical Coordinates with Dispersion and Advection for an Instantaneous Release, Symposium on Diffusion in Oceans and Fresh Water, August 31-September 2, 1964.

35. O'Connor, D. J. and DiToro, D. M., The Distribution of Dissolved Oxygen in a Stream with Time Varying Velocity, W.R.R., Vol. 4, No. 3, June 1968.

36. Orlob, G. T. and Selna, L. G., "Mathematical Simulation of Thermal Stratification in Deep Reservoirs", A.S.C.E. Specialty Conference on Water Quality, Portland, Oregon, January 1968.

37. Posey, Frank H. and DeWitt, J. W., Effects of Reservoir Impoundment on Water Quality, A.S.C.E. PO1, January 1970.

37a. Pritchard, D. W. and Carpenter, J. H., Appendix to "A Study of the Effects of a Submerged Weir in the Roanoke Rapids Reservoir Upon Downstream Water Quality", by F.F. Fish, C.H.J. Hull, B.J. Peters and W.E. Knight, Special Report No. 1, Roanoke River Studies.

38. Purcell, L. T., The Aging of Reservoir Waters, Journal of the American Water Works Association, 31, 10, October 1969.

39. Rehwer, C., Evaporation from Free Water Surfaces", U. S. Dept. of Agriculture, Technical Bulletin No. 271, December 1931.

40. Scalf, M. R., Witherow, J. L. and Priesing C. P., IRON-59 as Solids Tracer in Aqueous Suspensions, A.S.C.E., SA6, December 1968.

41. Shamir, U. Y. and Harleman, D. R. F., "Numerical and Analytical Solutions of Dispersion Problems in Homogeneous and Layered Aquifers", M.I.T. Hydrodynamics Laboratory Technical Report No. 89, May 1966.

42. Slotta, L. S. and Elwin, E. H., Entering Streamflow Effects on Currents of a Density Stratified Model Reservoir, Bulletin No. 44, Engineering Experiments Station, Oregon State University, Corvallis, Oregon, October 1969.

43. Slotta, L. S. and Terry, M. D., The Numac Method for Non-Homogeneous Unconfined Marker Cell Calculations Bulletin No. 44, Part II, Engineering Experiments Station, Oregon State University, Corvallis, Oregon, October 1969.

44. Stigter, C. and Siemons, J., Calculations of Longitudinal Salt-Distributions in Estuaries as a Function of Time, Delft Hydraulics Laboratory, Publication No. 52, October 1967.

45. Sundaram, T. R., et. al., An Investigation of the Physical Effects of Thermal Discharges into Cayuga Lake, Cornell Aeronautical Lab., Inc., Buffalo, New York, November 1969.

46. Symons, J. M., Irwin, W. H., Clark R. M. and Robeck, G. G., Management and Measurement of D.O. in Impoundments, U. S. Dept. of the Interior, FWPCA, Cincinnati, Ohio, September 1966.

47. Taylor, G. I., "The Dispersion of Matter in Turbulent Flow Through a Pipe", Proc. Royal Society (London) (A), 223 (1954).

48. Thackston, E. L. and Morris, M. W., Tracing Polluted Reservoir Inflows with Fluorescent Dyes, Vanderbilt University, TR 21, 1969.

49. Thirumurthi-Dhandapani, A Break-Through in the Tracer Studies of Sedimentation Tanks, Journal, Water Pollution Control Federation, Part 2, Vol. 41, No. 11, November 1969.

50. Thomas, H. A. and McKee, J. E., "Longitudinal Mixing in Aeration Tanks", Sewage Works Journal, Vol. 14, 1942.

51. Verduin, J., Primary Predictions in Lakes, Limnology and Oceanography, 1, 4, April 1956.

52. Villemonte, J. R., Rohlich, G. A. and Wallace, A. T., Hydraulic and Removal Efficiencies in Sedimentation Basins, Third International Conference on Water Pollution Research, Munich, Germany, Paper 16, 1966.

53. Ward, J. C., Annual Variating Stream Water Temperature, Proc. A.S.C.E., No. SA6, December 1963.

54. Water Resources Engineering, Inc., Mathematical Models for the Prediction of Thermal Energy Changes in Impoundments, Final Report to the FWPCA, Columbia River Thermal Effects Project, December 1969.

55. Wilson, James, U. S. Department of the Interior Techniques of Water Resources Investigation of the USGS - Fluorometric Procedures for Dye Tracing, Book 3, Chapter A12, 1968.

56. Wunderlich, W. O., "Heated Mass Transfer Between a Water Surface and the Atmosphere", Internal Memorandum, T.V.A. Engineering Laboratory, Norris, Tennessee, 1968.

57. Wunderlich, W. O. and Elder, R., "Graphical Temperature and D.O. Prediction Methods", Water Resources Research, T.V.A. Division of Water Control Planning, Engineering Laboratory, Norris, Tenn., April 1969.

APPRENDIX I

THE COMPUTER PROGRAM

In this appendix the FORTRAN computer program used to solve the finite volume representations of the temperature and water quality equations developed in Chapters 2 and 3 is presented. The program consists of a MAIN routine and sixteen subprograms. Temperatures are referred to by T and concentrations by C.

The MAIN routine performs all of the input and output except writing the output for the pulse injection concentrations and cumulative mass out information. This is done in subroutine SPECOT (N). The MAIN routine initializes many variables and constants, adjusts the surface elevation and calls for either solution to a pulse injection of a concervative tracer or for dissolved oxygen predictions.

At the beginning of the MAIN routine is a clock routine to indicate the time required for the computations (the subroutine CLOCK is a library program at the Massachusetts Institute of Technology Information Processing Services Center). The time required to compute both temperatures, D.O., B.O.D. profiles and outlet values for three hundred (300) time steps and fifty (50) distance steps is approximately three (3) minutes.

Comment cards are included in both the MAIN routine and in the subprograms to indicate points of interest and the specific function of each of the subprograms. A listing of the necessary input variables to the program is presented in APPENDIX II. In APPENDIX III, sample input data for the D.O. prediction model is presented for the case of

initial B.O.D. = 0., initial D.O. = 8 ppm, K = 0.05 day^{-1} and saturation of the entire euphotic zone.

```
C  RESERVOIR STRATIFICATION AND CONCENTRATION PREDICTION PROGRAM, 1970.

      COMMON T(60,2),EL(60),XL(60),A(60),TI(310),TA(310),SIGH(310)
      COMMON FIN(310),WIND(310),DD(310),QI(310),QO(310),P(50),NPR
      COMMON UOMAX(2),UIMAX(2),DTTI,DTTA,DTSIGH,DTFIN,DTWIND,DTDD,DTQI
      COMMON DTQO,JM,JOUT,JIN,KDIF,KSUR,KOH,KQ,KLOSS,YSUR,YOUT,DT,DY
      COMMON TSTOP,EVPCON,OMEGA,BZ,SPREAD,SIGMAI,SIGMAO,ETADY,TVARI
      COMMON TVARO,EVAP,RAD,TAIR,PSI,DERIV,HAFDEL,EPSIL,GJ
      COMMON YBOT,NN,BETA,DAJM,DELCON,V( 60,1),UI( 60,1),DTT
      COMMON RHO,HCAP,KMIX,RMIX,JMIXB,MIXED,QMIX,KAREA,DATRAD,ATRAD(310)
      COMMON AR,WINDY,CO,CI,B( 60),S( 60),EX( 60),EXO( 60),ARF,UO( 60,1)
      COMMON QIN(310),TIN(310),CC(20,60,2),CCC(20,310),COUT(20,310)
      COMMON CCT(20,310),QQMIX(60),XINF(60),OUTF(60),MIXH,MM
      COMMON SURF(310),GRAV,SLOPE,VISCOS,LAGTIM(310)
      COMMON PMASOT(20),PMASIN(20),ET,NTRAC(20),ITR,IST0,IS01,IS02
      COMMON ISTON,IST01,THICK1,THICK2,DOXLE(60,20),DO(306),BOD(306)
      COMMON NLEVE(306),VOL,NW,NDET,Z,Z1,DDOC,NGDET,DBOD,JEUP
      COMMON NBOUND,NGRID
      DIMENSION WH(20),AA(60),XXL(60)
      EQUIVALENCE (N,NN)
C READ IN ALL DATA FOR PROGRAM.
      READ (5,900) (WH(I),I=1,20)
      WRITE(6,900) (WH(I),I=1,20)
      READ (5,900) (WH(I),I=1,20)
      READ (5,901) JM,JOUT,KDIF,KSUR,KOH ,KQ,KLOSS,NPRINT,KAREA,KMIX,
     1MIXED
      READ (5,902) YSUR,YOUT,DT,TSTOP,TZERO,EVPCON,OMEGA,BZ
      READ (5,902) SPREAD,SIGMAI,ETA,BETA,RHO,HCAP,DELCON,RMIX
      READ (5,901) NTI,NTA,NSIGH,NFIN,NSURF,NDD,NQI,NQO
      READ (5,902) DTTI,DTTA,DTSIGH,DTFIN,DSURF,DTDD,DTQI,DTQO
      READ (5,902) (TI(I),I=1,NTI)
      READ (5,902) (TA(I),I=1,NTA)
      READ (5,902) (SIGH(I),I=1,NSIGH)
      READ (5,902) (FIN(I),I=1,NFIN)
      READ (5,902) (SURF(I),I=1,NSURF)
      READ (5,902) (DD(I),I=1,NDD)
      READ (5,902) (QI(I),I=1,NQI)
      READ (5,902) (QO(I),I=1,NQO)
      READ(5,903) SLOPE,GRAV,VISCOS
  903 FORMAT(3F12.2)
      READ(5,901) NGDET,NBOUND,NGRID
C  NBOUND=1=EUPHOTIC ZONE SATURATED
C  NBOUND=2=SATURATION OF ARBITRARY SURFACE LAYER THICKNESS TO BE SPECIFIED.
C  NBOUND=3=ZERO SURFACE LAYER THICKNESS FOR SATURATION.
C  NGDET=1=DETENTION TIME MODEL
C  NGDET=2=DO CALCULATION
      GO TO (15298,15299),NGDET
C  READ DATA FOR PULSE INJECTION.
15298 READ(5,927) ITR,(NTRAC(I),I=1,ITR)
927   FORMAT (I5/16I5)
      READ(5,901) NDET
13334 NDOCA=10000
      GO TO 15297
C  READ DATA FOR DO,BOD PREDICTIONS.
```

```
15299 READ(5,901) NDISSO,NBOD
      READ(5,902) DDOC,DBOD
      READ(5,902) (DO(I),I=1,NDISSO)
      READ(5,902)(BOD(I),I=1,NBOD)
      READ (5,901) NPROF
C  NPROF=1=UNIFORM INITIAL DO,BOD PROFILES.
C  NPROF=2=LINEAR INITIAL DO,BOD PROFILES.
      GO TO (12357,12358),NPROF
12357 READ(5,902) DOI,BODI
      GO TO 12359
12358 READ (5,902) DOB,DOT,BODB,BODT
12359 CONTINUE
      ITR=2
      NTRAC(1)=-2
      NTRAC(2)=-1
13333 READ (5,1563) Z,Z1,NDOCA
1563  FORMAT(2F10.5,I5)
15297 CONTINUE
      READ (5,902) THICK1,THICK2
      DY = (YSUR-YOUT)/FLOAT(JM-JOUT)
      YBOT = YOUT-DY*FLOAT(JOUT-1)
      GO TO (4,2), KAREA
C READ IN DATA FOR OTHER THAN LABORATORY RESERVOIR IF INDICATED.
    2 READ (5,901) NAA,NXXL,NWIND,NATRAD,JMP
      READ (5,902) DAA,DXXL,DTWIND,DATRAD,AAB,XXLB,ARF
      READ (5,902) (AA(I),I=1,NAA)
      READ (5,902) (XXL(I),I=1,NXXL)
      READ (5,902) (WIND(I),I=1,NWIND)
      READ (5,902) (ATRAD(I),I=1,NATRAD)
      DO 3 I=1,JMP
      T(I,1) = TZERO
      T(I,2)=TZERO
      EL(I) = YBOT+DY*FLOAT(I-1)
      RA = (EL(I)-AAB)/DAA
      L = RA
      A(I) = AA(L+1)+(RA-FLOAT(L))*(AA(L+2)-AA(L+1))
      A(I) = A(I)*ARF
      RA = (EL(I)-XXLB)/DXXL
      L = RA
      XL(I) = XXL(L+1)+(RA-FLOAT(L))*(XXL(L+2)-XXL(L+1))
    3 B(I) = BZ*ARF*EXP(OMEGA*EL(I))
C THE NUMBER 0.3989423=1.0/SQRT(2*PI).
      P(32) = 0.3989423/BZ/ARF
      P(33) = OMEGA*OMEGA/2.0
      P(34) = YOUT*OMEGA
      P(35) = P(32)*EXP(-P(33)*SIGMAI*SIGMAI)
      GO TO 5
    4 JMP = JM+IFIX((33.0-YSUR)/DY+0.5)
C THE NUMBER 0.01308866=1.0/30.48/SQRT(2*PI).
      CO = 0.01308866
      CI = 0.01308866
      ARF = 1.0
      AR = 0.7888E-10    *(TA(1)+273.16)**4
      P(22) = SIGMAI/CI
      DO 8 I=1,JMP
      B(I) = 30.48
      EL(I) = YBOT+DY*FLOAT(I-1)
      T(I,1) = TZERO
```

```
      IF (EL(I)-22.4) 6,7,7
    6 XL(I) = 10.0*(EL(I)+87.0)
      GO TO 8
    7 XL(I) = 1093.5
    8 A(I) = XL(I)*30.48
    5 BB = DT/A(JOUT+1)/DY
      E0=(A(1)+A(JM))/2.0+A(JM)*(SURF(1)-EL(JM))/DY
      JM1=JM-1
      DO 13 I=2,JM1
   13 E0=E0+A(I)
      E0=E0*DY*TZERO*0.1E04
      DTT=DT
      BBETA = QOUT(0)*BB
      WRITE (6,900) (WH(I),I=1,20)
      WRITE (6,904) JM,YSUR,RHO
      WRITE (6,905) JOUT,YOUT,HCAP
      WRITE (6,906) DY,YBOT,ETA
      WRITE (6,907) DT,TZERO,BETA
      WRITE (6,908) BBETA,SIGMAI,OMEGA
      WRITE (6,909) TSTOP,SPREAD,BZ
      WRITE (6,910) KDIF,KSUR,KOH ,KQ,KLOSS,KAREA,EVPCON,DELCON,KMIX
      WRITE (6,923) MIXED,RMIX,ARF
C INITIALIZE MANY VARIABLES.
      DO 850 N=1,310
      QIN(N)=0.0
      TIN(N)=0.0
      DO 851 M=1,ITR
      CCC(M,N)=0.0
      COUT(M,N)=0.0
      PMASOT(M)=0.0
      PMASIN(M)=0.0
  851 CCT(M,N)=0.0
  850 CONTINUE
      DO 852 I=1,60
      DO 853 M=1,ITR
      CC(M,I,1)=0.0
  853 CC(M,I,2)=0.0
      OUTF(I)=0.0
      QQMIX(I)=0.0
852   XINF(I)=0.0
      GO TO (38000,38001),NGUET
38001 GO TO (19488,19487),NPROF
19487 DO 87123 J=1,JM
      CC(1,J,1)=DOB+(FLOAT(J)*DY-DY)/(YSUR-YBOT)*(DOT-DOB)
      CC(1,J,2)=CC(1,J,1)
      CC(2,J,1)=BOUB+(FLOAT(J)*DY-DY)/(YSUR-YBOT)*(BOUT-BOUB)
87123 CC(2,J,2)=CC(2,J,1)
      GO TO 87124
19488 DO 83002 J=1,JM
      CC(1,J,1)=DOI
      CC(1,J,2)=DOI
      CC(2,J,2)=BOUI
83002 CC(2,J,1)=BOUI
87124 CONTINUE
38000 CONTINUE
      NW=0
      VOL=(A(1)+A(JM))*DY/2.
```

```
      DO 2131 J=2,JM1
2131  VOL=VOL+A(J)*DY
8555  CONTINUE
      NPR=NPRINT
      JXM=JM
      N = 0
      JMIXB = JM-MIXED
      QMIX = 0.0
      ET = 0.0
      RAD = 0.0
      EVAP = 0.0
      E2=0.0
      E3=0.0
      TAIR = 0.0
      EPSIL = 0.0
      HAFDEL = 0.0
      NDO1=NUOCA-1
      JIN = JM
      YSURP = YSUR
      ETADY = ETA*DY
      TVARI = 2.0*SIGMAI*SIGMAI
      DO 150 I=1,JMP
      S(I) = (DY*FLOAT(I-1))**2
      ARG = S(I)/TVARI
      IF (ARG-20.0) 145,145,146
  145 EX(I) = EXP(-ARG)
      GO TO 150
  146 EX(I) = 0.0
  150 CONTINUE
      P(25) = FLOAT(MIXED)*(B(JM)+B(JMIXB))
      IF(P(25)-0.0) 801,802,801
  802 P(25)=0.000001
  801 P(31) = OMEGA*SIGMAI*SIGMAI
      GO TO (9,11), KDIF
    9 DIF = D(1,1)
   11  IF (JM-50) 15,15,16
   15 JP = JM
      GO TO 17
   16 JP = 50
   17 GO TO (20,18), KQ
   18 UIMAX(1)=0.0
      UOMAX(1) = 0.0
      DO 19 J=1,JM
      SIGMAO = 1.0
      UI(J,1) = 0.0
   19 V(J,1) = 0.0
C  STATEMENT 20 IS BEGINNING OF MAIN ITERATION LOOP OF PROGRAM.
   20 GO TO (21,47), KQ
   21 GO TO (24,22), KMIX
C MIX INFLOW WATER IF INDICATED.
   22 QQ =QQIN(N+1)
  806 P(29) = RMIX/DY*2.0/P(25)
      QMIX = RMIX*QQ
      TP = 0.0
      DO 23 J=JMIXB,JM
   23 TP = TP+T(J,1)
      TP = TP/FLOAT(MIXED+1)
      TS = (TTIN(N+1)+TP*RMIX)/(1.0+RMIX)
```

```
      GO TO 25
   24 TS =TTIN(N+1)
25    CONTINUE
C  LOCATE ACTUAL LEVEL OF DAYS INPUT
      DO 4745 I=1,JM
      J=JM+1-I
      IF(TS-T(J,1)) 4745,4746,4746
4745  CONTINUE
4746  JIN=J+1
      IF(JIN-JM) 4747,4747,4748
4748  JIN=JM
4747  CONTINUE
      NW=NW+1
      JEUP=JM-4.6/ETA/DY
      GO TO (19000,19001),NGUET
19001 IF(JIN-JEUP) 19002,19003,19003
19003 NLEVE(N+1)=1
      GO TO 19000
19002 NLEVE(N+1)=2
19000 CONTINUE
      GO TO (45,31), KSUR
C COMPUTATIONS WHEN SURFACE ELEVATION VARIES WITH TIME.
   31 RA = (ET+DT)/DSURF
      TSUR=T(JM,1)
      L = RA
      YSUR = SURF(L+1)+(RA-FLOAT(L))*(SURF(L+2)-SURF(L+1))
      DYS = (YSUR+YSURP)/2.0-EL(JM)
      IF (ABS(DYS)-DY/2.0) 45,45,35
   35 M = 1+IFIX((ABS(DYS)-DY/2.0)/DY)
      JM = JM+IFIX(SIGN(1.0,DYS))*M
      T(JM,1)=TSUR
      JMIXB = JM-MIXED
      P(25) = FLOAT(MIXED)*(B(JM)+B(JMIXB))
      IF (JM-50) 37,37,38
   37 JP = JM
      GO TO 39
   38 JP = 50
   39 IF (DYS) 45,45,40
   40 JJM = JM-M
      DO 42 I=1,M
      J = JM+1-I
   42 CONTINUE
   45 N=N+1
65483 FORMAT( 8E12.5)
      NDDI=NDDI+1
      ET = ET+DT
      MM=0
      DO 18001 I=1,ITR
      IF (N-NTRAC(I)) 18001,18002,18002
18002 MM=MM+1
18001 CONTINUE
      IF(MM) 11010,11010,11011
11011 CONTINUE
C  NEW SURFACE CONCENTRATIONS DUE TO CHANGE IN SURFACE ELEVATION.
      DO 891 M=1,MM
      IF(JM-JXM) 890,891,892
C  IF SURFACE FELL.
```

```
  890 CC(M,JM,1)=2.0*CC(M,JM,1)+CC(M,JXM,1)*A(JXM)/A(JM)
      GO TO 891
892   CC(M,JXM,1)=0.5* CC(M,JXM,1)*A(JXM)/(A(JXM)+0.5*A(JM))
      CC(M,JM,1)=CC(M,JXM,1)
  891 CONTINUE
C  THIS IS THE LAGTIME DETERMINATION.
11010 CONTINUE
      JXM=JM
      QLIT=QQIN(N)*(1.0+RMIX)/B(JM)
      IF(JM-2-JIN) 870,870,871
  870 VELF=QLIT/THICK1
      JIN=JM
      XLAG=XL(JM)/VELF
      GO TO 872
  871 DELRHO=6.6E-06*((T(JM,1)-4.0)**2-(TS-4.0)**2)/2.0
      GPRIME=GRAV*DELRHO
      GO TO (873,874),KAREA
  874 SLOPE=(EL(JM)-EL(JIN))/(XL(JM)-XL(JIN))
873   CONTINUE
      DFLOW=(1.92      )*(QLIT*VISCOS/GPRIME/SLOPE)**0.33
      VELF=QLIT/DFLOW
      HVELF=QLIT/THICK2
      SLDIST=FLOAT(JM-JIN)*DY/SLOPE
      XLAG=SLDIST/VELF+XL(JIN)/HVELF
  872 LAGTIM(N)=XLAG/DT
C  END OF THE LAGTIME DETERMINATION.
      ML=N+LAGTIM(N)
      QIN(ML)=QIN(ML)+QQIN(N)
      TIN(ML)=(TIN(ML)*(QIN(ML)-QQIN(N))+TTIN(N)*QQIN(N))/QIN(ML)
      WRITE(6,875) N,LAGTIM(N)
875   FORMAT(' LAGTIME(',I3,')=',I3)
      TP=0.0
      DO 1023 J=JMIXB,JM
 1023 TP=TP+T(J,1)
      TP=TP/FLOAT(MIXED+1)
      TS=(TIN(N)+TP*RMIX)/(1.0+RMIX)
      DO 27 I=1,JM
      J = JM+1-I
      IF (TS-T(J,1)) 27,30,30
   27 CONTINUE
   30 JIN=J+1
      IF(JIN-JM) 1691,33,33
   33 JIN=JM
 1691 CONTINUE
      QQ=QIN(N)
   81 F = TIN(N)
      QMIX=RMIX*QQ
      CALL SPEED(N)
      P(24) = TS
   47 GJ = (FLXIN(N)+FLXIN(N+1))/ARF
C  ASSURES THAT V*DT/DY LESS THAN UNITY FOR STABILITY.
      VVV=ABS(V(2,1))
      DO 501 J=3,JM
      IF(VVV-ABS(V(J,1)))502,501,501
  502 VVV=ABS(V(J,1))
  501 CONTINUE
      VM=DY/DTT
      IF(VVV-VM) 503,504,504
```

```
  504 DT=DY/VVV
      IDT=DTT/DT+1
      DT=DTT/IDT
      GO TO 505
  503 IDT=1
C  END STABILITY CHECK.
  505 DO 79 M=1,IDT
      CALL SPEED(N)
C SUB SPEED COMPUTES WITHDRAWAL THICKNESS AND VELOCITIES AT EACH TIME STEP.
C  SUB XMIX CALCULATES COMPOSITION OF INFLOW.
      CALL XMIX(N)
C  SUB SPECAL CALCULATES DISTRIBUTION OF SPECIFIED INPUTS OF DO,BOD.
      CALL SPECAL(N)
      JMM=JM-1
      DO 1114 J=2,JMM
      DELTA=(1.0-BETA)*FLXIN(N)*(EXP(-ETA*(EL(JM)-EL(J)-DY/2.0))*A(J)-
     1EXP(-ETA*(EL(JM)-EL(J)+DY/2.0))*A(J-1))/A(J)/DY/HCAP/RHO
C  CHECKS DIRECTION OF VELOCITY TO ASSURE PROPER TEMPERATURE AND CONCENTRATION
C  ASSIGNMENT.
      IF(V(J,1)) 1160,1160,1161
 1160 IF(V(J+1,1))1170,1170,1171
 1170 DELTB=(V(J,1)*T(J,1)*(A(J)+A(J-1))/2.0-V(J+1,1)*T(J+1,1)*(A(J+1)+
     1A(J))/2.0)/A(J)/DY
      GO TO 1162
 1171 DELTB=(V(J,1)*T(J,1)*(A(J)+A(J-1))/2.0-V(J+1,1)*T(J,1)*(A(J+1)+
     1A(J))/2.0)/A(J)/DY
      GO TO 1162
 1161 IF(V(J+1,1))1172,1172,1173
 1173 DELTB=(V(J,1)*T(J-1,1)*(A(J)+A(J-1))/2.0-V(J+1,1)*T(J,1)*(A(J+1)+
     1A(J))/2.0)/A(J)/DY
      GO TO 1162
 1172 DELTB=(V(J,1)*T(J-1,1)*(A(J)+A(J-1))/2.0-V(J+1,1)*T(J+1,1)*(A(J+1)
     1+A(J))/2.0)/A(J)/DY
 1162 DELTE=(UI(J,1)*TS-   UO(J,1)*T(J,1))*B(J)*DY/A(J)/DY
      DELTC=DD(1)*(T(J+1,1)+T(J-1,1)-2.0*T(J,1))/DY/DY
      DELTD=DD(1)*(T(J-1,1)-T(J+1,1))*(A(J-1)-A(J+1))/A(J)/DY/DY/4.0
      DELT=(DELTA+DELTB+DELTC+DELTD+DELTE)*DT
 1114 T(J,2)=T(J,1)+DELT
      IF (V(JM,1))1163,1164,1164
 1164 DELTJM=DT*((1.0-BETA)*FLXIN(N)*(A(JM)-EXP(-ETA*DY/2.0)*
     1A(JM-1))/A(JM)/DY*2.0/HCAP/RHO+
     1V(JM,1)*(T(JM-1,1)-T(JM,1))/DY*2.0+UI(JM,1)*(TS    -T(JM,1))*B(JM)
     1/A(JM)-DD(1)*(T(JM,1)-T(JM-1,1))
     3 /DY/DY*2.0+(BETA*FLXIN(N)-FLXOUT(N))/RHO/HCAP/DY*2.0)
      GO TO 1165
 1163 DELTJM=DT*((1.0-BETA)*FLXIN(N)*(A(JM)-EXP(-ETA*DY/2.0)*
     1A(JM-1))/A(JM)/DY*2.0/HCAP/RHO+UI(JM,1)*(TS-T(JM,1))*B(JM)
     1/A(JM)-DD(1)*(T(JM,1)-T(JM-1,1))
     3 /DY/DY*2.0+(BETA*FLXIN(N)-FLXOUT(N))/RHO/HCAP/DY*2.0)
 1165 T(JM,2)=T(JM,1)+DELTJM
      FLUXOT=FLXOUT(N)
      IF(V(2,1)) 1166,1167,1167
 1167 DELT1=DT*((1.0-BETA)*FLXIN(N)*EXP( -ETA*(EL(JM)-EL(1)-DY/2.0))
     1/RHO/HCAP-V(2,1)*T(1,1)*2.0/DY+(UI(1,1)*TS-UO(1,1)*T(1,1))*B(1
     1)/(A(1)+A(2))*2.0+DD(1)*(T(2,1)-T(1,1))/DY/DY*2.0
     4+(1.0-BETA)*FLXIN(N)*EXP(-ETA*(EL(JM)-EL(1)+DY/4.0))/DY/2.0/RHO/
     5HCAP)
```

```
      GO TO 1163
 1166 DELT1=DT*((1.0-BETA)*FLXIN(N)*EXP( -ETA*(EL(JM)-EL(1)-DY/2.0))
     1/RHO/HCAP-V(2,1)*T(2,1)*2.0/DY+(U1(1,1)*TS     -U0(1,1)*T(1,1))*B(1
     1)/(A(1)+A(2))*2.0+DU(1)*(T(2,1)-T(1,1))/DY/DY*2.0
     4+(1.0-BETA)*FLXIN(N)*EXP(-ETA*(EL(JM)-EL(1)+DY/4.0))/DY/2.0/RHO/
     5HCAP)
 1163 T(1,2)=T(1,1)+DELT1
      GO TO (1115,1117),KAREA
 1115 DO 1116 J=1,JM
      PHIM=0.79E-10*(T(J,1)+273.0)**4-AR
      DELT=(2.0*(XL(J)+B(J))*PHIM/RHO/HCAP/A(J))*DT
      FLUXOT=FLUXOT+PHIM*2.0*(XL(J)+B(J))*DT*DY
 1116 T(J,2)=T(J,2)-DELT
 1117 DO 1118 J=1,JM
 1118 T(J,1)=T(J,2)
      YSURP = YSUR
C CHECK REASONABLENESS OF RESULTS.
      IF (ABS(T(JM,2))-100.0) 60,57,57
   57 TSTOP = ET
      GO TO 80
C SUB AVER MIXES SURFACE LAYERS IN THE EVENT OF A SURFACE INSTABILITY.
   60 IF (T(JM,2)+0.01-T(JM-1,2)) 63,779,779
   63 CONTINUE
C  SUB AVER PERFORMS CONVECTIVE MIXING OF TEMPERATURE IN MIXING LAYERS.
      CALL AVER(N)
C  SUB SPECAV PERFORMS CONVECTIVE MIXING OF SPECIFIED MATERIAL IN MIXING LAYER
      CALL SPECAV(N)
  779 CONTINUE
      CALL SPECOT(N)
C  SUB SPECOT CALCULATES PROPORTION OF SPECIFIED MATERIAL IN OUTFLOW.
   79 CONTINUE
      DT=DTT
C  SUB TOUT CALCULATES OUTFLOW TEMPERATURE.
      CALL TOUT(YNT,YNT1)
      TOUTC = YNT/YNT1
      TOUTF = 1.8*TOUTC+32.0
      IF(N-NPR) 100,100,80
   80 NPR = NPR+NPRINT
      WRITE (6,900) (WH(I),I=1,20)
      WRITE (6,912) ET,YSUR,F
      WRITE (6,913) N,EL(JM),TAIR
      WRITE (6,914) JM,EL(JIN),PSI
      F = FLXIN(N)
      WRITE (6,915) JIN,EVAP,F
      QOU = QOUT(N)
      BBETA = QOU*BB
      WRITE (6,925) BBETA,AR,WINDY
      QQ = QIN(N)
      WRITE (6,916) DIF,RAD,QQ
      WRITE (6,917) DERIV,FLUXOT,QOU
      GO TO (85,89), KN
   85 F = 2.0*HAFDEL
      WRITE (6,918) EPSIL,F,SIGMAO
      WRITE (6,919) DUMAX(1),UIMAX(1),TOUTC,TOUTF
      GO TO (86,86), KMIX
   86 WRITE (6,924) TS,TS
   89 WRITE (6,920)
      DO 90 I=1,19
```

```
   90 WRITE (6,921) (J,EL(J),T(J,1),J=I,JP,10)
      IF (JM-50) 100,100,91
   91 WRITE (6,920)
      IF (JM-60) 92,93,93
   92 LL = JM
      GO TO 94
   93 LL = 60
   94 DO 95 I=51,LL
   95 WRITE (6,921) (J,EL(J),T(J,1),J=I,JM,10)
100   IF(NDOCA-ND01) 1709,1710,1709
1710  WRITE(6,59645) ET
59645 FORMAT(' ELAPSED TIME =',F10.5)
      WRITE(6,30020)
30020 FORMAT  (/5('   J    ELEV   DO(PPM)'))
      DO 3000 I=1,10
3000  WRITE (6,921) (J,EL(J),CC(1,J,2),  J=I,JP,10)
      IF(JM-50) 32222,32222,32223
32223 IF(JM-60) 30021,30022,30022
30021 LL=JM
      GO TO 30025
30022 LL=60
30025 WRITE(6,30020)
      DO 30026 I=51,LL
30026 WRITE (6,921) (J,EL(J),CC(1,J,2),  J=I,JM,10)
32222 WRITE (6,9021) COUT(1,N)
9021  FORMAT (//' DO IN OUTFLOW IN PREVIOUS TIMESTEP =',F10.5 )
      ND01=0
1709  IF (ET-TSTOP) 20,1,1
    1 CONTINUE
  900 FORMAT (20A4)
  901 FORMAT (16I5)
  902 FORMAT (8F10.5)
  904 FORMAT (' NUMBER OF GRID POINTS='I3,17X,'SURFACE ELEVATION='F7.2,
     11X,'DENSITY='E12.5)
  905 FORMAT (' OUTLET LEVEL='I3,  26X,'OUTLET ELEVATION='F8.2,18X,
     1'HEAT CAPACITY='F8.5)
  906 FORMAT (' DY='F6.2,33X,'BOTTOM ELEVATION='F8.2,18X,'ETA='F6.3)
  907 FORMAT (' DT='F5.2,33X,'INITIAL TEMPERATURE='F6.2,17X,'BETA='F5.2)
  908 FORMAT (' BRIAN BETA='F5.2,26X,'INFLOW STD. DEV.='F6.2,20X,'COEF.
     1OMEGA IN AREA FORMULA='E12.5)
  909 FORMAT (' STOP AT TIME='F7.2,22X,'OUTFLOW SPREAD CONST.='F5.2,16X,
     1'WIDTH AT Y=0 IN AREA FORMULA='E12.5)
  910 FORMAT (' KDIF='I2,13X,'KSUR='I2,13X,'KOH ='I2,15X,'KQ='I2,16X,
     1'KLOSS='I2,13X,'KAREA='I2/' EVAPORATION CONSTANT='E11.4,10X,
     2 'CONST IN EQN FOR OUTFLOW DELTA='F5.2,7X,'KMIX='I2)
  911 FORMAT ( 'DN='I3,', ABOUT TO ENTER SUBROUTINE AVER.')
  912 FORMAT (  ' ELAPSED TIME='F7.2,22X,'ACTUAL SURFACE ELEVATION='
     1F7.2,11X,'INFLOW TEMPERATURE='F6.2)
  913 FORMAT (' NO. OF TIME STEPS='I4,20X,'SURFACE ELEVATION USED='
     1F9.2,11X,'AIR TEMPERATURE='F6.2)
  914 FORMAT (' NO. OF GRID POINTS='I3,20X,'ELEVATION OF INFLOW='F7.2,
     116X,'RELATIVE HUMIDITY='F5.2)
  915 FORMAT (' LEVEL OF INFLOW='I3,23X,'EVAPORATION FLUX='E12.5,14X,
     1'INSOLATION FLUX='E12.5)
  916 FORMAT (' DIFFUSION COEFFICIENT='E12.5,8X,'RADIATION FLUX='E12.5,
     116X,'INFLOW RATE='F11.1)
  917 FORMAT (' OUTFLOW TEMP GRADIENT='F8.5,12X,'HEAT LOSS FLUX='E12.5,
```

```
     1 16X,'OUTFLOW RATE='F10.1)
  918 FORMAT (' EPSILON='E11.4,23X,'WITHDRAWAL THICKNESS='F7.2,15X,
     1'OUTFLOW STD. DEV.='F6.2)
  919 FORMAT (' MAX SINK VELOCITY='F9.3,15X,'MAX SOURCE VELOCITY='F9.3,
     1 12X,'$OUTFLOW TEMPERATURE='F6.2,' C AND 'F6.2,' F.')
  920 FORMAT (/5('   J   ELEV    TEMP(C)'))
  921 FORMAT (5(I4,F7.1,F10.5,1X))
  922 FORMAT (/' TIME FROM BEGINNING OF CALCULATIONS FOR THIS DATA SET='
     1I3,' MINUTES,'I3,' SECONDS.')
  923 FORMAT (' NO. GRID SPACES IN MIXED LAYER='I3,8X,'MIXING RATIO='
     1F5.2,25X,'AREA REDUCTION FACTOR='F5.2)
  924 FORMAT (' TEMP OF MIXING LAYER='F6.2,15X,'MIXED INFLOW TEMP='
     1F6.2)
  925 FORMAT (' BRIAN BETA='F5.2,26X,'ATMOSPHERIC RADIATION='E12.5,
     1 9X,'WIND SPEED='F5.2)
      CALL EXIT
      END



      FUNCTION FLXOUT(N)
C CALCULATION OF SURFACE LOSSES DUE TO EVAPORATION, CONDUCTION, AND RADIATION.
      COMMON T(60,2),EL(60),XL(60),A(60),TI(310),TA(310),SIGH(310)
      COMMON FIN(310),WIND(310),DD(310),QI(310),QO(310),P(50),NPR
      COMMON UOMAX(2),UIMAX(2),DTTI,DTTA,DTSIGH,DTFIN,DTWIND,DTDD,DTQI
      COMMON DT,DX,JM,JOUT,JIN,KDIF,KSUR,KOM,KQ,KLOSS,YSUR,YOUT,DT,DY
      COMMON TSTOP,EVPCON,OMEGA,HZ,SPREAD,SIGMAI,SIGMAO,ETADY,TVARI
      COMMON TVARO,EVAP,RAD,TAIR,PSI,DERIV,HAFDEL,EPSIL,GJ
      COMMON YBOT,NN,BETA,DAJM,DELCON,V( 60,1),UI( 60,1),DTT
      COMMON RHO,HCAP,KMIX,RMIX,JMIXB,MIXED,QMIX,KAREA,DATRAD,ATRAD(310)
      COMMON AR,W,CO,CI,B(60),S(60),EX(60),EXO(60),ARF,UO(60,1)
      COMMON QIN(310),TIN(310),CC(20,60,2),CCC(20,310),COUT(20,310)
      COMMON CCT(20,310),QQMIX(60),XINF(60),OUTF(60),MIXH,MM
      COMMON SURF(310),GRAV,SLOPE,VISCOS,LAGTIM(310)
      COMMON PMASOT(20),PMASIN(20),ET,NTRAC(20),ITR,IST0,IS01,IS02
      COMMON IST0N,IST01,THICK1,THICK2,DOXLE(60,20),DO(306),BOD(306)
      COMMON NLEVE(306),VOL,NW,NDET,Z,Z1,DDOC,NGDET,DBOD
C KLOSS = 1 FOR LABORATORY USING ROHWER FORMULA.
C         2 FOR FIELD USING KOHLER FORMULA.
C         3 FOR FIELD USING ROHWER FORMULA.
      TVARO = 1.0
      ET=DTT*FLOAT(N)
      R = ET/DTTA
      L = R
      RR = R-FLOAT(L)
      TAIR = TA(L+1)+RR*(TA(L+2)-TA(L+1))
      R = ET/DTSIGH
      L = R
      RR = R-FLOAT(L)
      PSI = SIGH(L+1)+RR*(SIGH(L+2)-SIGH(L+1))
      TS = T(JM,1)
      H = 597.3-0.56*TS
C PARABOLIC APPROXIMATION FOR VAPOR PRESSURES IN MM HG.
      ES = 0.0418*TS*TS-0.6216*TS+13.0068
      EA = PSI*(0.0418*TAIR*TAIR-0.6216*TAIR+13.0068)
      DE = ES-EA
      GO TO (10,20,20), KLOSS
```

```
C CALCULATIONS FOR LABORATORY USE ROHWER FORMULA.
   15 CHI = RHO*(H*DE+TS*HCAP*DE+269.1*(TS-TAIR))
      EVAP = CHI*EVPCON
C UNITS OF RADIATION ARE CAL/CM-CM-MIN.
      AR = 0.7888E-10    *(TAIR+273.16)**4
      RAD = 0.7888E-10    *(273.16+TS)**4-AR
      W = 0.0
      P(30) = EVAP+RAD
      FLXOUT = P(30)
      RETURN
C FOR FIELD DATA. WIND SPEED IS IN M/SEC.
   20 R = ET/DTWIND
      L = R
      W = WIND(L+1)+(R-FLOAT(L))*(WIND(L+2)-WIND(L+1))
C FOR FIELD. ATMOSPHERIC RADIATION IS INCLUDED AS AN INPUT TO PROGRAM.
      R = ET/DAT+1.0
      L = R
      AR = ATRAD(L+1)+(R-FLOAT(L))*(ATRAD(L+2)-ATRAD(L+1))
      RAD = 1.1356E-6*(TS+273.16)**4-AR
      GO TO (15,25,30), KLOSS
C CALCULATION OF FIELD EVAPORATION USING KOHLER FORMULA.
C VAPOR PRESSURES IN MM.
   25 DE = DE/0.750062
      EVAP = H*DE+HCAP*DE*TS+372.0*(TS-TAIR)
      EVAP = EVPCON*RHO*W*EVAP
      P(30) = EVAP+RAD
      FLXOUT = P(30)/ARF
      RETURN
C CALCULATION OF FIELD EVAPORATION USING ROHWER FORMULA.
   30 CHI = RHO*(H*DE+TS*HCAP*DE+269.1*(TS-TAIR))
      FW = 0.0308+0.0148*W
      EVAP = CHI*FW*EVPCON
      P(30) = EVAP+RAD
      FLXOUT = P(30)/ARF
      RETURN
      END



      SUBROUTINE TOUT(YNT,YNT1)
C COMPUTE WEIGHTED AVERAGE OF OUTFLOW TEMPERATURE.
C USE COMPUTED INSTEAD OF GIVEN OUTFLOW RATE FOR YNT1.
C YNT1 WILL BE GREATER THAN TOUT FOR NARROW WITHDRAWAL LAYERS.
C HENCE. USE SAME METHOD TO CALCULATE J IN BOTH YNT AND YNT1.
C CALCULATED TOUT =YNT/YNT1.
      COMMON T(50,2),EL(50),XL(60),A(60),TI(310),TA(310),SIGH(310)
      COMMON FIN(310),WIND(310),DD(310),QI(310),QO(310),P(50),NPR
      COMMON DOMAX(2),QIMAX(2),DTTI,DTTA,DTSIGH,DTFIN,DTFOUT,DTDD,DTQI
      COMMON DTWD,JM,JOUT,JIN,KDIF,KSUR,KOM,KQ,KLOSS,YSUR,YOUT,DT,DY
      COMMON TSTOP,EVPCON,OMEGA,BZ,SPREAD,SIGMAI,SIGMAO,ETADY,TVARI
      COMMON IVAPO,EVAP,RAD,TAIR,PSI,DERIV,HAFDEL,EPSIL,GJ
C UNITS OF RADIATION ARE KCAL/M-M-DAY.
      COMMON YOUT,JJ,BETA,DAJM,DELCON,V( 60,1),UI( 60,1),DTT
      COMMON RHO,HCAP,KMIX,RMIX,JMIXO,MIXED,QMIX,KAREA,DATRAD,ATRAD(310)
      COMMON AP,INDY,CO,CI,S( 60),S( 60),EX( 60),EXO( 60),ARF,UO( 60,1)
      COMMON W(310),TIN(310),CC(20,60,2),CCC(20,310),COUT(20,310)
```

```
      COMMON CC(20,310),QQMIX(60),XINF(60),OUTF(60),MIXH,MM
      COMMON SURF(310),GRAV,SLOPE,VISCOS,LAGTIM(310)
      COMMON PMASOT(20),PMASIN(20),ET,NTRAC(20),ITR,ISTO,IS01,IS02
      COMMON ISTON,ISTO1,THICK1,THICK2,DOXLE(60,20),DO(306),BOD(306)
      COMMON NLEVE(306),VOL,NW,NDET,Z,Z1,DDOC,NGDET,DBOD
      YNT = 0.0
      YNT1 = 0.0
      JJM = JM
      M = JM-1
      IF ((M+1)/2-M/2) 5,10,5
    5 YNT = 1.5*(T(JM,1)*B(JM)*EXO(JM)+T(JM-1,1)*B(JM-1)*EXO(JM-1))
      YNT1 = 1.5*(B(JM)*EXO(JM)+B(JM-1)*EXO(JM-1))
      JJM = JM-1
   10 YNT = YNT+T(1,1)*B(1)*EXO(1)-T(JJM,1)*B(JJM)*EXO(JJM)
      YNT1 = YNT1+B(1)*EXO(1)-B(JJM)*EXO(JJM)
      DO 20 J=2,4,2
      M = JJM-1
      YNT = YNT+4.0*T(J,1)*B(J)*EXO(J)+2.0*T(J+1,1)*B(J+1)*EXO(J+1)
   20 YNT1 = YNT1+4.0*B(J)*EXO(J)+2.0*B(J+1)*EXO(J+1)
      YNT = YNT*DY/3.0
      YNT1 = YNT1*DY/3.0
      RETURN
      END



      SUBROUTINE SPEED(N)
C COMPUTATION OF VERTICAL AND SOURCE AND SINK VELOCITIES.
C ALSO, COMPUTATION OF WITHDRAWAL THICKNESS.
C SOURCE AND SINK VELOCITIES ARE ASSUMED TO HAVE GAUSSIAN DISTRIBUTION.
C VARIABLE WIDTH ACCOUNTED FOR IN CALCULATIONS BY ASSUMING EXP DISTRIBUTION.
C FORMULA USED FOR WIDTH IS B(Y) = BZ*EXP(OMEGA*Y).
C APPROXIMATION FORMULA (FUNCT PROB) USED TO EVALUATE PROBABILITY INTEGRAL.
      COMMON T(60,2),EL(60),XL(60),A(60),TI(310),TA(310),SIGH(310)
      COMMON FIN(310),WIND(310),DO(310),QI(310),QO(310),P(50),NPR
      COMMON UUMAX(2),UIMAX(2),DTTI,DTTA,DTSIGH,DTFIN,DTFOUT,DTDD,DTQI
      COMMON DTQO,JM,JOUT,JIN,KOIF,KSUR,KOH,KQ,KLOSS,YSUR,YOUT,DT,DY
      COMMON TSTOP,EVPCON,OMEGA,BZ,SPREAD,SIGMAI,SIGMAO,ETADY,TVARI
      COMMON TVARO,EVAP,RAD,TAIR,PSI,DERIV,HAFDEL,EPSIL,GJ
      COMMON YBOT,NN,BETA,DAJM,DELCON,V( 60,1),UI( 60,1),DTT
      COMMON RHO,HCAP,KMIX,RMIX,JMIXB,MIXED,QMIX,KAREA,DATRAD,ATRAD(310)
      COMMON AR,WINDY,CO,C1,B( 60),S( 60),EX( 60),EXO( 60),ARF,UO( 60,1)
      COMMON QIN(310),TIN(310),CC(20,60,2),CCC(20,310),COUT(20,310)
      COMMON CCT(20,310),QQMIX(60),XINF(60),OUTF(60),MIXH,MM
      COMMON SURF(310),GRAV,SLOPE,VISCOS,LAGTIM(310)
      COMMON PMASOT(20),PMASIN(20),ET,NTRAC(20),ITR,ISTO,IS01,IS02
      COMMON ISTON,ISTO1,THICK1,THICK2,DOXLE(60,20),DO(306),BOD(306)
      COMMON NLEVE(306),VOL,NW,NDET,Z,Z1,DDOC,NGDET,DBOD
C COMPUTE WITHDRAWAL THICKNESS.
C NOTE THAT ONLY HALF THE WITHDRAWAL THICKNESS IS COMPUTED.
      DERIV = (T(JOUT+1,1)-T(JOUT-1,1))/2.0/DY
C  CRITERION FOR EXISTANCE OF A WITHDRAWAL LAYER.
      IF(DERIV-0.001) 2,2,5
    2 JOUT1=JOUT+2
      DO 200 J=JOUT1,JM
      IF((T(J+1,1)-T(J,1))/DY-.001) 200,202,202
  200 CONTINUE
```

```
      SIGMA0=100.0*DY
      GO TO 5
  202 HAFDEL=FLOAT(J-JOUT)*DY
      SIGMA0=HAFDEL/SPREAD
      GO TO 4
C APPROXIMATING FORMULA USED FOR DENSITY IS RHO=1.0-0.00000663*(T-4.0)**2.
    5 EPSIL= 2.0*(T(JOUT,1)-4.0)/(151000.0-(T(JOUT,1)-4.0)**2)*DERIV
      GO TO (3,1), KOH
C CALCULATION OF WITHDRAWAL THICKNESS USING KAO FORMULA.
    1 QPOW = (QOUT(J)+QOUT(J+1))*0.5/B(JOUT)
      HAFDEL = DELCON*SQRT(QPOW)/EPSIL**0.25
      GO TO 4
C CALCULATION OF WITHDRAWAL THICKNESS USING KOH FORMULA.
    3 HAFDEL = DELCON/EPSIL**0.1666667
    4 SIGMA0 = HAFDEL/SPREAD
      IF(SIGMA0) 300,300,301
  300 SIGMA0=1.0
  301 CONTINUE
    6 TVAR0 = 2.0*SIGMA0*SIGMA0
      OMSOSQ = SIGMA0*SIGMA0*OMEGA
C FIRST COMPUTE MAXIMUM VELOCITIES, THEN OTHERS.
    7 XXI = PROB(YBOT,EL(JIN)+P(31),SIGMAI)
      XX0 = PROB(YBOT,YOUT+OMSOSQ,SIGMA0)
      GO TO (8,11), KAREA
    8 IF (YSUR-YOUT-2.58*SIGMA0) 15,15,9
    9 IF (YOUT-YBOT-2.58*SIGMA0) 15,10,10
   10 UOMAX(1) = QOUT(N)/SIGMA0*C0
      GO TO 25
   11 C0 = P(32)*EXP(-P(33)*SIGMA0*SIGMA0-P(34))
   15 X0 = C0/SIGMA0/(PROB(EL(JM),YOUT+OMSOSQ,SIGMA0)-XX0)
      UOMAX(1) = QOUT(N)*X0
      GO TO (25,35),KAREA
   25 IF (EL(JM)-EL(JIN)-2.58*SIGMAI) 35,35,30
   30 UIMAX(1) = QIN(N)/SIGMAI*CI
      GO TO 50
35    IF(JM-JIN) 40,40,41
C  THIS IS THE UNIFORM VELOCITY DISTRIBUTION IF THE FLOW IS SURFACE FLOW
C  ISTO IS THE NUMBER OF GRID POINTS BELOW SURFACE INTO WHICH FLOW WILL ENTER
40    ISTO=THICK1/DY-0.5
      ISTON=JM-ISTO-1
      DO 700 I=1,ISTON
700   UI(I,1)=0.
      ISTO1=ISTON+1
      DO 701 I=ISTO1,JM
      UI(I,1)=QIN(N)/(ISTO+.5)/DY/B(I) *(1.0+RMIX)
701   CONTINUE
      GO TO 52
   41 CI = P(35)*EXP(-EL(JIN)*OMEGA)
      P(22) = SIGMAI/CI
   45 XI = CI/SIGMAI/(PROB(EL(JM),EL(JIN)+P(31),SIGMAI)-XXI)
      UIMAX(1) = QIN(N)*XI
   50 GO TO (52,51), KMIX
   51 UIMAX(1) = UIMAX(1)*(1.0+RMIX)
      YY = QIN(N)*RMIX/P(25)
      ZZ = QMIX/P(25)
   52 SA0 = SIGMA0/C0
C COMPUTE VERTICAL ADVECTIVE VELOCITY AND SOURCE VELOCITY.
```

```
      DO 70 J=1,JM
      XO = SAO*(PROB(EL(J),YOUT+OMSOSQ,SIGMAO)-XXO)
      IF(JM-JIN) 703,703,56
56    XI = P(22)*(PROB(EL(J),EL(JIN)+P(31),SIGMAI)-XXI)
      I = IABS(J-JIN)+1
      UI(J,1) = UIMAX(1)*EX(I)
703   CONTINUE
70    CONTINUE
C COMPUTE EXPONENTIAL PART OF SINK VELOCITY FOR USE IN SUB TOUT AND FUNCT UO.
      IF (JM-2*JOUT+1) 75,75,80
   75 LUP = JOUT-1
      LDN = JM-JOUT
      IS = -1
      GO TO 85
   80 LUP = JM-JOUT
      LDN = JOUT-1
      IS = 1
   85 EXO(JOUT) = 1.0
      DO 100 I=1,LUP
      J = JOUT+IS*I
      ARG = S(I+1)/TVARO
      IF (ARG-20.0) 87,89,89
   87 EXO(J) = EXP(-ARG)
      GO TO 90
89    EXO(J)=0.0
90    IF (I-LDN) 91,91,100
   91 JJ = JOUT-IS*I
      EXO(JJ) = EXO(J)
  100 CONTINUE
      IF(JM-JIN) 705,705,706
705   IS02=JM-IST0
      IS01=IS02-1
      DO 710 J=1,IS01
710   UO(J,1) =UOMAX(1)*EXO(J)
      DO 712 J=IST01,JM
      UO(J,1)=UOMAX(1)*EXO(J)
712   CONTINUE
706   DO 36 J=1,JM
      GO TO (31,32),KMIX
32    IF(J-JM1A5) 31,33,33
   33 QQMIX(J)=QIN(N)*RMIX/(MIXED+1)
      UO(J,1)=QQMIX(J)/B(J)/DY
      IF(J.EQ.JM) UO(JM,1)=2.0*UO(J,1)
      GO TO 36
   31 UO(J,1)=0.0
   36 UO(J,1)=UO(J,1)+UOMAX(1)*EXO(J)
711   CONTINUE
      V(1,1)=0.0
      V(2,1)=(UI(1,1)-UO(1,1))*B(1)*DY/(A(1)+A(2))
      JMX=JM+1
      DO 500 J=3,JMX
      V(J,1)=(V(J-1,1)*(A(J-2)+A(J-1))/2.0+(UI(J-1,1)-UO(J-1,1))*B(J-1)
     1*DY)/(A(J)+A(J-1))*2.0
 500  CONTINUE
      RETURN
      END
```

```
      SUBROUTINE AVER(N)
C PERFORMS CONVECTIVE MIXING OF SURFACE LAYERS.
      COMMON T(50,2),EL(60),XL(60),A(60),TI(310),TA(310),SIGH(310)
      COMMON FIN(310),WIND(310),DD(310),QI(310),QO(310),P(50),NPR
      COMMON DDMAX(2),DIMAX(2),DTTI,DTTA,DTSIGH,DTFIN,DTWIND,DTDD,DTQI
      COMMON DT00,JM,JOUT,JIN,KDIF,KSUR,KOH,KQ,KLOSS,YSUR,YOUT,DT,DY
      COMMON ISTOP,EVPCON,OMEGA,BZ,SPREAD,SIGMAI,SIGMAO,ETADY,TVARI
      COMMON TVARO,EVAP,RAD,TAIR,PSI,DERIV,HAFDEL,EPSIL,GJ
      COMMON YOUT,NN,BETA,DAJM,DELCON,V( 60,1),UI( 60,1),DTT
      COMMON RHO,HCAP,KMIX,XMIX,JMIXB,MIXED,QMIX,KAREA,DATRAD,ATRAD(310)
      COMMON AR,WINDY,C1,C2,B( 60),S( 60),EX( 60),EXO( 60),ARF,UO( 60,1)
      COMMON QIN(310),TIN(310),CC(20,60,2),CCC(20,310),COUT(20,310)
      COMMON CCI(20,310),JJMIX(60),XINF(60),OUTF(60),MIXH,MM
      COMMON SUMF(310),GRAV,SLOPE,VISCOS,LAGTIM(310)
      COMMON PMASOT(20),PMASIN(20),ET,NTRAC(20),ITR,IST0,IS01,IS02
      COMMON ISTON,IST01,THICK1,THICK2,DOXLE(60,20),DO(306),BOD(306)
      COMMON NLEVE(306),VOL,NW,NDET,Z,Z1,DOOC,NGDET,DBOD
      DIMENSION VV(60),V(60),WH(20),TT(60),AA(60),XXL(60),C3(60)
      AV1=0.0
      AV2=0.0
      JMM=JM-1
      DO 5 I=1,JMM
      J=JM-I+1
      JJ=J-1
      IF(T(J,1)-T(JJ,1)) 6,7,7
    6 CONTINUE
      IF(J-2) 8,8,9
    8 T(2,1)=(T(2,1)*A(2)+T(1,1)*A(1)/2.0)/(A(2)+A(1)/2.0)
      T(1,1)=T(2,1)
      GO TO 7
    9 DO 10 K=1,JJ
      KJ=J+1-K
      KJJ=KJ-1
      IF(JM-KJ) 2,2,3
    2 FAC=0.5
      GO TO 4
    3 FAC=1.0
    4 AV1=AV1+T(KJ,1)*A(KJ)*FAC
      AV2=AV2+A(KJ)*FAC
      TAV=AV1/AV2
      IF(TAV-T(KJJ,1)) 10,20,20
   10 CONTINUE
   20 IF(J.EQ.JM) KJ=K
      DO 30 L=KJ,J
   30 T(L,1)=TAV
    7 AV1=0.0
      AV2=0.0
    5 CONTINUE
      RETURN
      END



      FUNCTION PROB(Y,YAV,SIG)
```

```
C COMPUTES AREA UNDER NORMAL ERROR CURVE BY RATIONAL APPROXIMATION.
      XX = (Y-YAV)/SIG
      X = ABS(XX)
      IF(X-10.0) 1,1,2
    2 X=10.0
    1 XT = 1.0/(1.0+0.33267*X)
      XA = EXP(-X*X/2.0)*0.3989423
      XA = XA*(0.436184*XT-0.120167*XT*XT+0.937298*XT**3)
      IF (XX) 5,5,10
    5 PROB = XA
      RETURN
   10 PROB = 1.0-XA
      RETURN
      END



      FUNCTION TTIN(N)
C COMPUTE INFLOW TEMPERATURE FROM READ IN VALUES.
C LINEAR INTERPOLATION BETWEEN READ IN VALUES.
      COMMON T(60,2),EL(60),XL(60),A(60),TI(310),TA(310),SIGH(310)
      COMMON FIN(310),WIND(310),DD(310),QI(310),QO(310),P(50),NPR
      COMMON UOMAX(2),UIMAX(2),DTTI,DTTA,DTSIGH,DTFIN,DTWIND,DTDD,DTQI
      COMMON DTJD,JM,JOUT,JIN,KDIF,KSUR,KOH,KQ,KLOSS,YSUR,YOUT,DT,DY
      COMMON TSTOP,EVPCON,OMEGA,HZ,SPREAD,SIGMAI,SIGMAO,ETADY,TVARI
      COMMON TVARO,EVAP,RAD,TAIR,PSI,DERIV,HAFDEL,EPSIL,GJ
      COMMON YOUT,NN,BETA,DAJM,DELCON,V( 60,1),UI( 60,1),DTT
      COMMON RHO,HCAP,KMIX,RMIX,JMIXB,MIXED,QMIX,KAREA,DATRAD,ATRAD(310)
      COMMON AR,JNDX,CO,CI,B( 60),S( 60),EX( 60),EXO( 60),ARF,UO( 60,1)
      COMMON JJ(310),TI1(310),CC(20,60,2),CCC(20,310),COUT(20,310)
      COMMON CCI(20,310),QMIX(60),XINF(60),OUTF(60),MIXH,MM
      COMMON SLOPE(310),GRAV,SLOPE,VISCOS,LAGTIM(310)
      COMMON PHASOI(20),PHASIN(20),ET,NTRAC(20),ITR,IST0,IS01,IS02
      COMMON ISTON,IST01,THICK1,THICK2,DOXLE(60,20),DO(306),BOD(306)
      COMMON NLEVE(305),VOL,NW,NDET,Z,Z1,DDOC,NGDET,DBOD
      ET=DTT*FLOAT(N)
      R = ET/DTTI
      L = R
      RR = R-FLOAT(L)
      TTIN=TI(L+1)+RR*(TI(L+2)-TI(L+1))
      RETURN
      END



      FUNCTION ELAIN(N)
C COMPUTE INCOMING SOLAR RADIATION FROM READ IN VALUES.
C READ IN VALUES TREATED AS A STEP FUNCTION.
      COMMON T(60,2),EL(60),XL(60),A(60),TI(310),TA(310),SIGH(310)
      COMMON FIN(310),WIND(310),DD(310),QI(310),QO(310),P(50),NPR
      COMMON UOMAX(2),UIMAX(2),DTTI,DTTA,DTSIGH,DTFIN,DTWIND,DTDD,DTQI
      COMMON DTJD,JM,JOUT,JIN,KDIF,KSUR,KOH,KQ,KLOSS,YSUR,YOUT,DT,DY
      COMMON TSTOP,EVPCON,OMEGA,HZ,SPREAD,SIGMAI,SIGMAO,ETADY,TVARI
      COMMON TVARO,EVAP,RAD,TAIR,PSI,DERIV,HAFDEL,EPSIL,GJ
      COMMON YOUT,NN,BETA,DAJM,DELCON,V( 60,1),UI( 60,1),DTT
      COMMON RHO,HCAP,KMIX,RMIX,JMIXB,MIXED,QMIX
```

```
      ET=DTT*FLOAT(N)
      R = ET/DTFIN
      L = R
      FLXIN = FIN(L+1)
      RETURN
      END



      FUNCTION QQIN(N)
C COMPUTE INFLOW RATE FROM READ IN VALUES.
C READ IN VALUES TREATED AS A STEP FUNCTION.
      COMMON T(60,2),EL(60),XL(60),A(60),TI(310),TA(310),SIGH(310)
      COMMON FIN(310),WIND(310),DD(310),QI(310),QO(310),P(50),NPR
      COMMON UOMAX(2),UIMAX(2),DTTI,DTTA,DTSIGH,DTFIN,DTWIND,DTDD,DTQI
      COMMON DTQQ,JM,JOUT,JIN,KDIF,KSUR,KOH,KQ,KLOSS,YSUR,YOUT,DT,DY
      COMMON TSTOP,EVPCON,OMEGA,BZ,SPREAD,SIGMAI,SIGMAO,ETADY,TVARI
      COMMON IVARQ,EVAP,RAD,TAIR,PSI,DERIV,HAFDEL,EPSIL,GJ
      COMMON YBOT,NN,BETA,DAJM,DELCON,V( 60,1),UI( 60,1),DTT
      COMMON RHO,HCAP,KMIX,RMIX,JMIXB,MIXED,QMIX
      ET=DTT*FLOAT(N)
      R = ET/DTQI
      L = R
      QQIN=QI(L+1)
      RETURN
      END



      FUNCTION QQOUT(N)
C COMPUTE OUTFLOW RATE FROM READ IN VALUES.
C READ IN VALUES TREATED AS A STEP FUNCTION.
      COMMON T(60,2),EL(60),XL(60),A(60),TI(310),TA(310),SIGH(310)
      COMMON FIN(310),WIND(310),DD(310),QI(310),QO(310),P(50),NPR
      COMMON UOMAX(2),UIMAX(2),DTTI,DTTA,DTSIGH,DTFIN,DTFOUT,DTDD,DTQI
      COMMON DTQQ,JM,JOUT,JIN,KDIF,KSUR,KOH,KQ,KLOSS,YSUR,YOUT,DT,DY
      COMMON TSTOP,EVPCON,OMEGA,BZ,SPREAD,SIGMAI,SIGMAO,ETADY,TVARI
      COMMON IVARQ,EVAP,RAD,TAIR,PSI,DERIV,HAFDEL,EPSIL,GJ
      COMMON YBOT,NN,BETA,DAJM,DELCON,V( 60,1),UI( 60,1),DTT
      COMMON RHO,HCAP,KMIX,RMIX,JMIXB,MIXED,QMIX
      ET=DTT*FLOAT(N)
      R = ET/DTQQ
      L = R
      QQOUT = QQ(L+1)
      RETURN
      END



      FUNCTION DIJ,N)
C COMPUTE DIFFUSIVITY FROM READ IN VALUES.
C ANY ASSUMED VARIATION OF THE DIFFUSIVITY MAY BE PROGRAMMED IN THIS FUNCTION
C HERE. A CONSTANT VALUE OF D IS ASSUMED.
      COMMON T(60,2),EL(60),XL(60),A(60),TI(310),TA(310),SIGH(310)
```

```
      COMMON FIN(310),WIND(310),DD(310),QI(310),QO(310),P(50),NPR
      COMMON UOMAX(2),UIMAX(2),DTTI,DTTA,DTSIGH,DTFIN,DTFOUT,DTDD,DTQI
      COMMON DTQO,JM,JOUT,JIN,KDIF,KSUR,KOH,KQ,KLOSS,YSUR,YOUT,DT,DY
      COMMON TSTOP,EVPCON,OMEGA,BZ,SPREAD,SIGMAI,SIGMAO,ETADY,TVARI
      COMMON TVARO,EVAP,RAD,TAIR,PSI,DERIV,HAFDEL,EPSIL,GJ
      COMMON YBOT,NN,BETA,DAJM,DELCON,V( 60,1),UI( 60,1),DTT
      COMMON RHO,HCAP,KMIX,RMIX,JMIXB,MIXED,QMIX
      D = DD(1)
      RETURN
      END



      SUBROUTINE XMIX(N)
C   CALCULATION OF COMPOSITION OF INFLOW
      COMMON T(50,2),EL(60),XL(60),A(60),TI(310),TA(310),SIGH(310)
      COMMON FIN(310),WIND(310),DD(310),QI(310),QO(310),P(50),NPR
      COMMON UOMAX(2),UIMAX(2),DTTI,DTTA,DTSIGH,DTFIN,DTWIND,DTDD,DTQI
      COMMON DTQO,JM,JOUT,JIN,KDIF,KSUR,KOH,KQ,KLOSS,YSUR,YOUT,DT,DY
      COMMON TSTOP,EVPCON,OMEGA,BZ,SPREAD,SIGMAI,SIGMAO,ETADY,TVARI
      COMMON TVARO,EVAP,RAD,TAIR,PSI,DERIV,HAFDEL,EPSIL,GJ
      COMMON YBOT,NN,BETA,DAJM,DELCON,V( 60,1),UI( 60,1),DTT
      COMMON RHO,HCAP,KMIX,RMIX,JMIXB,MIXED,QMIX,KAREA,DATRAD,ATRAD(310)
      COMMON AR,WINDY,CO,CI,B( 60),S( 60),EX( 60),EXO( 60),ARF,UO( 60,1)
      COMMON QIN(310),TIN(310),CC(20,60,2),CCC(20,310),COUT(20,310)
      COMMON CCT(20,310),QQMIX(60),XINF(60),OUTF(60),MIXH,MM
      COMMON SURF(310),GRAV,SLOPE,VISCOS,LAGTIM(310)
      COMMON PMASOT(20),PMASIN(20),ET,NTRAC(20),ITR,IST0,IS01,IS02
      COMMON ISTON,IST01,THICK1,THICK2,DUXLE(60,20),DO(306),BOD(306)
      COMMON NLEVE(306),VOL,NW,NDET,Z,Z1,DDOC,NGDET,DBOD
      XQ=QIN(N)*(1.0+RMIX)
      IF(XQ.EQ.0.0) GO TO 5
      JMIXH=JM-MIXED
      JMM=JM-1
      GO TO (300,301),NGDET
C  PULSE INJECTION CALCULATION.
300   IF(MM) 11010,11010,11011
11011 CONTINUE
      DO 1 M=1,MM
      YQ=0.0
21    DO 2 I=JMIXH,JM
    2 YQ=YQ+QQMIX(I)*CC(M,I,1)
24    CONTINUE
    1 CCC(M,N)=YQ/XQ
11010 CONTINUE
      IF(N-40) 7,7,8
    8 NX=40
      GO TO 9
    7 NX=N
    9 DO 3 I=1,NX
      NLM=N+1-I
      IF(N-(NLM+LAGTIM(NLM))) 3,11,3
11    IF(MM) 3,3,4
4     DO 30 M=1,ITR
      IF(NLM-NTRAC(M)) 30,5,30
5     CCC(M,N)=QIN(NLM)/XQ +YQ/XQ
51    CONTINUE
```

```
30      CONTINUE
    3 CONTINUE
    6 CONTINUE
      RETURN
C   DO.BOD CALCULATION.
301   MM=2
      YQ=QQMIX(JM)*CC(1,JM,1)
      YQQ=QQMIX(JM)*CC(2,JM,1)
      DO 17000 J=JMIXH,JMM
      YQ=YQ+QQMIX(J)*CC(1,J,1)
17000 YQQ=YQQ+CC(2,J,1)*QQMIX(J)
      CCC(1,N)=YQ/XQ
      CCC(2,N)=YQQ/XQ
      IF(N-60) 17332,17332,17333
17333 NX=60
      GO TO 1242
17332 NX=N
1242  CONTINUE
      DO 18000 I=1,NX
      NLM=N+1-I
      IF(N-(NLM+LAGTIM(NLM))) 18000,18001,18000
18001 CCC(1,N)=CCC(1,N)+QQIN(NLM)*QQQ(NLM)/XQ
      CCC(2,N)=CCC(2,N)+QQIN(NLM)*BBOD(NLM)/XQ
18000 CONTINUE
      RETURN
      END



      SUBROUTINE SPECAL(N)
C   CALCULATION OF DISTRIBUTION OF SPECIFIED INPUTS
      COMMON T(50,2),EL(60),XL(60),A(60),TI(310),TA(310),SIGH(310)
      COMMON FIN(310),VIND(310),DD(310),QI(310),QO(310),P(50),NPR
      COMMON QQMAX(2),QTMAX(2),DTTI,DTTA,DTSIGH,DTFIN,DTWIND,DTDD,DTQI
      COMMON DTQQ,JM,JOUT,JIN,KDIF,KSUR,KOH,KQ,KLOSS,YSUR,YOUT,DT,DY
      COMMON ISTOP,EVPCON,OMEGA,RZ,SPREAD,SIGMAI,SIGMAO,ETADY,TVARI
      COMMON TVARO,EVAP,RAD,TAIR,PSI,DERIV,HAFDEL,EPSIL,GJ
      COMMON YBOT,NN,BETA,DAJM,DELCON,V( 60,1),QI( 60,1),DTT
      COMMON RHO,HCAP,KMIX,XMIX,JMIXB,MIXED,QMIX,KAREA,DATRAD,ATRAD(310)
      COMMON AR,WINDY,CO,CI,B( 60),S( 60),EX( 60),EXQ( 60),ARF,QO( 60,1)
      COMMON QIN(310),TIN(310),CC(20,60,2),CCC(20,310),COUT(20,310)
      COMMON CCI(20,310),QQMIX(60),XINF(60),OUTF(60),MIXH,MM
      COMMON SURF(310),GRAV,SLOPE,VISCOS,LAGTIM(310)
      COMMON PMASOT(20),PMASIN(20),ET,NTRAC(20),ITR,IST0,IS01,IS02
      COMMON ISTON,IST01,THICK1,THICK2,DDXLE(60,20),DD(306),BOD(306)
      COMMON NLEVE(305),VOL,NW,NDET,Z,Z1,DDDC,NGDET,DBOD,JEUP
      COMMON NBOUND,NGRID
      JMM=JM-1
      DO 1 I=2,JMM
      IF(V(I,1)) 2,2,3
    2 OUTF(I)=(QQ(I,1)*B(I)*DY-V(I,1)*(A(I)+A(I-1))/2.0)*DT
      XINF(I)=-V(I+1,1)*(A(I)+A(I+1))/2.0*DT
    1 CONTINUE
      GO TO 1
    3 OUTF(I)=(QQ(I,1)*B(I)*DY+V(I+1,1)*(A(I)+A(I+1))/2.0)*DT
      XINF(I)=V(I,1)*(A(I)+A(I-1))/2.0*DT
```

```
83      CONTINUE
    1   CONTINUE
        IF(MM) 11010,11010,11011
11011   CONTINUE
        DO 53 M=1,MM
        DO 51 I=2,JMM
733     CONST1=0.0
        CONST2=0.0
        GO TO (7213,7112),NGDET
7112    IF(I -JBUP) 7211,7211,7212
7212    CONST1=0.0
        CONST2=0.0
        GO TO 7213
7211    IF(M-1) 736,736,737
736     CONST1=1
        CONST2=21
        GO TO 735
737     CONST1=1
        CONST2=0.0
735     CONTINUE
7213    CONTINUE
        IF(V(I,1))6,6,7
    6   IF(V(I+1,1)) 20,20,21
   20   CC(M,I,2)=(CC(M,I,1)*A(I)*DY-OUTF(I)*CC(M,I,1)+CCC(M,N)*UI(I,1)*
       1DT*B(I)*DY+XINF(I)*CC(M,I+1,1))/A(I)/DY-CONST1*CC(2,I,1)*DT
        GO TO 5
   21   CC(M,I,2)=(CC(M,I,1)*A(I)*DY-OUTF(I)*CC(M,I,1)+CCC(M,N)*UI(I,1)*
       1DT*B(I)*DY+XINF(I)*CC(M,I,1))/A(I)/DY -CONST1*CC(2,I,1)*DT
        GO TO 5
    7   IF(V(I+1,1)) 22,22,23
   23   CC(M,I,2)=(CC(M,I,1)*A(I)*DY-OUTF(I)*CC(M,I,1)+CCC(M,N)*UI(I,1)*
       1DT*B(I)*DY+XINF(I)*CC(M,I-1,1))/A(I)/DY -CONST1*CC(2,I,1)*DT
        GO TO 5
   22   CC(M,I,2)=(CC(M,I,1)*A(I)*DY-UO(I,1)*B(I)*DY*DT*CC(M,I,1)
       1-V(I+1,1)*(A(I)+A(I+1))/2.0*DT*CC(M,I+1,1)+CCC(M,N)*UI(I,1)*
       1DT*B(I)*DY+XINF(I)*CC(M,I-1,1))/A(I)/DY -CONST1*CC(2,I,1)*DT
5       IF (CC(M,I,2) -0.1E-30) 50,50,51
50      CC(M,I,2)=0.0
51      CONTINUE
C  CALCULATION ON SURFACE LAYER.
        GO TO (423,424), NGDET
424     J=JM
        DOSA=14.4776-0.3579*T(J,1)+0.0043*(T(J,1)**2)
        CONST1=0.0
        IF (M-1) 45895,45895,45896
45895   CONST2=1
        GO TO 45897
45896   CONST2=0.0
45897   CONTINUE
423     CONTINUE
        IF(V(JM,1)) 9,9,10
    9   CC(M,JM,2)=(CC(M,JM,1)*A(JM)*DY/2.0-(UO(JM,1)*B(JM)*DY/2.0*CC(M,JM
       1,1)-CCC(M,N)*UI(JM,1)*B(JM)*DY/2.0-V(JM,1)*(A(JM)+A(JM-1))/2.0*
       2CC(M,JM,1))*DT)/A(JM)/DY*2.0     -CONST1*CC(2,JM,1)*DT
       2 +CONST2*(DOSA-CC(1,JM,1))*DT
        GO TO 11
   10   CC(M,JM,2)=(CC(M,JM,1)*A(JM)*DY/2.0-(UO(JM,1)*B(JM)*DY/2.0*CC(M,JM
       1,1)-CCC(M,N)*UI(JM,1)*B(JM)*DY/2.0-V(JM,1)*(A(JM)+A(JM-1))/2.0*
```

```
     1CC(M,JM-1,1))*DT)/A(JM)/DY*2.0 -CONST1*CC(2,JM,1)*DT
     2 +CONST2*(DOSA-CC(1,JM,1))*DT
11    GO TO (76555,76556), NGDET
76556 IF(M-1) 76557,76557,76558
76557 CONST1=1
      CONST2=1
      GO TO 76555
76558 CONST1=1
      CONST2=0.0
C  CALCULATION ON BOTTOM LAYER.
76555 IF(V(2,1))12,12,13
   12 CC(M,1,2)=(CC(M,1,1)*A(1)*DY/2.0-(UO(1,1)*B(1)*DY/2.0*CC(M,1,1)-
     1CCC(M,N)*UI(1,1)*B(1)*DY/2.0+V(2,1)*(A(1)+A(2))/2.0*CC(M,2,1))*DT)
     2/A(1)/DY/0.5 -CONST1*CC(2,1,1)*DT
      GO TO 4
   13 CC(M,1,2)=(CC(M,1,1)*A(1)*DY/2.0-(UO(1,1)*B(1)*DY/2.0*CC(M,1,1)-
     1CCC(M,N)*UI(1,1)*B(1)*DY/2.0+V(2,1)*(A(1)+A(2))/2.0*CC(M,1,1))*DT)
     2/A(1)/DY*2.0 -CONST1*CC(2,1,1)*DT
    4 CONTINUE
      IF(CC(M,JM,2)-0.1E-30) 54,54,55
54    CC(M,JM,2)=0.0
55    CONTINUE
      IF (CC(M,1,2) -0.1E-30) 52,52,53
52    CC(M,1,2)=0.0
53    CONTINUE
11010 CONTINUE
      GO TO (7536,7537),NGDET
7537  DO 3547 J=1,JM
      DOSA=14.4776-0.3579*T(J,2)+0.0043*(T(J,2)**2)
      IF(CC(1,J,2)) 3699,3699,3655
3699  CC(1,J,2)=0.
      GO TO 3547
3655  IF(CC(1,J,2)-DOSA) 3547,3547,3548
3548  CC(1,J,2)=DOSA
3547  CONTINUE
C  SURFACE ASSUMPTION FOR DO.
      GO TO (12587,12588,7536),NBOUND
12587 DO 79965 J=JEUP,JM
      DOSA=14.4776-0.3579*T(J,2)+0.0043*(T(J,2)**2)
79965 CC(1,J,2)=DOSA
      GO TO 12589
12588 KCALC=JM-NGRID
      DO 17588 J=KCALC,JM
      DOSA=14.4776-0.3579*T(J,2)+0.0043*(T(J,2)**2)
17588 CC(1,J,2)=DOSA
12589 CONTINUE
7536  CONTINUE
      RETURN
      END



      SUBROUTINE SPECAV(N)
C  AVERAGING OF SPECIFIED MATERIAL IN MIXED LAYERS
      COMMON T(60,2),EL(60),XL(60),A(60),TI(310),TA(310),SIGH(310)
      COMMON FIN(310),WIND(310),DO(310),QI(310),QO(310),P(50),NPR
```

```
      COMMON UOMAX(2),UIMAX(2),DTTI,DTTA,DTSIGH,DTFIN,DTWIND,DTDD,DTQI
      COMMON DTUO,JM,JOUT,JIN,KDIF,KSUR,KOH,KQ,KLOSS,YSUR,YOUT,DT,DY
      COMMON ISTOP,EVPCON,OMEGA,HZ,SPREAD,SIGMAI,SIGMAO,ETADY,TVARI
      COMMON TVARO,EVAP,RAD,TAIR,PSI,DERIV,HAFDEL,EPSIL,GJ
      COMMON YBOT,NN,BETA,DAJM,DELCON,V( 60,1),UI( 60,1),DTT
      COMMON RHO,HCAP,KMIX,RMIX,JMIXB,MIXED,QMIX,KAREA,DATRAD,ATRAD(310)
      COMMON AR,WINDY,CU,CI,H( 60),S( 60),EX( 60),EXU( 60),ARF,UO( 60,1)
      COMMON QIN(310),TIN(310),CC(20,60,2),CCC(20,310),COUT(20,310)
      COMMON CCT(20,310),QQMIX(60),XINF(60),OUTF(60),MIXH,MM
      COMMON SURF(310),GRAV,SLOPE,VISCOS,LAGTIM(310)
      COMMON PMASOT(20),PMASIN(20),ET,NTRAC(20),ITR,IST0,IS01,IS02
      COMMON IST0N,IST01,THICK1,THICK2,DOXLE(60,20),DO(306),BOD(306)
      COMMON NLEVE(306),VOL,NW,NDET,Z,Z1,DDOC,NGDET,DBOD
      JMIXH=JM-MIXH+1
      IF(MM) 11010,11010,11011
11011 CONTINUE
      DO 1 M=1,MM
      XCC=0.0
      XA=0.0
      JMM=JM-1
      DO 2 J=JMIXH,JMM
      XCC=CC(M,J,2)*A(J)*DY+XCC
    2 XA=XA+A(J)*DY
      XCC=XCC+CC(M,JM,2)*A(JM)*DY/2.0
      XA=XA+A(JM)*DY/2.0
      DO 3 I=JMIXH,JM
    3 CC(M,I,2)= XCC/XA
    1 CONTINUE
      GO TO (7536,7537),NGDET
C  DO CALCULATIONS.
7537  DO 3547 J=JMIXH,JM
      DOSA=14.4776-0.3579*T(J,2)+0.0043*(T(J,2)**2)
      IF(CC(1,J,2)) 3699,3699,3655
3699  CC(1,J,2)=0.
      GO TO 3547
3655  IF(CC(1,J,2)-DOSA) 3547,3547,3548
3548  CC(1,J,2)=DOSA
3547  CONTINUE
7536  CONTINUE
11010 CONTINUE
      RETURN
      END




      SUBROUTINE SPECOT(N)
C PROPORTION OF SPECIFIED INFLOWS IN OUTFLOWS
      COMMON T(60,2),EL(60),XL(60),A(60),TI(310),TA(310),SIGH(310)
      COMMON FIN(310),WIND(310),DD(310),QI(310),QO(310),P(50),NPR
      COMMON UOMAX(2),UIMAX(2),DTTI,DTTA,DTSIGH,DTFIN,DTWIND,DTDD,DTQI
      COMMON DTUO,JM,JOUT,JIN,KDIF,KSUR,KOH,KQ,KLOSS,YSUR,YOUT,DT,DY
      COMMON ISTOP,EVPCON,OMEGA,HZ,SPREAD,SIGMAI,SIGMAO,ETADY,TVARI
      COMMON TVARO,EVAP,RAD,TAIR,PSI,DERIV,HAFDEL,EPSIL,GJ
      COMMON YBOT,NN,BETA,DAJM,DELCON,V( 60,1),UI( 60,1),DTT
      COMMON RHO,HCAP,KMIX,RMIX,JMIXH,MIXED,QMIX,KAREA,DATRAD,ATRAD(310)
      COMMON AR,WINDY,CU,CI,H( 60),S( 60),EX( 60),EXU( 60),ARF,UO( 60,1)
      COMMON QIN(310),TIN(310),CC(20,60,2),CCC(20,310),COUT(20,310)
```

```
      COMMON CCT(20,310),QQMIX(60),XINF(60),OUTF(60),MIXH,MM
      COMMON SURF(310),GRAV,SLOPE,VISCOS,LAGTIM(310)
      COMMON PMASOT(20),PMASIN(20),ET,NTRAC(20),ITR,IST0,IS01,IS02
      COMMON ISTON,IST01,THICK1,THICK2,DOXLE(60,20),DO(306),BOD(306)
      COMMON NLEVE(306),VOL,NW,NDET,Z,Z1,DDOC,NGDET,DBOD
      JMM=JM-1
      IF(MM) 11010,11010,11011
11011 CONTINUE
      DO 1 M=1,MM
21    XC=CC(M,JM,1)*(B(JM)*DY/2.0*UO(JM,1)-QQMIX(JM))+CC(M,1,1)*B(1)*DY/
     1 2.0*UO(1,1)
      XCC=CC(M,JM,2)*A(JM)*DY/2.0+CC(M,1,2)*A(1)*DY/2.0
      DO 2 J=2,JMM
      IF(J-JMIXH) 10,11,11
   10 XC=XC+CC(M,J,1)*UO(J,1)*B(J)*DY
      GO TO 12
   11 XC=XC+CC(M,J,1)*(UO(J,1)*B(J)*DY -QQMIX(J))
   12 XCC=XCC+CC(M,J,2)*A(J)*DY
    2 CONTINUE
      IF(QOUT(N)) 50,50,51
50    COUT(M,N)=0.
      CCT(M,N)=0.
      GO TO (800,1),NGDET
800   NM=NTRAC(M)
      GO TO 52
51    XF=QOUT(N)*DT
      XC=XC*DT
      COUT(M,N)=XC/XF
      GO TO (802,1),NGDET
802   NM=NTRAC(M)
80    CCT(M,N)=XC/QQIN(NM)/DTT/XF
52    CONTINUE
      PMASIN(M)=XCC/QQIN(NM)/DTT
      PMASOT(M) =CCT(M,N)*XF+PMASOT(M)
    1 CONTINUE
      GO TO (811,300),NGDET
811   IF(NW-NDET) 300,301,300
301   WRITE(6,5) ET
5     FORMAT (' ELAPSED TIME =', F7.2)
      WRITE(6,92756)
92756 FORMAT(' TRACE COUT/MASSIN   COUT      TRACOT       % REMAINING')
      WRITE(6,4) (M,CCT(M,N),COUT(M,N),PMASOT(M),PMASIN(M),M=1,MM)
    4 FORMAT(I4,4F12.5)
      NW=0
300   DO 16 M=1,MM
      DO 15 I=1,JM
   15 CC(M,I,1)=CC(M,I,2)
   16 CONTINUE
11010 CONTINUE
      RETURN
      END



      FUNCTION DDO(N)
C  COMPUTE INPUT DO FROM READ IN VALUES
```

```
      COMMON T(60,2),EL(60),XL(60),A(60),TI(310),TA(310),SIGH(310)
      COMMON FIN(310),WIND(310),DD(310),QI(310),QO(310),P(50),NPR
      COMMON UOMAX(2),UIMAX(2),DTTI,DTTA,DTSIGH,DTFIN,DTWIND,DTDD,DTQI
      COMMON DTQO,JM,JOUT,JIN,KDIF,KSUR,KOH,KQ,KLOSS,YSUR,YOUT,DT,DY
      COMMON TSTOP,EVPCON,OMEGA,BZ,SPREAD,SIGMAI,SIGMAO,ETADY,TVARI
      COMMON TVARO,EVAP,RAD,TAIR,PSI,DERIV,HAFDEL,EPSIL,GJ
      COMMON YBOT,NN,BETA,DAJM,DELCON,V( 60,1),UI( 60,1),DTT
      COMMON RHO,HCAP,KMIX,RMIX,JMIXB,MIXED,QMIX,KAREA,DATRAD,ATRAD(310)
      COMMON AR,WINDY,CO,CI,B( 60),S( 60),EX( 60),EXO( 60),ARF,UO( 60,1)
      COMMON QIN(310),TIN(310),CC(20,60,2),CCC(20,310),COUT(20,310)
      COMMON CCT(20,310),QQMIX(60),XINF(60),OUTF(60),MIXH,MM
      COMMON SURF(310),GRAV,SLOPE,VISCOS,LAGTIM(310)
      COMMON PMASOT(20),PMASIN(20),ET,NTRAC(20),ITR,IST0,IS01,IS02
      COMMON ISTON,IST01,THICK1,THICK2,DOXLE(60,20),DO(306),BOD(306)
      COMMON NLEVE(306),VOL,NW,NDET,Z,Z1,DDOC,NGDET,DBOD
      ET=DTT*FLOAT(N)
      P=ET/DDOC
      L=P
      NGOT=NLEVE(N)
      DDO=DO(L+1)
      IF(LAGTIM(N)) 1,1,78
78    GO TO (1,2),NGOT
C  SUBSURFACE ENTRANCE
2     DDO=DO(L+1)-BBOD(N)*( 1.-EXP(LAGTIM(N)*DTT*(-Z)))/(EXP(LAGTIM(N)
     2*DTT*(-Z)))
1     CONTINUE
      RETURN
      END
      FUNCTION BBOD(N)



C  CALCULATES INPUT BOD FROM READ IN VALUES
      COMMON T(60,2),EL(60),XL(60),A(60),TI(310),TA(310),SIGH(310)
      COMMON FIN(310),WIND(310),DD(310),QI(310),QO(310),P(50),NPR
      COMMON UOMAX(2),UIMAX(2),DTTI,DTTA,DTSIGH,DTFIN,DTWIND,DTDD,DTQI
      COMMON DTQO,JM,JOUT,JIN,KDIF,KSUR,KOH,KQ,KLOSS,YSUR,YOUT,DT,DY
      COMMON ISTOP,EVPCON,OMEGA,BZ,SPREAD,SIGMAI,SIGMAO,ETADY,TVARI
      COMMON TVARO,EVAP,RAD,TAIR,PSI,DERIV,HAFDEL,EPSIL,GJ
      COMMON YBOT,NN,BETA,DAJM,DELCON,V( 60,1),UI( 60,1),DTT
      COMMON RHO,HCAP,KMIX,RMIX,JMIXB,MIXED,QMIX,KAREA,DATRAD,ATRAD(310)
      COMMON AR,WINDY,CO,CI,B( 60),S( 60),EX( 60),EXO( 60),ARF,UO( 60,1)
      COMMON QIN(310),TIN(310),CC(20,60,2),CCC(20,310),COUT(20,310)
      COMMON CCT(20,310),QQMIX(60),XINF(60),OUTF(60),MIXH,MM
      COMMON SURF(310),GRAV,SLOPE,VISCOS,LAGTIM(310)
      COMMON PMASOT(20),PMASIN(20),ET,NTRAC(20),ITR,IST0,IS01,IS02
      COMMON ISTON,IST01,THICK1,THICK2,DOXLE(60,20),DO(306),BOD(306)
      COMMON NLEVE(306),VOL,NW,NDET,Z,Z1,DDOC,NGDET,DBOD
      ET=DTT*FLOAT(N)
      P=ET/DBOD
      L=P
      NGOT=NLEVE(N)
      GO TO (2,1),NGOT
2     BBOD=BOD(L+1)
      GO TO 253
C  SUBSURFACE ENTRANCE
1     BBOD=BOD(L+1)*(    EXP(LAGTIM(N)*DTT*(-Z)))
```

```
253   CONTINUE
      RETURN
      END
```

APPENDIX II

INPUT VARIABLES TO THE COMPUTER PROGRAM

Card 1, FORMAT 20A4

WH = Alphanumeric variable used to print a title at beginning of output. Anything printed on this card will appear as the first line of output

Card 2, FORMAT 20A4

WH = Alphanumeric variable used to list units used in computation prior to output at each time step.

Card 3, FORMAT 1615

JM = Initial number of grid points = number of the surface grid point.

JOUT = Number of the grid point corresponding to outlet elevation.

KDIF = 1 for a constant diffusion coefficient.

= 2 for a variable diffusion coefficient.

KSUR = 1 for a constant surface elevation.

= 2 for a variable surface elevation.

KOH = 1 for use of Koh's Equation 2-49 for computing the withdrawal thickness.

= 2 for use of Kao's Equation 4-26 of Huber and Harleman.

KQ = 1 for computations with inflow and outflow.

= 2 for computation with no inflow or outflow.

KLOSS = 1 for laboratory evaporation formula (Eq. 2-40).

= 2 for Kohler field evaporation formula (Eq. 2-23 of Huber and Harleman).

= 3 for Rohwer field evaporation formula (Eq. 2-43).

NPRINT = Number of time steps between print outs of calculations.

KAREA = 1 for laboratory reservoir calculations.

= 2 for calculations for any other reservoir.

KMIX = 1 for no entrance mixing.

= 2 to include entrance mixing.

MIXED = Number of grid spaces in surface layer for entrance mixing (defines d_m in Eq. 2-58).

Card 4, FORMAT 8F10.5

YSUR = Surface elevation at beginning of calculations.

YOUT = Elevation of outlet.

DT = Time step, Δt.

TSTOP = Time at which progress ceases calculations.

TZERO = Initial isothermal reservoir temperature.

EVPCON = Constant, a, in evaporation formulas of Chapter 2 for KLOSS = 1 or 2. For KLOSS = 3, EVPCON = 0.01.

OMEGA = Constant ω of Equation 5-2.

BZ = Constant B_o of Equation 5-2.

Card 5, FORMAT 8F10.5

SPREAD = Number of outflow standard deviations, σ_o,

equal to half the withdrawal thickness (see discussion of Equation 2-50).

SIGMAI = Inflow standard deviation, σ_i, Equation 2-51.

ETA = Radiation absorption coefficient, η, Equation 2-31

BETA = Fraction of solar radiation absorbed at the water surface, β, Equation 2-31.

RHO = Water density, ρ.

HCAP = Water specific heat, c_p.

DELCON = Half the value of the constant of Equation 4-4b used to predict the withdrawal thickness, δ.

RMIX = Mixing ratio, r_m, Equation 2-55.

Card 6, FORMAT 1615

NTI = Number of inflow temperatures to be read in.

NTA = Number of air temperatures to be read in.

NSIGH = Number of relative humidities to be read in.

NFIN = Number of insolation values to be read in.

NSURF = Number of surface elevations to be read in.

NDD = Number of values of the diffusion coefficient to be read in.

NQI = Number of inflow rates to be read in.

NQO = Number of outflow rates to be read in.

Card 7, FORMAT 8F10.5

DTTI = Time interval between input values of TI.

DTTA = Time interval between input values of TA.

DTSIGH = Time interval between input values of SIGH.

DTFIN = Time interval between input values of FIN.

DSURF = Time interval between input values of SURF.

DTDD = Time interval between input values of DD.

DTQI = Time inverval between input values of QI.

DTQO = Time inverval between input values of QO.

Card Group 8, FORMAT 8F10.5

TI = Values of inflow temperatures, T_{in}.

Card Group 9, FORMAT 8F10.5

TA = Values of air temperature, T_a.

Card Group 10, FORMAT 8F10.5

SIGH = Values of relative humidities, ψ, in decimal form.

Card Group 11, FORMAT 8F10.5

FIN = Values of insolation, ϕ_o.

Card Group 12, FORMAT 8F10.5

SURF = Values of surface elevations, y_s.

Card Group 13, FORMAT 8F10.5

DD = Values of diffusion coefficients, D.

Card Group 14, FORMAT 8F10.5

QI = Values of inflow rates, Q_i.

Card Group 15, FORMAT 8F10.5

QO = Values of outflow rates, Q_o.

Card 16, FORMAT 3F12.2

SLOPE = Average slope at the inlet end of the reservoir.

GRAV = Acceleration of gravity = 3528000 cm/min^2

(KAREA = 1) and 73156608000 m/day^2 (KAREA = 2).

VISCOUS = Viscosity of water

Card 17, FORMAT 2I5

NGDET = 1 for pulse injection solution.

= 2 for D.O. calculation.

NBOUND = 1 for entire euphotic zone saturated.

= 2 for specified number of grid points for saturated region.

= 3 for no saturation assumption, reaeration only mechanism.

Card 18, FORMAT 2I5

ITR = Number of pulse injections to be traced (if NGDET = 1).

or

NDISSO = Number of input D.O.'s to be read in. (if NGDET = 2).

NBOD = Number of input B.O.D.'s to be read in.

The following sequence holds if NGDET = 1.

Card Group 19, FORMAT 16I5

NTRAC(I) = Time steps at which pulse injections were input. (This will depend on DT for example if DT = 2 minutes and the first trace was input at 10 min., NTRAC(I) = 5).

Card 20, FORMAT I5

NDET = Number of time steps to be passed between printout of TRACOT (Equation 3-38).

Go to card 25.

The following sequence holds if NGDET = 2.

Card 19, 2F10.5

DDOC = Time interval between input values of D.O.

DBOD = Time interval between input values of B.O.D.

Card Group 20, FORMAT 8F10.5

DO = Values of inflow D.O.

Card Group 21, FORMAT 8F10.5

B.O.D. = Values of inflow B.O.D.

Card 22, FORMAT I5

NPROF = 1 for a constant initial B.O.D. and D.O. profile.

= 2 for a linear initial B.O.D. and D.O. profile.

Card 23, FORMAT 4F10.5

If NPROF = 1

DOI = Initial D.O. value.

BODI = Initial B.O.D. value.

or if NPROF = 2

DOB = Initial D.O. value at the reservoir bottom.

DOT = Initial D.O. value at the surface of the reservoir.

BODB = Initial B.O.D. value at the reservoir bottom.

BODT = Initial B.O.D. value at the reservoir surface.

Card 24, FORMAT 2F10.5, I5

Z = First order decay constant for B.O.D. (Eq. 3-14).

Z1 = First order reaeration constant at surface.

NDOCA = Time interval between printout of D.O. profiles.

Card 25, FORMAT 2F10.5

THICK1 = Thickness of surface layer for lagtime calculation (Equation 2-92).

THICK2 = Thickness of subsurface layer for lagtime calculation (Equation 2-92).

If lagtime is not to be considered set THICK1 and THICK2 = 0.00001 meters.

The following parameters are read in when KAREA = 2.

Card 26, FORMAT 1615

NAA = Number of areas to be read in.

NXXL = Number of lengths to be read in.

NWIND = Number of wind values to be read in.

NATRAD = Number of atmospheric radiation values to be read in.

JMP = Number of grid points for which program variables should be initialized. (This should be the maximum value of JM expected to occur in the calculations.)

Card 27, FORMAT 8F10.5

DAA = Vertical distance interval between input values of AA.

DXXL = Vertical distance interval between input values of XXL.

DTWIND = Time interval between input values of WIND.

DATRAD = Time interval between input values of ATRAD.

AAB = Elevation of first (lowest) value of AA.

XXLB = Elevation of first (lowest) value of XXL.

ARF = Area reduction factor, $a_r = 1$.

Card Group 28, FORMAT 8F10.5

AA = Values of horizontal cross-sectional areas, A.

Card Group 29, FORMAT 8F10.5

XXL = Values of reservoir lengths, L.

Card Group 30, FORMAT 8F10.5

WIND = Values of wind speeds, w.

Card Group 31

ATRAD = Values of atmospheric radiation, ϕ_a.

APPENDIX III

SAMPLE INPUT DATA FOR FONTANA D.O. PREDICTIONS

This appendix contains typical input for the prediction of temperature and D.O. profiles and outlet values. This particular input set is for the case of initial B.O.D. = 0, initial D.O. = 8 ppm and K = 0.05 day^{-1} and saturation in the entire euphotic zone.

Cards or card groups are separated by blanks in the computer listing. This is only for illustrative purposes and would not be present in the actual data deck. Data contained on the card or card groups are titled with a card prefaced by an asterisk (*) that would not appear in the actual computer input.

```
1FIELD DATA FOR FONTANA RESERVOIR FOR MARCH 1 TO DECEMBER 31, 1966.
0ALL UNITS IN METERS, DAYS, KILOCALORIES, KILOGRAMS, AND DEGREES CENTIGRADE.
   47   22    1    2    1    1    3   10    2    2    4
493.0      443.0      1.0       300.0      6.7       0.01      0.0133    0.855
1.96       4.0        0.75      0.50       997.0     0.998     1.00000   1.00
  306  306  306  306  306    2  306  306
1.0        1.0        1.0       1.0        1.0       306.0     1.0       1.0
*  INFLOW TEMPERATURES.(DEGREES CENTIGRADE).
      7.58      7.24      6.93      8.27      8.35      6.34      5.62      5.51
      6.06      6.67      7.61      8.29      9.13      9.96     10.70     10.97
     10.84     10.83     11.41     11.39     10.94     11.36     12.11     11.68
      9.40      8.52      8.25      8.27      8.50      8.73      9.83      9.93
      9.91     10.23     10.93      9.75      9.47      9.55      9.45      9.48
      9.95     10.41     11.63     12.29     12.32     12.66     12.45     12.92
     13.87     13.55     12.81     13.31     13.97     14.25     15.29     15.42
     15.68     15.00     14.55     14.79     14.93     14.30     13.59     12.86
     13.26     13.41     13.93     14.38     15.14     15.11     13.81     12.83
     12.59     12.28     13.28     14.30     13.81     13.86     14.16     14.51
     15.80     16.46     16.97     17.25     16.26     15.73     15.81     15.51
     16.36     17.13     17.06     16.20     15.68     15.31     15.78     16.91
     17.98     18.00     18.37     18.65     18.46     18.00     18.58     20.45
     19.39     19.28     19.34     19.87     19.67     20.57     19.39     19.75
     19.73     19.25     18.53     18.91     19.42     18.07     18.42     18.88
     19.47     19.29     18.76     18.81     20.31     20.81     20.55     20.59
     20.43     21.06     20.75     22.16     23.63     24.24     23.73     23.74
     23.22     21.49     21.64     22.30     22.84     21.37     20.65     20.48
     20.54     21.25     21.19     21.03     21.33     21.08     20.63     19.01
     18.04     18.45     18.44     18.27     18.31     18.48     18.48     18.20
     18.49     18.71     18.48     17.83     17.62     17.74     18.14     18.91
     19.55     20.86     19.96     19.89     19.70     19.54     19.18     19.86
     19.30     18.65     18.48     18.62     19.12     19.58     18.84     18.44
     18.79     18.95     19.04     18.84     19.17     19.08     18.26     18.88
     18.77     19.00     18.76     18.18     17.16     17.37     17.30     17.28
     17.21     16.43     15.36     16.03     16.28     15.85     16.00     16.10
     15.75     15.14     15.89     15.95     16.36     16.32     15.20     13.84
     13.69     14.29     14.44     13.94     13.97     13.80     13.98     14.28
     11.23     10.82     10.84     11.11     11.58     12.46     12.79     12.56
     14.12     13.78     13.84     14.25     14.28     13.04     13.02     11.74
     12.11     11.81     11.49     10.93     11.38     12.03     10.81      9.20
      8.43      8.81     10.01     10.92     11.14     11.87     11.14     12.52
     12.22     12.04     11.60     10.71      9.91      9.64     10.14     10.27
      9.72      8.65      8.61      8.53      8.04      8.55      9.47      9.08
      8.55      6.68      6.29      6.33      6.46      6.27      5.68      5.26
      6.21      7.78      8.84      9.88      9.19      8.24      7.22      7.02
      6.82      6.47      6.24      6.46      6.49      6.59      6.46      6.31
      6.45      6.63      5.82      4.08      3.76      4.12      5.05      5.38
      4.69      4.82
*  AIR TEMPERATURES.(DEGREES CENTIGRADE).
     6.034     5.248     8.752    11.746     0.281    -3.432    -2.560    -1.432
```

1.090	4.079	5.834	7.473	9.306	12.868	11.472	11.003
11.451	10.478	10.325	10.118	10.673	15.065	13.138	4.107
2.285	1.421	2.408	1.612	2.176	6.157	6.616	7.283
7.706	9.062	7.009	4.490	4.008	6.440	5.253	6.247
3.872	8.492	14.036	14.995	10.948	9.377	7.864	9.398
14.503	14.329	15.785	16.072	15.669	15.946	16.830	16.717
15.288	15.481	17.253	15.828	16.199	16.398	14.063	12.950
12.760	14.871	16.124	17.406	16.865	13.309	9.056	12.204
13.810	14.753	16.077	14.543	12.711	19.122	17.264	18.814
18.252	15.990	18.244	19.780	15.585	17.954	17.391	17.497
19.289	15.884	15.868	11.156	10.545	12.878	15.439	17.855
19.189	18.040	20.001	20.130	20.709	20.640	19.662	20.206
19.782	17.334	18.962	18.722	18.485	16.408	18.199	18.628
19.087	19.119	20.022	20.839	21.466	20.298	21.017	21.295
20.961	20.126	19.251	21.147	22.369	20.963	22.457	21.289
20.705	20.615	21.225	22.387	24.086	24.779	23.719	24.490
21.894	21.837	21.199	23.723	21.759	22.718	20.908	21.449
20.201	20.539	22.264	22.816	23.756	23.990	22.134	20.767
19.991	20.521	20.838	20.266	20.037	20.121	20.964	20.303
21.359	20.835	20.423	21.372	20.924	22.145	22.389	22.619
23.398	24.036	22.820	21.810	22.092	22.846	21.757	20.887
18.303	18.157	18.172	17.669	19.054	20.546	18.785	19.387
19.851	19.873	20.279	20.783	20.950	18.379	18.892	18.478
18.398	17.520	18.019	16.330	16.854	18.640	15.742	17.059
15.840	14.965	16.749	18.101	16.357	14.567	15.396	13.470
13.559	14.208	18.583	17.673	16.044	15.379	10.724	8.225
10.174	13.469	13.655	8.635	9.879	11.651	13.383	16.243
9.510	9.866	12.215	14.964	17.684	14.084	6.452	10.002
8.749	8.107	7.193	10.727	14.354	14.866	13.859	11.152
8.250	7.339	8.602	8.783	9.233	10.010	2.928	-1.490
6.428	5.304	10.523	10.444	10.746	12.747	14.179	12.162
13.076	10.286	10.962	6.450	5.769	6.126	9.373	10.575
6.940	3.493	4.233	4.929	5.464	7.803	11.906	10.372
-0.207	-1.522	1.251	0.795	2.252	0.443	-0.513	1.178
5.543	9.435	13.233	16.696	10.667	3.067	2.058	1.567
0.497	-0.226	1.092	1.279	2.979	3.808	3.705	3.997
5.695	5.164	-4.045	-4.841	-0.781	0.409	4.788	-1.212
-3.691	1.715						

* RELATIVE HUMIDITIES. (DECIMALS).

0.687	0.707	0.899	0.800	0.845	0.989	0.992	0.807
0.726	0.674	0.660	0.688	0.767	0.730	0.943	0.841
0.612	0.730	0.661	0.544	0.696	0.669	0.797	0.637
0.655	0.852	0.654	0.609	0.658	0.569	0.609	0.652
0.480	0.618	0.835	0.546	0.583	0.597	0.785	0.567
0.592	0.568	0.681	0.769	0.793	0.795	0.715	0.653
0.629	0.757	0.755	0.852	0.922	0.796	0.699	0.750
0.899	0.907	0.857	0.924	0.960	0.929	0.888	0.684
0.620	0.643	0.670	0.647	0.708	0.767	0.562	0.565
0.849	0.950	0.789	0.739	0.945	0.781	0.915	0.806
0.693	0.818	0.861	0.740	0.882	0.871	0.948	0.950
0.811	0.856	0.671	0.666	0.668	0.683	0.739	0.730
0.704	0.775	0.771	0.806	0.858	0.806	0.751	0.697
0.751	0.905	0.744	0.825	0.798	0.906	0.774	0.753
0.740	0.771	0.741	0.765	0.778	0.825	0.848	0.846
0.878	0.886	0.951	0.860	0.819	0.848	0.833	0.874
0.851	0.827	0.799	0.811	0.772	0.778	0.828	0.847
0.901	0.847	0.888	0.827	0.900	0.761	0.801	0.743

0.741	0.707	0.703	0.779	0.764	0.775	0.920	0.912
0.818	0.816	0.832	0.850	0.825	0.859	0.858	0.878
0.876	0.873	0.888	0.920	0.931	0.886	0.875	0.853
0.855	0.832	0.875	0.912	0.882	0.837	0.917	0.807
0.818	0.876	0.834	0.840	0.852	0.818	0.901	0.878
0.855	0.854	0.859	0.888	0.853	0.824	0.786	0.804
0.829	0.837	0.837	0.897	0.951	0.846	0.899	0.823
0.870	0.945	0.960	0.876	0.858	0.873	0.793	0.851
0.873	0.978	0.915	0.937	0.789	0.859	0.904	0.846
0.800	0.862	0.785	0.820	0.836	0.867	0.971	0.809
0.751	0.800	0.748	0.850	0.880	0.832	0.920	0.969
0.846	0.720	0.769	0.842	0.887	0.925	0.895	0.937
0.855	0.805	0.816	0.800	0.814	0.861	0.951	0.869
0.794	0.731	0.816	0.838	0.866	0.937	0.967	0.949
0.873	0.932	0.851	0.870	0.812	0.840	0.894	0.873
0.790	0.891	0.878	0.816	0.858	0.843	0.981	0.940
0.917	1.000	0.866	0.814	0.816	0.874	0.749	0.639
0.812	0.991	0.921	0.782	0.937	0.831	0.883	0.917
0.854	0.892	0.860	0.887	0.887	0.853	0.745	0.739
0.848	0.979	0.822	1.000	0.776	0.825	0.904	0.906
0.965	0.988						

* PREDICTED SOLAR RADIATION INCREASED BY 15%.(KCAL/M-M-DAY).

3641.306	3036.242	1405.145	2366.663	3389.045	3178.336	3706.230	4183.367
4230.890	4277.375	4075.889	4121.945	2184.633	3463.941	2257.337	3540.808
3880.664	4407.632	4458.660	4787.433	4797.453	4600.007	4120.648	4480.558
5068.949	3017.081	4882.390	5104.730	5294.582	5027.503	5256.492	5147.203
4949.656	5221.113	3312.271	4769.910	4474.335	5474.960	3506.479	5315.125
5826.902	5365.847	4677.152	4125.269	2184.112	3667.411	4911.644	6003.707
5734.128	3084.714	3109.574	3135.408	3160.601	5932.941	6309.335	5197.585
2403.948	3279.037	3591.128	4542.375	5541.695	3717.163	2505.267	6769.914
7044.164	6846.023	6056.968	6851.671	6590.136	6674.550	7490.031	7076.789
7048.488	3290.461	4516.882	6450.632	3038.519	4536.125	3737.138	5331.566
7015.250	6038.246	6572.835	6089.093	2816.871	5467.761	3833.682	3703.543
5559.433	6334.777	7410.359	7421.414	8283.511	8105.980	7436.792	7040.878
7924.957	6920.195	5703.226	4914.359	4918.878	5014.085	5628.730	8528.562
6625.542	3473.046	7676.363	5991.449	6541.578	3080.518	5969.429	7752.050
7283.171	7874.636	8255.234	6878.277	7389.199	6626.492	3079.269	3083.042
3086.595	3089.930	3093.043	4223.714	5660.726	3504.713	3103.319	6212.761
5713.582	5293.636	7111.910	4933.843	7870.976	7483.988	3743.357	5742.476
4666.128	6914.285	4290.578	7004.328	6108.664	7893.617	7362.968	8674.496
8765.703	7922.957	8499.023	8206.128	7379.195	8731.785	4827.902	4752.949
7352.761	8427.101	4519.984	5979.816	6725.464	4487.039	6720.617	3054.296
3576.029	6027.007	6161.382	3859.921	5848.308	3224.782	6898.820	6777.746
7157.363	7423.613	2982.816	2974.871	6760.871	7236.601	4727.816	7908.640
7006.195	3184.957	6643.335	2902.418	2931.037	3847.717	3647.045	3789.301
5692.394	6765.558	7256.316	5962.210	6051.398	7635.425	6418.589	7223.468
7688.058	6005.988	5875.125	4150.406	2694.489	5788.476	3130.831	6886.003
2635.140	2620.025	3766.197	5512.746	4632.312	3936.839	7065.171	6485.597
6453.460	2491.281	4740.066	4966.089	6499.613	4273.535	3538.553	5879.285
4987.582	6679.105	6059.664	6013.750	5967.421	5920.703	2255.749	5331.382
6296.011	6163.191	6183.347	4702.656	2139.097	4582.531	5443.476	2079.610
2783.813	4513.261	4534.425	5081.917	1979.240	1959.093	1938.940	2338.230
1898.651	5133.597	5162.824	5026.875	4445.445	2977.059	1778.650	4176.777
4913.996	4644.339	3883.798	3627.605	1662.454	1644.110	1625.914	1607.875
4285.332	1572.299	3816.518	2723.992	3480.351	2300.179	1486.542	1469.986
3541.468	1755.157	3506.288	3187.323	3431.094	1375.295	2689.957	1345.624

1331.164 1316.963 2519.199 3620.786 2712.884 3135.385 3103.937 1237.375
1225.085 1213.083 1201.373 2190.775 1178.839 1168.023 2306.022 1147.303
2561.509 2820.626 3129.675 1427.263 1706.202 2733.521 2160.580 2702.813
1824.208 1062.705 2111.588 2846.838 1778.112 1768.080 1032.739 2868.579
1023.124 1018.830

* WATER SURFACE ELEVATIONS.(METERS).
492.493 492.928 493.355 495.120 496.147 496.845 497.354 497.848
498.287 498.640 498.948 499.238 499.506 499.790 499.991 500.277
500.582 500.631 500.908 501.122 501.256 501.481 501.554 501.746
501.771 501.646 501.524 501.399 501.387 501.365 501.375 501.311
501.298 501.451 501.457 501.408 501.317 501.228 501.061 500.911
500.856 500.673 500.737 500.737 500.619 500.667 500.719 500.868
500.792 500.591 500.442 500.341 500.649 500.829 501.042 501.094
501.109 501.478 501.885 502.493 503.383 504.334 505.124 505.739
506.218 506.632 507.025 507.349 507.623 507.897 507.986 508.175
508.382 508.687 508.958 509.125 509.183 509.312 509.406 509.507
509.522 509.650 509.760 509.766 509.900 509.924 510.107 510.229
510.555 510.769 510.945 511.052 511.082 511.064 511.028 511.003
511.101 511.098 511.040 511.076 511.189 511.399 511.357 511.375
511.308 511.253 511.186 511.082 511.015 511.076 511.156 511.012
510.863 510.769 510.677 510.570 510.540 510.521 510.339 510.198
510.052 509.936 509.939 510.034 510.000 510.022 509.973 509.936
509.970 509.939 509.836 509.823 509.686 509.586 509.491 509.357
509.253 509.125 509.162 509.028 508.946 508.860 508.799 508.684
508.580 508.571 508.333 508.153 507.937 507.693 507.501 507.260
506.977 506.641 506.245 505.885 505.572 505.279 504.947 504.617
504.267 503.950 503.694 503.578 503.511 503.301 503.280 503.225
503.161 503.109 503.084 503.103 503.212 503.206 503.130 503.030
502.911 502.764 502.670 502.578 502.603 502.457 502.280 502.136
501.941 501.832 501.670 501.518 501.341 501.143 501.021 500.829
500.646 500.469 500.289 500.021 499.902 499.854 499.686 499.521
499.323 499.395 499.323 499.323 499.241 499.149 498.951 498.735
498.610 498.418 498.302 498.119 497.979 497.650 497.372 497.193
496.818 496.400 496.001 495.632 495.355 495.144 494.919 494.794
494.568 494.303 494.102 493.803 493.547 493.431 493.160 493.105
494.504 495.095 495.553 495.909 496.159 496.120 496.092 496.050
495.912 495.809 495.729 495.742 495.507 495.385 495.723 495.894
495.928 496.004 495.979 495.983 495.940 495.912 496.229 496.757
497.491 498.080 498.415 498.787 499.180 499.445 499.671 499.823
499.951 499.674 499.421 499.146 498.835 498.372 497.994 497.671
497.400 497.199 497.068 496.799 496.580 496.330 496.034 495.635
495.330 495.029 494.751 494.641 495.193 495.550 495.650 495.611
495.361 495.074 494.867 494.678 494.446 494.206 493.983 493.754
493.514 493.282 493.111 492.834 492.551 492.264 492.163 492.380
492.343 492.264

* DIFFUSIVITIES.(M-M/DAY).
0.01245 0.01245

* INFLOW RATES.(M-M-M/DAY).
14679452.012110548.014740613.045212688.028991888.019939568.016636713.014679452.0
13700822.012942384.012122780.0 9859698.0 9847465.010911726.010177753.010520274.0
10165521.0 9737370.0 8734274.0 7645548.0 7241862.0 8171561.0 8196027.010520274.0
10336781.0 9761834.010226685.0 9272520.0 8379520.0 8134862.0 7890205.0 7951369.0
7608849.0 6728081.0 9847465.0 8049233.0 7046136.0 7021670.0 6923806.0 7241862.0
6850409.0 6463424.0 6605752.0 8012533.0 8514081.0 8318355.0 6923807.0 6581287.0
5969643.0 6139835.0 6728082.0 6972739.010887261.0 9541643.0 7951369.0 8196026.0

8196027.012355206.012783357.017615328.026545328.028624912.025566672.020306560.0
16636713.015413425.013823151.011988219.010141055.010887260.010838329.010226685.0
10226685.010948424.010764931.0 9125725.0 8636410.0 9541643.0 9052328.0 9052328.0
8318355.0 7278561.0 6373328.0 7596616.0 7486519.0 7780109.0 9248055.011743562.0
12844521.010092123.0 8685342.0 7388658.0 7229630.0 7462054.0 6728081.0 7119534.0
5896246.0 6140903.0 6373327.0 6923807.0 9125726.0 7829041.0 6972738.0 5015478.0
5504794.0 6605752.0 6226533.0 5945178.0 7975834.0 6434492.0 5039944.0 5076643.0
5309067.0 5186738.0 5003244.0 5492560.0 5150040.0 4660724.0 5321300.0 6140903.0
5504794.0 5749450.0 7608849.0 7339725.0 4403835.0 5504794.0 5431396.0 5773917.0
5822848.0 5932944.0 5125574.0 4146943.0 3731024.0 3792190.0 3559765.0 4110245.0
4293738.0 5357998.0 4171408.0 3767724.0 4403834.0 4966547.0 4257040.0 4330437.0
4293738.0 3302875.0 3376273.0 3865588.0 4110246.0 4171410.0 4721890.0 8477384.0
6874876.0 5455862.0 5272368.0 5198971.0 8269424.0 8281657.0 5884012.0 5529259.0
5578191.0 5945177.0 8391753.013015782.015046440.010826095.0 9321451.0 9431548.0
8269423.0 7963602.0 7608849.0 8049232.0 8807671.0 7767876.0 6801478.0 7229630.0
6312163.0 6067506.0 7413122.0 6091971.0 4770820.0 4342670.0 4991012.0 4819752.0
4991012.0 4893149.0 4770820.0 4305971.0 4648492.0 4991012.0 5688285.0 4379370.0
4330438.0 4330438.0 3498601.0 3449670.0 7706712.010642602.0 6752548.0 5406930.0
5162273.0 5211204.010030957.011205315.0 8514083.0 6899342.0 6287698.0 5406930.0
4501697.0 4893149.0 5627122.0 6752547.0 7046137.0 6079739.0 9052329.0 8440683.0
6361094.0 6263232.0 5422847.0 5504793.0 5284602.0 5137807.0 5015478.0 6581287.0
6018573.0 5504793.0 5565953.0 5431396.0 5003245.0 7486521.0 6544588.0 9908631.0
29236544.016881360.012355206.0 9969794.0 7095067.0 8073697.0 8930001.011865891.0
10948425.0 9590576.0 8954466.0 6238766.0 6728080.0 8134863.020184240.018716288.0
13896549.011131918.0 9676204.0 9431548.0 9113493.0 9419313.018055712.020257632.0
20551232.016710111.014924110.013333836.012306274.011804725.010948425.010397945.0
7462053.0 8196026.0 8991163.0 8832137.0 6801479.0 7254096.0 7474288.0 6617985.0
9296986.0 9345917.0 8807671.0 8709808.0 8440685.0 7095066.0 6238766.0 6728081.0
6850410.0 7192931.0 7767877.0 8318355.027279296.019633760.014924110.012905685.0
11621233.010532507.0 9125726.0 8538547.0 7315259.0 7168464.0 7706711.0 7278560.0
7192930.0 7657780.0 8624177.0 6544588.0 6165369.0 6165369.0 9174657.018716288.0
12416370.011254247.0

* OUTFLOW RATES,(M-M-M/DAY).
1223287.0 1100959.0 1223287.0 978630.3 1957260.0 1467945.0 2691233.0 1345616.0
1223287.0 2935891.0 3180548.0 1957260.0 1957260.0 1957260.0 3865589.0 2446575.0
1712603.0 9663974.0 978630.3 978630.3 3180548.0 1467945.0 6605755.0 5627124.0
8563015.013333838.013211510.012722194.0 9052330.0 8563015.0 8318358.0 9296988.0
8073700.0 2446575.0 9052330.010764934.010275618.0 9296988.010642605.010642605.0
8318358.011743564.0 4893151.0 8073700.011743564.0 6605755.0 5382467.0 2691233.0
7339727.012232879.010764934.010030961.0 1957260.0 4159179.0 1223287.0 6361097.0
7829042.0 2446575.0 1467945.0 0.0 0.0 0.0 0.0 183493.2
856301.5 733972.7 0.0 733972.7 489315.1 733972.7 7584385.0 3302877.0
2691233.0 244657.6 733972.7 3914521.0 6361097.0 5137809.0 5627124.0 4893151.0
6850412.0 2446575.0 2446575.0 6850412.0 2446575.0 6605755.0 4648494.0 7339727.0
978630.3 1467945.0 1712603.0 3180548.0 5871782.0 7951371.0 7829042.0 7829042.0
2201918.0 6116439.0 8073700.0 6116439.0 7339727.0 1345616.0 8318358.0 4159179.0
8073700.0 8440686.0 8563015.0 9786303.010520276.0 3669863.0 1957260.0 9908632.0
10520276.0 8318358.0 8196029.0 8807673.0 6361097.0 4893151.011498906.011009591.0
10520276.0 9786303.0 5627124.0 2935891.0 5260138.0 4770823.0 7095070.0 7584385.0
4403836.0 6361097.0 8563015.0 4159179.0 8073700.0 7095070.0 7095070.0 8563015.0
8196029.0 9786303.0 3302877.0 7706714.0 7217398.0 7584385.0 6361097.0 7829042.0
7829042.0 3425206.011009591.010030961.011254249.011865893.011743564.014190140.0
15535757.016392058.017370688.016881360.016881360.016514387.016881360.016147401.0
16881360.016636716.015658085.015168770.015168770.016881360.0 9052330.010275618.0
9052330.0 8807673.0 9541646.0 7829042.0 7095070.0 8563015.0 9296988.010030961.0
9786303.010030961.0 9541646.0 8807673.0 4159179.0 8807673.010275618.0 9296988.0

10397947.0 8073700.0 9541646.0 9541646.010275618.010764934.0 8073700.0 9786303.0
9541646.0 9296988.0 8807673.011254249.011621235.011498906.011449975.010275618.0
10397947.0 4159179.010520276.010030961.0 9786303.0 9296988.011254249.011254249.0
7829042.010764934.0 8563015.012232879.010764934.014679455.015902743.012232879.0
16147401.016392058.015658085.014190140.011254249.010397947.010642605.0 9052330.0
11743564.011988222.010764934.012232879.011254249.0 8807673.011988222.010275618.0
1467945.0 489315.1 0.0 0.0 0.0 8318358.0 9296988.012232879.0
13700825.012232879.010520276.0 5871782.011988222.010520276.010764934.013700825.0
12232879.0 8563015.0 9786303.0 8685344.0 9419317.0 9541646.0 7339727.0 4893151.0
611643.9 0.0 4648494.0 1957260.0 489315.1 3547535.0 3669863.0 5504795.0
4159179.015655085.015658085.015658085.017126016.016392058.017370688.014801784.0
15413428.014924113.012956852.014924113.013211510.014190140.013945482.014924113.0
13945482.014190140.013945482.0 9786303.010030961.0 9296988.010030961.012232879.0
17003696.017003696.014679455.012232879.012232879.012232879.012232879.012232879.0
12232879.012232879.012232879.012232879.012232879.012110550.012110550.012232879.0
12477537.012477537.0

.00271 73156608000. .0864

2 1 1

306 2

1.0 306.0

* DISSOLVED OXYGEN IN INFLOW,(PPM).

12.444	11.193	10.142	9.678	10.674	11.496	11.271	11.649
10.360	11.688	10.614	9.712	10.158	10.282	9.894	9.956
10.156	10.503	9.708	9.028	10.191	9.553	9.590	9.780
11.464	9.827	9.600	10.101	10.399	10.281	11.619	10.234
9.537	9.052	9.213	10.053	9.401	10.108	9.407	10.141
9.948	10.200	10.681	9.204	9.531	9.435	8.832	8.950
10.079	9.583	9.462	9.572	8.856	9.074	8.785	8.682
8.804	8.561	9.171	8.370	8.954	8.510	8.928	8.584
9.462	9.885	8.713	8.536	8.322	8.869	9.879	9.698
9.639	9.487	9.041	8.980	8.599	9.268	9.020	8.908
9.054	8.813	8.677	8.955	8.679	8.836	8.795	9.050
8.124	7.507	8.488	8.883	8.675	8.752	8.692	8.686
8.479	7.866	8.293	8.516	7.617	8.829	8.439	8.457
8.275	8.573	8.329	8.207	8.377	8.309	8.559	8.557
8.361	8.355	8.413	7.855	7.547	7.966	8.956	9.078
8.836	8.484	8.894	8.911	9.099	7.938	7.505	8.817
9.275	8.072	8.550	8.575	7.173	7.483	7.621	7.575
7.904	8.405	8.076	6.909	7.436	7.971	8.185	8.176
8.282	8.276	7.891	7.948	7.958	8.092	7.570	8.590
9.047	8.430	8.608	8.020	8.107	7.994	8.430	7.920
7.595	8.231	8.341	8.251	8.640	8.595	8.047	7.928
8.124	8.321	8.284	7.569	8.091	7.885	8.372	7.691
8.036	8.180	7.793	8.334	8.202	7.884	9.293	9.596
8.691	9.249	8.965	9.449	8.303	9.341	9.270	8.775
9.442	9.481	9.367	7.992	9.003	9.498	9.869	9.900
9.802	10.075	8.279	9.389	9.989	9.738	9.453	9.782
8.659	8.277	8.301	7.930	8.480	8.315	7.928	8.466
8.776	9.117	8.354	8.640	8.827	8.662	8.643	8.494
7.929	8.828	9.295	8.475	8.694	8.696	8.525	8.641
9.003	9.653	9.213	9.079	8.778	8.201	8.226	8.009
8.843	9.257	9.178	9.052	9.829	9.198	9.555	9.851
10.984	10.713	9.904	9.684	9.883	10.128	8.768	8.758

```
     8.981      9.020      9.415      9.817     10.524      9.350      9.342      9.288
     9.113      8.785      8.604      8.612      8.929      8.232      8.322      8.086
     8.696      8.752      9.390      9.780      8.928      9.724      9.315      9.472
     8.677      9.749      9.524      8.162      8.122      8.472      8.779      8.798
     9.500      9.970      9.782      9.692      9.302      9.155      9.497      9.643
     9.380      9.422      9.496     10.089     11.549     11.708     11.326     10.870
    10.993     10.501

*  BOD IN INFLOW,ASSUMED,(PPM)
     8.0        8.0

     1

8.0           0.0

   0.05        0.00        10

8.0           8.0

     9     9   306   306    58

*  AREAS,(M-M).
15.24      15.24      1.0        1.0        396.24     396.24     1.0
283279.9  1699680.  4249199.  7243872.  10643231. 14487744. 21286463. 30027672.
40468560.

*  LENGTHS,(M).
1770.278  10863.07  16077.34  23480.33  28211.80  34552.62  41038.27  43259.17
45737.56

*  WIND SPEEDS,(M/DAY).
     5.193      2.405      1.921      3.429      6.901      7.768      5.466      3.086
     1.618      0.992      1.035      2.853      1.644      0.889      0.642      3.361
     2.653      3.775      6.938      4.893      1.839      2.643      3.134     10.144
     5.603      1.949      6.130      5.487      3.184      8.166      6.914      6.889
     9.852      3.328      5.095      6.488      3.390      4.515      2.674      8.374
     2.680      3.288      4.248      5.726      5.434      3.313      2.674      1.958
     3.187      2.649      1.969      0.756      0.322      2.455      4.126      2.821
     0.788      1.355      1.731      0.430      0.721      0.972      2.521      4.524
     2.281      1.862      1.942      1.666      1.205      4.386      2.721      2.672
     0.533      0.152      4.120      2.054      0.259      2.256      0.454      1.541
     2.899      0.721      1.734      2.097      0.844      1.101      0.217      0.202
     1.586      1.550      3.277      4.091      2.774      1.630      0.903      1.006
     0.979      0.887      1.967      1.293      0.875      2.457      2.107      1.478
     0.848      0.251      1.081      1.867      1.564      0.382      1.029      1.094
     1.058      0.802      0.534      0.586      1.413      1.089      1.268      0.721
     1.043      0.639      0.418      1.129      1.561      0.163      2.760      2.133
     2.386      1.435      0.929      1.309      1.676      1.735      1.550      1.329
     1.359      1.506      0.909      1.157      0.727      2.642      1.517      2.137
     1.464      0.891      1.181      1.291      0.909      1.662      1.027      0.482
     1.257      0.849      1.628      0.885      2.238      0.843      0.777      0.789
     0.623      1.211      0.824      1.176      0.724      0.462      1.483      1.681
     1.345      1.215      1.028      0.717      1.313      1.690      0.733      2.076
     2.250      0.842      1.151      0.870      0.654      0.497      0.390      0.714
     0.691      0.646      0.819      1.134      1.564      1.488      1.654      0.924
     0.741      0.592      0.328      0.456      0.346      2.400      0.745      1.705
     0.729      0.229      0.121      1.180      1.802      2.178      2.115      1.302
```

1.626	0.241	0.439	0.635	4.610	1.279	3.110	1.121
1.315	1.378	2.961	1.881	0.439	0.650	0.328	4.608
2.737	1.000	1.324	2.234	1.934	2.138	1.951	0.515
3.889	2.956	1.661	0.962	0.555	0.956	1.208	0.381
1.394	1.261	1.455	2.289	1.284	2.372	5.438	7.725
1.780	2.100	2.028	0.763	0.500	0.471	1.273	0.713
1.655	1.234	1.435	0.875	0.703	0.960	0.631	1.459
1.729	0.414	1.010	0.303	0.415	0.474	0.381	2.876
10.203	12.457	6.320	0.787	4.825	2.617	1.822	0.319
0.332	0.569	1.388	3.839	3.702	4.136	0.841	1.305
3.984	1.179	0.346	0.423	0.320	1.007	3.952	1.731
0.590	0.966	6.726	6.212	3.251	0.388	1.767	7.885
0.592	0.745						

* ATMOSPHERIC RADIATION.(KCAL/M-M-DAY).

5359.863	5688.148	6561.992	6726.355	4716.891	4418.652	4470.258	4479.535
4751.516	5168.273	5329.066	5536.418	6547.926	6811.750	6803.648	6515.793
6059.133	5946.840	5860.254	5818.348	6395.285	6877.480	6804.520	5295.703
4844.613	5268.578	4951.293	4768.641	4901.270	5650.805	5523.246	5532.844
5563.699	6222.957	6089.039	5304.258	5186.629	5403.684	5479.039	5328.777
5066.102	6249.648	6990.770	7127.250	6657.328	6409.637	5656.371	5769.660
6647.836	7204.191	7469.715	7473.594	7352.336	7115.891	6959.629	7336.344
7476.668	7381.379	7521.145	7414.383	7334.086	7499.074	7236.090	6135.754
6121.160	6517.695	7202.363	7320.734	7075.352	6282.387	5659.367	6227.539
6784.809	7338.680	7170.375	6572.730	6812.238	7898.969	7567.121	7732.457
7229.883	7303.203	7506.473	7809.570	7539.875	7616.016	7670.324	7732.340
7679.789	7024.758	6530.402	5955.070	5804.230	6149.875	6748.168	6984.199
6979.082	7283.109	7931.371	8076.301	8137.871	7906.078	7472.082	7157.809
7456.379	7296.387	7184.180	7413.969	7594.602	7555.770	7352.023	7167.137
7371.031	7024.102	7124.500	7408.723	7457.172	7907.836	8425.734	8442.891
8397.141	8236.129	8109.238	8148.437	8150.547	8283.824	8607.852	7919.309
7948.527	7782.410	7603.152	8224.410	8191.645	8113.930	8767.758	8590.437
8385.234	7933.770	8112.770	8157.992	7899.594	7615.902	7695.609	7329.574
7111.285	7430.930	7484.805	7619.887	8073.980	7767.598	8149.699	7942.430
7484.746	7312.430	8139.949	7657.551	7533.656	8023.031	7916.973	8248.227
8456.773	7911.742	7910.773	8286.695	8054.516	8446.711	7904.047	8006.719
8051.590	8111.734	8672.945	8511.437	7937.074	8026.980	8064.906	7314.211
7172.234	7778.113	7246.906	7823.852	8033.828	8120.164	7847.305	7812.555
7612.547	7500.578	7621.980	7872.359	7780.195	7038.840	7214.680	7055.676
6904.562	7334.477	7337.852	7252.727	7731.406	7522.094	7469.223	7047.305
7492.859	7426.094	7384.020	7509.039	7437.426	6908.430	6482.023	6458.586
6446.547	7223.926	7535.242	7093.656	6696.422	7397.156	6460.887	5851.910
6089.328	6254.922	6492.477	5860.102	6032.348	6270.711	7118.867	6726.227
5683.039	5787.109	6088.355	6770.586	7805.184	6690.336	5657.578	6612.137
6212.402	5745.551	5771.695	6197.914	7323.012	7402.449	7231.988	6738.133
6428.273	5739.641	5842.367	5840.879	5997.723	6459.695	5706.117	4758.484
4690.746	5601.930	6322.152	6285.121	6800.262	7113.973	7264.023	7015.832
6455.687	6696.348	6213.141	5854.039	5677.031	5947.832	6686.859	6690.953
5780.590	5732.281	5407.797	5575.625	5514.562	6404.789	6588.035	6673.324
5342.922	5226.633	5103.184	4706.953	5340.715	4976.117	4839.344	5500.930
6122.422	6620.082	7186.574	7554.059	6732.836	5731.562	5346.113	5550.945
5075.309	4825.215	4758.594	5431.008	5605.648	5335.344	5526.586	5338.875
5729.340	6006.320	4583.145	4200.000	4903.750	5178.578	5878.484	4487.641
4974.980	5551.066						

APPENDIX IV

LIST OF TABLES AND FIGURES

FIGURES

TABLES

APPENDIX V

DEFINITION OF NOTATION

Representative units of variables are given in cm,gm,min,cal, and °C.

a	Constant in evaporation formula (cm/min-millibar)·
a	Constant in Dougal-Bowmann equation (min^{-1})
a_t	Atmospheric transmission coefficient
c	Concentration (gm/cm^3)
c'	Turbulent concentration fluctuations (gm/cm^3)
c_E	Concentration of tracer E (gm/cm^3)
c_{mix}	Concentration in convectively mixed region (gm/cm^3)
cout	Concentration in outlet (gm/cm^3)
c_p	Specific heat (cal/gm°C)
c_{sat}	D.O. saturation concentration (gm/cm^3)
d	Depth of fluid (cm)
d_e	Depth of euphotic zone (cm)
d_m	Depth of surface layer for entrance mixing (cm)
d_s	Depth of entering stream (cm)
d_{sat}	Depth for saturation in the water quality model (cm)
e	Base of Naperian logarithms
e_a	Saturated water vapor pressure at temperature of air (millibars)
g	Gravitational acceleration (cm/min^2)
h	Thickness of horizontal layer for lag time (cm)
i	Direction

j	Direction
k	Bulk depletion factor (min^{-1})
k_1	Reoxygenation rate constant (min^{-1})
k_2	Reoxygenation rate constant (min^{-1})
m	Optical air mass
n	Number of time steps
n	Direction parallel to reservoir bottom (cm)
n_{max}	Location of maximum velocity for sinking flow (cm)
p	Pressure (millibar)
q_i	Inflow rate per unit vertical distance (cm^2/min)
q_o	Outflow rate per unit vertical distance (cm^2/min)
r	Normalized distance between the sun and the earth
r_H	Stratification criterion ratio
r_m	Entrance mixing ratio
$sinks_m$	Sinks of mass (gm/cm^3-min)
$sinks_T$	Sinks of heat (cal/cm^3-min)
t	Time (min)
t_d	Detention time (min)
t_i	Start of water quality calculations (min)
t_i'	Start of pulse injection calculation (min)
t_{it}	Time to drain volume of water above center line of intake (min)
t_L	Total lag time (min)
t_{LH}	Horizontal lag time component (min)
t_{Ly}	Time for incoming water to reach its density level (min)

u	Horizontal advective velocity (cm/min)
u'	Turbulent advective velocity fluctuations (cm/min)
u_i	Interfacial velocity (cm/min)
u_{max}	Maximum velocity in lower layer of surface entrance (cm/min)
v	Vertical convective velocity (cm/min)
v	Voltage
v_{max}	Maximum vertical velocity in numerical scheme (cm/min)
w	Wind velocity (cm/min)
x	Horizontal distance (cm)
y	Vertical distance, elevation (cm)
y_b	Reservoir bottom elevation (cm)
y_i	Elevation of inflow (cm)
y_{mix}	Elevation of bottom of mixed convective layer (cm)
y_{out}	Elevation of outflow (cm)
y_s	Surface elevation (cm)
z	Transverse direction (cm)
A	Horizontal cross-sectional area (cm^2)
B	Reservoir width (cm)
B_{av}	Average width of surface layers subject to entrance mixing (cm)
B_o	Width at elevation zero (cm)
B.O.D.	Initial condition for B.O.D. (ppm)
C	Cloudiness
D	D.O. deficit

D, D_T	Diffusivity of heat (cm^2/min)
D_L	Longitudinal dispersion coefficient (cm^2/min)
D_M	Diffusivity of mass (cm^2/min)
D_ρ	Numerical dispersion (cm^2/min)
D_p	Dispersion coefficient ($cm^2 min$)
D_r	Vertical eddy diffusivity (cm^2/min)
$D.O._{out}$	D.O. in outlet (ppm)
E	Turbulent diffusivity of heat (cm^2/min)
IF_r	Reservoir Froude number
G	Dummy variable
J	Number of spatial grid points in finite difference equations
K	B.O.D. decay constant (min^{-1})
K_1	Decay constant (min^{-1})
L	Reservoir length (cm)
L'	Reservoir length for lag time (cm)
L	Latent heat of vaporization (cal/gm)
M	Mass (gm)
P	Reservoir perimeter
P	Rate of photosynthetic oxygen production (min^{-1})
P_r	Prandtl number
Q	Volume rate of flow (cm^3/min)
Q_i	Inflow rate to reservoir (cm^3/min)
Q_i'	Total inflow rate with entrance mixing (cm^3/min)
Q_m	Portion of mixed inflow withdrawn from surface layers (cm^3/min)

Q_o Outflow rate from reservoir (cm^3/min)

Q_v Vertical flow rate in reservoir (cm^3/min)

R Reynolds number

R Rate of oxygen demand by algae (min^{-1})

S Dummy variable

S_c Schmidt number

T Temperature (°C)

T' Turbulent temperature fluctuation (°C)

T_a Air temperature (°C)

T_{a_2} Air temperature, measured two meters above surface (°C)

T_i Inflow temperature (°C)

T_{in}' Inflow temperature with entrance mixing (°C)

T_m Temperature of mixed surface layer

T_m Average temperature of surface layers for use with entrance mixing (°C)

T_{mix} Temperature of convective mixed layers

T_o Initial uniform temperature (°C)

T_{out} Outflow temperature (°C)

T_r Reservoir temperature (°C)

T_s Surface temperature (°C)

T_w Water temperature (°C)

$\bar{U}$ Average advective velocity (cm/min)

U_i Inflow velocity (cm/min)

$U_{i_{max}}$ Maximum inflow velocity (cm/min)

U_m Uniform outflow velocity from surface layer subject to entrance mixing (cm/min)

U_o Outflow velocity (cm/min)

$U_{o_{max}}$ Maximum outflow velocity (cm/min)

V_{it} Volume of reservoir above intake (cm^3)

V_o Vertical equivalent outflow advective velocity (cm/min)

$\forall$ Volume (cm^3)

V_Q Volume of inflow (cm^3/min)

$\forall_r$ Reservoir volume (cm^3)

W Work (gm-cm/min^2)

W_L Load of tracer (gm-cm/min^2)

α Solar altitude (degrees)

α, α_o Parameters in Koh's prediction formula for the withdrawal thickness ($cm^{-2/3}$)

β Fraction of solar radiation absorbed at water surface

β_o Vertical density gradient (gm/cm^4)

γ Specific weight (gm/cm-min)

δ Thickness of withdrawal layer (cm)

$\delta(x)$ Dirac delta function

Δ Increment (min)

ε Radiative emissivity

ε Normalized density gradient (cm^{-1})

ε_a Saturated vapor pressure at temperature of air (millibars)

ε_s Saturated vapor pressure at temperature of water (millibars)

η Radiation absorption or extinction coefficient (cm^{-1})

θ Dummy variable

θ Angle between reservoir entrance slope on the reservoir surface

λ Dummy variable

μ Dynamic viscosity (gm/cm-min)

ν Kinematic viscosity (cm^2/min)

ρ Density (gm/cm^3)

ρ_o Reference density (gm/cm^3)

ℓ Biochemical oxygen demand (ppm)

ℓ_{mix} B.O.D. in convectively mixed layers (ppm)

ℓ_o B.O.D. in incoming streams (ppm)

σ Stefan-Boltzman constant (cal/cm^2-min-°K)

σ_i Standard deviation of inflow velocity distribution (cm)

σ_o Standard deviation of outflow velocity distribution (cm)

τ Dummy variable

τ_o Shear stress ($gm/cm\text{-}min^2$)

ϕ Heat flux (cal/cm^2-min)

ϕ_a Atmospheric radiation flux (cal/cm^2-min)

ϕ_b Solar radiation absorbed internally (cal/cm^2-min)

ϕ_c Conductive heat flux (cal/cm^2-min)

ϕ_E Total evaporation heat flux (cal/cm^2-min)

ϕ_e Evaporation heat flux from vaporization of surface water (cal/cm^2-min)

ϕ_L Heat flux from surface heat losses (cal/cm^2-min)

ϕ_m Heat flux from heat transfer through reservoir sides (cal/cm^2-min)

ϕ_o Solar radiation (insolation) heat flux (cal/cm^2-min)

ϕ_r Longwave radiation heat flux from water surface (cal/cm^2-min)

ϕ_{sc} Solar constant (cal/cm^2-min)

ϕ_v Evaporation heat flux from heat advected from water surface (cal/cm^2-min)

ψ Dummy variable

ψ Relative humidity

ω Parameter in reservoir width-elevation relationship (cm^{-1})